Class Mobility in the Era of Rising Inequality: A Synthetic Dynasty Analysis

Geoffrey T. Wodtke[1], Weiqi Wang[2], Kristina Butaeva[2], and Steven N. Durlauf[2]

[1]*Department of Sociology, University of Chicago*
[2]*Harris School of Public Policy, University of Chicago*

October 9, 2026

Abstract

Widely regarded as a barometer for equality of opportunity, intergenerational mobility has attracted renewed attention amid concerns that it has declined in the wake of rising economic inequality since the 1970s. Although earlier research documents stability, or even modest increases, in mobility among cohorts who entered the labor market before this period, evidence for more recent cohorts is limited and inconsistent. In this study, we analyze contemporary trends in class mobility using a new approach based on the "synthetic dynasties" represented in Markov chains. This approach yields several novel measures of *movement* and *memory*, which respectively capture how class positions differ from one generation to the next and how the influence of class origins dissipates across generations. Applying these methods to data from the U.S., we find that overall levels of movement and memory have remained remarkably stable across cohorts born between 1945 and 1990. These trends are highly robust to the use of alternative data sources, sample definitions, measurement strategies, and class typologies. Taken together, our findings provide little evidence of a decline in intergenerational mobility over this period, despite substantial increases in economic inequality.

Keywords: class, occupations, mobility, inequality, trends, Markov chains

Direct correspondence to Geoffrey T. Wodtke, Department of Sociology, University of Chicago, 1126 E. 59th St. Chicago, IL 60637, email: wodtke@uchicago.edu.

1 Introduction

Intergenerational mobility concerns the extent to which socioeconomic attainments are linked across generations within families. This linkage has been conceptualized in several different ways. First, it can be understood as *association*, or the strength of the relationship between the social origins of parents and the destinations of children. Second, it can also be conceived in terms of *memory*, or how the association of a family's social origins with the destinations of descendants dissipates across generations. Lastly, mobility can be viewed as *movement*, or whether a descendant's social position differs from that of an ancestor.

Mobility—whether conceptualized as association, memory, or movement—is widely regarded as a key indicator of societal openness and equality of opportunity (Blau and Duncan, 1967; Featherman and Hauser, 1978; Roemer, 1998). Both scholarly and public interest in mobility stems largely from its connection to these ideals, and nowhere has this interest been more pronounced than in the U.S., where national mythology has cast the country as a "land of opportunity," promising abundant possibilities for advancement regardless of class background. The belief in American exceptionalism has not been confined to domestic observers. For example, Friedrich Engels famously described the U.S. as "a country rich, vast, expanding...unleavened by feudal remnants or monarchical traditions and without a permanent and hereditary proletariat [where] everyone could become, if not a capitalist, at all events an independent man" (Marx and Engels 1942:449).

In recent decades, however, concerns about the prospect of declining mobility have increased (DeParle, 2012; Haldane, 2025; Krueger, 2012; Putnam, 2015), as economic growth has slowed and inequality has widened since the 1970s. These trends—sluggish growth coupled with a steep rise in income and wealth inequality—have renewed public interest in mobility and revived controversies over whether American society is straying from its professed commitment to equality of opportunity. They have also spurred a renaissance of empirical research on mobility and its contemporary dynamics (Chetty et al., 2017; Davis and Mazumder, 2024; DiPrete, 2020; Mitnik et al., 2016).

Trends in mobility have long been the subject of vibrant theoretical debate, and recent concerns have drawn fresh attention to competing perspectives on how mobility evolves over time. Modernization theory, for example, anticipates a steady increase in mobility as societies develop economically (Featherman and Hauser, 1978; Lipset and Bendix, 1959; Treiman, 1970). In particular, as modernization expands access to education and increases the importance of skills for occupational attainment, it is thought to weaken

the influence of family background and foster greater mobility over time (Hout, 1988; Pfeffer and Hertel, 2015). An alternative perspective, articulated in the Featherman-Jones-Hauser (FJH) hypothesis, contends that the link between class origins and destinations remains largely stable in market-based societies with nuclear family systems, and that any fluctuations in mobility mainly reflect structural shifts in the distribution of occupations (Erikson and Goldthorpe, 1992; Featherman et al., 1975).

These long-run perspectives contrast with more recent arguments that rising inequality reduces mobility. Many of these arguments are motivated by "The Great Gatsby Curve," an empirical proposition that higher cross-sectional inequality is associated with lower intergenerational mobility (Andrews and Leigh, 2009; Corak, 2006, 2013; Hertel and Groh-Samberg, 2019). DiPrete (2020) and Durlauf et al. (2022) describe mechanisms that can generate this association. One mechanism operates through schooling and labor markets, where Hassler et al. (2007) show how shifts in the distribution of education interact with skill premia to produce an inverse relationship between inequality and mobility. A second set of mechanisms emphasizes social processes, where rising inequality reduces mobility by increasing segregation and deepening disparities in resources between upper- and lower-class families, which then polarize investments in children. These disparities reinforce class differences in the acquisition of human, social, and cultural capital, strengthening the capacity of more advantaged families to transmit their social position across generations (Andrews and Leigh, 2009; Durlauf, 1996; Fogli et al., 2025; Mitnik et al., 2016). Together, these arguments depart from earlier sociological theories that emphasized steady growth or stability in intergenerational mobility over long time horizons.

Prior research on mobility trends in the U.S. provides mixed support for these competing perspectives, particularly during the recent period of rising inequality. For cohorts born well before this period, a large body of evidence indicates that the link between class origins and destinations either remained stable or weakened over much of the twentieth century (e.g., Featherman et al. 1975; Featherman and Hauser 1978; Grusky and Hauser 1984; Hauser et al. 1975; Hout 1988). However, research covering more recent cohorts—those who grew up or entered the labor market during the era of rising inequality—is both more limited and more inconsistent. Among studies of occupational mobility, some report continued stability in origin-destination associations (Song et al., 2020), others suggest a modest decline in the influence of parental background (Beller and Hout, 2006; Pfeffer and Hertel, 2015), and still others point to signs of increasing persistence across generations (Beller, 2009; Mitnik et al., 2016). Research on income mobility during this period is similarly inconclusive: while some studies report little

change (Bloome, 2015; Chetty et al., 2014; Lee and Solon, 2009), others suggest a decline in mobility for cohorts entering the labor force after 1980 (Aaronson and Mazumder, 2008; Davis and Mazumder, 2024). In sum, the evaluation of recent trends in intergenerational mobility—whether measured using occupations or income—remains "plagued with inconsistent findings" (Torche 2015:56).

Some of these inconsistencies may stem from limitations in how recent trends have been analyzed. Most studies focus on income-based measures of mobility, which are sensitive to earnings volatility over the life course and may capture individuals' positions within a complex, multidimensional system of social stratification less effectively than occupation-based measures (Connelly et al., 2016; Nybom and Stuhler, 2016). Occupational classes, in particular, are strongly associated with a wide range of life chances (Wodtke, 2017), and they are closely tied to the growth of income inequality in recent decades (Mouw and Kalleberg, 2010; Weeden et al., 2007; Zhou and Wodtke, 2019).

Prior studies of occupational mobility, while more robust to life-course volatility, suffer their own drawbacks. They have largely relied on small samples of recent cohorts (e.g., Pfeffer and Hertel 2015; Mitnik et al. 2016), reducing their ability to detect change during the period of rising inequality. Moreover, the most influential analyses of trends in occupational mobility were conducted before this period and draw on data that exclude recent cohorts entirely (e.g., Erikson and Goldthorpe 1992; Featherman and Hauser 1978; Hout 1988).

Finally, nearly all studies of trends in occupational mobility employ log-linear or log-multiplicative models, whose coefficients represent odds ratios capturing the strength of the association between parental origins and child destinations. Although widely used and analytically powerful, these models capture only one dimension of mobility—namely, association—and do not directly reflect movement or memory. They also typically impose restrictive functional form assumptions about the evolution of mobility over time. When these assumptions are violated, they can obscure meaningful changes and introduce bias (Bucca and Urbina, 2021). In addition, estimates derived from these models are often imprecise due to the instability of odds ratios, particularly in sparse contingency tables (Zhou, 2015).[1] Taken together, these limitations complicate efforts to assess whether, and how, mobility has shifted in recent decades.

In this study, we analyze cohort trends in class mobility during the era of rising inequality. To this end, we draw on the most recent data available from the U.S., apply nonparametric smoothing techniques to improve the precision of estimates for recent cohorts, and use a new set of mobility measures based on the "synthetic dynasties" represented in Markov chains. These measures adapt the logic of synthetic cohort analysis

and stable population models—widely used in demography (Wachter, 2014)—to study class mobility. Rather than tracking actual family lineages over multiple generations, we use cross-sectional data on parent-child pairs to simulate the long-run trajectories of hypothetical dynasties initiated by individuals in a given birth cohort. This approach allows us to characterize a cohort's mobility not only in terms of the observed transitions from parental origins to child destinations, but also through the extent to which class origins would continue to influence subsequent, synthetic generations formed as if patterns of occupational inheritance were to remain stable indefinitely.

Our approach yields several novel and complementary measures of mobility conceptualized as movement. First, we distinguish between *overall mobility* and *steady-state mobility*. Overall mobility is defined conventionally as the total amount of movement across classes observed among parent-child pairs in a given cohort. It reflects both shifts in the occupational distribution and the association of parental origins with child destinations. It is also commonly decomposed into two components: structural mobility, which reflects movements necessitated by changes in the marginal distribution of occupations, and exchange mobility, which captures residual movements (Featherman and Hauser, 1978; Jones, 1985; McClendon, 1977; Sobel et al., 1985).[2]

Steady-state mobility, by contrast, measures the amount of movement between classes after a Markov chain has reached its stationary distribution, where the marginal proportions of different classes become invariant across generations and thus structural mobility ceases to exist (Butaeva et al., 2025). In other words, steady-state mobility reflects the movement that would persist among descendants of synthetic dynasties once the class structure has stabilized. These movements are driven solely by the association—or lack thereof—between parental origins and child destinations.

Second, we also introduce several measures of mobility conceptualized as memory. In particular, we analyze a measure of *aggregate intergenerational memory*, defined as the distance between the observed transition probabilities among parent-child pairs and the limiting transition probabilities of a Markov chain (Blume et al., 2025), where the influence of class origins on the destinations of descendants has dissipated entirely. This measure captures how the influence of class origins fades out over successive generations of a synthetic dynasty. Mobility is higher when origins lose their influence quickly, such that descendants from different class backgrounds rapidly converge to a state in which they have equal chances of attaining any destination.

These measures extend a long tradition of using Markov chains to study the intergenerational transmission of social status (Bartholomew, 1967; Boudon, 1973; Dardanoni, 1993; Prais, 1955; Singer and Spilerman, 1976), and offer several advantages over conven-

tional approaches to analyzing mobility. They provide simple, interpretable summary indices of movement and memory that can also be disaggregated to reveal more granular, class-specific patterns. They are fully nonparametric, imposing no assumptions about the distribution of parental origins and child destinations or how it changes over time. And lastly, they can be readily combined with smoothing techniques to produce more precise estimates of trends, particularly for cohorts that are sparsely represented in the data.

Applying these methods to data from the General Social Survey (GSS), we find that overall mobility in the U.S. has remained remarkably stable across cohorts born between 1945 and 1990. In addition, the link between class origins and destinations—as captured by our measures of steady-state mobility and aggregate intergenerational memory—also appears largely unchanged over this period. An extensive set of robustness analyses indicates that the stable patterns we observe are highly robust to the use of alternative data sources, sample definitions, measurement strategies, and class typologies, including those based on income rather than occupations.

Beneath this apparent stability, however, lies a more complex set of underlying dynamics. The stable level of overall mobility results from offsetting trends in its component parts: structural mobility has declined, reflecting a slowdown in occupational upgrading, while exchange mobility has increased. Similarly, there is at least some evidence that the flat trends in steady-state mobility and intergenerational memory may conceal variation across class origins. Among those from the upper and lower classes, movement has declined and memory has increased, albeit slightly. Conversely, among those from middle-class origins, movement has risen while memory has weakened. These class-specific trends should be interpreted cautiously because the smaller effective sample sizes within individual origin classes make them difficult to estimate with precision. In general, sample size and other data limitations prevent us from precisely estimating trends among certain subpopulations that may be of interest, including separate trends by race and ethnicity.

Despite these limitations, the present study makes several contributions to research on class mobility. Empirically, it provides the most up-to-date and comprehensive estimates of American trends in intergenerational mobility during the era of rising inequality. Theoretically, these estimates help adjudicate among competing accounts of how mobility evolves over time, offering limited evidence for modernization theory, mixed support for the inequality perspective, and partial alignment with the FJH hypothesis. Methodologically, we introduce novel measures that capture multiple dimensions of class mobility, are easy to interpret, and do not rely on restrictive parametric assump-

tions.

In the sections that follow, we begin by reviewing different theoretical perspectives and prior research on trends in mobility. Next, we introduce Markov models of class mobility and describe our synthetic dynasty measures based thereon. We then outline the data and methods used to estimate these measures, present their trends across cohorts, and conclude by considering the broader implications of our findings for theory and future research.

2 Trends in Class Mobility: Continuity or Change?

Different theoretical perspectives offer contrasting predictions about trends in class mobility over time. The modernization perspective—also known as the liberal theory of industrialization—anticipates steadily rising mobility as societies develop and expand access to education. The FJH hypothesis, by contrast, contends that the influence of class origins on destinations remains largely invariant. "Great Gatsby" perspectives advance historically contingent arguments about how certain types of socioeconomic economic change may shape intergenerational mobility, suggesting that recent increases in income and wealth inequality are disrupting patterns of mobility that were once relatively stable.

Modernization theory views rising class mobility as a natural consequence of economic development and the institutional changes that accompany it (Featherman and Hauser, 1978; Lipset and Bendix, 1959; Treiman, 1970). As societies industrialize, they are thought to transition from "particularistic" forms of social stratification—where opportunities are allocated primarily on the basis of kinship and ascribed status—to more meritocratic systems, in which occupational attainment depends increasingly on individual achievement and formal qualifications (Featherman and Hauser 1978:12). This process was expected to intensify in the post-industrial era, as service-based economies place an even greater premium on education and human capital, and rapid technological change accelerates the obsolescence of occupational skills, limiting parents' ability to directly transmit competencies that remain relevant in an evolving labor market (Bell, 1976; Featherman and Hauser, 1978).

Expansion of the formal education system plays an especially important role in promoting mobility, according to the modernization perspective. Mobility is thought to increase not only because of a decline in the direct influence of class origins on destinations, but also through changes brought about by expanded access to education (Beller and Hout, 2006; Hout, 1988). In principle, educational expansion could reduce the importance of family background for attaining higher levels of education, thereby at-

tenuating the indirect link between class origins and destinations that operates through differences in schooling. Empirically, however, class disparities in educational attainment have largely persisted—and in some cases even widened—during recent episodes of expansion (Bailey and Dynarski, 2011; Lucas, 2001; Raftery and Hout, 1993).

But even when disparities in educational attainment persist, expansion nonetheless increases the share of the population attaining higher levels of schooling, particularly college degrees. Because the association of class origins with destinations tends to be weaker among those more education, expansion may promote greater mobility through a compositional mechanism—that is, by shifting more people into subpopulations where social origins seem to exert less influence. In this way, post-secondary expansion may generate increases in mobility at the population level even when class disparities in educational attainment remain pronounced. While there is considerable evidence that educational expansion promotes mobility through this type of compositional change (Breen, 2010; Hout, 1988; Pfeffer and Hertel, 2015; van de Werfhorst, 2024), several recent studies also raise doubts about the equalizing role of post-secondary education (Fiel, 2020; Zhou, 2019).

In contrast to modernization theory, the FJH hypothesis rejects the possibility that class mobility follows an upward, developmentally driven trajectory. Rather than anticipating that mobility will increase steadily with economic development, this perspective posits that the association between class origins and destinations—typically measured using odds ratios—remains relatively stable over time in societies with market economies and a nuclear family system (Featherman et al., 1975). While overall rates of mobility—conceptualized as movement—may rise or fall, these fluctuations are thought to reflect changes in the occupational structure, driven by technological development, shifting labor demand, or educational expansion, and not by any systematic strengthening or weakening of the association between class origins and destinations. The FJH hypothesis thus distinguishes between a "genotypic" pattern of mobility, referring to stable origin-destination associations, and a "phenotypic" pattern based on observed levels of movement between classes, which vary in response to shifts in the distribution of occupations over time (Featherman et al. 1975:339-340).

Empirical research on the U.S. largely supports the modernization or FJH perspectives for cohorts born earlier in the 20th century. Studies of occupational mobility covering these groups generally find that the association between class origins and destinations—the "genotypic pattern of mobility"—either remained stable or declined modestly (Featherman et al., 1975; Featherman and Hauser, 1978; Grusky and Hauser, 1984; Hauser et al., 1975; Hout, 1988). Similar patterns also appear in Europe, where

early studies pointed to "trendless fluctuation" in origin-destination associations across cohorts (Erikson and Goldthorpe, 1992) and later reanalyses suggested that these associations had actually weakened in some countries (Breen, 2004; Breen and Müller, 2020). However, most evaluations of the modernization and FJH perspectives are based on data that largely predate the contemporary period of rising inequality.

Since the 1970s, income and wealth inequality in the U.S. have increased (Killewald et al., 2017; Morris and Western, 1999; Piketty and Saez, 2003; Saez and Zucman, 2016). Much of this increase has been driven by disproportionate gains at the top of the distribution. For example, the share of national income held by the top 1% of families has roughly doubled, climbing from under 10% in the 1970s to around 20% today (Saez and Zucman, 2020). The recent shifts in economic inequality also map closely onto occupational classes (Mouw and Kalleberg, 2010; Weeden et al., 2007; Zhou and Wodtke, 2019), with the earnings of professionals and managers increasingly pulling away from the rest of the labor force. The emergence of this high-inequality regime marks a potentially new phase in the long-term dynamics of class reproduction (Andrews and Leigh, 2009; DiPrete, 2020; Mitnik et al., 2016).

Specifically, a number of scholars have argued that rising inequality may reduce intergenerational mobility by exacerbating disparities in the resources that families invest in their children (Andrews and Leigh, 2009; Mitnik et al., 2016). As affluent families consolidate income and wealth, they may become increasingly effective at transmitting their advantages to the next generation, while families with fewer resources find it harder to facilitate upward mobility for their children. A growing body of evidence suggests that upper-class parents now invest more heavily in their children's human, social, and cultural capital—through high-quality childcare and extracurricular activities, enrollment in private or well-resourced public schools, and access to selective colleges and universities (Bailey and Dynarski, 2011; Kornrich and Furstenberg, 2013; Schneider et al., 2018). Moreover, parental investments may extend beyond adolescence and the transition to adulthood, as affluent parents are also better positioned to support their children later in life—for example, by financing graduate and professional degrees or subsidizing prolonged job searches. All of these investments are thought to increase the likelihood of class reproduction, particularly among those at the top of the occupational hierarchy (Mitnik et al., 2016). This evidence is complemented by research showing that policies which expand investments in disadvantaged children can generate medium- and long-term improvements in educational outcomes (Heckman et al., 2010; Johnson and Jackson, 2019; Gray-Lobe et al., 2022).

Beyond polarizing the resources that families invest in their children's development,

rising inequality may also promote intergenerational persistence by reshaping the social contexts in which children grow up. Greater income inequality is associated with higher levels of residential and school segregation, particularly among families with children (Logan et al., 2020; Owens et al., 2016), and the spatial concentration of poverty and affluence is linked, in turn, to disparities in educational attainment and labor market outcomes (Chetty et al., 2016; Wodtke et al., 2011, 2016). Through these mechanisms, higher inequality may further suppress intergenerational mobility by deepening the contextual differences that enhance the development of advantaged children while constraining the life chances of their more disadvantaged counterparts. Consistent with this account, formal theoretical models and a growing body of empirical studies highlight how segregation and peer effects can generate persistent intergenerational inequalities (Bénabou, 1996; Durlauf, 1996; Durlauf and Seshadri, 2017; Fogli et al., 2025).

According to this perspective, then, mobility should decline following the rise in economic inequality, with a lag determined by the timing and nature of parental investments and any contextual effects on their children. If these influences are concentrated in childhood and adolescence, shifts in mobility may only become apparent once cohorts raised during the era of growing inequality reach adulthood. However, if parental support and neighborhood contexts later in life also play an important role, changes could emerge more quickly. In either case, the effects are likely to appear as a stronger link between class origins and destinations among cohorts who grew up or entered the labor market after the 1970s. Because the largest gains in income and wealth have accrued to those in professional and managerial occupations, the consequences of rising inequality for mobility may also be more pronounced among their children. In this scenario, rising inequality would not necessarily produce uniform changes in mobility across class origins but would instead engender a growing capacity for upper class families in particular to secure desirable positions for the next generation (Mitnik et al., 2016).

Research on the relationship between inequality and mobility has produced mixed and sometimes contradictory findings. Cross-national comparisons consistently show that countries with higher levels of income inequality tend to exhibit lower levels of income mobility (Andrews and Leigh, 2009; Blanden, 2013; Corak, 2013)—an empirical pattern that Krueger (2012) termed "The Great Gatsby Curve." However, this inverse relationship is weaker, or altogether absent, when occupational class rather than income is used to measure mobility between parental origins and child destinations (Bukodi and Goldthorpe, 2018; DiPrete, 2020; Torche, 2015). At the same time, Hertel and Groh-Samberg (2019) find that cross-national associations between economic inequality and class mobility are more evident when inequality is measured across occupational classes

rather than individuals or households, suggesting that the link may depend on how these concepts are operationalized. Research examining the association between income inequality and income mobility across American states also has not uncovered a strong relationship (Bloome, 2015).

A second line of evidence comes from trend analyses, which examine whether mobility has declined with rising inequality since the 1970s. Findings from this literature are inconsistent as well. Among studies of income mobility, some report little change over time (Bloome, 2015; Chetty et al., 2014; Lee and Solon, 2009), while others document a decline in mobility for more recent cohorts (Aaronson and Mazumder, 2008; Davis and Mazumder, 2024). Research on occupational mobility during this period is less extensive but similarly divided. Some studies report that the association between parental origins and child destinations has remained largely unchanged (Song et al., 2020). Others find evidence of growing persistence across generations (Beller, 2009; Mitnik et al., 2016). And still others suggest a decline in the influence of parental origins (Beller and Hout, 2006; Pfeffer and Hertel, 2015). Taken together, these findings do not support a clear or consistent conclusion. Whether class mobility has changed during the era of rising inequality thus remains an unsettled question.

One reason this question remains unresolved is that the most reliable data on the occupations of children and their parents contain relatively small samples of cohorts who grew up or entered the labor market after the 1970s. To compensate, prior studies have typically grouped cohorts into broad, arbitrarily defined bins in an effort to boost statistical power, yet even then, the ability to detect change is limited and potentially distorted.

In addition, nearly all modern studies of trends have relied on log-linear or log-multiplicative models, such as the "unidiff" or log-multiplicative layer effect model (Erikson and Goldthorpe, 1992; Xie, 1992), to analyze mobility conceptualized as association. Despite their many advantages, these models directly capture only this single dimension of mobility, their parameter estimates can be quite noisy when based on sparse contingency tables, and they impose strong assumptions about the nature of change over time. For example, layer effect models assume that the pattern of association between class origins and destinations remains the same across cohorts, allowing only the strength of these relationships to vary according to a single set of parameters. These constraints can make it difficult to detect changes in mobility over time and may introduce bias into estimates of trends.

The present study aims to address these limitations and provide new evidence on trends in class mobility during the era of rising inequality. To assemble larger samples

of the cohorts most likely to be affected by higher inequality, we leverage the most recent data available on the occupations of children and their parents. We then employ nonparametric smoothing techniques to reduce random variation and enhance precision. Finally, we use these smoothed data to estimate a new set of measures that capture mobility conceptualized as movement and memory, while avoiding any restrictive assumptions about how mobility has changed over time. We conclude by comparing our measures with more conventional indicators of mobility as association and by investigating the sensitivity of our conclusions to alternative analytic choices.

3 Methods

3.1 Data

To study the dynamics of class mobility in the U.S., we use data from the 1972 to 2024 waves of the General Social Survey (GSS; Davern et al. 2025). The GSS is a repeated cross-sectional survey that collects demographic and employment information from nationally representative samples of non-institutionalized American adults. Surveys were conducted annually from 1972 to 1994—except in 1979, 1981, and 1992—and biennially thereafter. The GSS is well-suited for this analysis because it is one of the few long-running surveys that records information on both respondents' occupations and those of their parents, enabling comparisons across cohorts spanning multiple decades.

Our analytic sample consists of all GSS respondents who were born between 1945 and 1990, who were 25 to 55 years old at the time of their interview, and who reported complete information on both their own and their father's occupations. This yields a total of $n = 24,265$ respondents in birth cohorts that grew up or entered the labor market during the era of rising inequality. Sample sizes vary by cohort, ranging from 184 to 788 respondents. The birth-year and age-at-interview restrictions serve to maximize the size of our samples across cohorts while simultaneously limiting the potential for life-cycle bias in our trend estimates by ensuring that occupational destinations are observed at broadly comparable stages of respondents' working lives. Parallel analyses using alternative age restrictions (e.g., 25 to 64, 30 to 64, or 30 to 40) produced similar results, which are reported in Appendix A.

Table 1: A Five-class Version of the EGP Typology

Class	Description	Illustrative Occupations	EGP Labels
1	Higher-grade professionals, administrators, and managers	Accountants, postsecondary teachers, lawyers	I
2	Lower-grade professionals, administrators, and managers	Primary school teachers, registered nurses, managers (all other)	II
3	Higher-grade routine non-manual workers, technicians, and supervisors	Secretaries, office supervisors, bookkeepers	V + IIIa
4	Higher-grade manual workers, lower-grade technicians, and farmers	Carpenters, auto technicians, electricians	VI + IVc
5	Lower-grade routine non-manual and manual workers	Retail sales supervisors, nursing aides, truck drivers	VII + IIIb

Notes: The illustrative occupations for each class include the three most common occupational titles among sample members in the 2022 wave of the GSS. The self-employed (EGP Classes IVa and IVb) are allocated across all five of our classes based only on their occupation.

3.2 Occupational Classes

At each wave of the GSS, respondents are asked, *"What kind of work do you normally do?"* They are also asked retrospectively, *"What kind of work did [your father] usually do while you were growing up?"* Responses to both questions were coded using the 2010 Census Occupational Classification (COC) system, which we use to assign sample members to class origins based on their father's occupation and to class destinations based on their own occupation. These father-child pairs constitute the empirical basis for our analysis.

To translate detailed COC codes into occupational classes, we adopt a five-class version of the Erikson-Goldthorpe-Portocarero (EGP) typology (Erikson et al., 1979). Widely used in prior studies of intergenerational mobility, the EGP typology groups occupations according to their employment relations, skill requirements, and work conditions. We focus on a five-class version of the typology to preserve clear distinctions in skills, conditions, and employment relations while avoiding overly fine categories that would lead to excessive sparsity. The resulting classes—summarized in Table 1—include: (1) higher-

grade professionals, administrators, and managers; (2) lower-grade professionals, administrators, and managers; (3) higher-grade routine non-manual workers, technicians, and supervisors; (4) higher-grade manual workers, lower-grade technicians, and farmers; and (5) lower-grade routine non-manual and manual workers. Figure 1 displays the number of observations in each of these classes, separately by birth cohort.

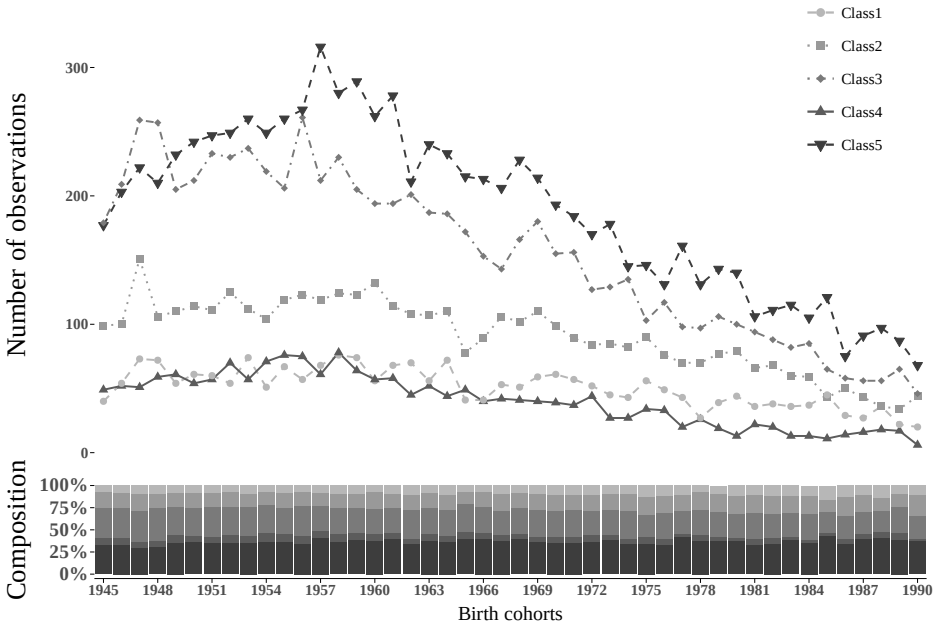
Although the EGP typology is widely used, the details of its implementation vary across studies. We implement our classification using the crosswalk developed by Morgan (2017). To assess the robustness of our key findings, we also conducted a series of parallel analyses based on several alternative implementations. These included versions of the typology that (i) omit farmers and the self-employed; (ii) follow the classification decisions adopted by Erikson and Goldthorpe (2010) and Pfeffer and Hertel (2015); and (iii) expand the typology to seven classes. As reported in Appendix B, trend estimates are highly consistent across different approaches to measuring occupational class.

3.3 Analyses

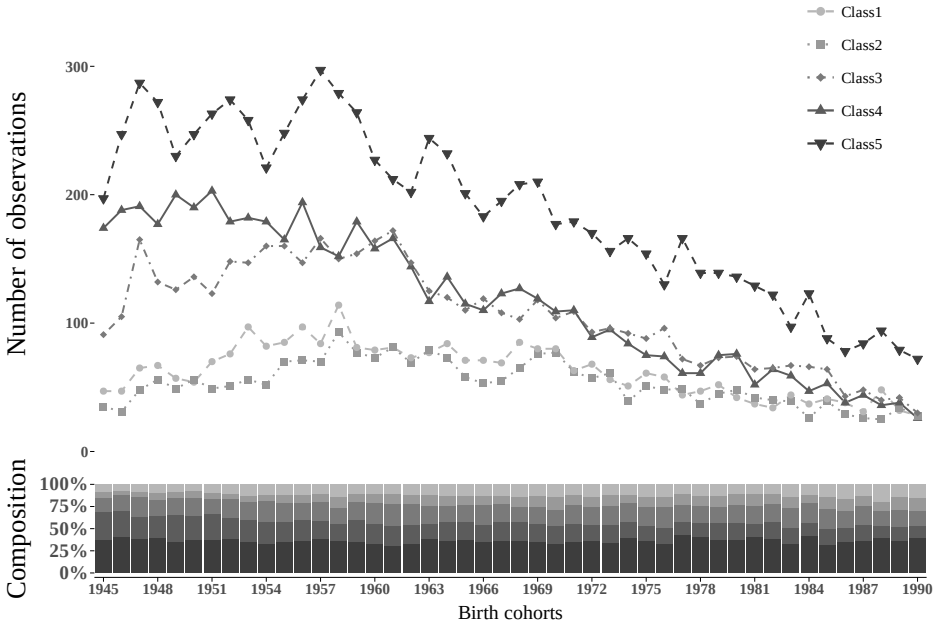
We analyze intergenerational mobility using a new class of measures based on the "synthetic dynasties" represented in Markov chains. This approach begins with the observed transition probabilities between fathers' and children's occupational classes in a particular birth cohort, and then asks what would happen if these probabilities were to remain constant across subsequent generations. In this way, it allows us to characterize mobility not only through the father-child transitions observed in the GSS but also through the long-run influence of class origins on hypothetical family dynasties constructed as if patterns of class transmission were indefinitely stable from one generation to the next.

Formally, let P denote a 5×5 transition matrix, where each element P_{ij} represents the probability of transitioning from origin class $i \in \{1, ..., 5\}$ to destination class $j \in \{1, ..., 5\}$. If μ_p denotes a 1×5 row vector of probabilities capturing the marginal distribution of parental origins, then the corresponding distribution of children's class destinations is given by $\mu_c = \mu_p \cdot P$. Now suppose that the intergenerational transmission of class observed in a given cohort and summarized by P were to remain unchanged across subsequent generations descended from this cohort. In this situation, the mobility process would take the form of a stationary Markov chain, where the probability of entering a particular destination class at any generation t is constant and depends only on the origin class of the preceding generation $t-1$. Under this process, the marginal distribution of classes at generation t evolves recursively as $\mu_t = \mu_{t-1} \cdot P$ or, similarly, from an initial distribution μ_0 in the founding generation as $\mu_t = \mu_0 \cdot P^t$.

Figure 1: Sample sizes by class origin, destination, and birth cohort



(A) Class destinations of children



(B) Class origins of fathers

Notes: Class 1 refers to higher-grade professionals; class 2 refers to lower-grade professionals; class 3 includes higher-grade routine non-manual workers and technicians; class 4 comprises higher-grade manual workers, lower-grade technicians, and farmers; and class 5 includes lower-grade routine non-manual and manual workers.

As $t \to \infty$, the marginal distribution of occupational classes converges to an invariant, or steady-state, distribution denoted by μ_∞. At the same time, the transition matrix converges to a limiting matrix, $P^t \to P^\infty$, in which every row is equal to μ_∞.[3] Substantively, this means that once the steady state is reached, the marginal distribution of classes remains constant across generations, and the influence of class origins in the founding generation $t = 0$ has dissipated entirely—that is, descendants share identical chances of occupying different class destinations, regardless of their dynasty's starting point. These limiting properties of Markov chains provide the foundation for our key measures of mobility.[4]

For any given cohort, the GSS captures only a single intergenerational transition—from fathers to their children—and does not observe subsequent generations of descendants. We therefore cannot directly test whether the underlying mobility process is first-order, which would require linked observations across at least three generations, or whether a cohort-specific transition matrix remains stable across subsequent generations. These assumptions are used only to characterize the implications of the observed father-child transitions, not to forecast future mobility or to claim that actual family lineages follow a stationary Markov process. In reality, transition probabilities may change across generations or depend on the class positions of more distant ancestors and broader kin networks (Mare, 2011; Song, 2021). If so, iterating a first-order transition matrix would not recover the true, but unobserved, multi-generational mobility process. We therefore refer to the resulting dynasties as *synthetic*: they are hypothetical lineages generated as if the father-child transition probabilities observed for a given cohort persisted indefinitely. In this sense, the Markov chain serves as an analytic device analogous to a period life table in demography. Just as a period life table summarizes mortality by exposing a synthetic cohort to the age-specific mortality rates observed at a given point in time, our approach summarizes mobility by exposing synthetic dynasties indefinitely to the transition probabilities observed for a given cohort.

Building on the limiting properties of Markov chains, we distinguish between two complementary notions of mobility: mobility as movement and mobility as memory. Measures of *movement* capture the extent to which children's class positions differ from those of their parents both in the observed data and within the synthetic dynasties implied by a Markov chain. Measures of *memory*, by contrast, assess how class origins shape the destinations of later generations within these synthetic dynasties and the rate at which their influence fades.

3.3.1 Mobility as Movement

With measures of movement, mobility is higher when children's occupational classes differ from those of their parents'. More specifically, these measures quantify how much probability mass lies off the main diagonal of the transition matrix. At one extreme, every child could remain in the same class as their parent, such that the transition matrix is equal to the identity matrix. At the other extreme, every child could enter a different class than their parent, producing a transition matrix with zeros along the main diagonal. In general, the greater this off-diagonal mass, the higher the level of mobility when conceptualized as movement.

Movement measures have a long history in empirical research on mobility. A classic example is the decomposition of overall mobility into "structural" and "exchange" components (Erikson and Goldthorpe, 1992; Featherman and Hauser, 1978; McClendon, 1977; Sobel et al., 1985). In this decomposition, overall mobility is defined as the proportion of children who occupy a different class than their parents; structural mobility refers to the portion of these movements driven by shifts in the marginal distribution of classes; and exchange mobility represents the residual movements that occur net of structural change.

Whereas prior studies evaluate these measures only for the observed transitions from fathers to children, we trace how they evolve across generations of synthetic dynasties governed by a stationary Markov chain. Specifically, we define *overall mobility* as the proportion of descendants in generation t that experience a change in occupational class compared to the previous generation $t-1$:

$$OM_t = 1 - \sum_i \mu_{i,t-1} \cdot P_{ii}. \tag{1}$$

where $\mu_{i,t-1}$ denotes the marginal proportion of descendants in class i at generation $t-1$, and P_{ii} represents the ith diagonal element of the transition matrix. This measure captures the total amount of movement between classes from one generation to the next within a set of synthetic dynasties.

At any generation of these dynasties, overall mobility can then be decomposed into structural and exchange components. *Structural mobility* is formally defined as follows:

$$SM_t = \frac{1}{2} \cdot \sum_i |\mu_{i,t-1} - \mu_{i,t}|. \tag{2}$$

It captures the movements necessitated by shifts in the marginal distribution of classes

from generation $t-1$ to t. *Exchange mobility* is defined residually as the difference between overall and structural mobility:

$$EM_t = OM_t - SM_t. \tag{3}$$

This formulation merely extends the familiar decomposition of overall mobility to each generation t of a Markov chain.

As the Markov chain converges to its steady state, the recursive relation $\mu_t = \mu_{t-1} \cdot P$ stabilizes at $\mu_\infty = \mu_\infty \cdot P$. In this state, structural mobility vanishes because the marginal distribution of classes no longer changes across generations, and thus overall mobility becomes equal to exchange mobility. We refer to this limiting quantity as *steady-state mobility*, which can be formally defined as follows:

$$SSM = 1 - \sum_i \mu_{i,\infty} \cdot P_{ii}. \tag{4}$$

Steady-state mobility measures the amount of intergenerational movement that persists among synthetic dynasties in a Markov chain, once the occupational structure has stabilized. In other words, SSM isolates an intrinsic level of movement that is not driven by changes in the marginal distribution of classes but is instead generated by the transition process itself (Butaeva et al., 2025).

To examine class-specific heterogeneity in intergenerational movement, we additionally compute the mean time to exit (MTE; Kemeny and Snell 1976) from each origin class in the founding generation of the synthetic dynasties. This measure can be formally defined as follows:

$$MTE_i = (1 - P_{ii}) \cdot \sum_{t=1}^{\infty} t \cdot P_{ii}^{t-1}. \tag{5}$$

In substantive terms, MTE_i represents the expected number of generations it takes for descendants to leave origin class i. Higher values reflect lower chances of movement away from the class, while lower values signal a greater likelihood of departure.

3.3.2 Mobility as Memory

In contrast to movement, measures of memory capture the enduring influence of class origins across multiple generations within synthetic dynasties. Mobility is higher when descendants from different origins quickly come to face similar chances of entering each destination. Conversely, mobility is lower when class origins continue to shape occupational outcomes many generations into the future.

More specifically, measures of memory variously reflect the concepts of distance, time, and decay. Some measures quantify the distance between a focal transition matrix and the limiting matrix of a stationary Markov chain, in which descendants share identical chances of entering each destination regardless of their dynasty's starting point. Other measures capture the amount of time required for the mobility process to reach this steady state, at which point class origins no longer predict the destinations of descendants. Still others capture the rate at which the association between class origins and the destinations of descendants is decaying across generations. In colloquial terms, measures of memory indicate how far, and how quickly, a set of synthetic dynasties moves toward a state of multi-generational "equality of opportunity."

Formally, equality of opportunity corresponds to a transition matrix in which all rows are the same. In a stationary Markov chain, this state arises in the limit as $\mu_t = \mu_0 \cdot P^t$ converges to the steady-state distribution μ_∞ and the transition matrix converges to P^∞, where each row equals μ_∞. Because P^∞ has identical rows, it represents a state in which class destinations are independent of origins in the founding generation of the dynasties.

Using this limiting matrix as a benchmark, we define *aggregate intergenerational memory* at generation t as follows:

$$AIM_t = \frac{1}{2} \cdot \sum_{i,j} |P^t_{ij} - \mu_{j,\infty}| \cdot \mu_{i,0}. \tag{6}$$

This measure captures the distance of P^t from the limiting matrix P^∞, whose rows are all equal to μ_∞. At generation $t = 1$, it provides a concise summary of how strongly class origins shape outcomes across future generations, with larger values signaling greater distance from the state of multi-generational equality of opportunity (Blume et al., 2025).

To examine class-specific heterogeneity, we decompose AIM_t into components that measure the distance between the transition probabilities of a given origin class and their limit at the steady state. This yields a measure of intergenerational memory for each origin class i at generation t, which can be defined as follows:

$$IM_{i,t} = \frac{1}{2} \cdot \sum_{j} |P^t_{ij} - \mu_{j,\infty}|. \tag{7}$$

By construction, the weighted average of $IM_{i,t}$ across origin classes, using their relative size as weights, is equal to AIM_t. Plotting these class-specific measures highlights variation in the influence of different origins across subsequent generations (Blume et al., 2025).

In addition to measures of distance, we also report measures that capture time and decay. Specifically, we examine the number of generations it takes for the influence of class origins to dissipate entirely, denoted by t^*, as well as $\Delta_{AIM} = (AIM_1 - AIM_2)/AIM_1$, which measures the rate at which the influence of class origins declines across generations (Durlauf et al., 2024). Taken together, AIM_t, t^*, and Δ_{AIM} jointly characterize the magnitude, persistence, and rate of decay of the link between a family's origins and the destinations of its descendants.

3.3.3 Estimation and Inference

We estimate all the measures outlined previously, separately for each birth cohort, using our analytic sample from the GSS. To improve the precision of our estimates and reduce sampling variability—especially for recent cohorts with fewer observations—we smooth our mobility tables using thin-plate splines before computing measures of movement and memory (Wood, 2003). Specifically, we smooth cell counts in the three-way contingency table of origin class (row), destination class (column), and birth cohort (layer) using the following model:

$$\log\left(n_{ijk}\right) = \alpha_{ij} + f_{ij}(k) + \epsilon_{ijk}, \tag{8}$$

where n_{ijk} denotes the number of respondents from origin class $i \in \{1, ..., 5\}$ observed in destination class $j \in \{1, ..., 5\}$ for cohort $k \in \{1945, ..., 1990\}$. The parameters α_{ij} represent a set of origin-by-destination fixed effects, while $f_{ij}(k)$ is a smooth function of cohort that is allowed to vary across each origin-destination pair. We specify these functions using thin-plate splines, which flexibly smooth over random variation in cell counts across cohorts.

The model is estimated via penalized maximum likelihood, where the penalty is designed to limit excessive curvature, or "wiggliness," in the spline functions. This is achieved by augmenting the likelihood with an additional term that takes the form an integrated second derivative multiplied by a smoothing parameter: $\sum_{i,j} \lambda_{ij} \int f''_{ij}(k)^2 \, dk$. Larger values of the smoothing parameters λ_{ij} produce smoother fits and greater resistance to deviations from linearity. We optimized these parameters using restricted maximum likelihood (Wood, 2011).

After fitting Equation 8, we generate predicted counts, denoted by $\hat{n}_{ijk}$, which are then used to compute all the probabilities on which our measures of movement and memory are based. For example, we estimate the transition matrix for a particular cohort k as $\hat{P}_{ij} = \hat{n}_{ijk} / \sum_j \hat{n}_{ijk}$. This approach smooths both the cell counts and the marginal totals

while avoiding restrictive assumptions about how mobility may vary across cohorts. It results in cohort-specific estimates for our focal measures that are less variable and more precise. It also obviates the need to pool adjacent cohorts into larger groups, a common but arbitrary strategy for dealing with sparsity that can distort trends. To assess the robustness of this approach, we experimented with a variety of alternative specifications, including models that did not smooth the marginal totals, that used different spline bases, and that optimized the smoothing parameters via generalized cross-validation, all of which produced similar results.

To quantify the uncertainty in our estimates, we use the nonparametric bootstrap. Specifically, we resample the observed data with replacement $b = 2000$ times and replicate our entire analysis on each bootstrap sample, including estimation of the smoothed counts. This procedure yields an approximate sampling distribution for every measure of interest. We then construct confidence intervals from these distributions using a percentile estimator that adjusts for any bias or skew (Davison and Hinkley, 1997). We report unweighted estimates throughout, as a parallel analysis incorporating survey weights that adjust for different features of the GSS design produced nearly identical results (see Appendix C for details). A full set of replication files for this analysis is available at https://github.com/vigiwang/synthetic_dynasty_analysis_replicate.

4 Results

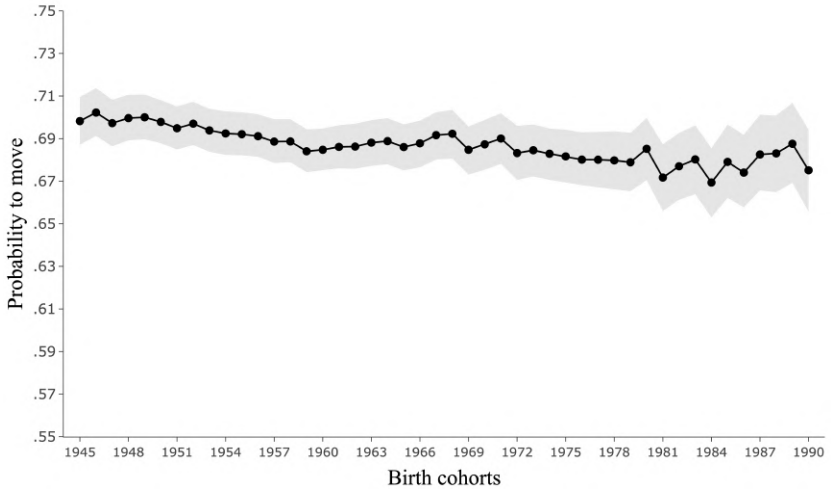
4.1 Overall, Structural, and Exchange Mobility

Panel A of Figure 2 displays trends in overall mobility at generation $t = 1$, which reflects the total amount of movement in the observed transitions between fathers and their children. Across cohorts who grew up or entered the labor market during the era of rising inequality, overall mobility remained remarkably stable. In the 1945 birth cohort, about 70% of children entered a different occupational class than their fathers. In the 1990 cohort, this share declined only slightly to about 68%. More broadly, across all cohorts born between 1945 and 1990, overall mobility hovered around 70%. These results indicate that the likelihood of children entering a different class than their fathers was largely invariant over time.

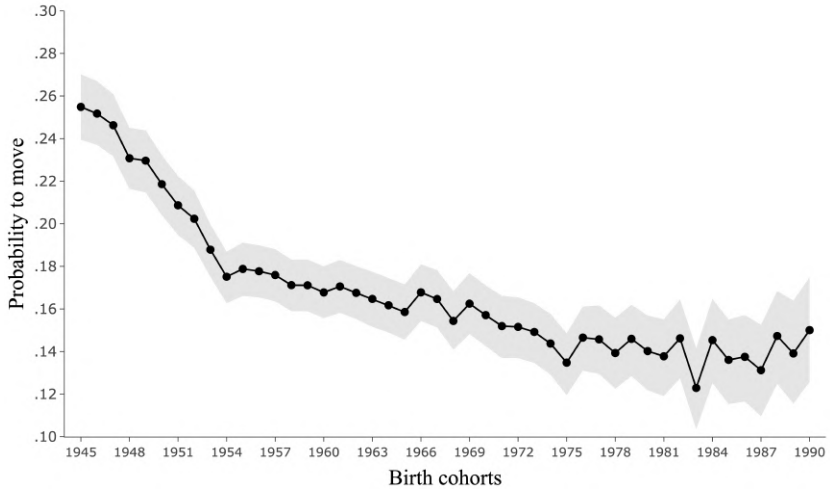
Overall mobility reflects differences in the marginal distribution of classes between fathers and children as well as the transition probabilities linking them. It can be decomposed into structural mobility, capturing the portion of movements driven by shifts in the marginal distribution of classes, and exchange mobility, which captures the residual

Figure 2: Measures of movement at generation $t = 1$.

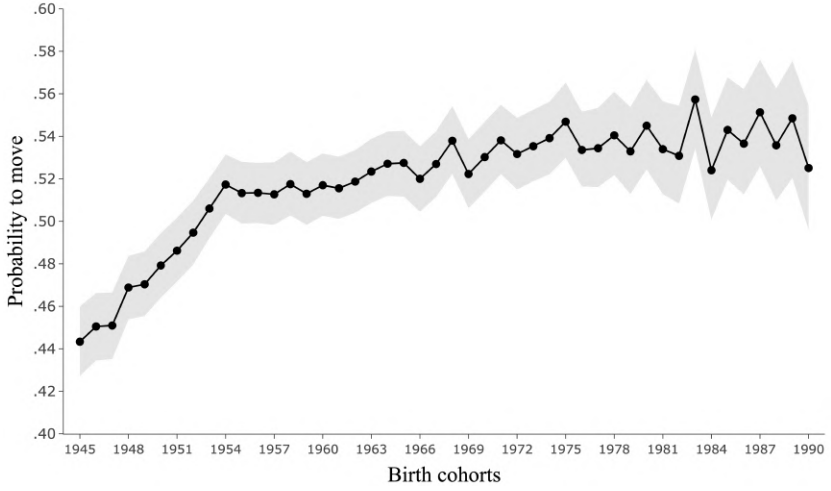
(A) Overall mobility (OM_1)



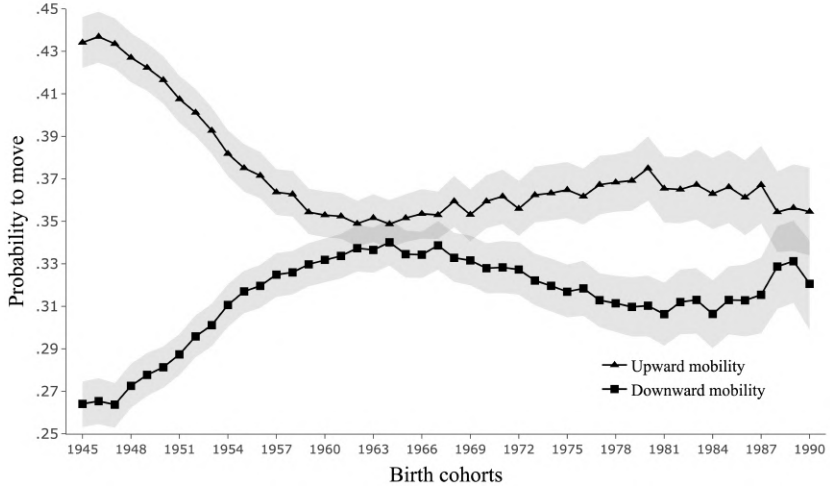
(B) Structural mobility (SM_1)



(C) Exchange mobility (EM_1)



(D) Upward and downward mobility



Notes: Shaded areas represent 95% confidence intervals.

movements net of these structural changes. Panels B and C of Figure 2 display trends in structural and exchange mobility, respectively, at generation $t = 1$, showing that the stability of overall mobility conceals offsetting trends in these components.

Specifically, structural mobility declined from about 25% in the 1945 birth cohort to less than 15% among those born after the mid-1970s. This decline was driven largely by two factors: the slowing contraction of class 4 (higher-grade manual workers, lower-grade technicians, and farmers), whose share of the workforce stabilized at a relatively low level, and the deceleration of growth in classes 2 (lower-grade professionals, administrators, and managers) and 3 (higher-grade routine non-manual workers, technicians, and supervisors).

By contrast, exchange mobility increased from about 45% to nearly 55% over the same period. The countervailing trends in structural and exchange mobility offset one another, producing a flat trajectory in overall mobility across cohorts. Together, they indicate that a growing share of intergenerational movements came to reflect transitions between fathers and their children that left the marginal distribution of occupational classes unchanged.

Overall mobility can also be decomposed into upward and downward movements, provided that an ordering is imposed on the occupational classes. Although the EGP typology does not natively encode a hierarchy, we assume our five classes are ordered by their numeric labels, such that a destination class j is considered higher in rank than an origin class i if $j < i$.[5] Under this ordering, overall mobility at generation $t = 1$ can be partitioned into upward mobility, or the proportion of children who attain a higher-ranked class than their fathers, and downward mobility, which captures the proportion of children who fall to a lower-ranked class.

Panel D of Figure 2 displays trends in upward and downward mobility across cohorts, showing that the stability of overall mobility also reflects offsetting changes in these components. Upward mobility declined sharply from about 45% in the 1945 cohort to approximately 35% in cohorts born in the late 1950s, while downward mobility increased over the same period. Both rates then stabilized, remaining mostly flat for cohorts born since the 1960s. In other words, upward mobility far exceeded downward mobility among cohorts born before mid-century, but the two metrics converged and are now at roughly similar levels among recent birth cohorts.

To summarize, overall mobility between classes in the observed transitions from fathers to children remained stable during the era of rising inequality. Beneath this stability, however, lies a more complex set of underlying dynamics: structural mobility declined, reflecting a slowdown in occupational upgrading and a corresponding drop

in upward movements, while exchange mobility increased. As a result, recent cohorts experienced levels of overall mobility comparable to earlier ones, but with less upward movement driven by professional-sector expansion and agricultural-sector contraction, and more circulation both up and down the class hierarchy.

4.2 Movement in Synthetic Dynasties

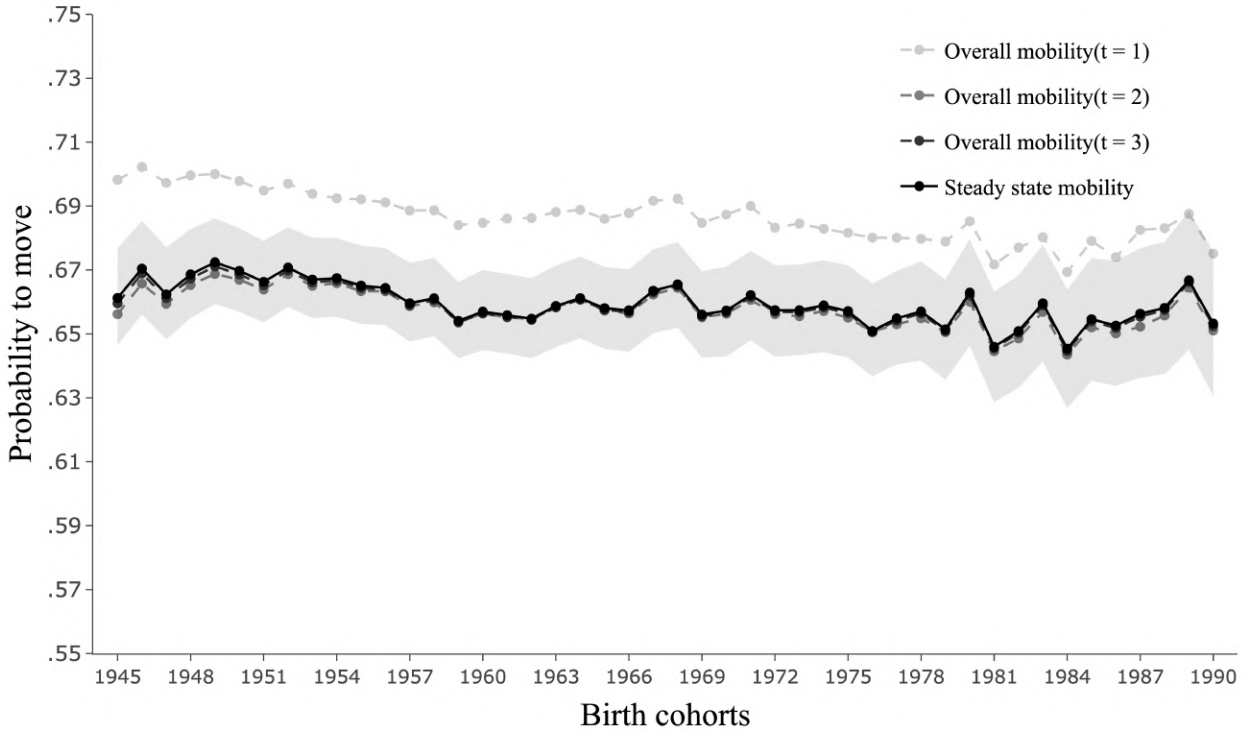
Figure 3 plots trends in overall mobility across generations in stationary Markov chains. At generation $t = 1$, the figure reproduces the empirical trend shown in Panel A of Figure 2. For subsequent generations ($t \geq 1$), it traces how mobility evolves as these synthetic dynasties unfold. The solid black line depicts steady-state mobility, which captures the total amount of intergenerational movement between classes once the Markov chain has reached its equilibrium. In this state, structural mobility is absent entirely, so all remaining movements are generated by the transition process itself rather than shifts in the marginal distribution of classes across generations.

Two key patterns are evident in this figure. First, the steady state is reached rather quickly: across all cohorts, the Markov chains converge to an invariant marginal distribution of classes within four generations. Even by generation $t = 2$, overall mobility has largely stabilized, with little change thereafter. Second, the level of steady-state mobility is also remarkably flat. Once the occupational structure has stabilized in each Markov chain, the probability that a descendant of a synthetic dynasty exits their parental class is close to 66% across all cohorts. This suggests that the "intrinsic" level of intergenerational movement has remained largely stable among those who grew up or entered the labor market during the period of rising inequality.

Nearly flat trends in overall and steady-state mobility suggest a stable concentration of probability mass along the diagonal of the cohort-specific transition matrices. Such stability, however, does not preclude heterogeneity in movement across origin classes and could reflect offsetting dynamics. To investigate this possibility, Figure 4 plots trends in the mean time to exit, which captures the average number of generations it takes for descendants of a given origin class to transition into a different destination. A higher mean time to exit indicates that descendants of synthetic dynasties tend to remain in their origin class for longer, signaling a lower likelihood of movement. For visual clarity, Figure 4 displays point estimates only. An analogous figure with 95% confidence intervals is provided in Appendix D.

The figure suggests potentially meaningful variation in trends across classes, although the class-specific estimates are noisy and accompanied by relatively wide con-

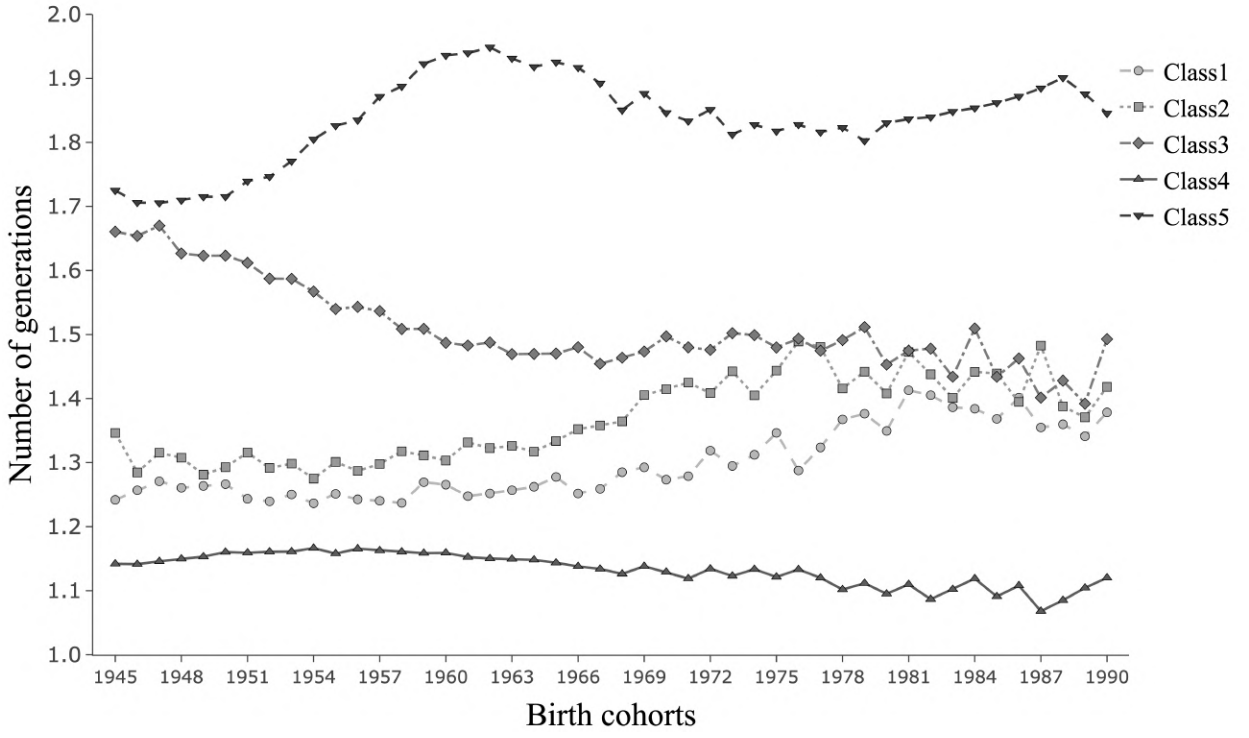
Figure 3: Overall mobility (OM_t) across synthetic generations



Notes: This figure illustrates the evolution of overall mobility across generations in a stationary Markov chain. By $t = 4$, the Markov chains for all cohorts have converged to their respective steady-state distributions, where there is no structural mobility. Shaded areas represent 95% confidence intervals, which are shown only for the trend in steady-state mobility.

fidence intervals, as reported in the Appendix. For classes 1 and 2 (higher- and lower-grade professionals, administrators, and managers), mean time to exit appears to have increased, consistent with greater persistence and reduced movement across cohorts. A similar pattern is visible for class 5 (lower-grade routine non-manual and manual workers), where the estimated mean time to exit rises from about 1.7 generations among the 1945 cohort to nearly two generations among more recent cohorts. Taken together, these patterns are suggestive of declining mobility at both the top and bottom of the occupational hierarchy. By contrast, for classes in the middle of the hierarchy—particularly class 3 (higher-grade routine non-manual workers, technicians, and supervisors)—mean time to exit appears to have declined, consistent with reduced persistence and greater movement. Thus, what appears as stability in overall levels of intergenerational movement may reflect countervailing dynamics, with growing persistence at the top and bottom and increasing movement in the middle, although these differences should be interpreted cautiously given the imprecision of the underlying estimates.

Figure 4: Mean time to exit from each origin class (MTE_i)



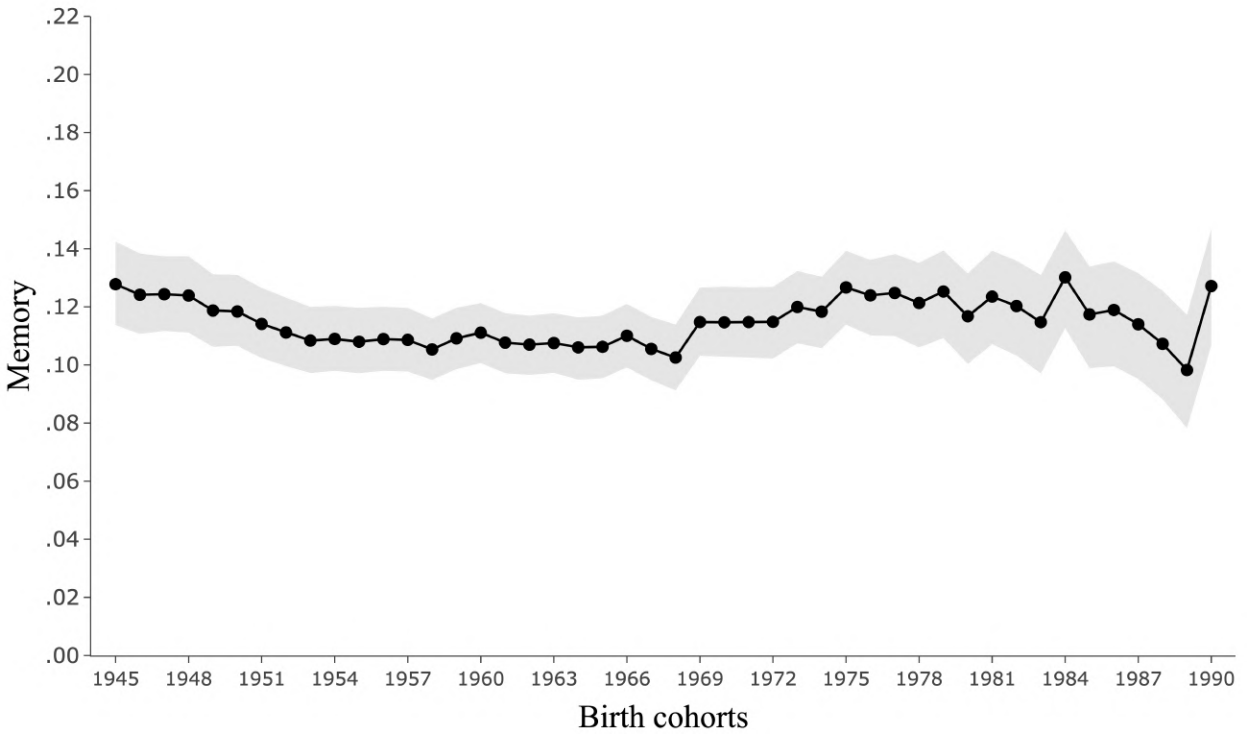
Notes: This figure plots the mean time to exit from each origin class (MTE_i), separately by cohort. Class 1 refers to higher-grade professionals, administrators, and managers; class 2 refers to lower-grade professionals, administrators, and managers; class 3 includes higher-grade routine non-manual workers, technicians, and supervisors; class 4 comprises higher-grade manual workers, lower-grade technicians, and farmers; and class 5 includes lower-grade routine non-manual and manual workers.

4.3 Intergenerational Memory

Figure 5 shows trends in aggregate intergenerational memory at generation $t = 1$. This measure captures the degree to which the observed transition matrix between fathers and children deviates from the limiting matrix of a stationary Markov chain. In the limit, each row of this matrix converges to the steady-state distribution of occupational classes, meaning that the destinations of descendants are completely independent of the founding generation's origins. Larger values therefore indicate greater distance from this benchmark of multi-generational "equality of opportunity."

As Figure 5 illustrates, aggregate intergenerational memory at generation $t = 1$ changed little across birth cohorts. For the 1945 cohort, the estimated AIM_1 is about .13. This metric then declines to .11 among cohorts born in the 1950s before rising slightly to just above .12 for more recent cohorts. These results suggest that the influence of class

Figure 5: Aggregate intergenerational memory at generation $t = 1$ (AIM_1)

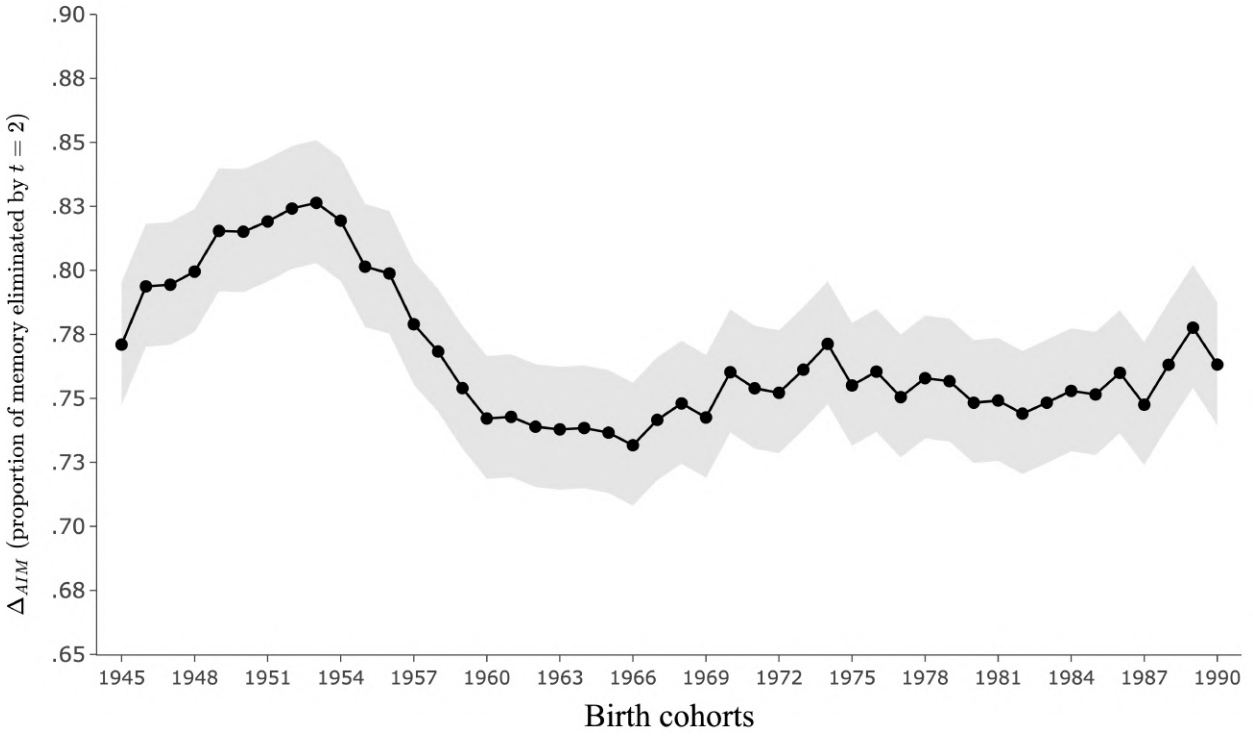


Notes: Shaded areas represent 95% confidence intervals.

origins across generations has persisted largely unchanged throughout the era of rising inequality. This stability mirrors the patterns we observed previously in our measures of overall and steady-state mobility.

In addition to measuring memory as distance, we also examine how quickly the influence of class origins dissipates across generations. As mentioned previously, the Markov chains converge to their steady state, at which point the influence of class origins has vanished entirely, within four generations for all cohorts—that is, $t^* \leq 4$. To characterize the pace of this convergence, Figure 6 reports Δ_{AIM}, which captures the proportion of memory eliminated by the second generation of the synthetic dynasties. In other words, the figure illustrates the rate at which memory decays over the first two generations of the dynasties. For all cohorts, more than 70% of memory is eliminated by generation $t = 2$, indicating a relatively rapid rate of decay throughout the period. This rate varies modestly across cohorts: memory loss hovers around 80% for cohorts born before 1955 and then declines to around 75% thereafter. Taken together, these results suggest that intergenerational memory—including its magnitude, persistence, and rate of decay—have

Figure 6: Rate of decay in aggregate intergenerational memory between generation $t = 1$ and $t = 2$



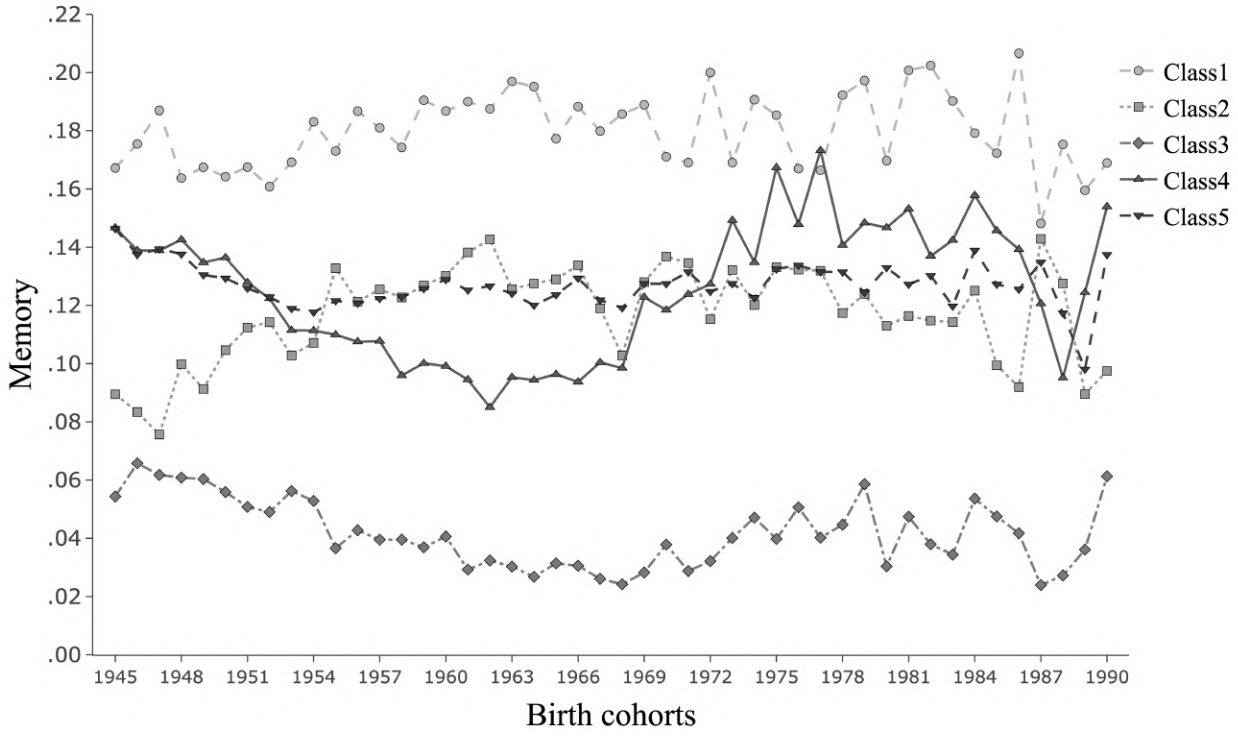
Notes: Shaded areas represent 95% confidence intervals.

remained largely stable during the era of rising inequality.

Figure 7 plots trends in intergenerational memory separately for each origin class. It displays only point estimates for visual clarity, but a version of this figure with 95% confidence intervals is provided in Appendix D. These measures highlight variation in how strongly different class origins shape the destinations of descendants across generations in synthetic dynasties. Higher values indicate that descendants from a given origin class are farther from the Markov steady-state and therefore take longer to converge toward equal opportunities.

The figure reveals nontrivial variation in memory across class origins. Class 1 (higher-grade professionals, administrators, and managers) consistently exhibits the highest level of memory, with point estimates suggesting a slight increase from about .17 among earlier cohorts to nearly .20 among more recent cohorts. Intergenerational memory for class 2 (lower-grade professionals, administrators, and managers) also appears to have increased, from below .10 for cohorts born in the 1940s to about .13 for those born since the 1960s.

Figure 7: Intergenerational memory at generation $t = 1$ by origin class ($IM_{i,1}$)



Notes: This figure plots intergenerational memory at generation $t = 1$, separately for each origin class ($IM_{i,1}$) and by cohort. Class 1 refers to higher-grade professionals, administrators, and managers; class 2 refers to lower-grade professionals, administrators, and managers; class 3 includes higher-grade routine non-manual workers, technicians, and supervisors; class 4 comprises higher-grade manual workers, lower-grade technicians, and farmers; and class 5 includes lower-grade routine non-manual and manual workers.

At the lower end of the class structure, memory has remained relatively stable for class 5 (lower-grade routine non-manual and manual workers). For class 4 (higher-grade manual workers, lower-grade technicians, and farmers), the estimates suggest a decline in memory among cohorts born through the 1960s, followed by an apparent upward shift among subsequent cohorts. Among several cohorts born since 1970, estimated memory for class 4 approaches the high levels observed at the top of the hierarchy for class 1. This pattern is consistent with a renewed influence of these origins on descendants' occupational destinations, although the trend should be interpreted cautiously given the imprecision of the underlying estimates, as shown in the Appendix.

By contrast, in the middle of the occupational hierarchy, class 3 (higher-grade routine non-manual workers, technicians, and supervisors) stands out for its consistently low level of memory across all cohorts. Moreover, our estimates suggest that the limited influence of these origins may have declined slightly over time.

Figure 8 plots measures of memory across generations, separately for the 1945 and 1990 birth cohorts, to illuminate change over time. At generation $t = 1$, the figure reproduces our estimates for these two cohorts shown earlier in Figures 5 and 7. For later generations ($t \geq 1$), it traces how memory decays as the synthetic dynasties unfold, converging to zero by generation $t = 4$, when the Markov chains reach their steady state. At this point, class origins in the founding generation of the dynasties no longer shape the class destinations of descendants. The rate at which memory declines to zero therefore captures how quickly the influence of class origins dissipates. Comparing this decay process across cohorts helps to describe how class mobility has changed over time.

Panels A and B of Figure 8 show that aggregate intergenerational memory decays in much the same way for both the 1945 and 1990 birth cohorts. In each case, it begins between .12 and .14 at generation $t = 1$, drops to about .04 by generation $t = 2$, and approaches zero thereafter. However, despite these aggregate similarities, Panels C and D suggest small shifts in the dissipation of memory for specific class origins. In particular, for the 1990 cohort, there are faint indications that memory associated with the professional, administrative, and managerial classes (classes 1 and 2) fades more slowly than for the 1945 cohort.

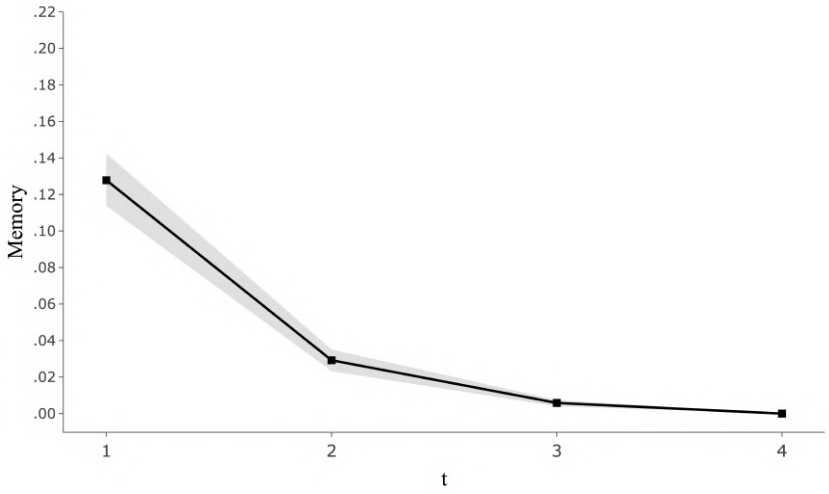
To summarize, intergenerational memory has remained mostly stable across cohorts who grew up or entered the labor market during the era of rising inequality. Beneath this aggregate stability, we uncover modest evidence that the influence of particular class origins may have shifted in offsetting ways. Over time, memory appears to increase at the top of the class structure, decrease in the middle, and either remain stable or rebound following a decline at the bottom, although these class-specific trends are estimated imprecisely and should therefore be interpreted cautiously.

4.4 Comparison with Traditional Measures of Association

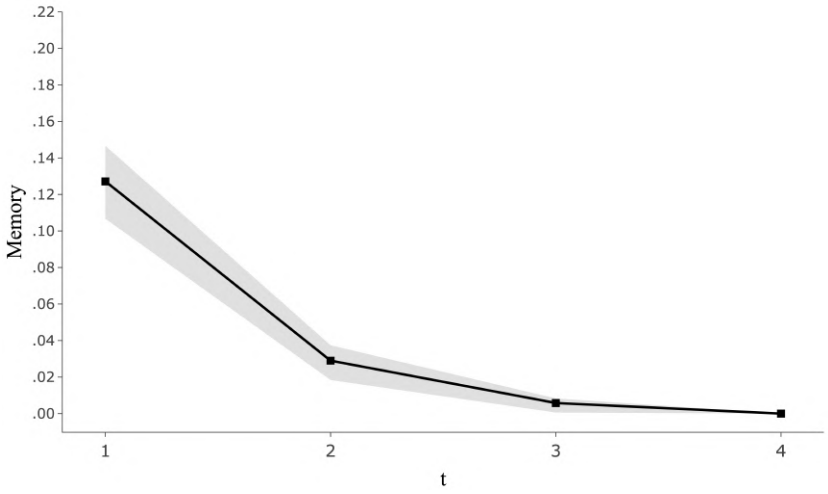
In this section, we compare results from our synthetic dynasty analysis, which conceptualized mobility as movement and memory, to more conventional measures that assess mobility as association. Whereas measures of movement capture departures from complete immobility, and measures of memory capture departures from multi-generational equality of opportunity, measures of association assess deviations from statistical independence between parental origins and child destinations. When child destinations are independent of parental origins, equality of opportunity holds not only for distal generations within synthetic dynasties but also in the immediate transition from parents to children. Thus, zero association implies zero memory. However, while higher levels

Figure 8: Memory across synthetic generations in the 1945 and 1990 birth cohorts

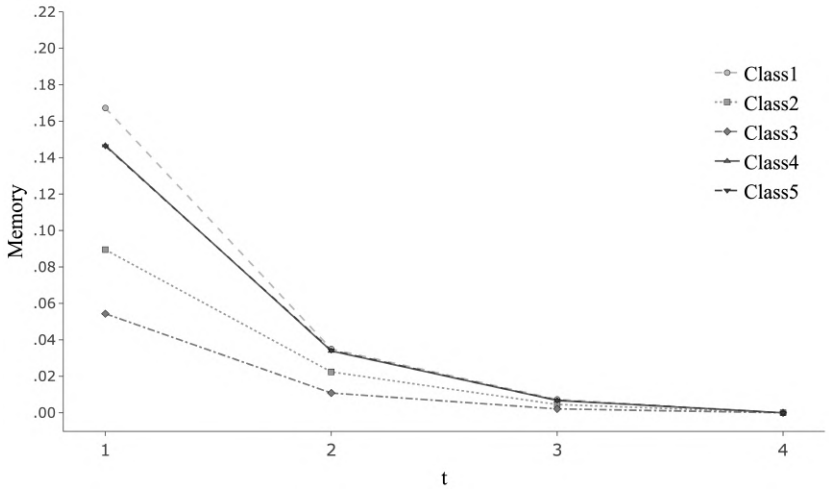
(A) AIM_t for the 1945 cohort



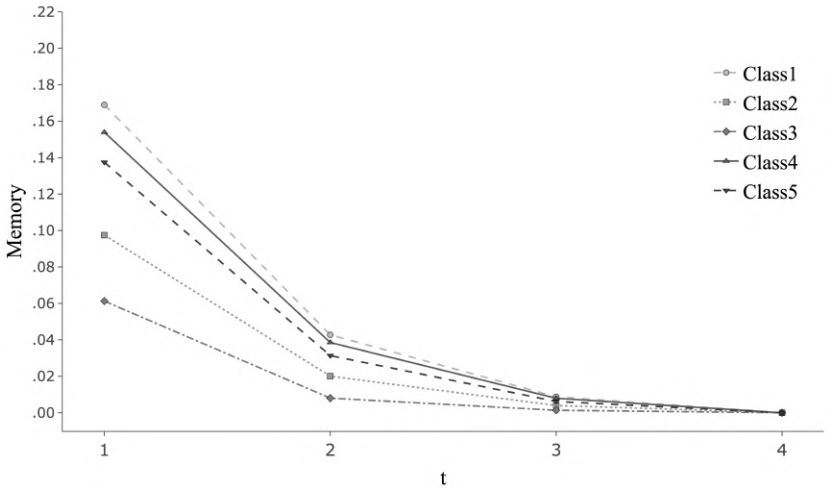
(B) AIM_t for the 1990 cohort



(C) $IM_{i,t}$ for the 1945 cohort



(D) $IM_{i,t}$ for the 1990 cohort



Notes: This figure illustrates the evolution of AIM_t and $IM_{i,t}$ across generations in a stationary Markov chain, separately for the 1945 and 1990 cohorts. By $t = 4$, both transition matrices have converged to the steady state, implying zero memory of class origins. Shaded areas represent 95% confidence intervals.

of association typically imply greater memory, nonzero measures of association alone do not directly indicate how far or how quickly dynasties converge to a state in which ancestral origins no longer predict the destinations of descendants.

Typically, measures of association aim to capture the strength of dependence between parental origins and child destinations while remaining insensitive to shifts in the marginal distribution of classes. To this end, a standard practice is to estimate a log-multiplicative layer effect model, in which the natural logarithms of odds ratios are given by functions of the model's coefficients. Formally, this model can be expressed as follows:

$$\log\left(n_{ijk}\right) = \tau + \tau_i + \tau_j + \tau_k + \tau_{ik} + \tau_{jk} + \theta_{ij}\phi_k + \epsilon_{ijk}, \tag{9}$$

where the parameters are normalized using baseline constraints but are otherwise unrestricted (Xie, 1992). With this specification, the θ_{ij} parameters capture the pattern of association between origins and destinations in a reference cohort, while the "layer effects" ϕ_k scale the magnitude of these associations up or down for each comparison cohort.

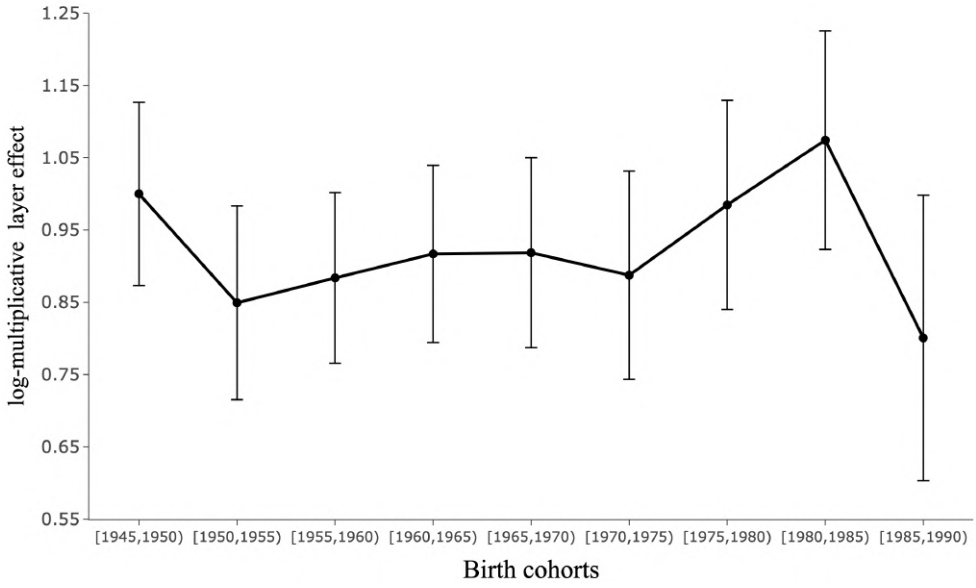
A distinctive feature of this model is that it cleanly distinguishes changes in class composition from changes in intergenerational associations. Variation in the marginal distribution of origins and destinations is absorbed by the τ parameters, which account for shifts in class size across cohorts. The θ_{ij} parameters, then, encode the dependence structure between origins and destinations, while the ϕ_k parameters capture whether the strength of these associations is rising or falling. Functions of θ_{ij} and ϕ_k yield the odds ratios that summarize how destinations depend on origins in each cohort k.

Figure 9 plots a series of estimated layer effects across cohorts. To improve the precision of these estimates, we fit the model in Equation 9 after grouping cohorts into 5-year or approximately 10-year bins. The results suggest that the strength of the origin-destination associations has remained fairly stable over time. For example, we estimate that the origin-destination associations for cohorts born after 1975 are only about 5% stronger than for cohorts born earlier. These differences are small, and they all lie well within the margin of sampling error. In general, any changes are difficult to detect in this analysis because the estimated layer effects are quite imprecise even after binning cohorts, with confidence intervals consistently spanning a wide range of values.

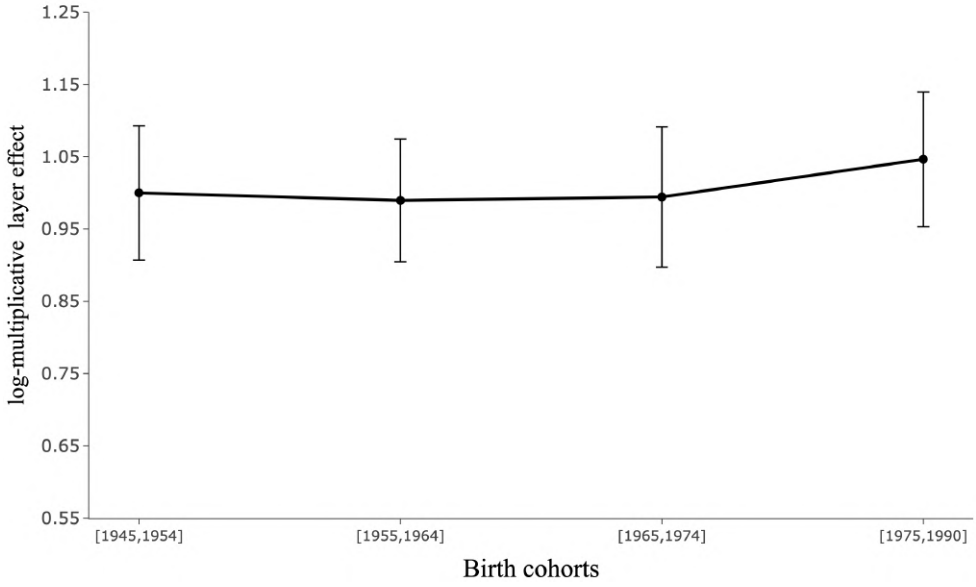
To summarize, our analysis of mobility as association, using log-multiplicative models, provides little evidence of an upward or downward trend. These findings are consistent with results from our analysis based on Markov chains, which capture mobility in terms of movement and memory. Each approach highlights a different aspect of class mobility and brings distinct advantages. Log-linear and log-multiplicative models iso-

Figure 9: Log-multiplicative layer effects

(A) Cohorts in 5-year bins



(B) Cohorts in ∼10-year bins



Notes: This figure plots the log-multiplicative layer effect across birth cohorts using 5-year and ∼10-year bins, respectively. The vertical bars represent 95% confidence intervals.

late the strength of origin-destination associations net of differences in class composition. Markov chains, by contrast, trace intergenerational transitions and the persistent influence of class origins across generations within synthetic dynasties. They also avoid functional form assumptions and generate measures that can be easily disaggregated to reveal class-specific dynamics. Taken together, these complementary approaches indicate that class mobility—whether conceptualized and measured as movement and memory in Markov chains or as association in parametric models—has remained largely unchanged throughout the era of rising inequality.

4.5 Robustness Analyses

To assess the robustness of our findings, we conducted a series of ancillary analyses examining the sensitivity of our conclusions to alternative data sources, measures, analytic samples, and smoothing techniques.

Appendix E presents trends in mobility based on several different measures of movement, memory, and association. For movement, we additionally consider class outflows—both in the observed transition matrix and in the steady state of a Markov chain—as well as mean first passage time, a measure that characterizes transitions between specific pairs of classes across generations within synthetic dynasties. For memory, we also compute the maximum distance to the stationary distribution and the second-largest eigenvalue of the transition matrix, which reflects how fast a Markov chain converges to its steady state (Levin et al., 2009; Sommers and Conlisk, 1979). Finally, for association, we examine the Altham index (Altham, 1970), which measures the extent to which the observed odds ratios in a mobility table depart from independence, and the Hellinger index, which is based on a discrete copula (Coleman and Lukina, 2025; Geenens and Lafaye de Micheaux, 2022). Across all these approaches, the results are broadly consistent: they indicate that each dimension of mobility has mostly remained stable.

To examine potential heterogeneity by gender, we estimated mobility trends separately for father-son, father-daughter, mother-son, and mother-daughter pairs, as well as for pooled mother-child pairs. These results are reported in Appendix F. Because the GSS only began collecting information on maternal occupations in 1994, analyses using these data cover fewer cohorts and rely on smaller samples, resulting in less precise estimates. Although *levels* of occupational mobility differ by gender, the *trends* are broadly similar: movement and memory remain stable across cohorts, with little consistent evidence of either upward or downward change. To further assess the role of maternal origins, we also conducted a parallel analysis of educational mobility using a five-category measure

of educational attainment, which affords a much larger sample and a longer series of cohorts. In analyses of educational transitions through maternal lineages, steady-state mobility again remains broadly stable, while memory declines sharply across cohorts. Taken together, these analyses provide little evidence that mobility has declined when maternal origins are incorporated and, in some cases, suggest movement away from greater persistence across generations.

This pattern appears to contrast with Beller (2009), who finds that incorporating mothers' class positions reveals an upturn in the importance of family background for men's mobility. The two sets of findings are not necessarily contradictory, however, because our analysis examines movement and memory within gender-specific lineages, whereas Beller (2009) measures intergenerational association using models that jointly incorporate both parents' class positions and other aspects of family structure. The joint influence of parental background could strengthen through changes in how mothers' and fathers' resources are correlated, combined, or invested within families, even if movement and persistence along either parent-child lineage remains unchanged. Although distinguishing between these processes lies beyond the scope of the present analysis, it will be an important task for future research on how the role of family origins has changed over time.

Our sample is not large enough to estimate trends separately for each racial group in the GSS, but we conducted a parallel analysis that excludes non-White respondents in an effort to explore potential heterogeneity by race. These results, reported in Appendix G, are nearly identical to those based on the full analytic sample discussed previously.

In addition to smoothing our data with penalized splines, we evaluated several other strategies for addressing sparsity and improving precision. Specifically, we replicated our analysis of movement and memory in synthetic dynasties using transition matrices constructed by binning cohorts into 5-year and 10-year intervals. For reference, we also computed estimates from the raw transition matrices for individual birth cohorts, without any smoothing. These results are presented in Appendix H. As expected, the raw transition matrices introduce considerable sampling variability, but the point estimates exhibit broadly similar patterns—despite fluctuating much more from cohort to cohort, they still show no discernible trend. Binning cohorts substantially reduces sampling variability and produces trend estimates for all our measures that align with those based on smoothing splines, albeit at a coarser temporal resolution.

We also examined whether our conclusions extend beyond occupational mobility to income mobility, as rising income inequality may have altered mobility across income classes even if occupational mobility remained stable. Because the GSS does not mea-

sure parental income, this analysis requires a different data source. In Appendix I, we replicate our analysis using the 1979 and 1997 National Longitudinal Surveys of Youth (NLSY; Bureau of Labor Statistics 2025; 2026), defining class positions based on family income. Across the cohorts represented in these surveys–children born between 1961–1964 in the NLSY79 and 1980–1984 in the NLSY97—aggregate intergenerational memory and steady-state mobility of income also show no appreciable signs of change. As a further benchmark, we also computed estimates of occupational mobility from the NLSY, which closely track the corresponding patterns observed in the GSS for the same cohorts.

Finally, we investigated the sensitivity of our inferences to sparsity. Although smoothing reduces random variation in the observed tables, it cannot fully address the uncertainty associated with small underlying cell counts. Sparsity in our analytic sample reflects two related processes. First, some origin-destination transitions are rare because of the occupational structure and its evolution across cohorts (e.g., as farming has declined, very few children with professional parents enter that occupation). Second, recent cohorts are represented by smaller samples, making these uncommon transitions more likely to be observed only a few times, or not at all. To assess the influence of these sparse cells on our results, Appendix K reports a perturbation analysis in which all cells in our mobility tables containing five or fewer observations are perturbed under two mechanisms: redistribution, which alters transition probabilities while holding the margins fixed, and augmentation, which allows both the margins and transition probabilities to change. Recomputing all trends shows that any perturbation-induced changes remain within the bootstrap confidence intervals reported previously and that none of the aggregate trends is significantly altered.

This robustness to sparsity contrasts with measures based on odds ratios, in which zero or small cells enter directly into local cross-product ratios and can therefore produce extreme or even undefined estimates. In comparison, our Markov-based measures incorporate sparse cells through the full system of transition probabilities, where a cell's influence depends on its dynamic leverage within the broader pattern of inflows, outflows, and retention. Consequently, sparse cells do not mechanically generate extreme values. Rather, they become problematic primarily when structural zeros render the transition matrix non-primitive and preclude a unique steady state.

5 Discussion

This study examined whether patterns of class mobility shifted during an era of rising inequality in the U.S. Focusing on Americans born between 1945 and 1990, we tracked

trends among cohorts who grew up or entered the labor market after inequality began to increase in the 1970s. To evaluate competing theoretical perspectives that predict different trends over this period, we adopted a nonparametric approach that constructs synthetic dynasties with Markov chains. This approach simulates the long-run trajectories of hypothetical family lines based on observed cross-sectional links between parents and their children. From these simulations, we analyzed novel measures of mobility that variously capture the amount of movement between classes and the persistent influence of class origins across generations.

Our analysis provides little evidence that mobility declined across cohorts born between 1945 and 1990. Overall mobility, which captures the amount of movement across classes from one generation to the next, was largely stable. This stability was evident both in the observed transitions between parents and their children and among synthetic generations in the Markov steady state, where movements no longer reflect changes in the marginal distribution of classes. Intergenerational memory, which captures how class origins influence the destinations of descendants within synthetic dynasties, also changed little throughout the era of rising inequality. These trends in movement and memory align with more traditional measures of mobility conceptualized as association, and they appear robust to alternative sample definitions, class typologies, and measurement strategies.

Despite this overall stability, trends in movement and memory varied by class origin. Among the upper and lower classes, we found declining movement and increasing memory across cohorts. In contrast, among the middle classes, we observed increases in movement and declines in memory. While these patterns suggest a potential decline in mobility at the top and bottom of the class structure, and an increase in the middle, the changes we document are small and noisy, and thus should be interpreted with caution. Nevertheless, there is at least some evidence that the flat trends in our summary measures may reflect offsetting dynamics among different classes.

These findings challenge several established theories of social mobility in different ways. First, they do not align with modernization theory (Lipset and Bendix, 1959; Featherman and Hauser, 1978), which predicts a steady increase in mobility as societies grow economically, develop technologically, and expand access to education. Second, our results provide only limited support for the contemporary view that rising inequality will reduce mobility (Andrews and Leigh, 2009; Durlauf and Seshadri, 2017; Mitnik et al., 2016). Although we observe some faint indications of declining mobility and increasing persistence at the poles of the class hierarchy, these changes are small and subject to considerable sampling uncertainty, while our aggregate measures are flat and

precisely estimated. Overall, then, our results are most consistent with the FJH hypothesis (Featherman et al., 1975), which predicts that the relationship between class origins and destinations should remain relatively stable over time. Even here, however, our findings are only partly consistent, as we observe stability in aggregate measures of movement, memory, and association that may reflect shifts in the underlying pattern of mobility across different class origins. Thus, all three perspectives warrant at least some reconsideration, as none fully align with the trends we observe during the contemporary period of rising inequality in the U.S.

What are the social and political implications of rising inequality alongside relatively stable levels of class mobility? When the pecuniary rewards attached to different classes of occupations become increasingly unequal (Weeden et al., 2007; Zhou and Wodtke, 2019), but the chances of moving across classes remain largely unchanged, public concerns about growing inequality may be tempered and support for redistribution blunted (Alesina et al., 2018; Manza and Brooks, 2020). At the same time, stable mobility in a context of rising inequality may amplify the significance of "mobility effects," which refer to the social and psychological consequences of moving up or down the class hierarchy (Sorokin, 1927; Wei and Xie, 2025). Upward mobility may feel especially rewarding, while downward mobility carries steeper penalties. As a result, when mobility is still prevalent but its stakes are higher, the divergent experiences of upward or downward movement could deepen social and political divisions.

Beyond its empirical and theoretical contributions, our study also introduced novel methods for analyzing class mobility using Markov chains. This approach conceptualizes mobility as patterns of movement and memory across generations of synthetic dynasties, highlighting aspects of the mobility process that may not be apparent from measures of association between parental origins and child destinations alone. In this way, it provides a valuable complement to established methods, such as log-linear models or other measures based on odds ratios. A key feature of our approach is that it requires no parametric assumptions, which may distort analyses of trends when violated. Markov chains and synthetic dynasty analyses therefore hold the potential for wide application in the social sciences, wherever there is interest in examining additional dimensions of the mobility process beyond origin-destination associations without restrictive modeling assumptions.

These contributions must, of course, be weighed against several limitations of our study. First, we are unable to provide precise estimates of trends separately by race or geographic region owing to small samples for certain subgroups. This is a nontrivial constraint, as patterns of mobility could have evolved quite differently across demographic

subpopulations during the era of rising inequality (e.g., Chetty et al. 2024; Durlauf et al. 2024).

Second, our analyses focused mainly on aggregate occupational classes. Although aggregate typologies provide a useful summary of an individual's location within a complex, multidimensional system of social stratification (Wodtke, 2017; Zhou and Wodtke, 2019), they inevitably obscure some features of the mobility process that are better captured by more detailed occupational categories or "microclasses" (Weeden and Grusky, 2005). In principle, Markov chains and synthetic dynasty measures can be constructed from transition matrices based on either aggregate or disaggregate class typologies. In practice, however, the GSS sample is too small for trend analyses of microclass mobility, as it produces extremely sparse tables at the level of detailed occupations that preclude reliable estimation.

Another limitation is that small sample sizes and the potential for life-cycle bias make it difficult to confidently analyze a longer series of cohorts. Expanding the analysis to include both younger and older cohorts introduces two problems: greater sparsity and systematic age differences in when members of these cohorts are observed. Older cohorts born before 1945 are disproportionately interviewed by the GSS later in their careers, when occupational attainment is at its peak and non-random selection out of the labor force is common. In contrast, younger cohorts born after 1990 are disproportionately observed when their careers are just beginning and many remain in school. These differences amplify the risk that apparent trends are actually artifacts of selection or life-cycle bias rather than genuine changes in mobility across cohorts.

Nevertheless, extending our series of cohort estimates backward suggests a noteworthy pattern. As shown in Appendix J, cohorts born before 1945 exhibit noisy but suggestive evidence of rising mobility—characterized by pronounced increases in movement and declines in memory and association. These trends level off around the time our focal series of cohorts begins, indicating that the stable pattern we observe from 1945 onward may not represent continuity with the past but rather a break with a previous trajectory of increasing mobility. One possible explanation is that the mechanisms highlighted by modernization theory, such as technological change and educational expansion, continued to promote mobility, while mechanisms emphasized by the inequality perspective, such as polarized investments in children and deepening segregation, began to suppress it, potentially offsetting one another. This interpretation is admittedly speculative, however, both because estimating reliable trends for distal cohorts is challenging in the GSS and because our study does not directly examine the mechanisms thought to underlie these trends.

The limitations of our study point toward promising directions for future research. Directly analyzing the influence of educational expansion versus polarized investments in children on movement and memory will be essential. This could be achieved by integrating our synthetic dynasty approach with inverse probability weighting to construct counterfactual trends in mobility under hypothetical scenarios where, for example, parental spending on children remains constant over time within each origin class. These empirical and methodological extensions would help disentangle the potentially opposing forces shaping trends in mobility over the past several decades.

In conclusion, the era of rising inequality in the U.S. has not been marked by a decline in class mobility, but the subtle changes we do observe warrant ongoing attention. The full impact of heightened inequality may still be unfolding, especially for cohorts entering the labor market today. These individuals spent their entire childhood in a highly unequal society and are now beginning careers amid technological and political changes that could transform labor demand and exacerbate inequality even further (Manning, 2024; Rockall et al., 2025). Although class mobility appears to have remained mostly stable thus far, continued scrutiny of signals suggesting a decline in equality of opportunity will remain essential as the economy and social policy continue to evolve.

Notes

1. As we illustrate below, our mobility measures are less sensitive to sparsity than measures based on odds ratios. Zero transition cells do not render our measures undefined, and a sparse-cell perturbation analysis demonstrates their considerable stability in Appendix K.

2. What we call exchange mobility has also been termed "circulation mobility" in earlier work (e.g., Featherman and Hauser 1978; Jones 1985). Sobel et al. (1985) use the terms structural and exchange mobility differently, defining them through a quasi-symmetry model in which exchange mobility consists of reciprocated flows between pairs of classes while structural mobility reflects marginal heterogeneity operating uniformly across origins. Our decomposition instead follows directly from the marginal distributions across generations: structural mobility is the minimum amount of movement required to transform one marginal distribution into the other, and exchange mobility is the remaining movement. Thus, exchange mobility in our formulation need not involve reciprocated flows within class pairs.

3. Formally, these limiting properties require that P is primitive, meaning that there exists a positive integer v such that P^v is strictly positive.

4. The observed parental margins are retrospective rather than a cross-sectional distribution of all adults in the parental generation. Because fathers enter the data through their sampled adult children who then report their occupations, μ_p is descendant-weighted, and thus it partly reflects differential fertility, survival, and family structure (Duncan 1966; Song and Mare 2015). Earlier demographic models sometimes explicitly incorporated differential fertility alongside occupational mobility to examine changes in occupational distributions (Matras 1961, 1967). Our synthetic dynasties, by contrast, merely summarize the observed father–child transitions without separately modeling fertility, mortality, or marriage, so their steady state should not be interpreted as a demographic projection for the actual population.

5. That is, we assume the class hierarchy begins with (1) higher-grade professionals, administrators, and managers at the top, followed by (2) lower-grade professionals, administrators, and managers, (3) higher-grade routine non-manual workers, technicians, and supervisors, (4) higher-grade manual workers, lower-grade technicians, and farmers, and lastly, (5) lower-grade routine non-manual and manual workers, who compose the lowest-ranked class.

Acknowledgments

This research was supported by the James M. and Cathleen D. Stone Foundation. We thank Michael Sobel, Xiang Zhou, Siwei Cheng, Tom Coleman, and participants in the Inequality Working Group and the Demography Workshop at the University of Chicago for helpful feedback and discussions. We used chatGPT for assistance with coding our statistical analyses and copyediting the manuscript. Responsibility for all content rests solely with the authors.

References

Aaronson, D. and Mazumder, B. (2008). Intergenerational Economic Mobility in the United States, 1940 to 2000. *Journal of Human Resources*, 43(1):139–172.

Alesina, A., Stantcheva, S., and Teso, E. (2018). Intergenerational Mobility and Preferences for Redistribution. *American Economic Review*, 108(2):521–554.

Altham, P. (1970). The Measurement of Association of Rows and Columns for an r×s Contingency Table. *Journal of the Royal Statistical Society: Series B (Statistical Methodology)*, 32(1):63–73.

Andrews, D. and Leigh, A. (2009). More Inequality, Less Social Mobility. *Applied Economics Letters*, 16(15):1489–1492.

Bailey, M. J. and Dynarski, S. M. (2011). Inequality in Postsecondary Education. In Duncan, G. J. and Murnane, R. J., editors, *Whither Opportunity? Rising Inequality, Schools, and Children's Life Chances*. Russell Sage Foundation, New York, NY.

Bartholomew, D. J. (1967). *Stochastic Models for Social Processes*. Wiley Series in Probability and Statistics. Wiley, New York.

Bell, D. (1976). *The Coming of Post-Industrial Society*. Basic Books, New York.

Beller, E. (2009). Bringing Intergenerational Social Mobility Research into the Twenty-first Century: Why Mothers Matter. *American Sociological Review*, 74(4):507–528.

Beller, E. and Hout, M. (2006). Intergenerational Social Mobility: The United States in Comparative Perspective. *The Future of Children*, 16(2):19–36.

Bhatia, R. (1997). *Matrix Analysis*. Graduate texts in mathematics. Springer, New York.

Blanden, J. (2013). Cross-Country Rankings in Intergenerational Mobility. *Journal of Economic Surveys*, 27:38–73.

Blau, P. M. and Duncan, O. D. (1967). *The American Occupational Structure*. Wiley, New York.

Bloome, D. (2015). Income Inequality and Intergenerational Income Mobility in the United States. *Social Forces*, 93(3):1047–1080.

Bloome, D. and Dyer, Shauna Zhou, X. (2018). Educational Inequality, EducatioExpansion, and Intergenerational Income Persistence in the United States. *American Sociological Review*, 83(6):1215–1253.

Blume, L., Cholli, N., Durlauf, S., and Lukina, A. (2025). Immobility as Memory: Some New Approaches to Characterizing Intergenerational Persistence via Markov Chains. *Sociological Methods & Research*, 54(4):1396–1434.

Boudon, R. (1973). *Mathematical Structures of Social Mobility*, volume 2. The Josey Bass, San Francisco, California.

Breen, R. (2004). *Social Mobility in Europe*. Oxford University Press, Oxford.

Breen, R. (2010). Educational Expansion and Social Mobility in the 20th Century. *Social Forces*, 89(2):365–388.

Breen, R. and Müller, W. (2020). *Education and Intergenerational Social Mobility in Europe and the United States*. Stanford University Press, Stanford.

Bucca, M. and Urbina, D. R. (2021). Lasso Regularization for Selection of Log-linear Models: An Application to Educational Assortative Mating. *Sociological Methods & Research*, 50(4):1763–1800.

Bukodi, E. and Goldthorpe, J. H. (2018). Social Inequality and Social Mobility: Is There an Inverse Relation? *SocArXiv*, 10:31235.

Bureau of Labor Statistics, U.S. Department of Labor (2025). National longitudinal survey of youth 1979 cohort, 1979–2022 (rounds 1–30). Produced and distributed by the Center for Human Resource Research (CHRR), The Ohio State University.

Bureau of Labor Statistics, U.S. Department of Labor (2026). National longitudinal survey of youth 1997 cohort, 1997–2023 (rounds 1–21). Produced and distributed by the Center for Human Resource Research (CHRR), The Ohio State University.

Butaeva, K., Chen, L., Durlauf, S., and Park, A. (2025). A Tale of Two Transitions: Mobility Dynamics in China and Russia after Central Planning. Working Paper 34124, National Bureau of Economic Research.

Bénabou, R. (1996). Heterogeneity, Stratification, and Growth: Macroeconomic Implications of Community Structure and School Finance. *The American Economic Review*, 86(3):584–609.

Chetty, R., Dobbie, W. S., Goldman, B., Porter, S., and Yang, C. (2024). Changing Opportunity: Sociological Mechanisms Underlying Growing Class Gaps and Shrinking Race Gaps in Economic Mobility. Working Paper 32697, National Bureau of Economic Research.

Chetty, R., Grusky, D., Hell, M., Hendren, N., Manduca, R., and Narang, J. (2017). The Fading American Dream: Trends in Absolute Income Mobility Since 1940. *Science*, 356(6336):398–406.

Chetty, R., Hendren, N., and Katz, L. F. (2016). The Effects of Exposure to Better Neighborhoods on Children: New Evidence from the Moving to Opportunity Project. *American Economic Review*, 106(4):855–902.

Chetty, R., Hendren, N., Kline, P., Saez, E., and Turner, N. (2014). Is the United States Still a Land of Opportunity? Recent Trends in Intergenerational Mobility. *American Economic Review*, 104(5):141–147.

Coleman, T. and Lukina, A. (2025). Discrete Copulas and Rank Correlation: New Measures for Assortative Matching. *University of Chicago Stone Center Working Paper Series*, 25-11.

Conlisk, J. and Sommers, P. (1979). Eigenvector Status Proxies in Markov Chain Mobility Models. *Sociological Methods & Research*, 8(2):159–178.

Connelly, R., Gayle, V., and Lambert, P. S. (2016). A Review of Occupation-based Social Classifications for Social Survey Research. *Methodological Innovations*, 9:2059799116638003.

Corak, M. (2006). Do Poor Children Become Poor Adults? Lessons for Public Policy from a Cross Country Comparison of Generational Earnings Mobility. In Creedy, J. and Kalb, G., editors, *Dynamics of Inequality and Poverty*, volume 13 of *Research on Economic Inequality*. Elsevier, Amsterdam.

Corak, M. (2013). Income Inequality, Equality of Opportunity, and Intergenerational Mobility. *Journal of Economic Perspectives*, 27(3):79–102.

Dardanoni, V. (1993). Measuring Social Mobility. *Journal of Economic Theory*, 61(2):372–394.

Davern, M., Bautista, R., Freese, J., Herd, P., and Morgan, S. L. (2025). General Social Survey 1972-2024 [Machine-readable data file]. Data accessed at https://gssdataexplorer.norc.org.

Davis, J. M. and Mazumder, B. (2024). The Decline in Intergenerational Mobility after 1980. *Review of Economics and Statistics*, 108(1):1–15.

Davison, A. C. and Hinkley, D. V. (1997). *Bootstrap Methods and Their Application*. University Press, Cambridge.

DeParle, J. (2012). Harder for Americans to Rise from Lower Rungs. *The New York Times*. Available from http://www.nytimes.com/2012/01/05/us/harder-for-americans-to-rise-from-lower-rungs.html.

DiPrete, T. A. (2020). The Impact of Inequality on Intergenerational Mobility. *Annual Review of Sociology*, 46(1):379–398.

Duncan, O. D. (1966). Methodological issues in the analysis of social mobility. In Smelser, N. J. and Lipset, S. M., editors, *Social Structure and Mobility in Economic Development*, chapter 2, pages 51–97. Aldine, Chicago.

Durlauf, S. N. (1996). A Theory of Persistent Income Inequality. *Journal of Economic Growth*, 1(1):75–93.

Durlauf, S. N., Kim, G., Lee, D., and Song, X. (2024). The Evolution of Black-White Differences in Occupational Mobility Across Post-Civil War America. Working Paper 32370, National Bureau of Economic Research.

Durlauf, S. N., Kourtellos, A., and Tan, C. M. (2022). The Great Gatsby Curve. *Annual Review of Economics*, 14(1):571–605.

Durlauf, S. N. and Seshadri, A. (2017). Understanding the Great Gatsby Curve. In *NBER Macroeconomics Annual 2017*, volume 32, pages 333–393. University of Chicago Press.

Erikson, R. and Goldthorpe, J. H. (1992). *The Constant Flux: A Study of Class Mobility in Industrial Societies*. Clarendon Press, Oxford.

Erikson, R. and Goldthorpe, J. H. (2010). Has Social Mobility in Britain Decreased? Reconciling Divergent Findings on Income and Class Mobility. *The British Journal of Sociology*, 61(2):211–230.

Erikson, R., Goldthorpe, J. H., and Portocarero, L. (1979). Intergenerational Class Mobility in Three Western European Societies: England, France and Sweden. *The British Journal of Sociology*, 30(4):415–441.

Featherman, D. L. and Hauser, R. M. (1978). *Opportunity and Change*. Academic Press, New York.

Featherman, D. L., Jones, F. L., and Hauser, R. M. (1975). Assumptions of Social Mobility Research in the US: The Case of Occupational Status. *Social Science Research*, 4(4):329–360.

Fiel, J. E. (2020). Great Equalizer or Great Selector? Reconsidering Education as a Moderator of Intergenerational Transmissions. *Sociology of Education*, 93(4):353–371.

Fogli, A., Guerrieri, V., Ponder, M., and Prato, M. (2025). The End of the American Dream? Inequality and Segregation in US Cities. *Journal of Political Economy*. Forthcoming.

Geenens, G. and Lafaye de Micheaux, P. (2022). The Hellinger Correlation. *Journal of the American Statistical Association*, 117(538):639–653.

Gray-Lobe, G., Pathak, P. A., and Walters, C. R. (2022). The Long-Term Effects of Universal Preschool in Boston. *The Quarterly Journal of Economics*, 138(1):363–411.

Grinstead, C. M. and Snell, J. L. (1997). *Introduction to Probability*. American Mathematical Society, Providence, RI.

Grusky, D. B. and Hauser, R. M. (1984). Comparative Social Mobility Revisited: Models of Convergence and Divergence in 16 Countries. *American Sociological Review*, 49(1):19–38.

Haldane, A. (2025). Governments are Chasing the Wrong Rainbows. *Financial Times*. Available from https://www.ft.com/content/50e79018-83ac-4cf0-8747-237a8696baa6?utm_source=chatgpt.com.

Hassler, J., Rodríguez Mora, J. V., and Zeira, J. (2007). Inequality and Mobility. *Journal of Economic Growth*, 12(3):235–259.

Hauser, R. M., Koffel, J. N., Travis, H. P., and Dickinson, P. J. (1975). Temporal Change in Occupational Mobility: Evidence for Men in the United States. *American Sociological Review*, 40(3):279–297.

Heckman, J. J., Moon, S. H., Pinto, R., Savelyev, P. A., and Yavitz, A. (2010). The Rate of Return to the HighScope Perry Preschool Program. *Journal of Public Economics*, 94(1):114–128.

Hertel, F. R. and Groh-Samberg, O. (2019). The Relation between Inequality and Intergenerational Class Mobility in 39 Countries. *American Sociological Review*, 84(6):1099–1133.

Hout, M. (1988). More Universalism, Less Structural Mobility: The American Occupational Structure in the 1980s. *American Journal of Sociology*, 93(6):1358–1400.

Hunter, J. J. (2005). Stationary distributions and mean first passage times of perturbed Markov chains. *Linear Algebra and its Applications*, 410:217–243.

Johnson, R. C. and Jackson, C. K. (2019). Reducing Inequality through Dynamic Complementarity: Evidence from Head Start and Public School Spending. *American Economic Journal: Economic Policy*, 11(4):310–49.

Jones, F. L. (1985). Structural and Circulation Mobility are Alive and Well. *Sociology*, 19(1):139–142.

Kemeny, J. and Snell, J. (1976). *Finite Markov Chains*, volume 26 of *Undergraduate Texts in Mathematics*. Springer-Verlag, New York.

Killewald, A., Pfeffer, F. T., and Schachner, J. N. (2017). Wealth Inequality and Accumulation. *Annual Review of Sociology*, 43:379–404.

Kornrich, S. and Furstenberg, F. (2013). Investing in Children: Changes in Parental Spending on Children, 1972–2007. *Demography*, 50(1):1–23.

Krueger, A. (2012). The Rise and Consequences of Inequality. *Presentation made to the Center for American Progress, January 12th*.

Lee, C.-I. and Solon, G. (2009). Trends in Intergenerational Income Mobility. *The Review of Economics and Statistics*, 91(4):766–772.

Levin, D. A., Peres, Y., and Wilmer, E. L. (2009). *Markov Chains and Mixing Times*. American Mathematical Society, Providence, RI.

Lipset, S. M. and Bendix, R. (1959). *Social Mobility in Industrial Society*. University of California Press, Berkeley.

Logan, J. R., Foster, A., Xu, H., and Zhang, W. (2020). Income Segregation: Up or Down, and for Whom? *Demography*, 57(5):1951–1974.

Lucas, S. R. (2001). Effectively Maintained Inequality: Education Transitions, Track Mobility, and Social Background Effects. *American Journal of Sociology*, 106(6):1642–1690.

Manning, S. (2024). AI's Impact on Income Inequality in the US: Interpreting Recent Evidence and Looking to the Future. *Brookings*. Available from https://www.brookings.edu/articles/ais-impact-on-income-inequality-in-the-us/.

Manza, J. and Brooks, C. (2020). Mobility Optimism in an Age of Rising Inequality. *The Sociological Quarterly*, 62(2):343–368.

Mare, R. D. (2011). A Multigenerational View of Inequality. *Demography*, 48(1):1–23.

Marx, K. and Engels, F. (1942). *Karl Marx and Frederick Engels: Selected Correspondence*. International Publishers, New York.

Matras, J. (1961). Differential Fertility, Intergenerational Occupational Mobility, and Change in the Occupational Distribution: Some Elementary Interrelationships. *Population Studies*, 15(2):187–197.

Matras, J. (1967). Social mobility and social structure: Some insights from the linear model. *American Sociological Review*, 32(4):608–614.

McClendon, M. J. (1977). Structural and Exchange Components of Vertical Mobility. *American Sociological Review*, 42(1):56–74.

Meyer, C. D. (2000). *Matrix Analysis and Applied Linear Algebra*. Society for Industrial and Applied Mathematics (SIAM), Philadelphia.

Mitnik, P. A., Cumberworth, E., and Grusky, D. B. (2016). Social Mobility in a High-inequality Regime. *The ANNALS of the American Academy of Political and Social Science*, 663(1):140–184.

Morgan, S. L. (2017). A Coding of Social Class for the General Social Survey. GSS Methodological Report 125, NORC at the University of Chicago, Chicago, IL.

Morris, M. and Western, B. (1999). Inequality in Earnings at the Close of the Twentieth Century. *Annual Review of Sociology*, 25:623–657.

Mouw, T. and Kalleberg, A. L. (2010). Occupations and the Structure of Wage Inequality in the United States, 1980s to 2000s. *American Sociological Review*, 75(3):402–431.

Nybom, M. and Stuhler, J. (2016). Heterogeneous Income Profiles and Lifecycle Bias in Intergenerational Mobility Estimation. *Journal of Human Resources*, 51(1):239–268.

Owens, A., Reardon, S. F., and Jencks, C. (2016). Income Segregation Between Schools and School Districts. *American Educational Research Journal*, 53(4):1159–1197.

Pfeffer, F. T. and Hertel, F. R. (2015). How has Educational Expansion Shaped Social Mobility Trends in the United States? *Social Forces*, 94(1):143–180.

Piketty, T. and Saez, E. (2003). Income Inequality in the United States, 1913–1998. *The Quarterly Journal of Economics*, 118(1):1–41.

Prais, S. J. (1955). Measuring Social Mobility. *Journal of the Royal Statistical Society. Series A (General)*, 118(1):56–66.

Putnam, R. D. (2015). *Our Kids: The American Dream in Crisis*. Simon & Schuster, New York, NY.

Raftery, A. E. and Hout, M. (1993). Maximally Maintained Inequality: Expansion, Reform, and Opportunity in Irish Education. *Sociology of Education*, 66(1):41–62.

Rockall, E., Mendes Tavares, M., and Pizzinelli, C. (2025). AI Adoption and Inequality. *IMF Working Papers*, 25(68):1–64.

Roemer, J. E. (1998). *Equality of Opportunity*. Harvard University Press, Cambridge, MA.

Saez, E. and Zucman, G. (2016). Wealth Inequality in the United States since 1913: Evidence from Capitalized Income Tax Data. *Quarterly Journal of Economics*, 131(2):519–578.

Saez, E. and Zucman, G. (2020). The Rise of Income and Wealth Inequality in America: Evidence from Distributional Macroeconomic Accounts. *Journal of Economic Perspectives*, 34(4):3–26.

Schneider, D., Hastings, O. P., and LaBriola, J. (2018). Income Inequality and Class Divides in Parental Investments. *American Sociological Review*, 83(3):475–507.

Shorrocks, A. (1978). The Measurement of Mobility. *Econometrica: Journal of the Econometric Society*, 46(5):1013–1024.

Singer, B. and Spilerman, S. (1976). The Representation of Social Processes by Markov Models. *American Journal of Sociology*, 82(1):1–54.

Sobel, M. E., Hout, M., and Duncan, O. D. (1985). Exchange, Structure, and Symmetry in Occupational Mobility. *American Journal of Sociology*, 91(2):359–372.

Sommers, P. M. and Conlisk, J. (1979). Eigenvalue Immobility Measures for Markov Chains. *Journal of Mathematical Sociology*, 6(2):253–276.

Song, X. (2021). Multigenerational Social Mobility: A Demographic Approach. *Sociological Methodology*, 51(1):1–43.

Song, X. and Mare, R. D. (2015). Prospective versus retrospective approaches to the study of intergenerational social mobility. *Sociological Methods & Research*, 44(4):555–584.

Song, X., Massey, C. G., Rolf, K. A., Ferrie, J. P., Rothbaum, J. L., and Xie, Y. (2020). Long-term Decline in Intergenerational Mobility in the United States Since the 1850s. *Proceedings of the National Academy of Sciences*, 117(1):251–258.

Sorokin, P. A. (1927). *Social Mobility*. Harper and Brothers, New York.

Torche, F. (2015). Analyses of Intergenerational Mobility: An Interdisciplinary Review. *The Annals of the American Academy of Political and Social Science*, 657:37–62.

Treiman, D. J. (1970). Industrialization and Social Stratification. *Sociological Inquiry*, 40(2):207–234.

van de Werfhorst, H. G. (2024). Is Meritocracy Not So Bad After All? Educational Expansion and Intergenerational Mobility in 40 Countries. *American Sociological Review*, 89(6):1181–1213.

Wachter, K. W. (2014). *Essential Demographic Methods*. Harvard University Press, Cambridge, MA.

Weeden, K. A. and Grusky, D. B. (2005). The Case for a New Class Map. *American Journal of Sociology*, 111(1):141–212.

Weeden, K. A., Kim, Y.-M., Di Carlo, M., and Grusky, D. B. (2007). Social Class and Earnings Inequality. *American Behavioral Scientist*, 50(5):702–736.

Wei, L. and Xie, Y. (2025). Social Mobility as Causal Intervention. *Sociological Methods & Research*, 54(4):1463–1504.

Wodtke, G. T. (2017). Social Relations, Technical Divisions, and Class Stratification in the United States: An Empirical Test of the Death and Decomposition of Class Hypotheses. *Social Forces*, 95(4):1479–1508.

Wodtke, G. T., Elwert, F., and Harding, D. J. (2016). Neighborhood Effect Heterogeneity by Family Income and Developmental Period. *American Journal of Sociology*, 121(4):1168–1222.

Wodtke, G. T., Harding, D. J., and Elwert, F. (2011). Neighborhood Effects in Temporal Perspective: The Impact of Long-Term Exposure to Concentrated Disadvantage on High School Graduation. *American Sociological Review*, 76(5):713–736.

Wood, S. N. (2003). Thin Plate Regression Splines. *Journal of the Royal Statistical Society Series B: Statistical Methodology*, 65(1):95–114.

Wood, S. N. (2011). Fast Stable Restricted Maximum Likelihood and Marginal Likelihood Estimation of Semiparametric Generalized Linear Models. *Journal of the Royal Statistical Society: Series B (Statistical Methodology)*, 73(1):3–36.

Xie, Y. (1992). The Log-multiplicative Layer Effect Model for Comparing Mobility Tables. *American Sociological Review*, pages 380–395.

Xie, Y. and Killewald, A. (2013). Intergenerational Occupational Mobility in Great Britain and the United States since 1850: Comment. *American Economic Review*, 103(5):2003–2020.

Zhou, X. (2015). Shrinkage Estimation of Log-odds Ratios for Comparing Mobility Tables. *Sociological Methodology*, 45(1):320–356.

Zhou, X. (2019). Equalization or Selection? Reassessing the Meritocratic Power of a College Degree in Intergenerational Income Mobility. *American Sociological Review*, 84(3):459–485.

Zhou, X. and Wodtke, G. T. (2019). Income Stratification among Occupational Classes in the United States. *Social Forces*, 97(3):945–972.

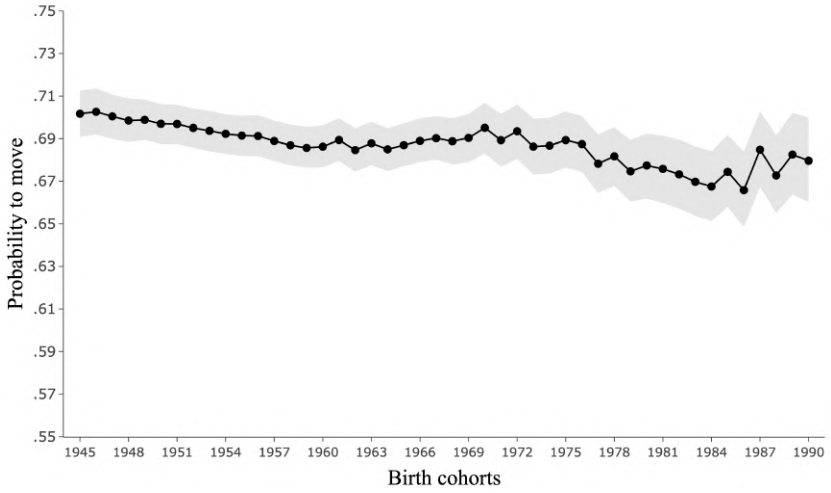
Appendix

A Alternative Age Restrictions

In this section, we replicate our main analyses after varying the age restriction applied to respondents at the time of their GSS interview, when information on their current occupations is collected. Specifically, we expand the sample to include older respondents by shifting the age window from 25–55 to 25–64 and also 30–64, and we additionally restrict the sample to a narrower age window of 30–40. As shown in Figures A.1 to A.12, these changes to the age range do not materially alter the estimated trends in movement, memory, or association. Across these samples, the trends remain largely flat, with at most a faint suggestion of declining mobility in some point estimates.

Figure A.1: Measures of movement at generation $t = 1$ computed from samples of respondents age 25-64

(A) Overall mobility (OM_1)



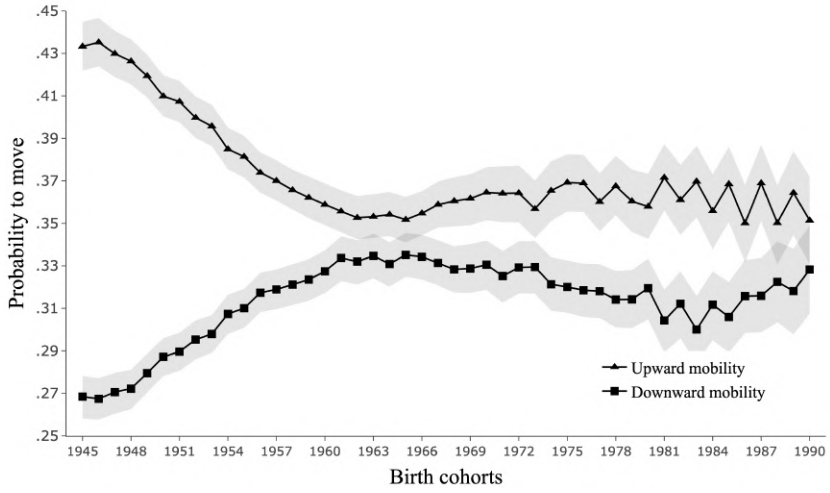
(B) Structural mobility (SM_1)



(C) Exchange mobility (EM_1)

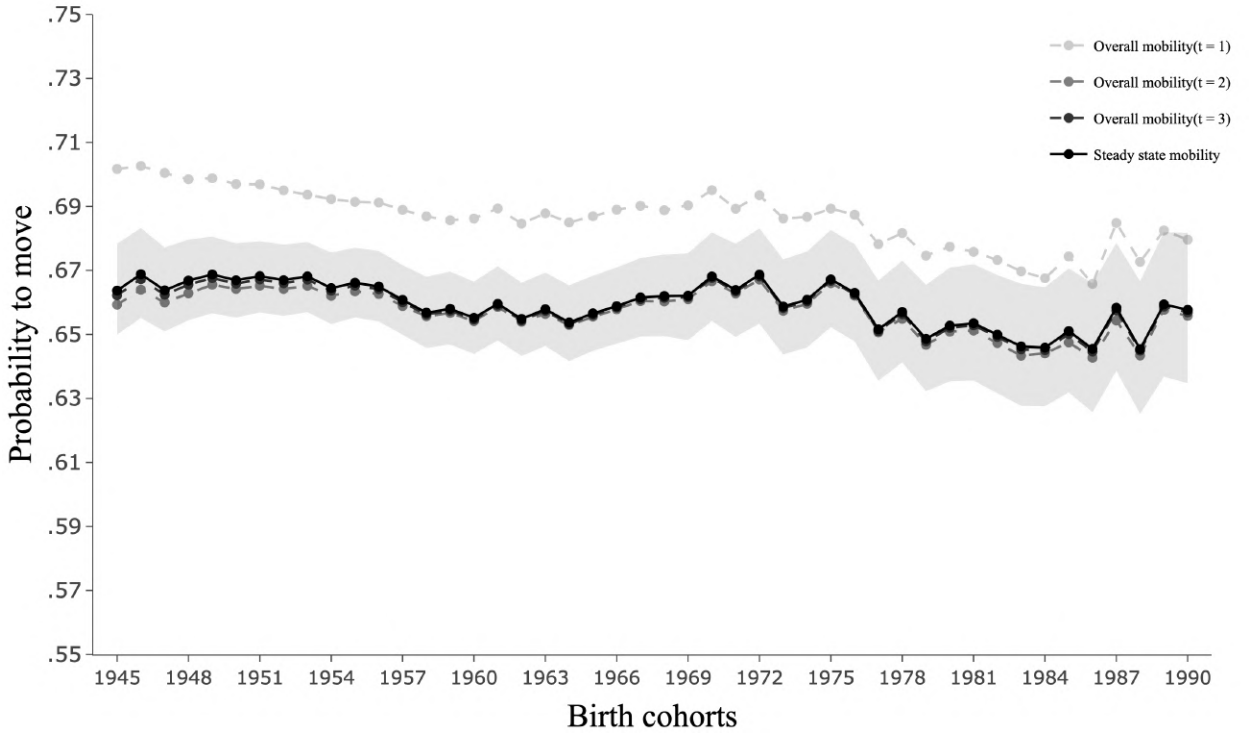


(D) Upward and downward mobility



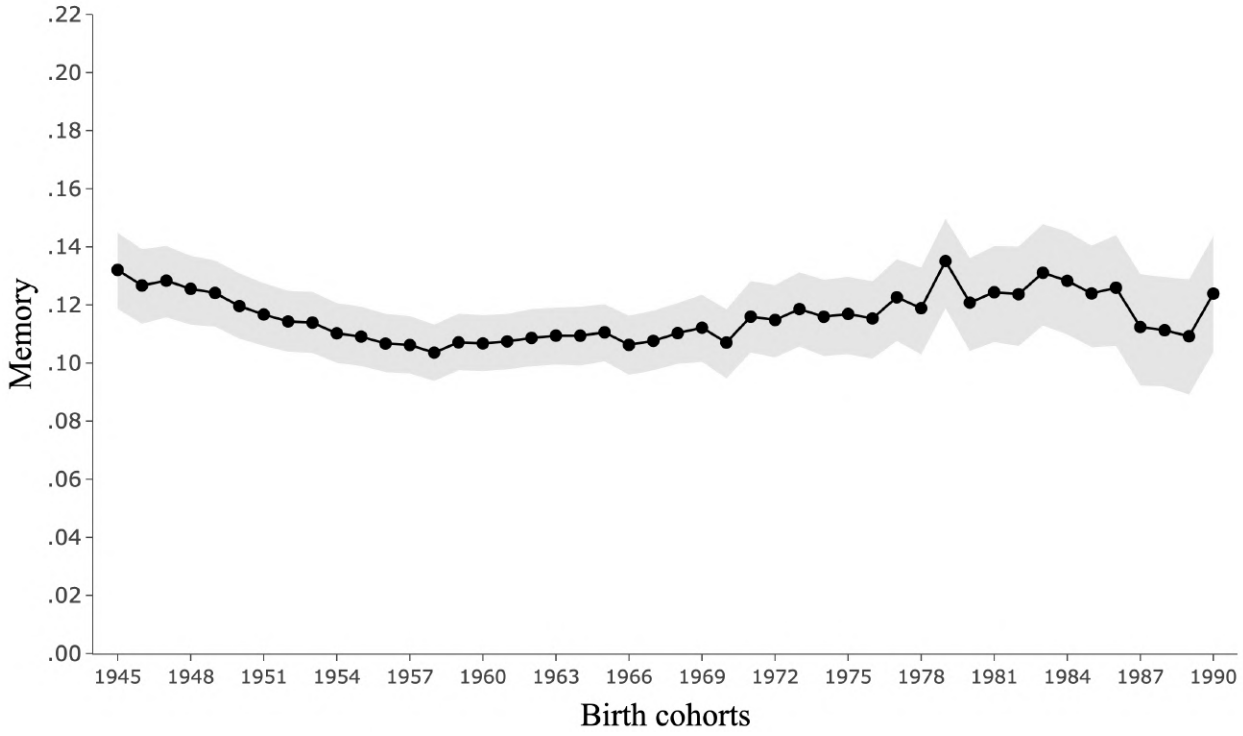
Notes: Shaded areas represent 95% confidence intervals.

Figure A.2: Overall mobility (OM_t) across synthetic generations computed from samples of respondents age 25-64



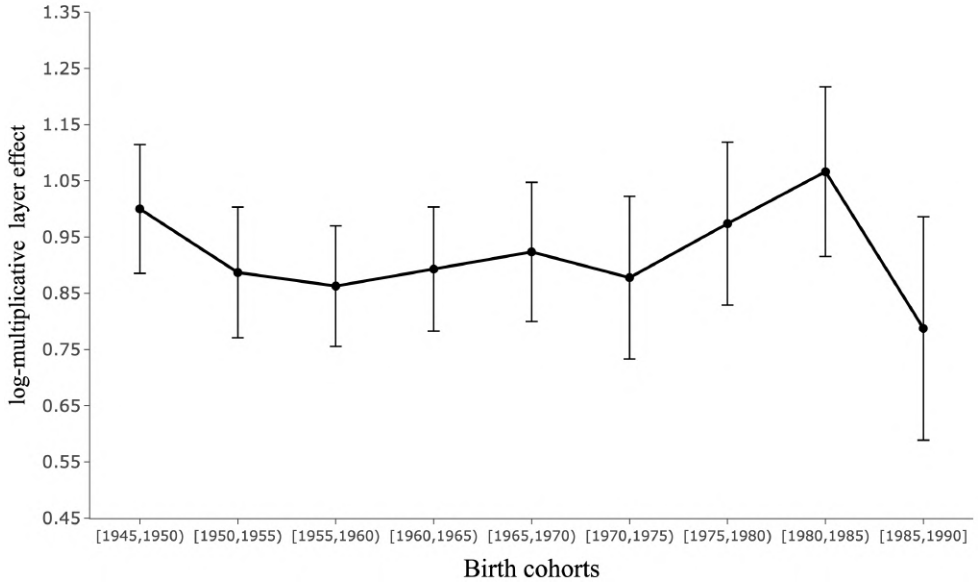
Notes: This figure illustrates the evolution of overall mobility across generations in a stationary Markov chain. By $t = 4$, the Markov chains for most of the cohorts have converged to their respective steady-state distributions, where there is no structural mobility. Shaded areas represent 95% confidence intervals, which are shown only for the trend in steady-state mobility.

Figure A.3: Aggregate intergenerational memory at generation $t = 1$ (AIM_1) computed from samples of respondents age 25-64



Notes: Shaded areas represent 95% confidence intervals.

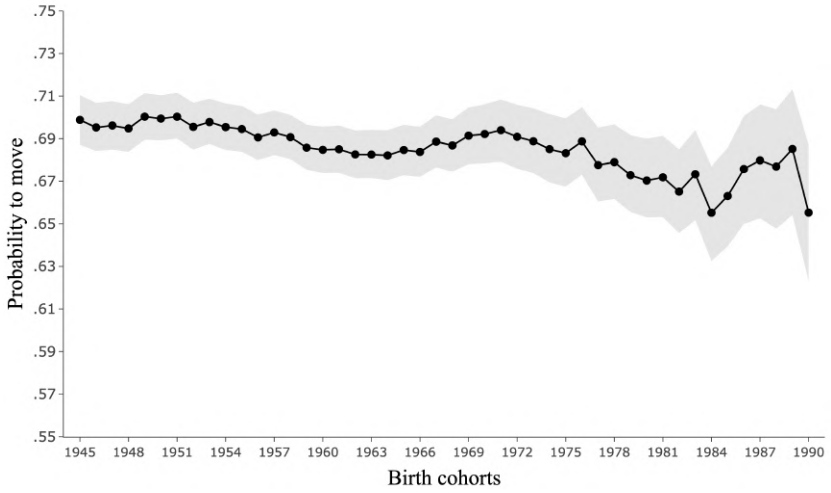
Figure A.4: Log-multiplicative layer effects computed from samples of respondents age 25-64



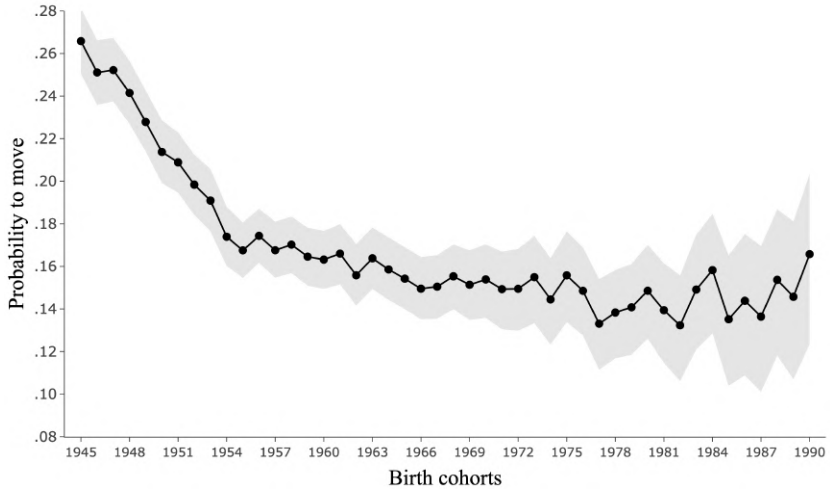
Notes: This figure plots the log-multiplicative layer effect across birth cohorts using 5-year bins. The vertical bars represent 95% confidence intervals.

Figure A.5: Measures of movement at generation $t = 1$ computed from samples of respondents age 30-64

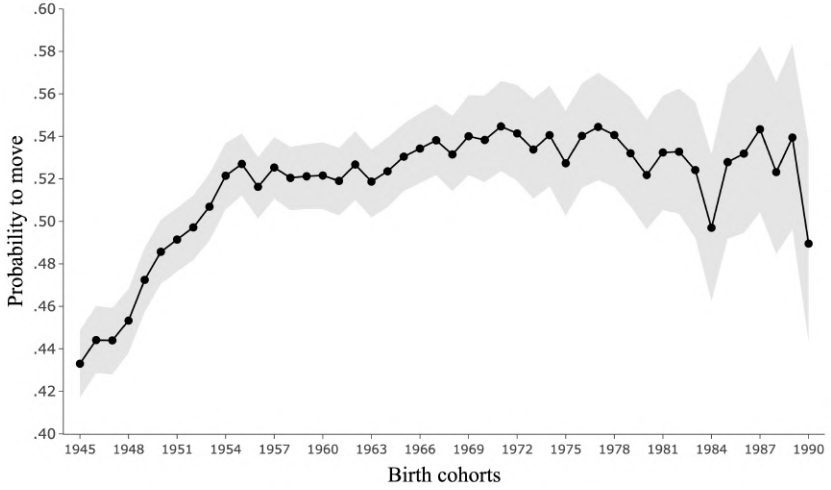
(A) Overall mobility (OM_1)



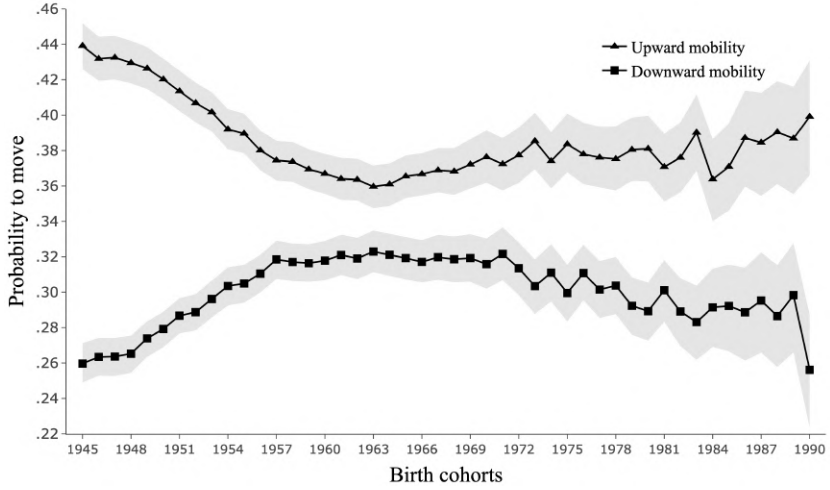
(B) Structural mobility (SM_1)



(C) Exchange mobility (EM_1)

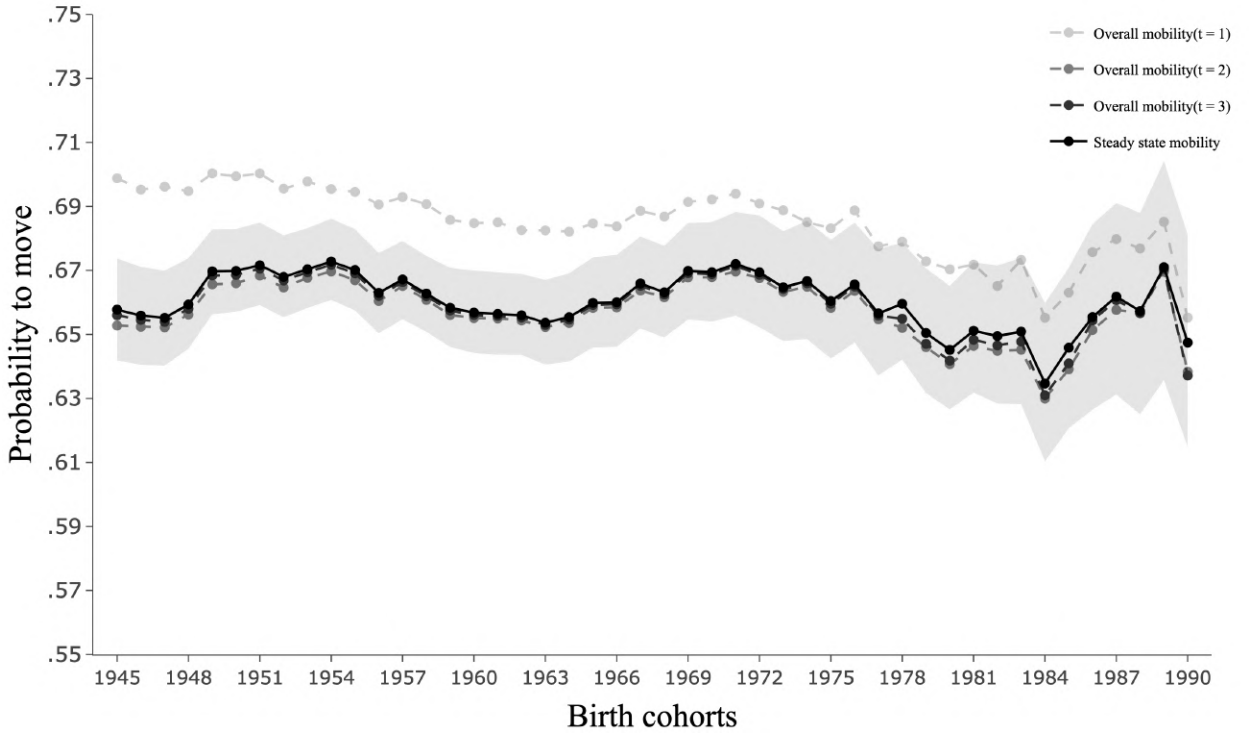


(D) Upward and downward mobility



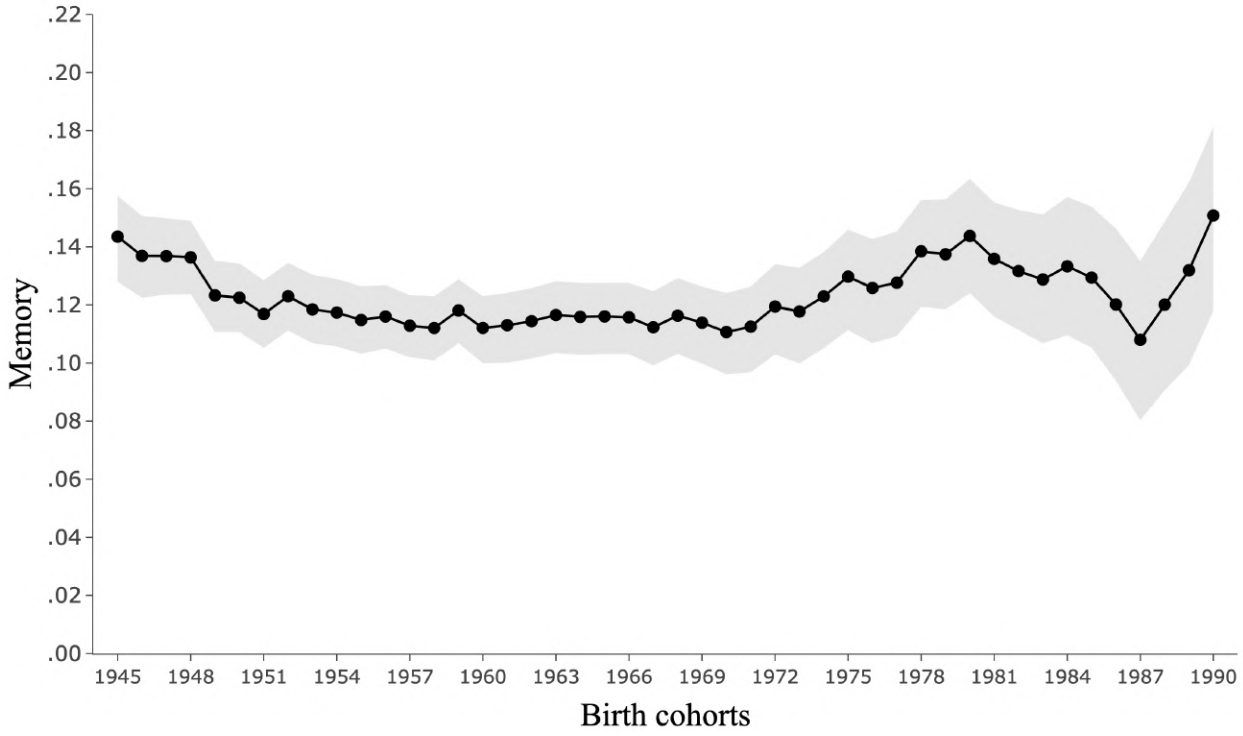
Notes: Shaded areas represent 95% confidence intervals.

Figure A.6: Overall mobility (OM_t) across synthetic generations computed from samples of respondents age 30-64



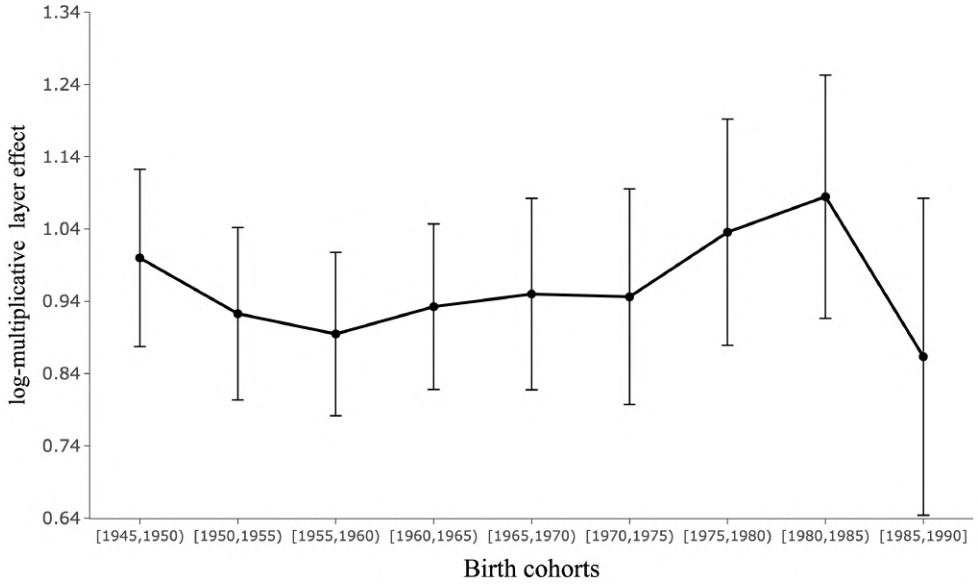
Notes: This figure illustrates the evolution of overall mobility across generations in a stationary Markov chain. By $t = 4$, the Markov chains for most of the cohorts have converged to their respective steady-state distributions, where there is no structural mobility. Shaded areas represent 95% confidence intervals, which are shown only for the trend in steady-state mobility.

Figure A.7: Aggregate intergenerational memory at generation $t = 1$ (AIM_1) computed from samples of respondents age 30-64



Notes: Shaded areas represent 95% confidence intervals.

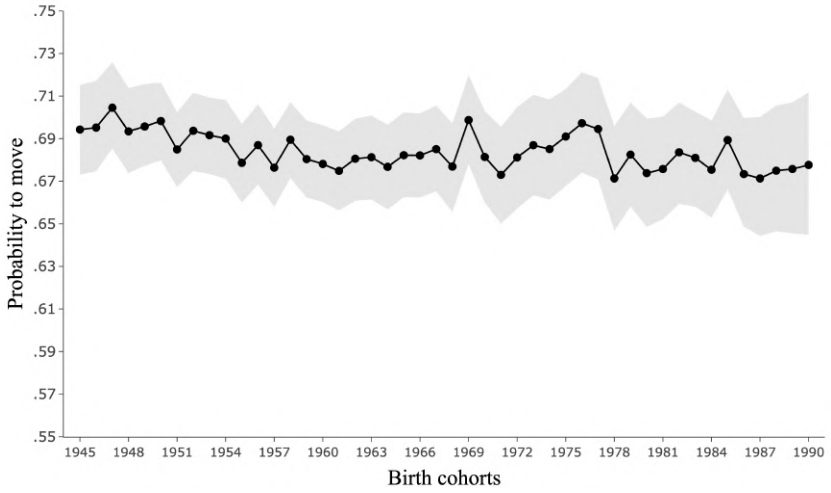
Figure A.8: Log-multiplicative layer effects computed from samples of respondents age 30-64



Notes: This figure plots the log-multiplicative layer effect across birth cohorts using 5-year bins. The vertical bars represent 95% confidence intervals.

Figure A.9: Measures of movement at generation $t = 1$ computed from samples of respondents age 30-40

(A) Overall mobility (OM_1)



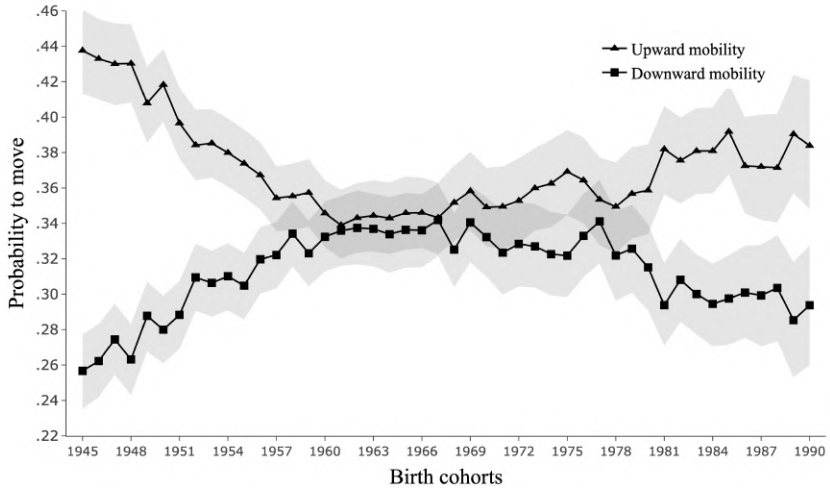
(B) Structural mobility (SM_1)



(C) Exchange mobility (EM_1)

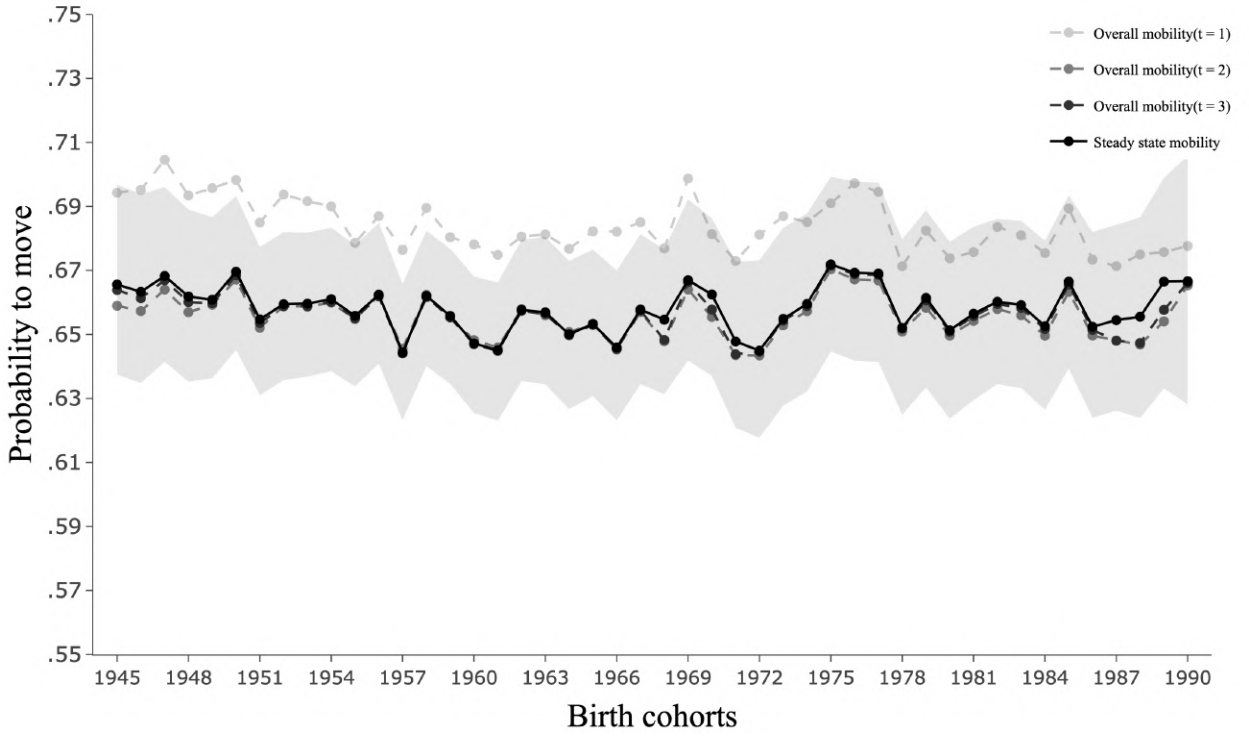


(D) Upward and downward mobility



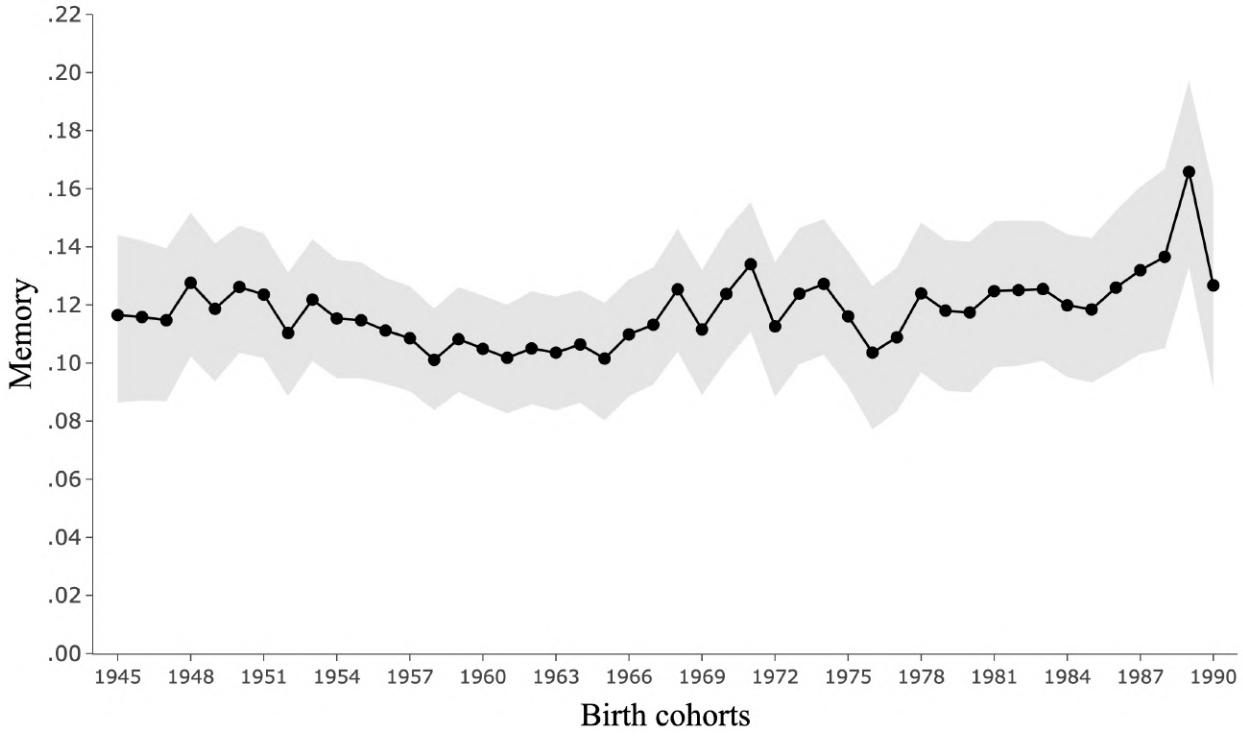
Notes: Shaded areas represent 95% confidence intervals.

Figure A.10: Overall mobility (OM_t) across synthetic generations computed from samples of respondents age 30-40



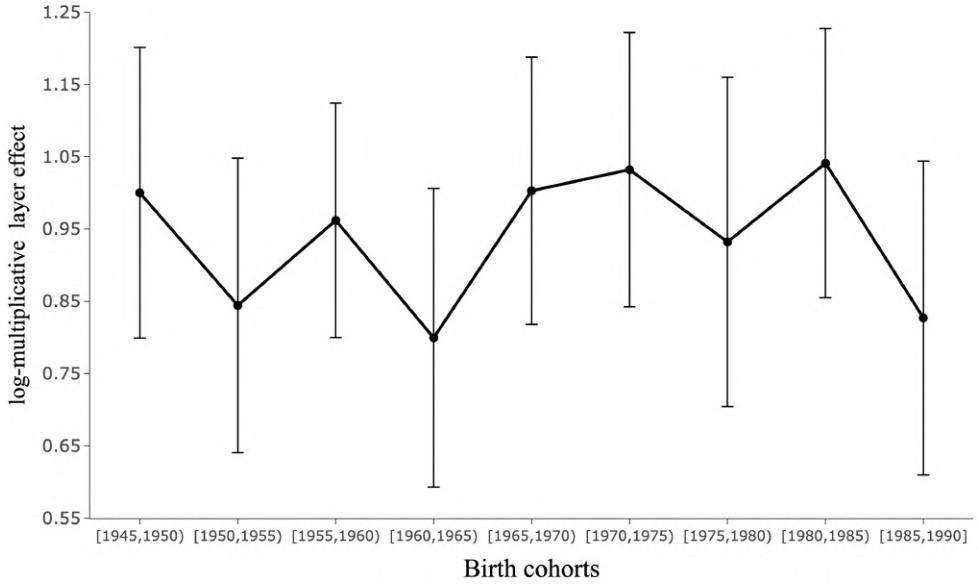
Notes: This figure illustrates the evolution of overall mobility across generations in a stationary Markov chain. By $t = 4$, the Markov chains for most of the cohorts have converged to their respective steady-state distributions, where there is no structural mobility. Shaded areas represent 95% confidence intervals, which are shown only for the trend in steady-state mobility.

Figure A.11: Aggregate intergenerational memory at generation $t = 1$ (AIM_1) computed from samples of respondents age 30-40



Notes: Shaded areas represent 95% confidence intervals.

Figure A.12: Log-multiplicative layer effects computed from samples of respondents age 30-40



Notes: This figure plots the log-multiplicative layer effect across birth cohorts using 5-year bins. The vertical bars represent 95% confidence intervals.

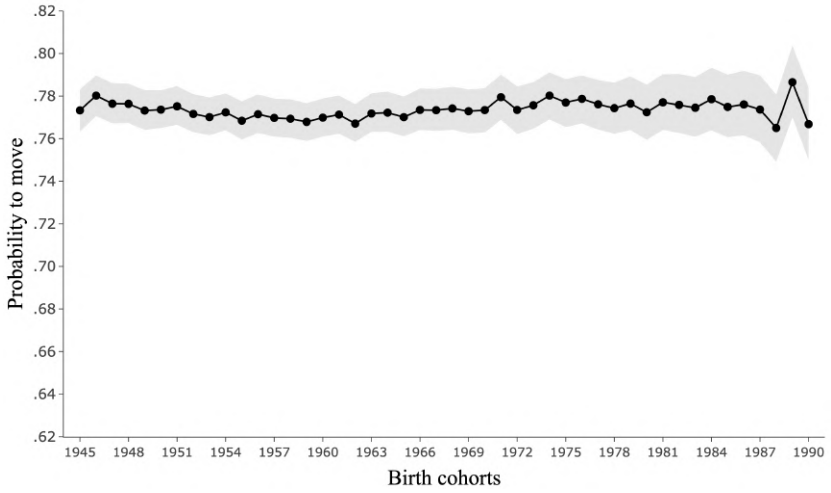
B Alternative Class Typologies

In this section, we replicate our main analyses using several alternative EGP typologies. Specifically, we employ the six-class typology adopted by Pfeffer and Hertel (2015) and the seven-class typology developed by Morgan (2017). The primary difference between our five-class typology and these alternatives is that we combine Class IIIa (higher-grade routine non-manual occupations) with Class V (lower-grade technicians) as a "middle class," while grouping Class IIIb (lower-grade routine non-manual occupations) with Class VII (unskilled manual workers). A second distinction is that both the six- and seven-class typologies classify all self-employed respondents outside the professional classes together with farmers in Class IV. We also replicate our analyses with the five-class typology after excluding all self-employed respondents, following the approach employed by Erikson and Goldthorpe (2010). In addition, we conduct replications excluding farmers, as prior research suggests that long-term trends in mobility can be particularly sensitive to changes involving this group (Xie and Killewald, 2013).

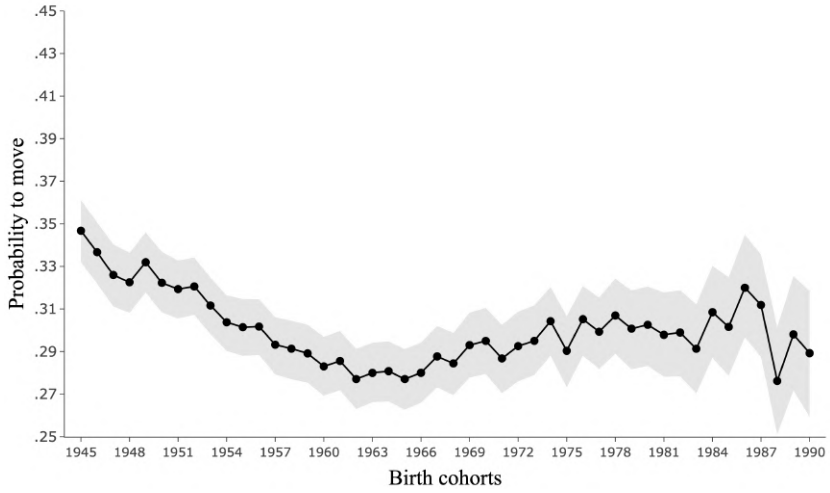
Overall, adopting these alternative typologies affects the levels of estimated mobility but not its trends. Across all approaches to measurement, we find relatively little evidence of an increase or decrease in mobility, whether assessed in terms of movement, memory, or association. With some of these typologies—particularly those employed by Pfeffer and Hertel (2015), Morgan (2017), our five-class typology excluding farmers—we find a slight downward shift in steady-state mobility and a slight upward shift in memory among cohorts born after the late 1960s. However, these changes are small, and we often cannot rule out that they are merely due to sampling variability.

Figure B.1: Measures of movement at generation $t = 1$ based on the Pfeffer and Hertel (2015) typology

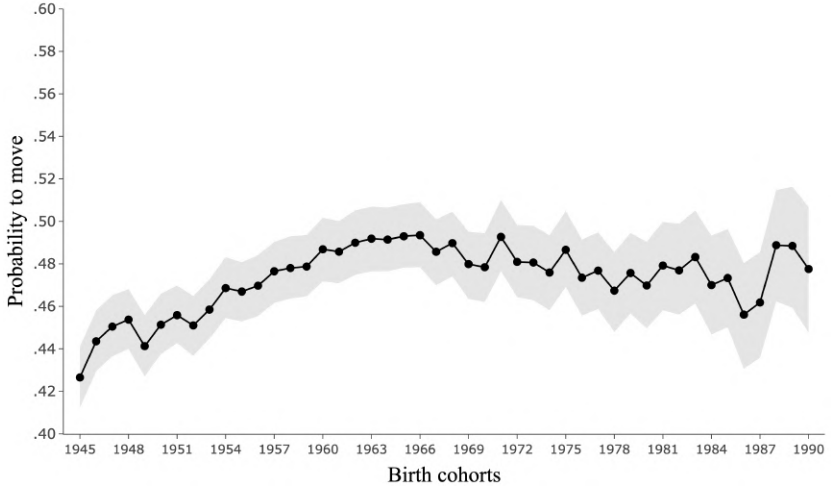
(A) Overall mobility (OM_1)



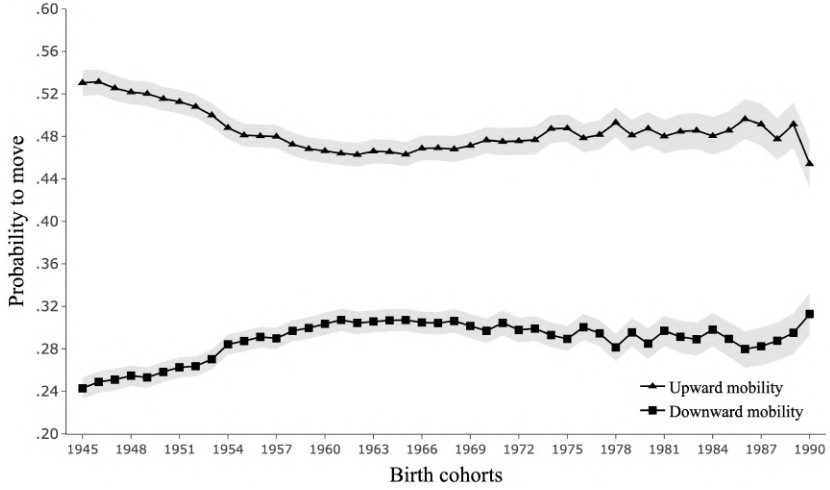
(B) Structural mobility (SM_1)



(C) Exchange mobility (EM_1)

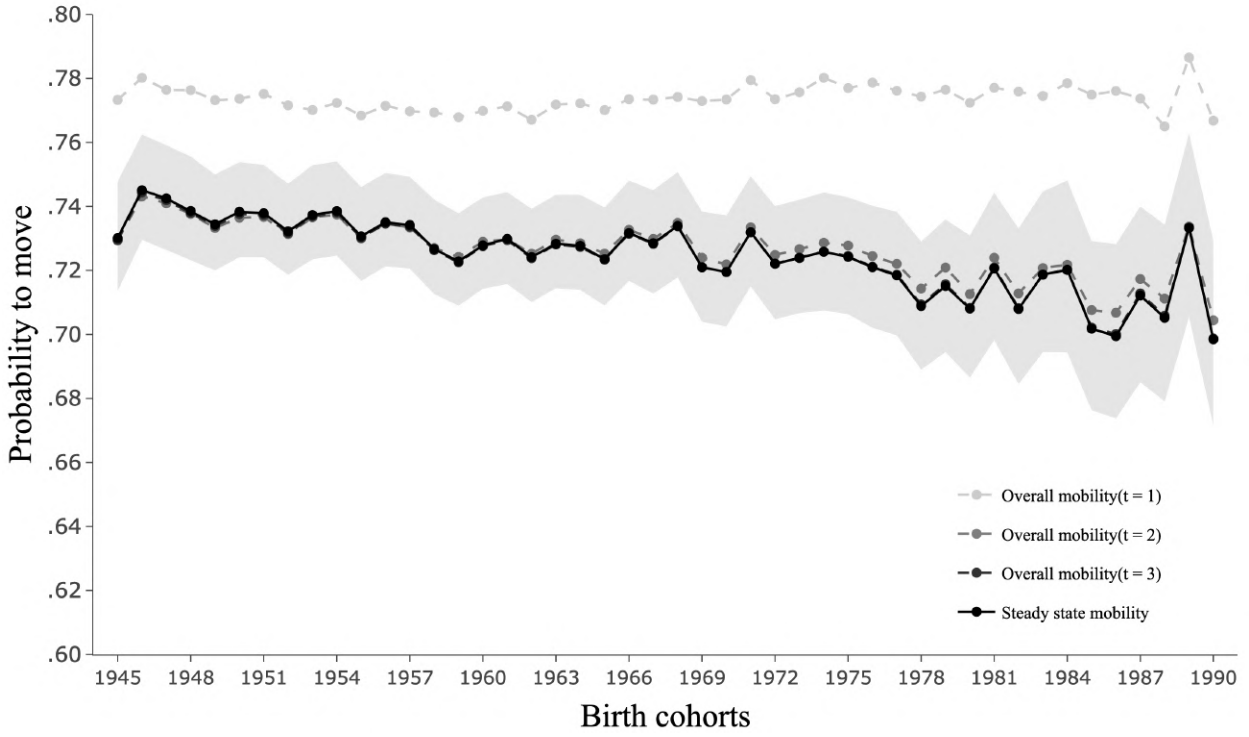


(D) Upward and downward mobility



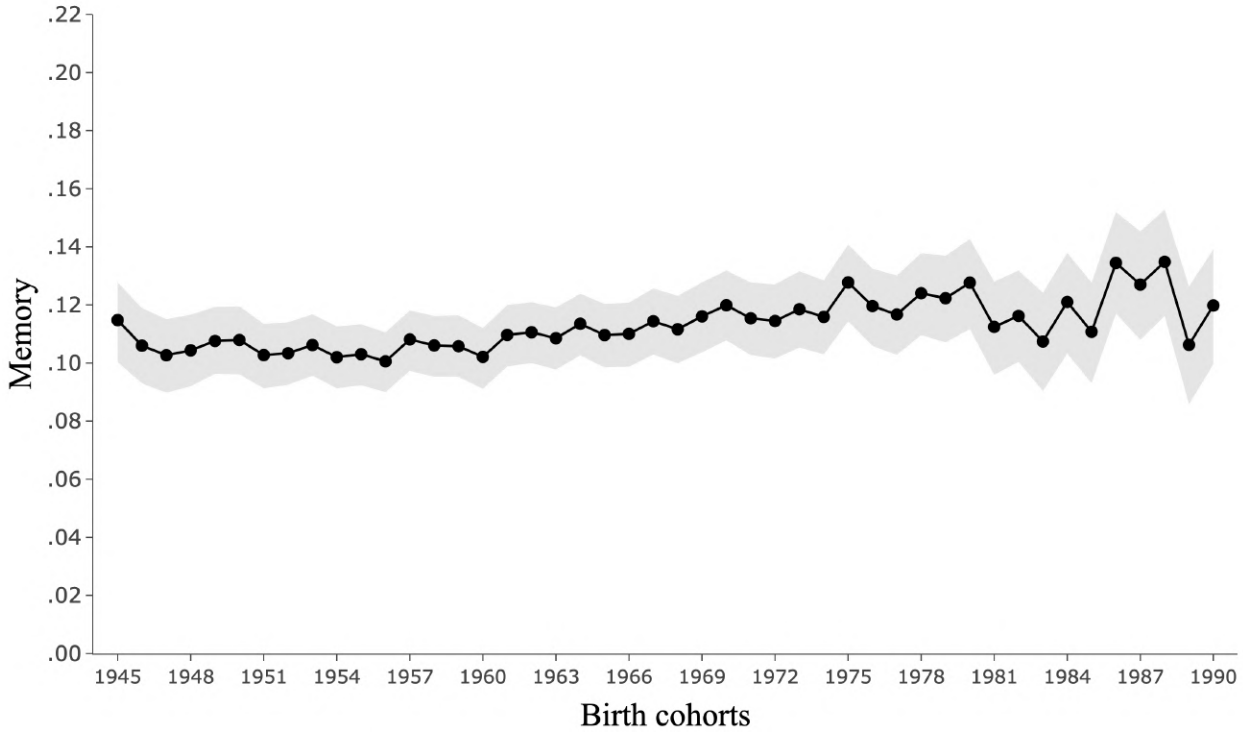
Notes: Shaded areas represent 95% confidence intervals.

Figure B.2: Overall mobility (OM_t) across synthetic generations based on the Pfeffer and Hertel (2015) typology



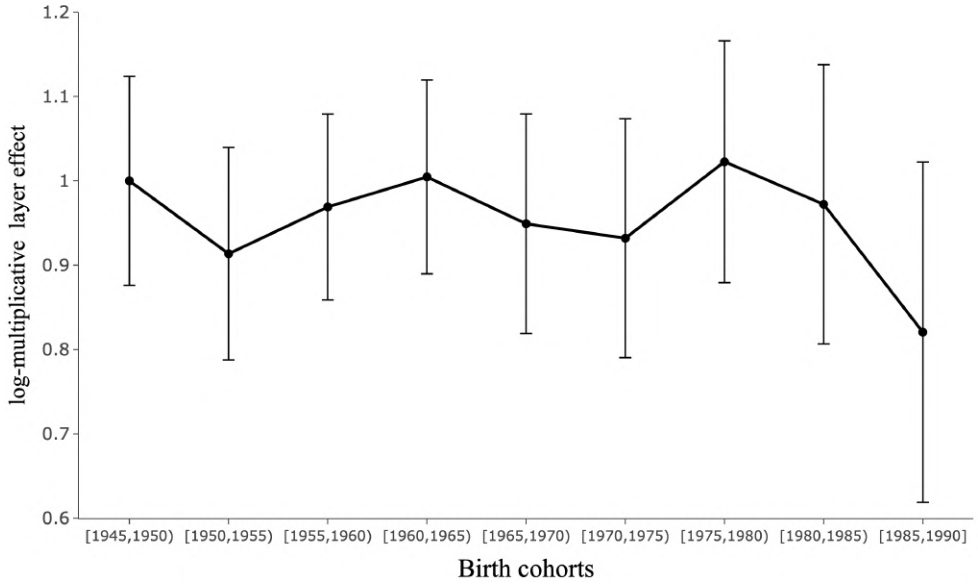
Notes: This figure illustrates the evolution of overall mobility across generations in a stationary Markov chain. By $t = 4$, the Markov chains for most of the cohorts have converged to their respective steady-state distributions, where there is no structural mobility. Shaded areas represent 95% confidence intervals, which are shown only for the trend in steady-state mobility.

Figure B.3: Aggregate intergenerational memory at generation $t = 1$ (AIM_1) based on the Pfeffer and Hertel (2015) typology



Notes: Shaded areas represent 95% confidence intervals.

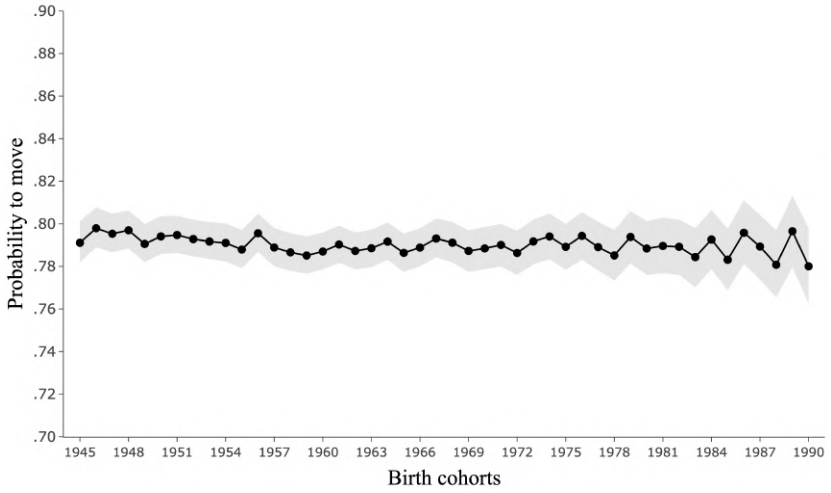
Figure B.4: Log-multiplicative layer effects based on the Pfeffer and Hertel (2015) typology



Notes: This figure plots the log-multiplicative layer effect across birth cohorts using 5-year bins. The vertical bars represent 95% confidence intervals.

Figure B.5: Measures of movement at generation $t = 1$ based on the Morgan (2017) typology

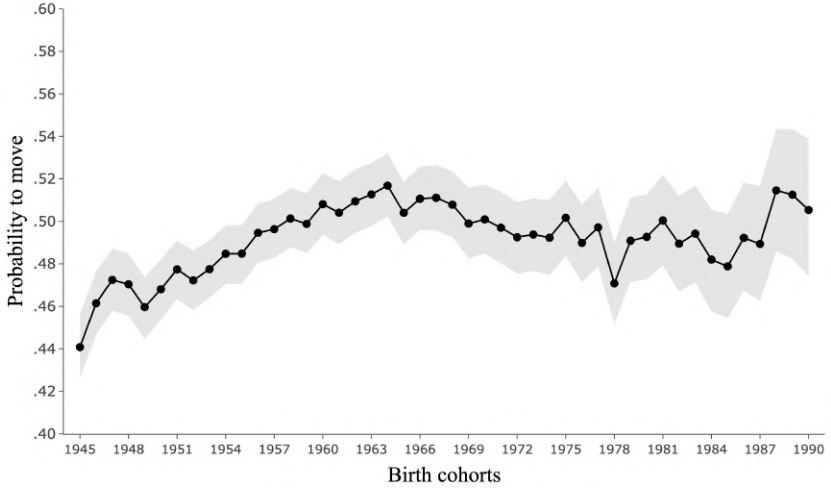
(A) Overall mobility (OM_1)



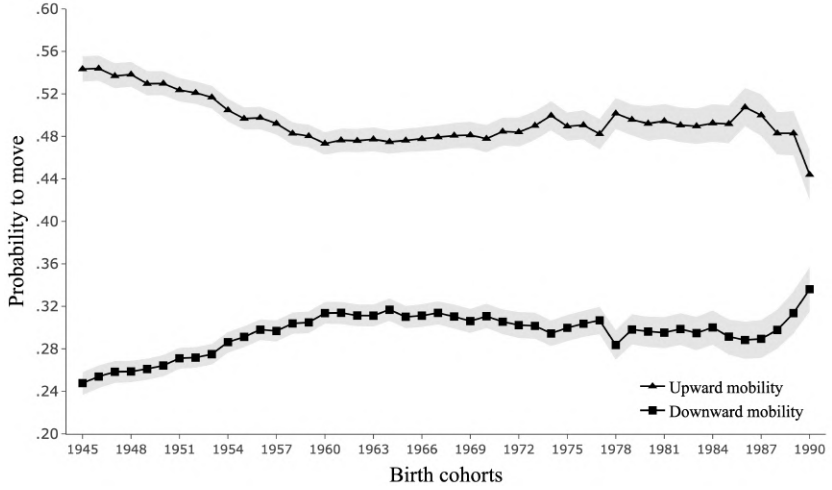
(B) Structural mobility (SM_1)



(C) Exchange mobility (EM_1)

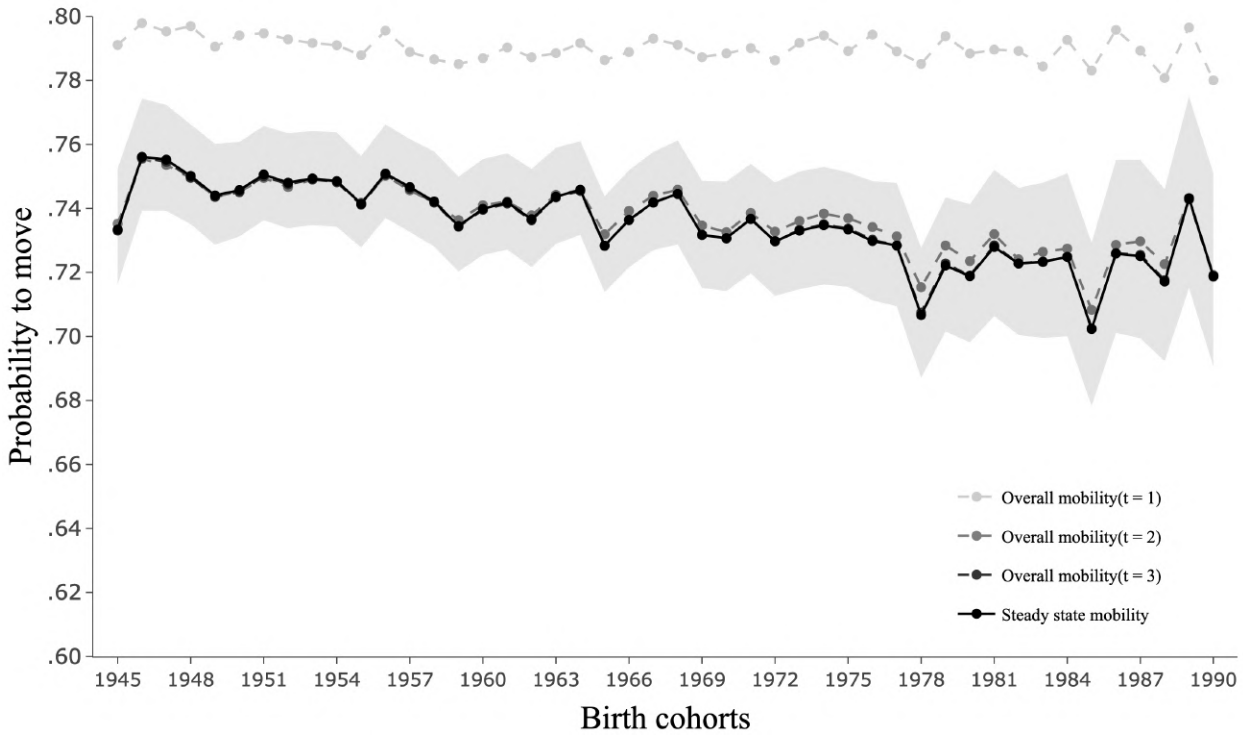


(D) Upward and downward mobility



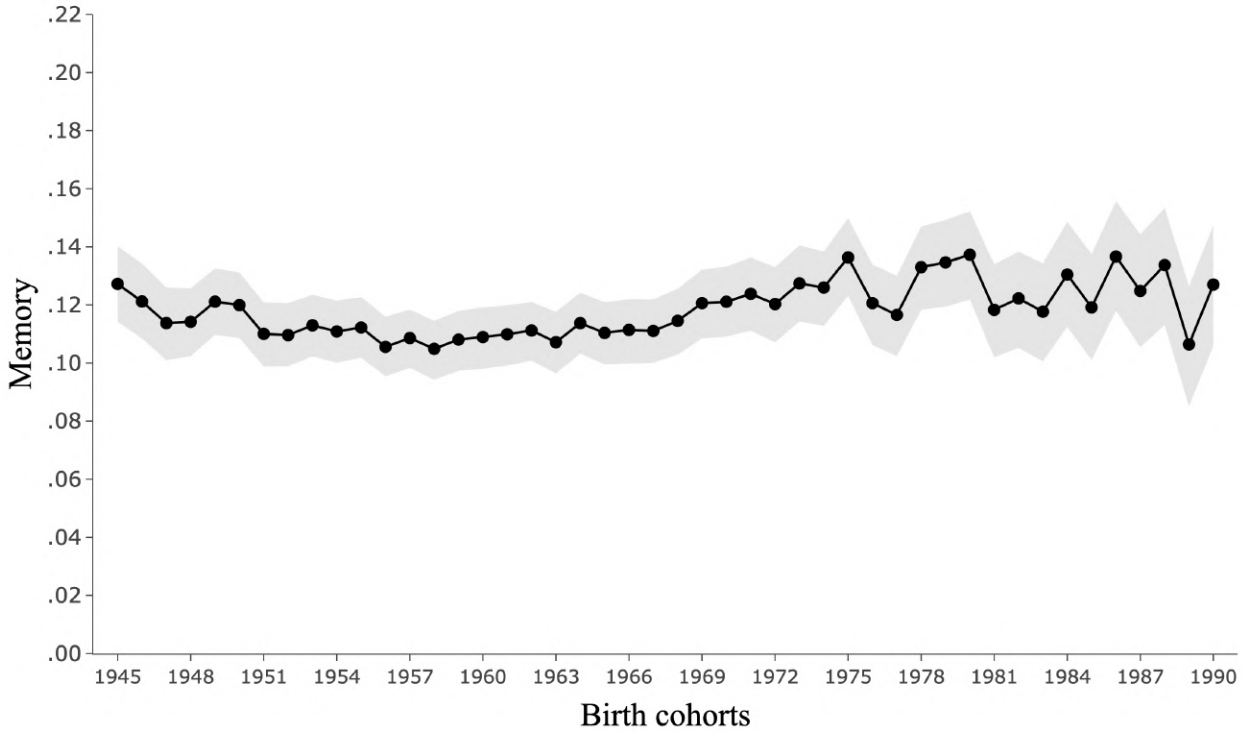
Notes: Shaded areas represent 95% confidence intervals.

Figure B.6: Overall mobility (OM_t) across synthetic generations based on the Morgan (2017) typology



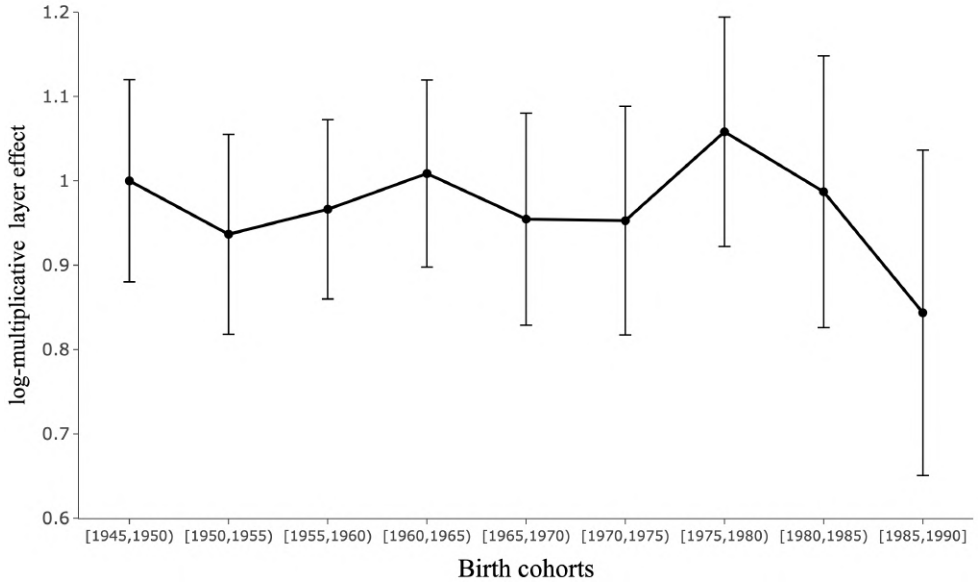
Notes: This figure illustrates the evolution of overall mobility across generations in a stationary Markov chain. By $t = 4$, the Markov chains for most of the cohorts have converged to their respective steady-state distributions, where there is no structural mobility. Shaded areas represent 95% confidence intervals, which are shown only for the trend in steady-state mobility.

Figure B.7: Aggregate intergenerational memory at generation $t = 1$ (AIM_1) based on the Morgan (2017) typology



Notes: Shaded areas represent 95% confidence intervals.

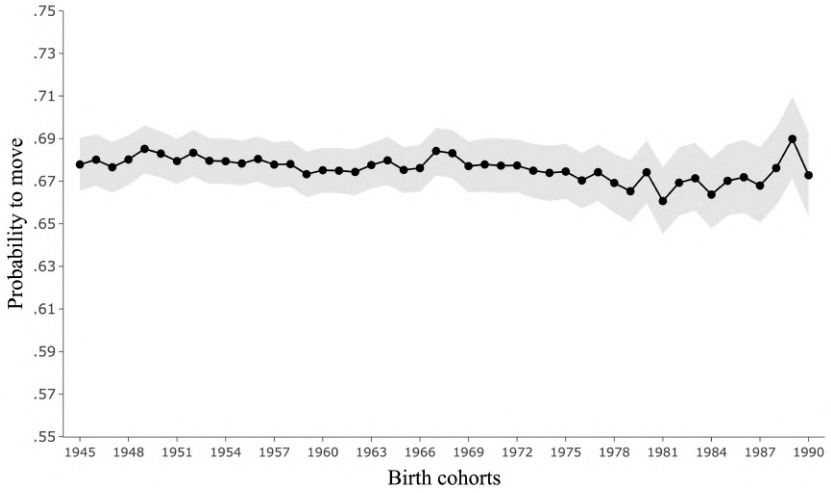
Figure B.8: Log-multiplicative layer effects based on the Morgan (2017) typology



Notes: This figure plots the log-multiplicative layer effect across birth cohorts using 5-year bins. The vertical bars represent 95% confidence intervals.

Figure B.9: Measures of movement at generation $t = 1$ excluding farmers

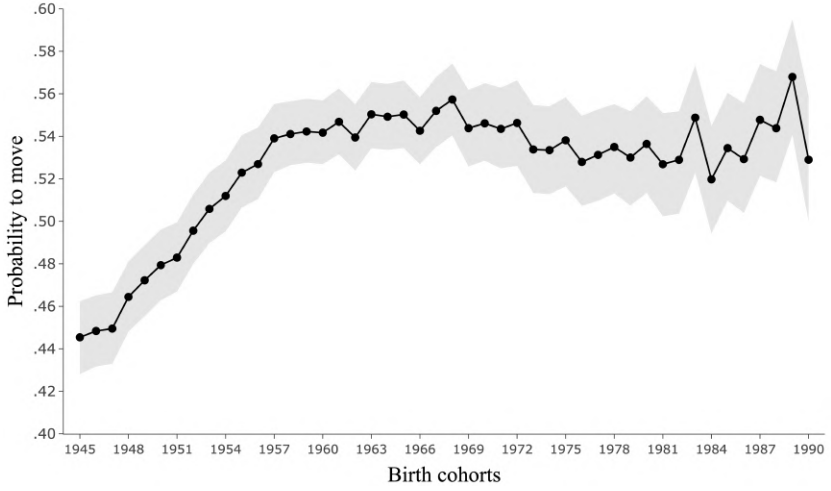
(A) Overall mobility (OM_1)



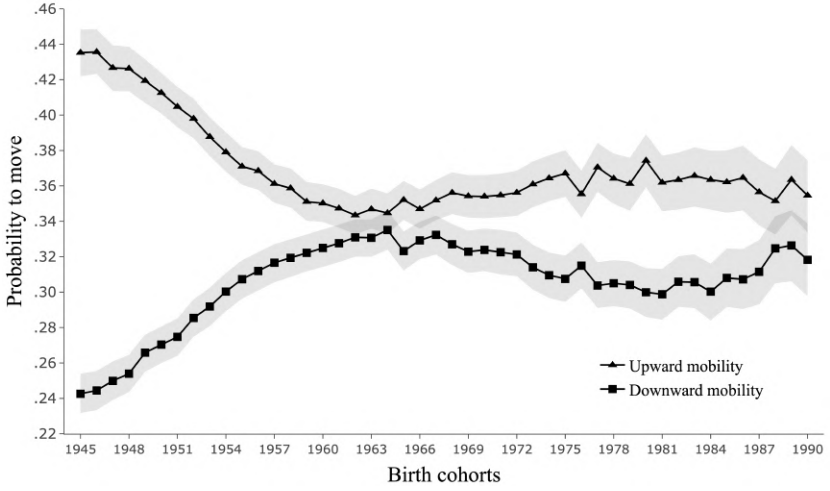
(B) Structural mobility (SM_1)



(C) Exchange mobility (EM_1)

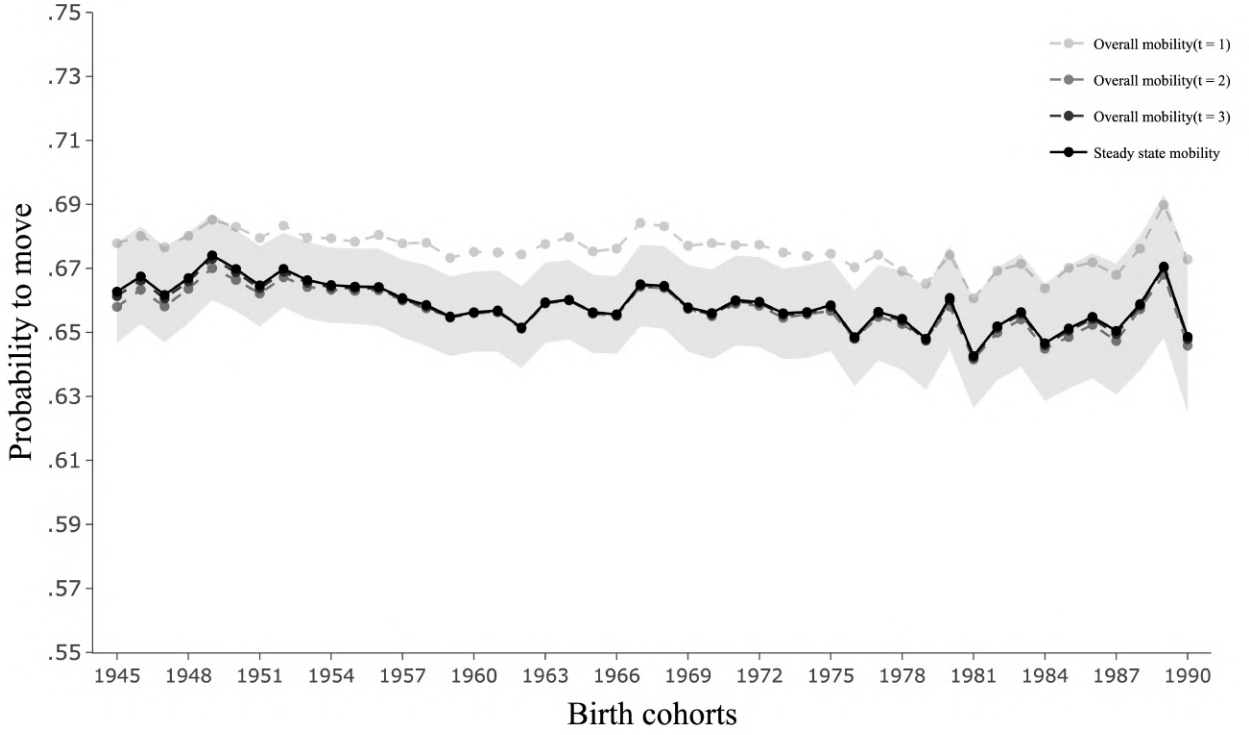


(D) Upward and downward mobility



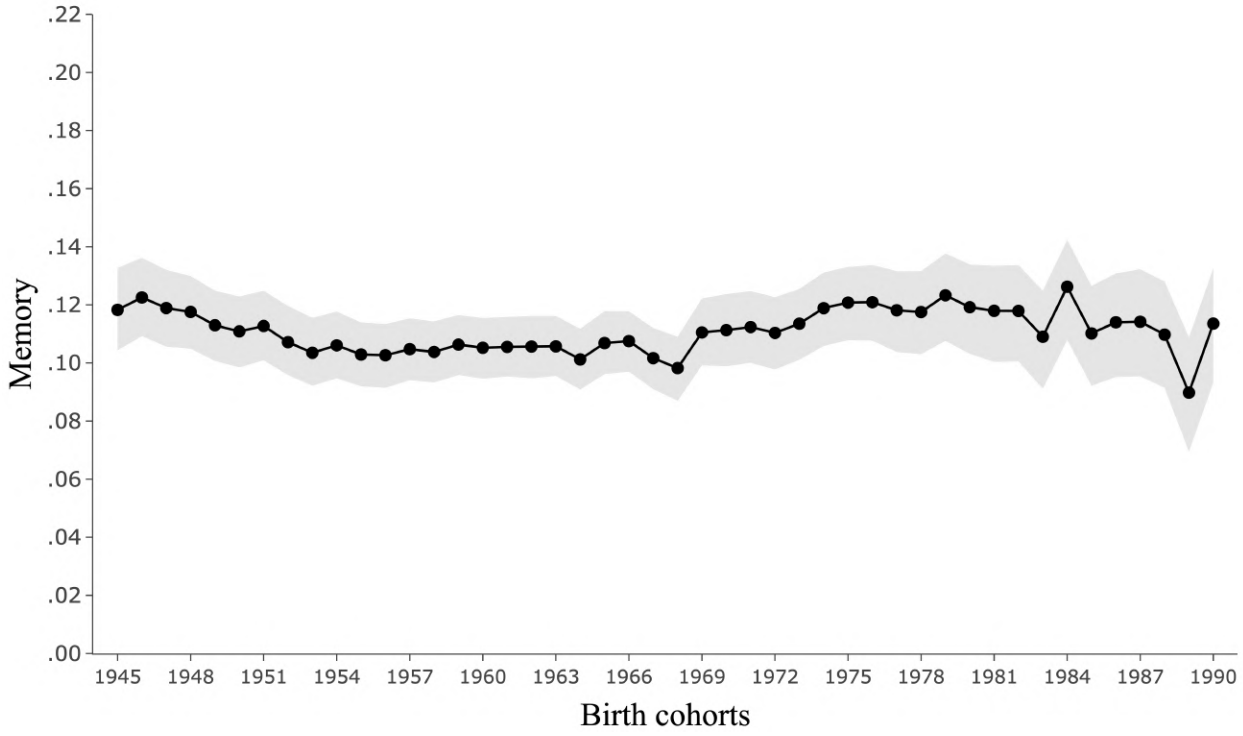
Notes: Shaded areas represent 95% confidence intervals.

Figure B.10: Overall mobility (OM_t) across synthetic generations excluding farmers



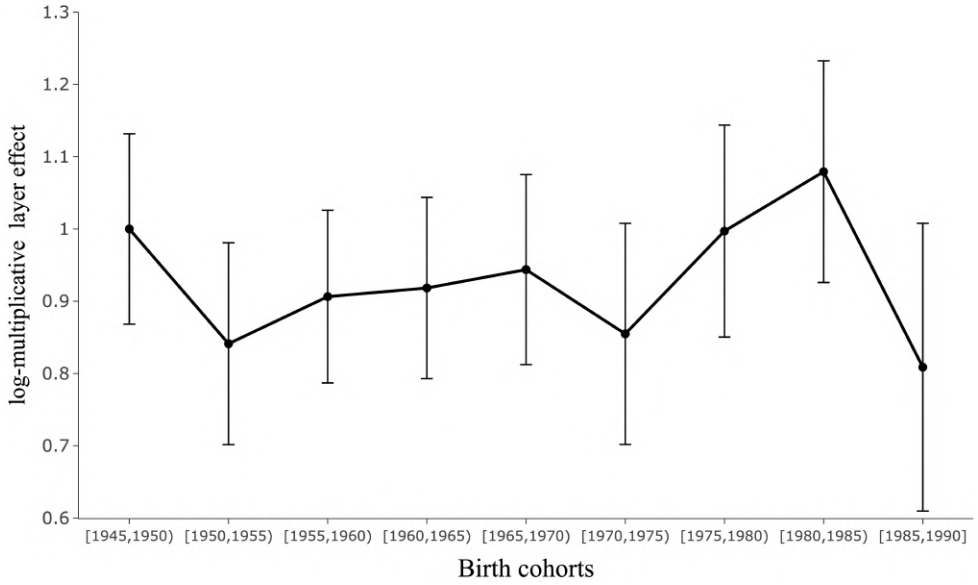
Notes: This figure illustrates the evolution of overall mobility across generations in a stationary Markov chain. By $t = 4$, the Markov chains for most of the cohorts have converged to their respective steady-state distributions, where there is no structural mobility. Shaded areas represent 95% confidence intervals, which are shown only for the trend in steady-state mobility.

Figure B.11: Aggregate intergenerational memory at generation $t = 1$ (AIM_1) excluding farmers



Notes: Shaded areas represent 95% confidence intervals.

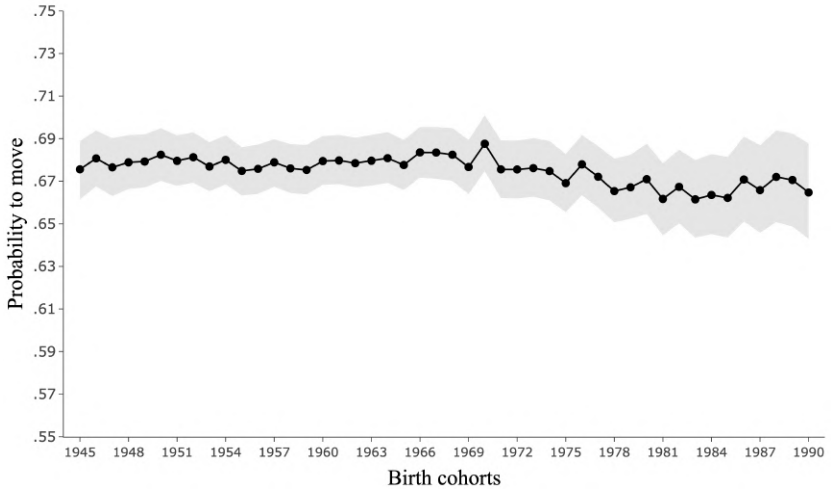
Figure B.12: Log-multiplicative layer effects excluding farmers



Notes: This figure plots the log-multiplicative layer effect across birth cohorts using 5-year bins. The vertical bars represent 95% confidence intervals.

Figure B.13: Measures of movement at generation $t = 1$ based on Erikson and Goldthorpe (2010) typology

(A) Overall mobility (OM_1)



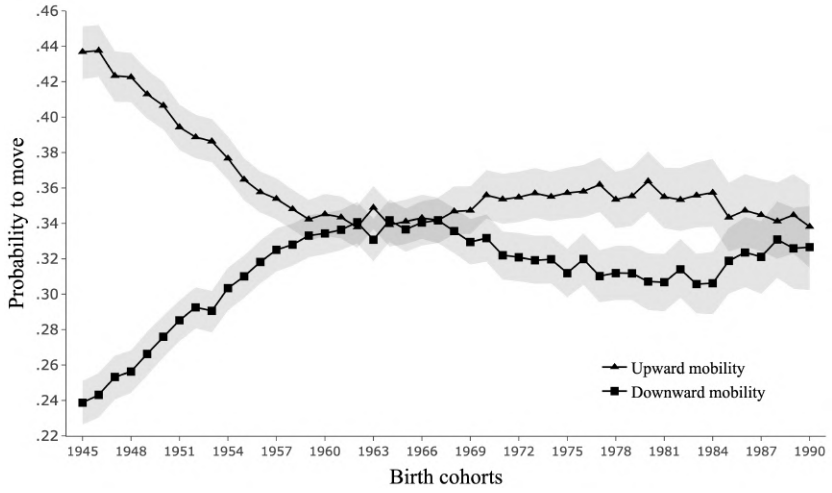
(B) Structural mobility (SM_1)



(C) Exchange mobility (EM_1)

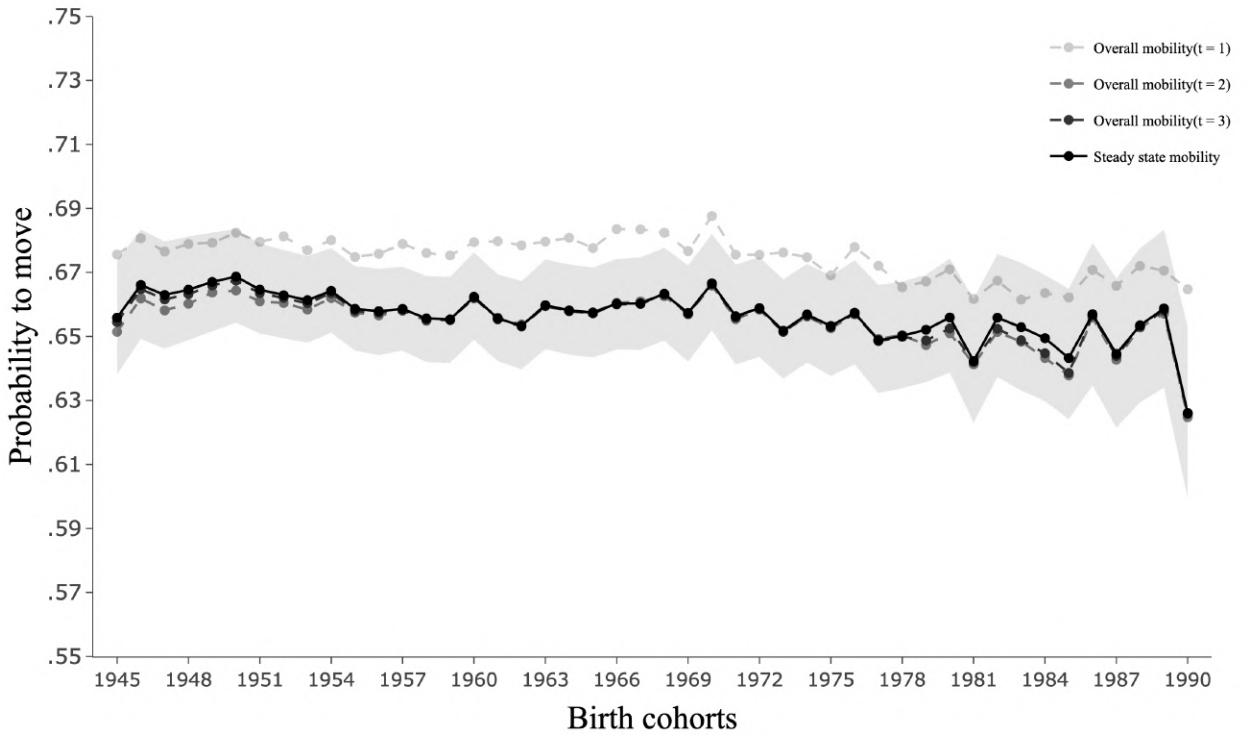


(D) Upward and downward mobility



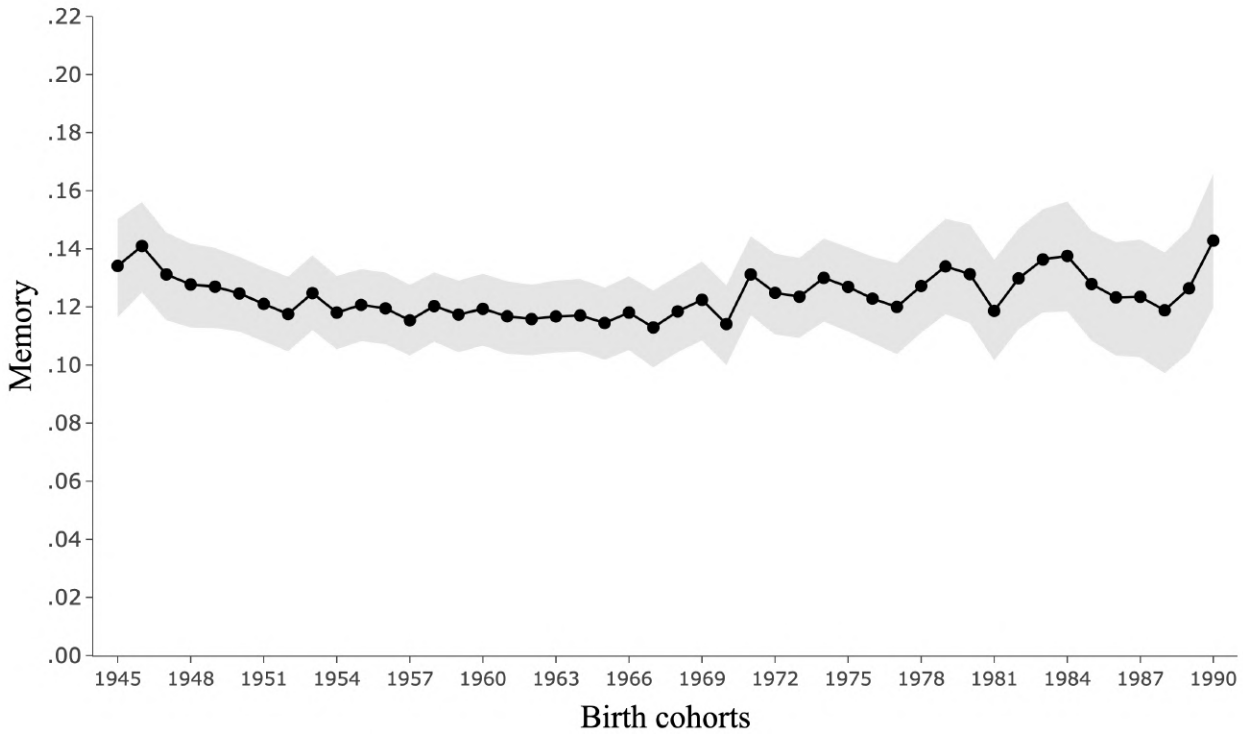
Notes: Shaded areas represent 95% confidence intervals.

Figure B.14: Overall mobility (OM_t) across synthetic generations based on Erikson and Goldthorpe (2010) typology



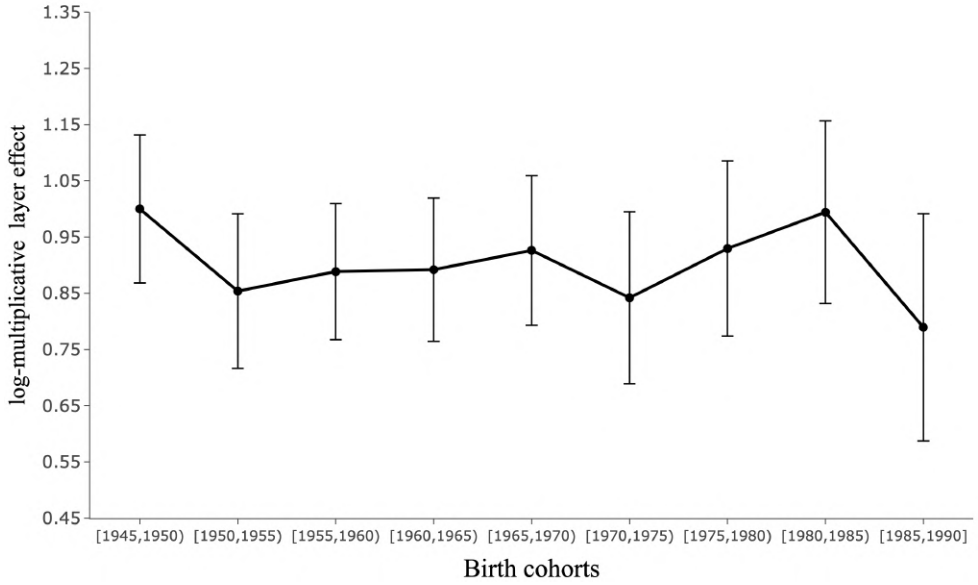
Notes: This figure illustrates the evolution of overall mobility across generations in a stationary Markov chain. By $t = 4$, the Markov chains for most of the cohorts have converged to their respective steady-state distributions, where there is no structural mobility. Shaded areas represent 95% confidence intervals, which are shown only for the trend in steady-state mobility.

Figure B.15: Aggregate intergenerational memory at generation $t = 1$ (AIM_1) based on Erikson and Goldthorpe (2010) typology



Notes: Shaded areas represent 95% confidence intervals.

Figure B.16: Log-multiplicative layer effects based on Erikson and Goldthorpe (2010) typology



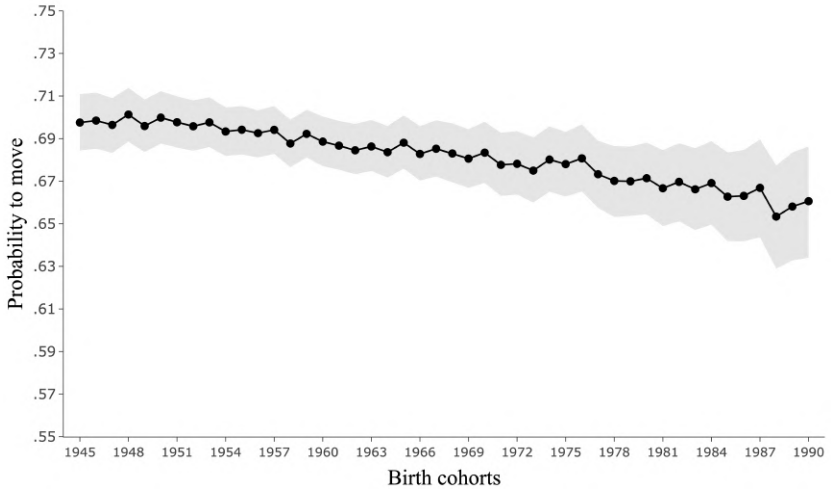
Notes: This figure plots the log-multiplicative layer effect across birth cohorts using 5-year bins. The vertical bars represent 95% confidence intervals.

C Weighted Estimates

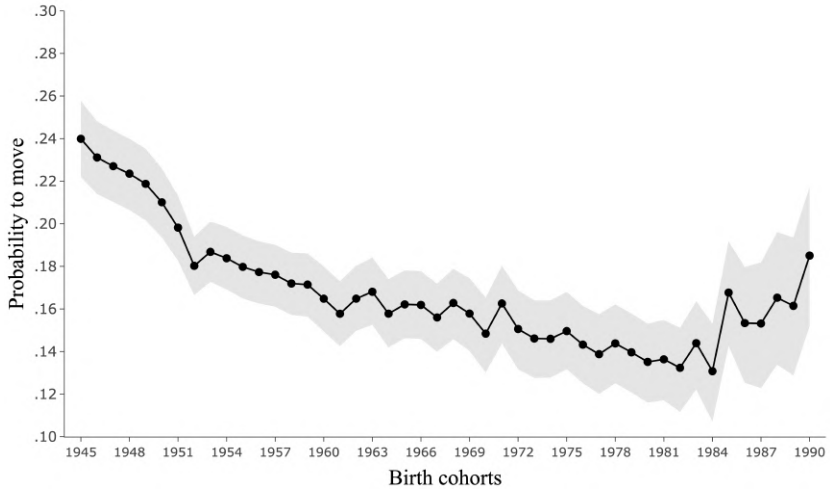
We conducted a parallel analysis using the GSS post-stratification weights, which adjust for unequal probabilities of sample selection, ballot and form assignment errors, and the Black oversamples in 1982 and 1987. The weighted results closely mirror our unweighted estimates. All measures of memory and association exhibit nearly identical patterns, and the weighted cell counts generally fluctuate only a little around the raw counts in the mobility tables. The only noteworthy difference involves our measures of movement, where we observe a slight downward trend in overall and steady-state mobility beginning with cohorts born in the 1950s.

Figure C.1: Measures of movement at generation $t = 1$.

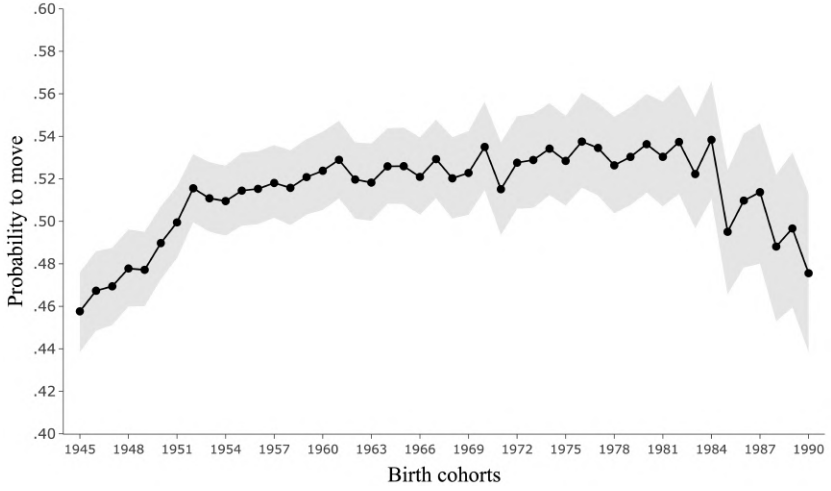
(A) Overall mobility (OM_1)



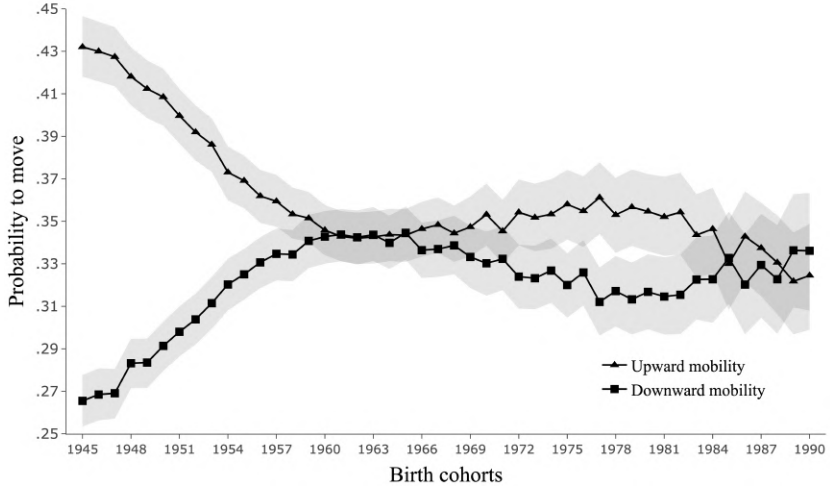
(B) Structural mobility (SM_1)



(C) Exchange mobility (EM_1)

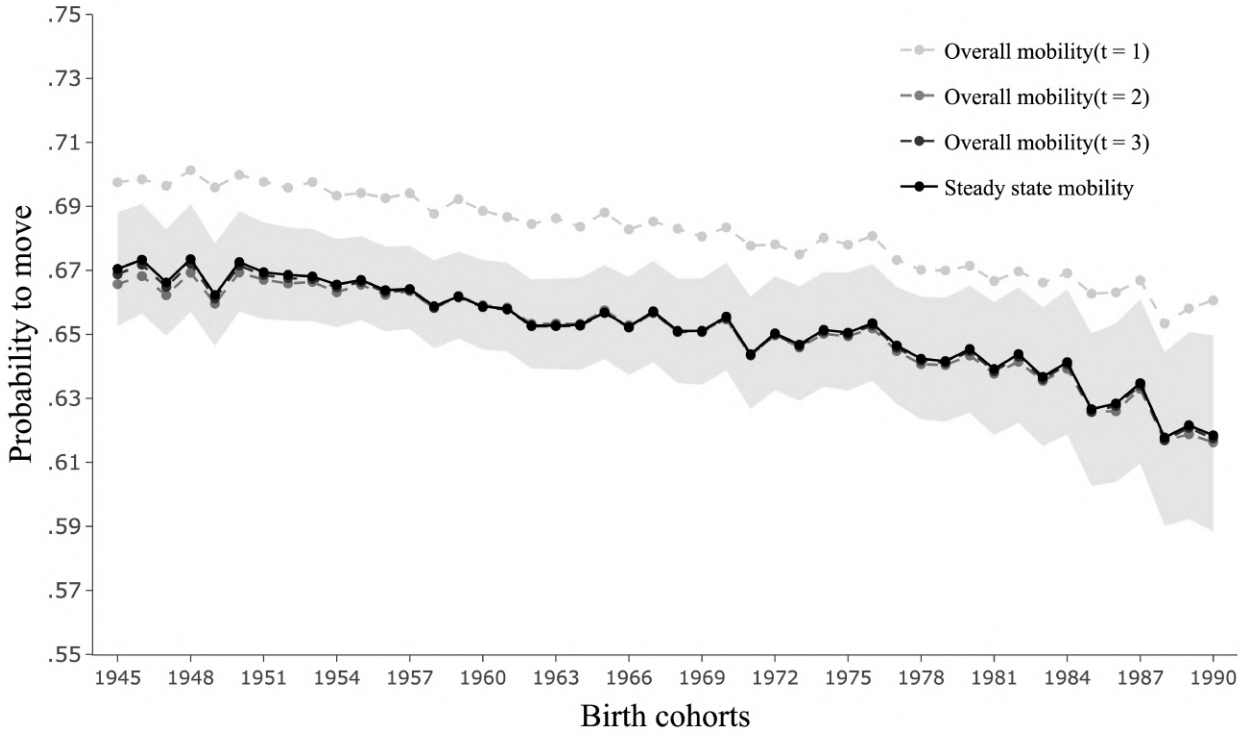


(D) Upward and downward mobility



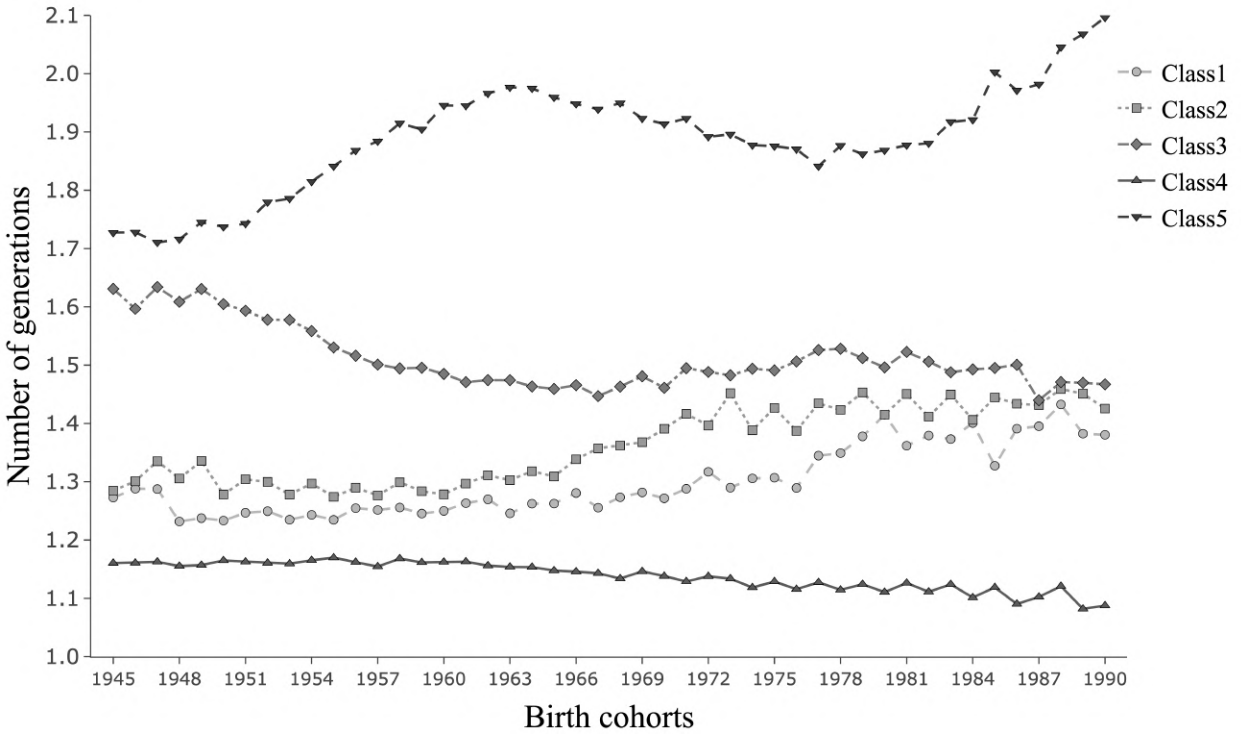
Notes: Shaded areas represent 95% confidence intervals.

Figure C.2: Overall mobility (OM_t) across synthetic generations



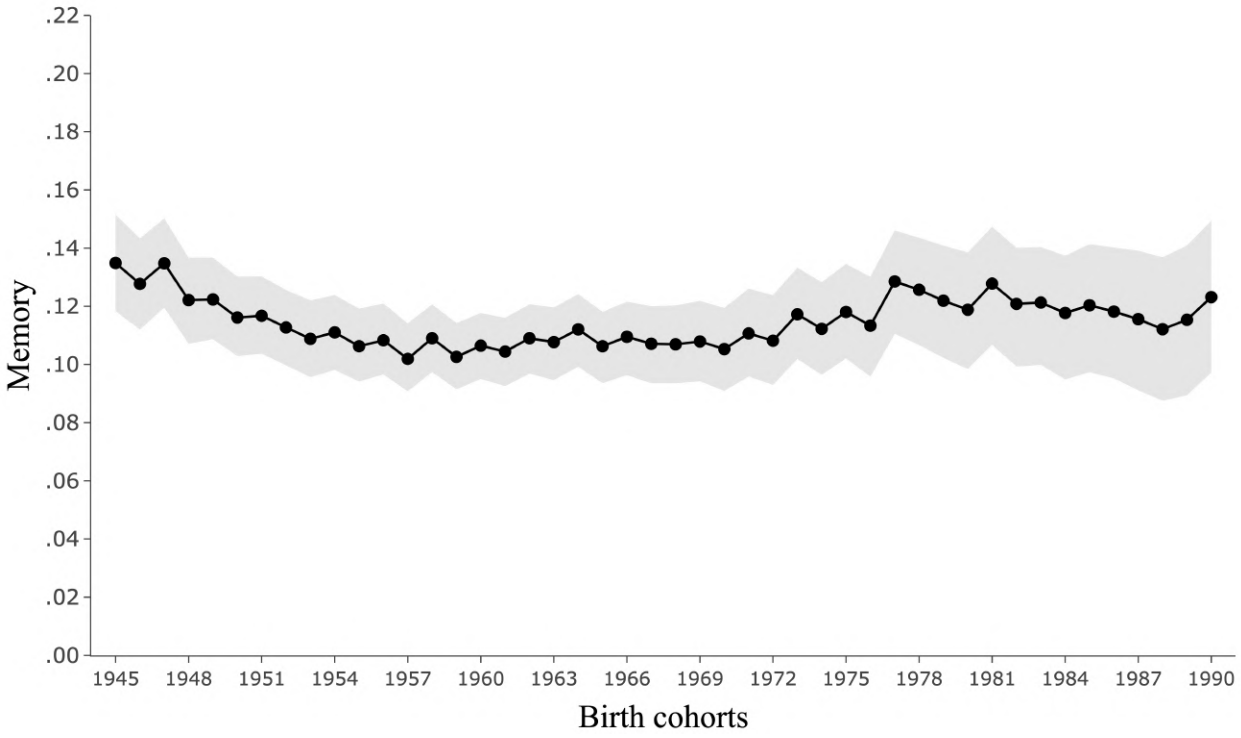
Notes: This figure illustrates the evolution of overall mobility across generations in a stationary Markov chain. By $t = 4$, the Markov chains for all cohorts have converged to their respective steady-state distributions, where there is no structural mobility. Shaded areas represent 95% confidence intervals, which are shown only for the trend in steady-state mobility.

Figure C.3: Mean time to exit from each origin class (MTE_i)



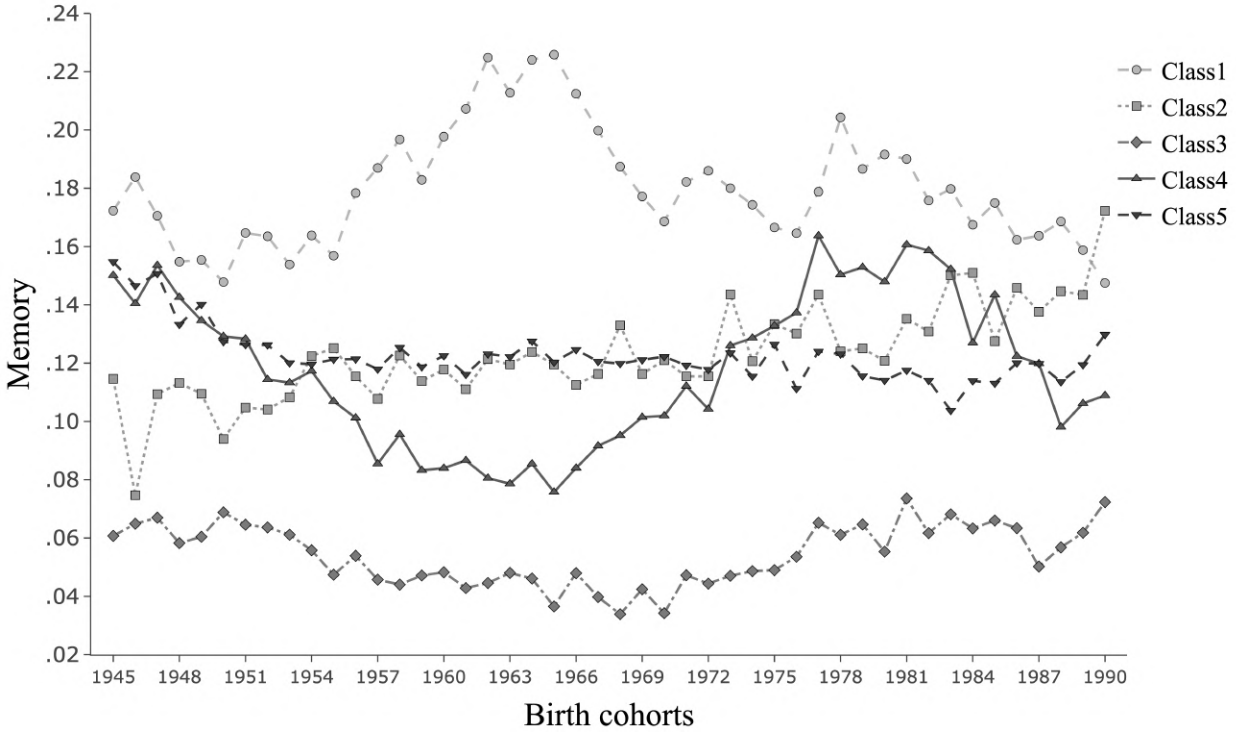
Notes: This figure plots the mean time to exit from each origin class (MTE_i), separately by cohort. Class 1 refers to higher-grade professionals, administrators, and managers; class 2 refers to lower-grade professionals, administrators, and managers; class 3 includes higher-grade routine non-manual workers, technicians, and supervisors; class 4 comprises higher-grade manual workers, lower-grade technicians, and farmers; and class 5 includes lower-grade routine non-manual and manual workers.

Figure C.4: Aggregate intergenerational memory at generation $t = 1$ (AIM_1)



Notes: Shaded areas represent 95% confidence intervals.

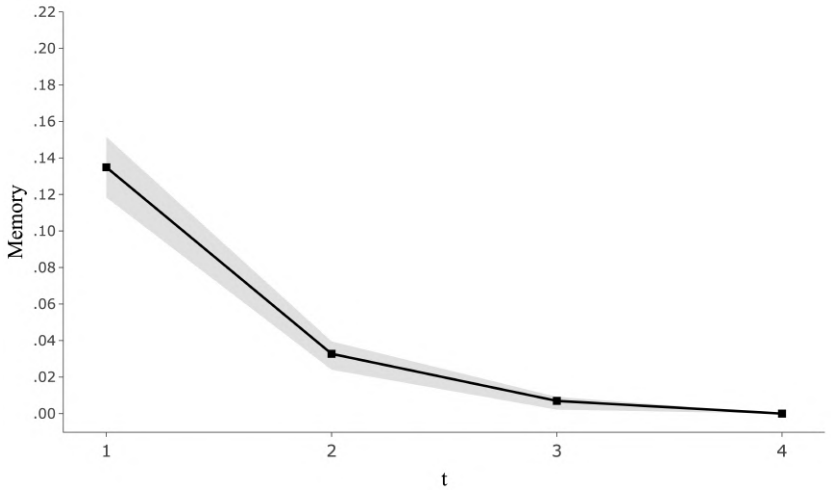
Figure C.5: Intergenerational memory at generation $t = 1$ by origin class ($IM_{i,1}$)



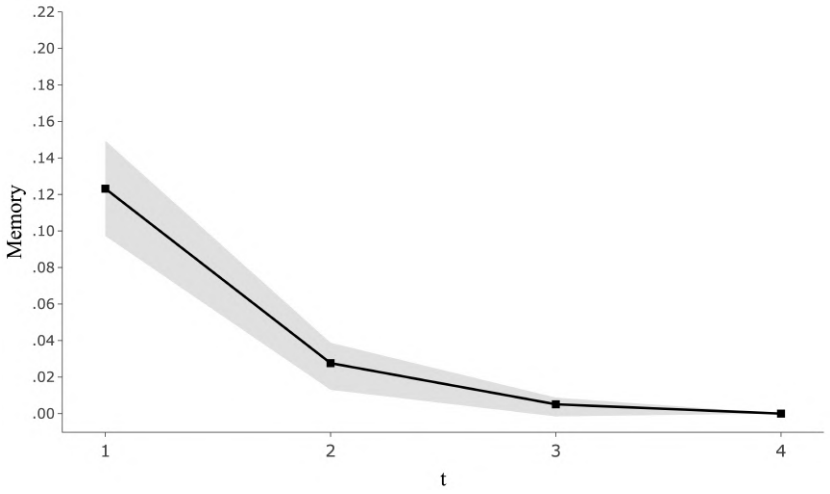
Notes: This figure plots intergenerational memory at generation $t = 1$, separately for each origin class ($IM_{i,1}$) and by cohort. Class 1 refers to higher-grade professionals, administrators, and managers; class 2 refers to lower-grade professionals, administrators, and managers; class 3 includes higher-grade routine non-manual workers, technicians, and supervisors; class 4 comprises higher-grade manual workers, lower-grade technicians, and farmers; and class 5 includes lower-grade routine non-manual and manual workers.

Figure C.6: Memory across synthetic generations in the 1945 and 1990 birth cohorts

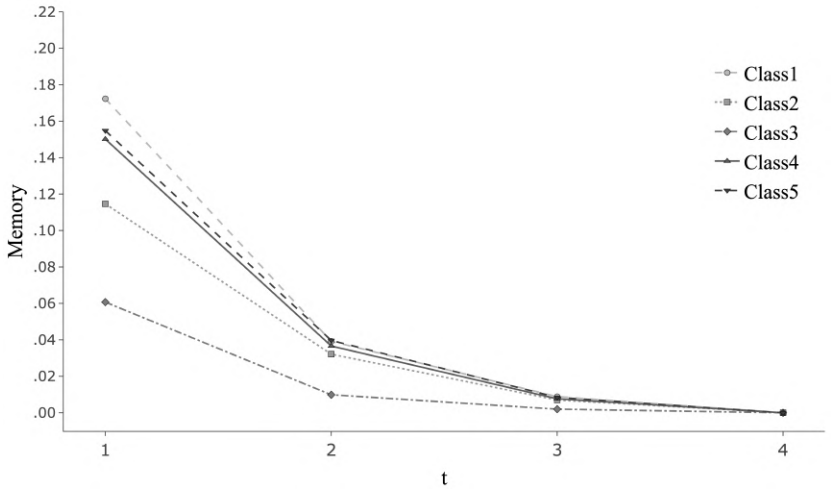
(A) AIM_t for the 1945 cohort



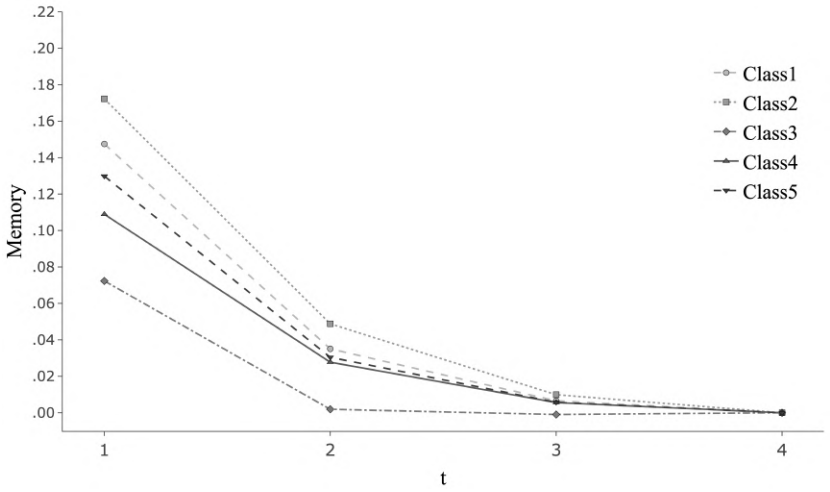
(B) AIM_t for the 1990 cohort



(C) $IM_{i,t}$ for the 1945 cohort



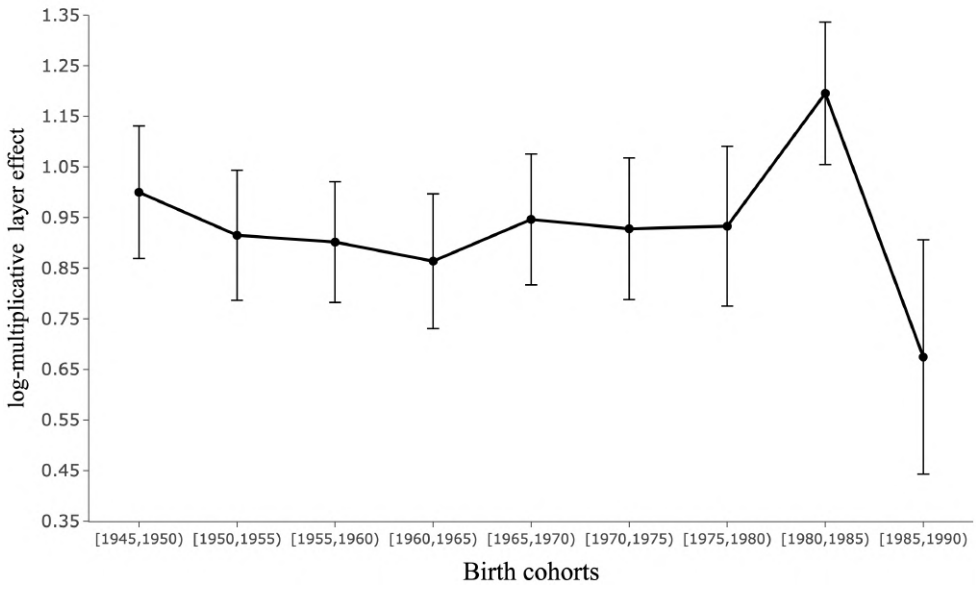
(D) $IM_{i,t}$ for the 1990 cohort



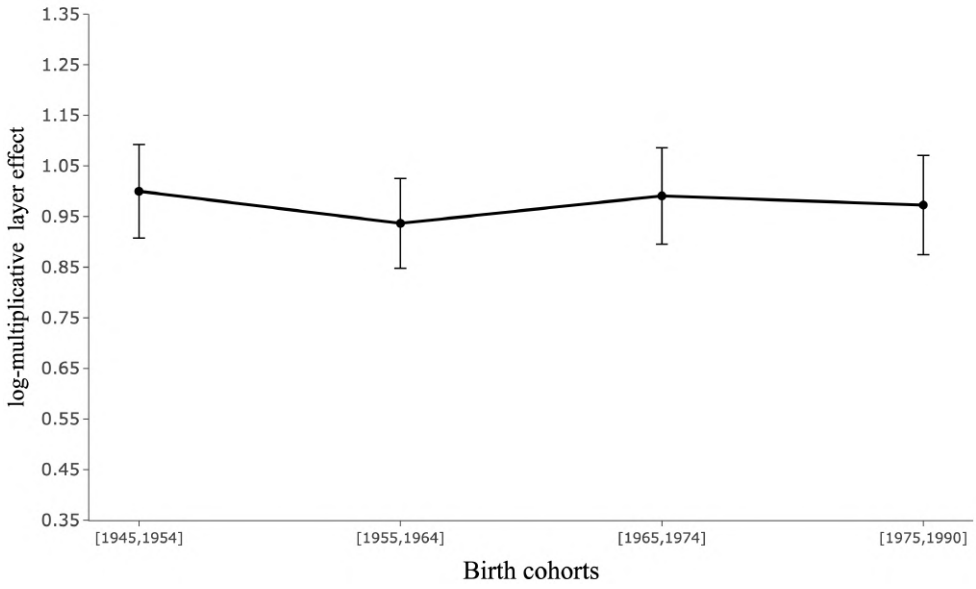
Notes: This figure illustrates the evolution of AIM_t and $IM_{i,t}$ across generations in a stationary Markov chain, separately for the 1945 and 1985 cohorts. By $t = 4$, both transition matrices have converged to the steady state, implying zero memory of class origins. Shaded areas represent 95% confidence intervals.

Figure C.7: Log-multiplicative layer effects

(A) Cohorts in 5-year bins



(B) Cohorts in ∼10-year bins

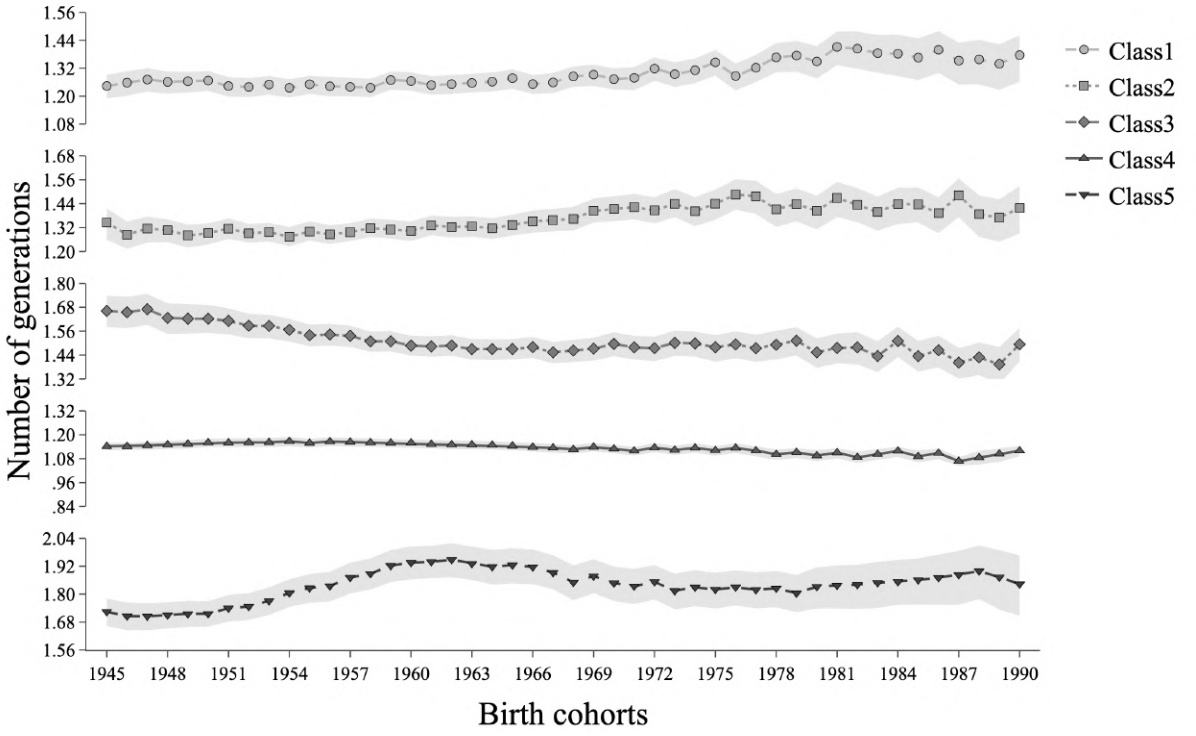


Notes: This figure plots the log-multiplicative layer effect across birth cohorts using 5-year and ∼10-year bins, respectively. The vertical bars represent 95% confidence intervals.

D Confidence Intervals for Class-Specific Measures of Movement and Memory

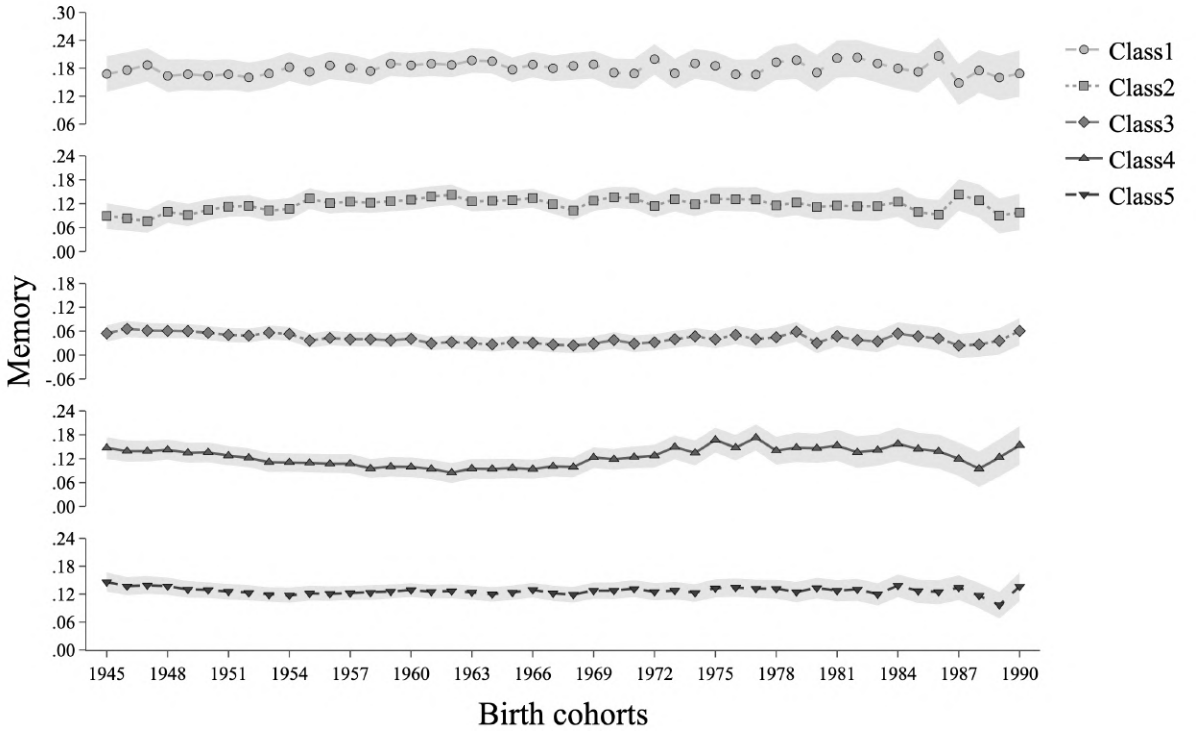
In this section, we report 95% confidence intervals for the class-specific measures of movement and memory presented in the main text. Specifically, Figures D.1 and D.2 reproduce the estimates of mean time to exit (MTE_i) and intergenerational memory at generation $t = 1$ ($IM_{i,1}$) shown in Figures 4 and 7, respectively, together with their 95% confidence intervals.

Figure D.1: Mean time to exit from each origin class (MTE_i) with 95% confidence intervals



Notes: This figure plots the mean time to exit from each origin class (MTE_i), separately by cohort. Shaded areas represent 95% confidence intervals. Class 1 refers to higher-grade professionals, administrators, and managers; class 2 refers to lower-grade professionals, administrators, and managers; class 3 includes higher-grade routine non-manual workers, technicians, and supervisors; class 4 comprises higher-grade manual workers, lower-grade technicians, and farmers; and class 5 includes lower-grade routine non-manual and manual workers.

Figure D.2: Intergenerational memory at generation $t = 1$ by origin class ($IM_{i,1}$) with 95% confidence intervals



Notes: This figure plots intergenerational memory at generation $t = 1$, separately for each origin class ($IM_{i,1}$) and by cohort. Shaded areas represent 95% confidence intervals. Class 1 refers to higher-grade professionals, administrators, and managers; class 2 refers to lower-grade professionals, administrators, and managers; class 3 includes higher-grade routine non-manual workers, technicians, and supervisors; class 4 comprises higher-grade manual workers, lower-grade technicians, and farmers; and class 5 includes lower-grade routine non-manual and manual workers.

E Alternative Measures of Mobility

In this section, we report estimates from several alternative measures of movement, memory, and association. We begin with an alternative measure of movement—class outflows—computed from both the observed transition matrices and the Markov steady state. Specifically, we estimate and report the follow quantity:

$$O_{i,t} = \sum_{j \neq i} P_{ij}^{t},$$

for $t = 1$ and for $t = \infty$. These results are presented in Figure E.1. The outflow patterns capture movement out of each origin class separately and thus tend to mirror the patterns in our measure of mean time to exit. They too are consistent with somewhat lower movement for the upper and lower classes and somewhat higher movement in the middle, particularly for class 3 (higher-grade routine non-manual workers, technicians, and supervisors).

We next turn to mean first passage time (MFPT; Grinstead and Snell 1997; Kemeny and Snell 1976). MFPT characterizes movement between specific pairs of classes across generations of synthetic dynasties. The MFPT estimates the expected number of generations it would take to reach destination class j when starting from origin class i in the founding generation of a dynasty. We follow the logic for computing this measure as outlined in Grinstead and Snell (1997). Consider an ergodic Markov chain, and let $MFPT_{ij}$ denote the expected number of generations needed to reach class j from class i (for $i \neq j$). If the process reaches j in the first generation, then the transition occurs with probability 1, and thus $MFPT_{ij} = 1$. However, if this direct transition does not occur, the process instead moves to some intermediate state k in the first generation. In this case, one generation has already passed, and the expected number of additional generations to reach j from k is given by $MFPT_{kj}$. The total expected number of generations from i to j can therefore be formally defined as follows:

$$MFPT_{ij} = P_{ij} + \sum_{k \neq j} P_{ik} \cdot (MFPT_{kj} + 1), \tag{E1}$$

or since $\sum_k P_{ik} = 1$,

$$MFPT_{ij} = 1 + \sum_{k \neq j} P_{ik} \cdot MFPT_{kj}. \tag{E2}$$

Therefore, $MFPT_{ij}$ can be computed from Equation (E2) by solving, in our case, a system of 20 equations. Since we are using a 5×5 transition matrix, there are 25 possible

(i, j) class combinations. Excluding the 5 diagonal elements where $i = j$, we are left with 20 off-diagonal unknowns, each corresponding to a distinct $MFPT_{ij}$, to be solved simultaneously.

Figure E.2 shows estimates of the MFPT from origin class i to destination class j, separately by cohort. Downward transitions appear in the top panel, while upward transitions are shown in the bottom panel. Except for class 4 (higher-grade manual workers, lower-grade technicians, and farmers), which is a rare destination for all origins, we generally observe longer times for upward than for downward transitions. Among the upward transitions, class 3 is the most readily attainable destination for classes 4 and 5. For downward transitions, class 3 is again the most common destination for the top two classes. These patterns change little across cohorts.

Next, we examine alternative measures of intergenerational memory, including the maximum distance to stationarity (Blume et al., 2025; Levin et al., 2009) and the second-largest eigenvalue of the transition matrix (Sommers and Conlisk, 1979; Conlisk and Sommers, 1979; Shorrocks, 1978). These measures respectively quantify the distance from the steady state, and the speed at which the Markov process converges to it. The maximum distance to stationarity can be formally defined as follows:

$$d_t = \max_i \sum_j |P_{ij}^t - \mu_{j,\infty}|, \tag{E3}$$

which represents the largest difference between any row of the observed transition matrix and the steady-state distribution μ_∞. The magnitude of d_t represents the worst-case distance of the Markov process from its steady state——the largest deviation from equality of opportunity across all class origins at generation t. Conceptually, it is analogous to aggregate intergenerational memory AIM_t defined in Equation (6), but with a key distinction: while AIM_t reflects the average distance to the steady state across all origin classes, d_t captures the maximal deviation. Equivalently, d_t can be interpreted as the maximum value of the individual memory metric $IM_{i,t}$ from Equation (7), taken across all origin classes i, thereby highlighting the "worst-case class origin" with respect to its distance from multi-generational equality of opportunity.

To provide an intuitive explanation of the second-largest eigenvalue as a measure of memory, recall the standard spectral decomposition for diagonalizable matrices (Meyer, 2000, pp. 517–518; Bhatia, 1997, pp. 4–5):

$$P = V\Lambda V^{-1} = V\Lambda U = \sum_i \lambda_i \mathbf{v}_i \mathbf{u}_i, \tag{E4}$$

where V is the matrix whose columns are the right eigenvectors $\mathbf{v}_i$, Λ is the diagonal matrix of eigenvalues λ_i, and $U = V^{-1}$ is the matrix whose rows are the left eigenvectors $\mathbf{u}_i$, normalized such that $\mathbf{u}_i\mathbf{v}_k = \delta_{ik}$. Recall that a vector $\mathbf{v}$ is a right eigenvector if $P\mathbf{v} = \lambda\mathbf{v}$, while a vector $\mathbf{u}$ is called a left eigenvector if $\mathbf{u}P = \lambda\mathbf{u}$.

Then, for the t-th generation in our setting, the expression can be written as:

$$P^t = \sum_i \lambda_i^t \mathbf{v}_i \mathbf{u}_i. \tag{E5}$$

To derive the expression for the distribution of classes in generation t, we apply the matrix P^t to the initial row distribution μ_0:

$$\mu_t = \mu_0 P^t = \mu_0 \sum_i \lambda_i^t \mathbf{v}_i \mathbf{u}_i = \sum_i \lambda_i^t (\mu_0 \mathbf{v}_i)\mathbf{u}_i = \sum_i \lambda_i^t \alpha_i \mathbf{u}_i, \tag{E6}$$

where $\alpha_i = (\mu_0 \mathbf{v}_i)$ denotes the scalar obtained by applying the initial distribution to the right eigenvector $\mathbf{v}_i$. Recall that the eigenvalues of P are ordered by modulus such that

$$|\lambda_1| = 1 > |\lambda_2| \geq \cdots \geq |\lambda_n|.$$

Because P is row-stochastic, the dominant eigenvalue λ_1 equals 1, with corresponding right eigenvector $\mathbf{v}_1 = \mathbf{1}$ and normalized left eigenvector $\mathbf{u}_1 = \mu_\infty$, the steady-state distribution (Sommers and Conlisk, 1979). Since $\mu_0\mathbf{1} = 1$, we can rewrite Equation (E6) in a form that is more intuitive for our analysis:

$$\mu_t = \mu_\infty + \lambda_2^t \alpha_2 \mathbf{u}_2 + \cdots + \lambda_n^t \alpha_n \mathbf{u}_n. \tag{E7}$$

For the purpose of studying mobility, the transient left eigenvectors $\mathbf{u}_i$, for $i \geq 2$, can be interpreted as the principal directions along which the current distribution μ_t converges toward the steady-state distribution μ_∞. Each $\mathbf{u}_i$ identifies a "barrier" that may slow this evolution, and the elements of $\mathbf{u}_i$ correspond to category-specific coordinates along that direction. The scalar coefficients α_i measure the initial distribution's loading, or relative weight, on each barrier, while the eigenvalues λ_i indicate the persistence of the corresponding barrier over generations t. Since $|\lambda_i| < 1$ for $i \geq 2$, as $t \to \infty$, all terms multiplied by λ_i^t converge to zero. Modes associated with smaller eigenvalue moduli decay more quickly, while the mode associated with $|\lambda_2|$ is asymptotically the slowest-decaying component, provided that its loading is nonzero. Consequently, the mode associated with $|\lambda_2|$ can be interpreted as the dominant, most persistent pattern constraining intergenerational mobility, and $|\lambda_2|$ governs the asymptotic rate of persis-

tence in the system. Larger values of $|\lambda_2|$ correspond to slower convergence and, therefore, lower mobility conceptualized as memory. Formally, the convergence rate can be bounded as

$$\|\mu_\infty - \mu_t\| \leq c\,|\lambda_2|^t, \quad \text{where} \quad c = \sum_{i=2}^{n} |\alpha_i|\,\|\mathbf{u}_i\|, \tag{E8}$$

with c a constant depending on the initial distribution and the left eigenvectors.

Figure E.3 plots trends in d_t and $|\lambda_2|$ across cohorts. These trends align closely with our results from the main text, showing a fairly stable pattern over time. Overall, the weight of the evidence suggests there has been little change in intergenerational memory.

Finally, we consider several alternative measures of association that are based on the joint distribution of parental and child occupations, in contrast to the conditional probabilities represented by the transition matrix. These include the Altham index (Altham, 1970) and the Hellinger dependence index (Coleman and Lukina, 2025; Geenens and Lafaye de Micheaux, 2022). Both summarize the degree of dependence in the joint probability distribution of parental origins and child destinations.

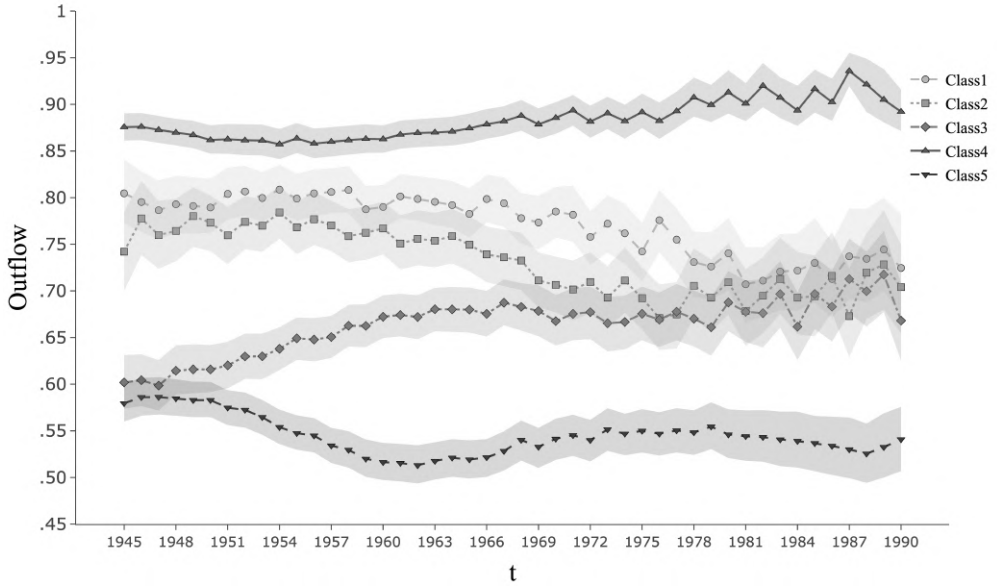
The Altham index provides a summary measure of dependence in a contingency table by quantifying the deviation of an observed probability matrix from the independence matrix. Formally, it is defined as the square root of the sum of squared deviations of all log-odds ratios from zero. Recall that, under perfect independence, all odds ratios equal one, and their logarithms equal zero. The index ranges from 0 to ∞, where 0 indicates no association, and higher values signify stronger dependence between origins and destinations, corresponding to lower mobility. The index has no finite upper bound because, in theory, the odds ratios can become arbitrarily large, reflecting extreme persistence of status across generations.

The Hellinger index uses iterative proportional fitting to transform the marginal proportions of the probability matrix to a uniform distribution while preserving the underlying dependence structure (i.e., the odds ratios). The transformed matrices with uniform marginals are then contrasted with the independence matrix under uniform marginals. The measure ranges from 0 to 1, where 0 indicates complete independence between origins and destinations and 1 indicates perfect dependence.

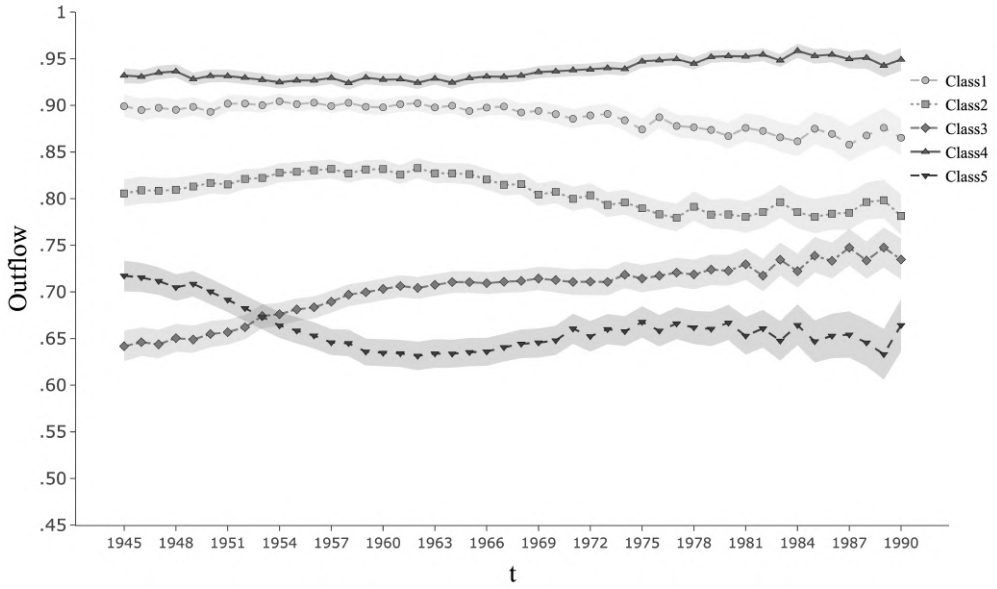
Figure E.4 displays estimates of the Altham and Hellinger indices computed from the smoothed mobility tables. As with our other measures of association—in particular, the log-multiplicative layer effects from the model in Equation 9—these trends provide little evidence of an upward or downward shift. The point estimates fluctuate in no clear direction, especially among more recent cohorts, but these changes generally cannot be statistically distinguished from the levels observed among earlier cohorts.

Figure E.1: Class outflows at generation $t = 1$ and at the steady state

(A) Outflows at generation $t = 1$

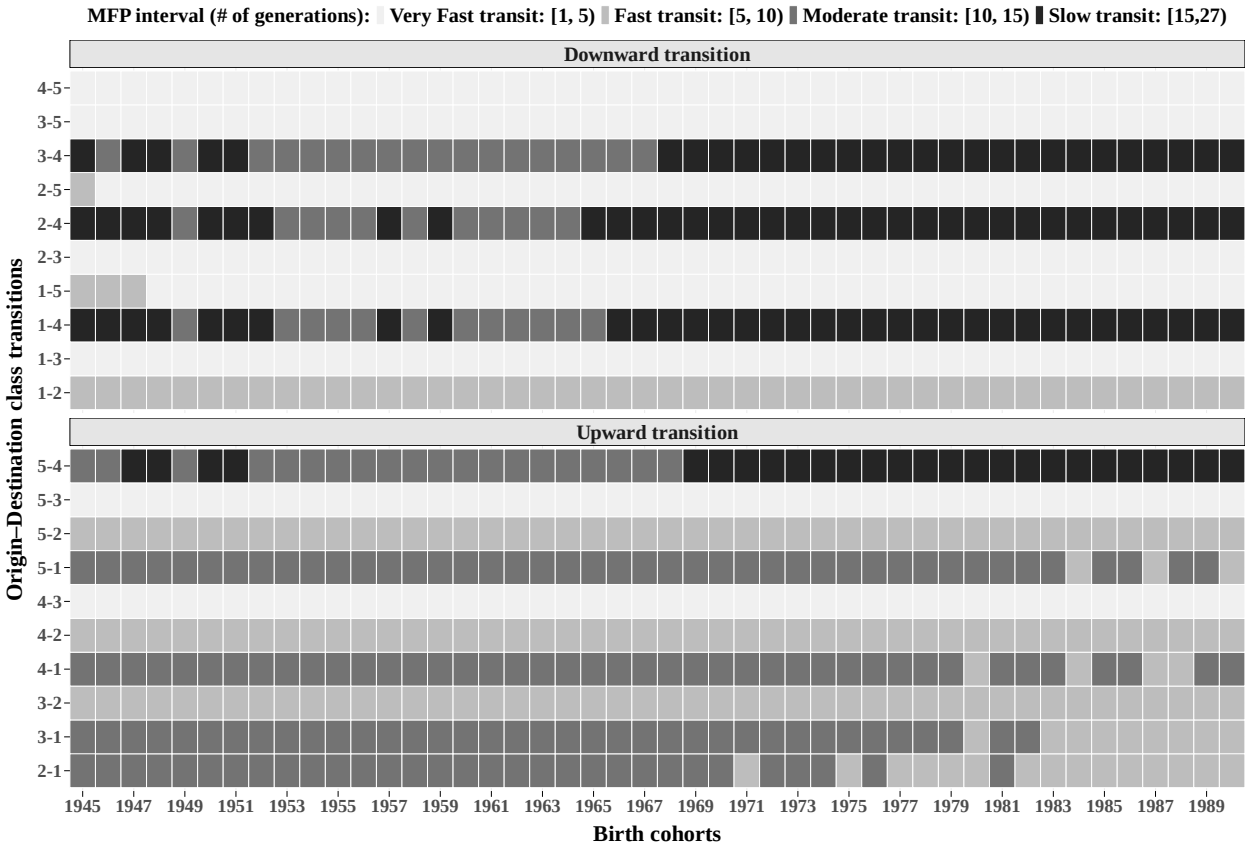


(B) Outflows at the steady state



Notes: Shaded areas represent 95% confidence intervals. Class 1 refers to higher-grade professionals, administrators, and managers; class 2 refers to lower-grade professionals, administrators, and managers; class 3 includes higher-grade routine non-manual workers, technicians, and supervisors; class 4 comprises higher-grade manual workers, lower-grade technicians, and farmers; and class 5 includes lower-grade routine non-manual and manual workers.

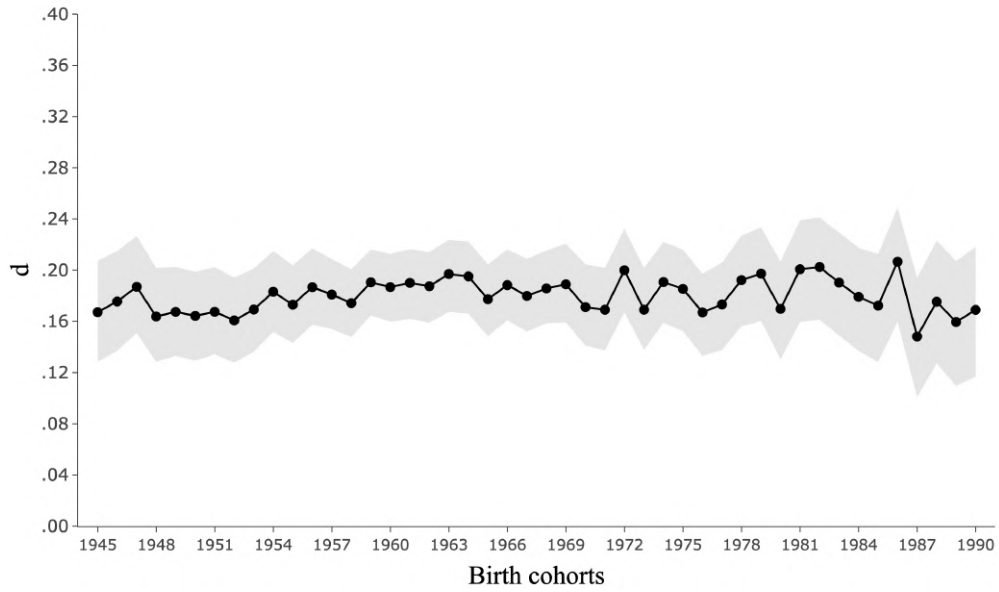
Figure E.2: Mean first passage time



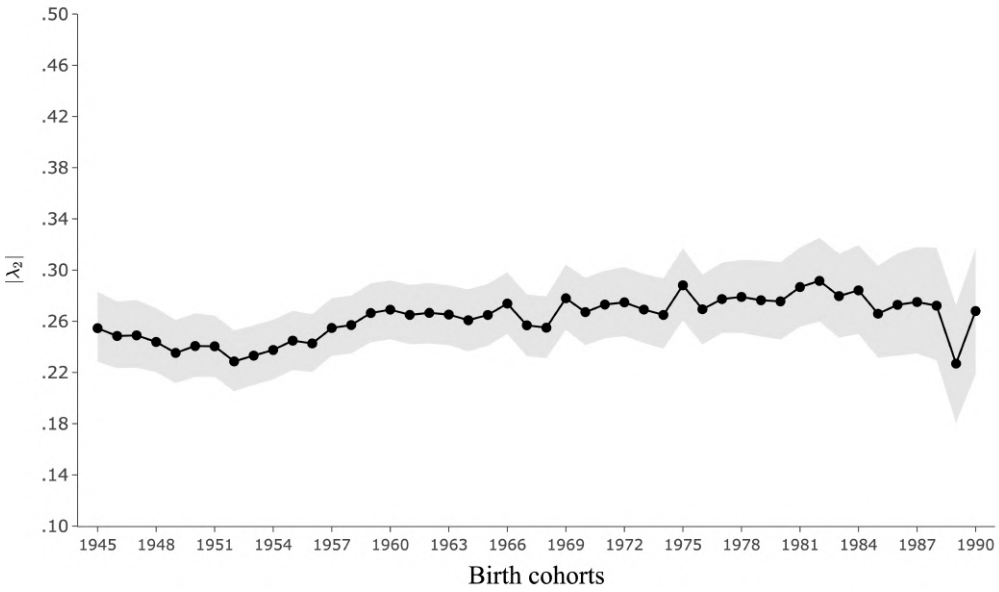
Notes: Class 1 refers to higher-grade professionals, administrators, and managers; class 2 refers to lower-grade professionals, administrators, and managers; class 3 includes higher-grade routine non-manual workers, technicians, and supervisors; class 4 comprises higher-grade manual workers, lower-grade technicians, and farmers; and class 5 includes lower-grade routine non-manual and manual workers.

Figure E.3: Alternative measures of memory

(A) Maximum distance to stationarity (d_t)



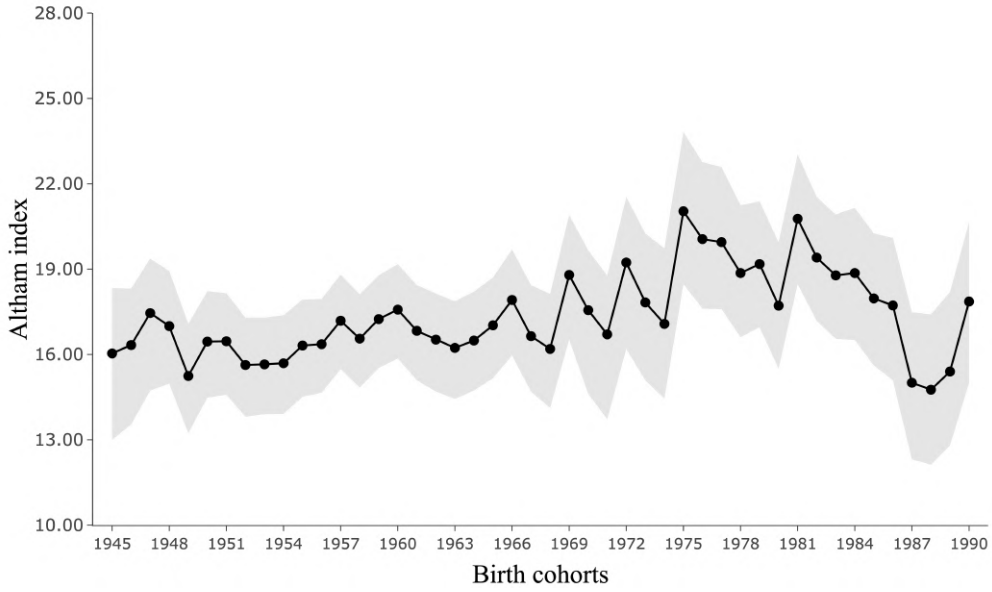
(B) Second largest eigenvalue modulus ($|\lambda_2|$)



Notes: Shaded areas represent 95% confidence intervals.

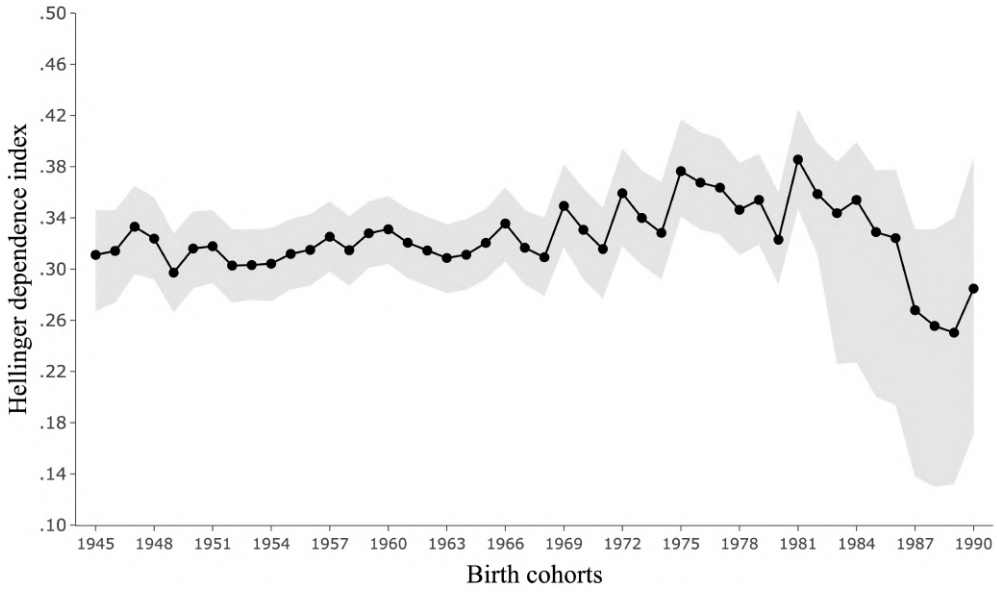
Figure E.4: Alternative measures of dependence

(A) Altham index



Notes: Shaded areas represent 95% confidence intervals.

(B) Hellinger dependence index



Notes: Shaded areas represent 95% confidence intervals.

F Trends by Gender

In this section, we examine potential gender differences in mobility patterns across cohorts. Specifically, we replicate our main analyses using transition matrices constructed separately from father-daughter, father-son, mother-child, mother-son, and mother-daughter pairs, rather than from the pooled father–child pairs used in the main text. We also construct transition matrices based on the highest-ranked class of either parent. Trend estimates based on father-daughter pairs are presented in Figures F.1 to F.4, while those based on father-son pairs appear in Figures F.5 to F.8. Estimates based on mother-child pairs are shown in Figures F.9 to F.12, while those based on mother-son pairs appear in Figures F.13 to F.16 and those based on mother-daughter pairs in Figures F.17 to F.20. Estimates based on the highest-ranked class of either parent are presented in Figures F.21 to F.24. Owing to sample-size limitations—particularly the small number of female observations in Class 4—the retained samples include 15,560 mother-child pairs (respondents aged 25–55, born between 1948 and 1990), 5,206 mother-son pairs (respondents aged 25–55, born between 1952 and 1979), 7,273 mother-daughter pairs (respondents aged 25–55, born between 1952 and 1983), 11,046 father-daughter pairs (respondents aged 25–55, born between 1945 and 1977), and 11,879 higher-status-parent-child pairs (respondents aged 25–55, born between 1945 and 1990). A narrower range of cohorts is retained in some of these ancillary analyses because we exclude cohorts for which more than 5% of the bootstrap replications yield non-primitive transition matrices.

Compared with the baseline father-child results, upward mobility is generally higher among father-daughter dyads and among mother-child dyads in the earlier cohorts. These patterns reflect changes in women's occupational positions across generations. Among the occupational specifications presented here, the higher-status-parent-child specification is the only one in which the origin is defined as a function of both parents' occupational classes, although it summarizes them in a single origin class. In contrast to the parent-specific origin measures, it shows substantially higher downward than upward mobility for most cohorts, while overall mobility remains broadly stable. Since the higher-status-parent dyads are restricted to respondents with occupational-class information available for both parents, whereas parent-specific dyads need not impose the same restriction, these dyad constructions may differ in their composition with respect to family structure and parental employment. These differences may then be related to social processes such as assortative marriage and parental occupational role modeling. Given the limited sample available for respondents raised in single-parent families, examining whether occupational mobility trends differ across family structures remains a

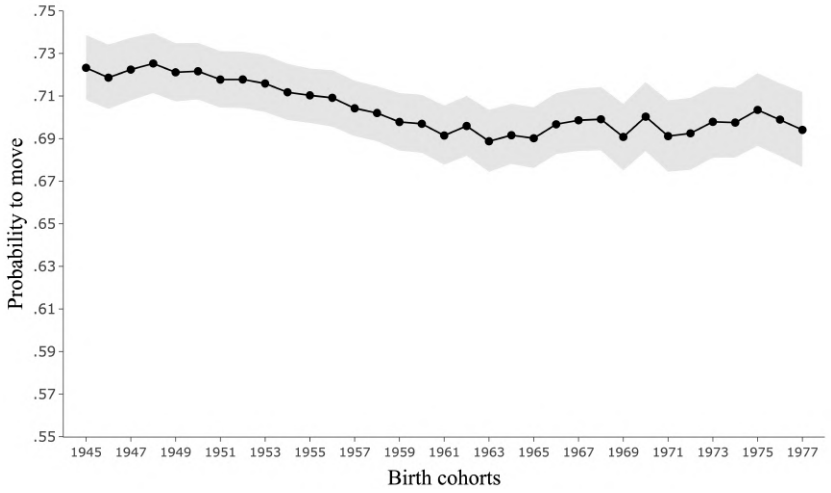
direction for future research. Overall, our results provide little consistent evidence of declining occupational mobility along maternal lineages.

To examine whether the broadly stable mobility pattern is specific to occupational class and to further explore the maternal role in mobility, we replicate a subset of our analyses using educational attainment as an alternative outcome. Here, we classify parents' and respondents' completed years of schooling into five categories: more than 16 years, 16 years, 13–15 years, 12 years, and fewer than 12 years, with category 1 representing the highest attainment. The sample consists of respondents born between 1945 and 1990 who were aged 25-55 at the time of the survey. As in our analysis from the main text, we apply generalized additive model (GAM) smoothing to reduce sampling variability. Figures F.25 to F.36 present aggregate intergenerational memory at t=1, steady-state mobility, and log-multiplicative layer effects for mother-child, mother-son, mother-daughter, and highest-educated-parent-child pairs.

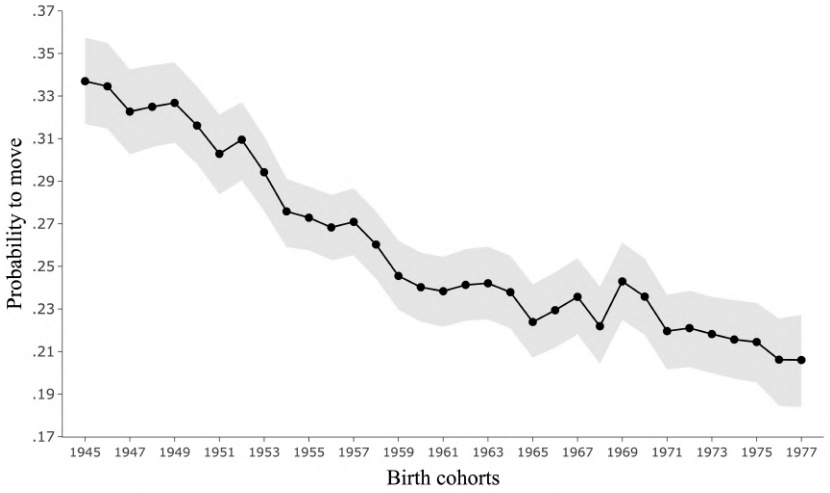
Educational mobility exhibits some different patterns compared with occupational mobility, particularly for memory. Aggregate intergenerational memory generally declines across cohorts for all dyads examined. The log-multiplicative layer effects generally show declining point estimates as well, although they remain imprecise. Steady-state mobility, on the other hand, remains broadly stable. Taken together, then, the results of all these ancillary analyses still provide essentially no evidence of declining mobility even after incorporating maternal origins and stratifying the analysis in different ways by gender.

Figure F.1: Measures of movement at generation $t = 1$ based on father-daughter pairs

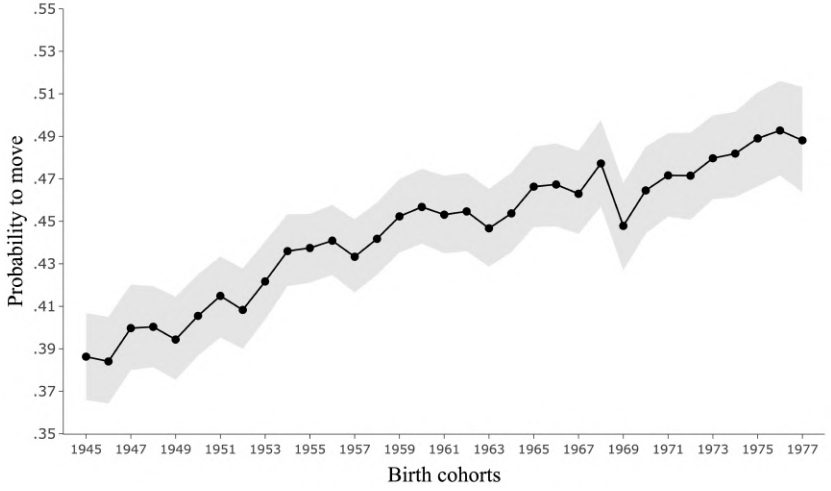
(A) Overall mobility (OM_1)



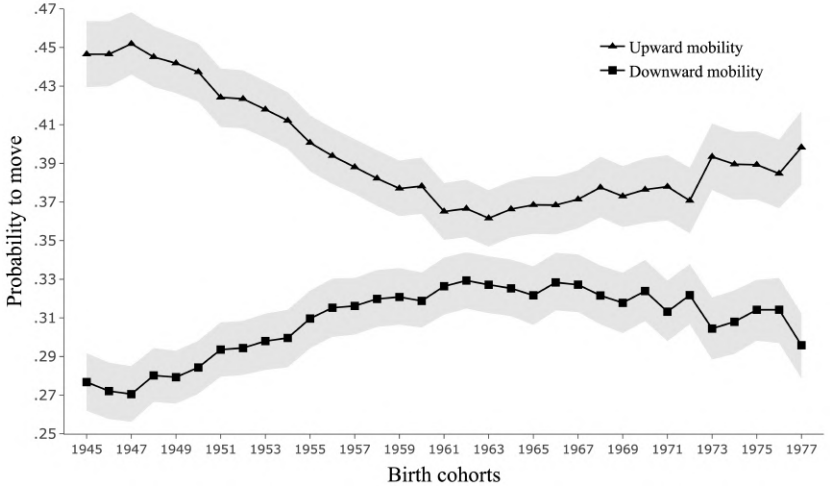
(B) Structural mobility (SM_1)



(C) Exchange mobility (EM_1)

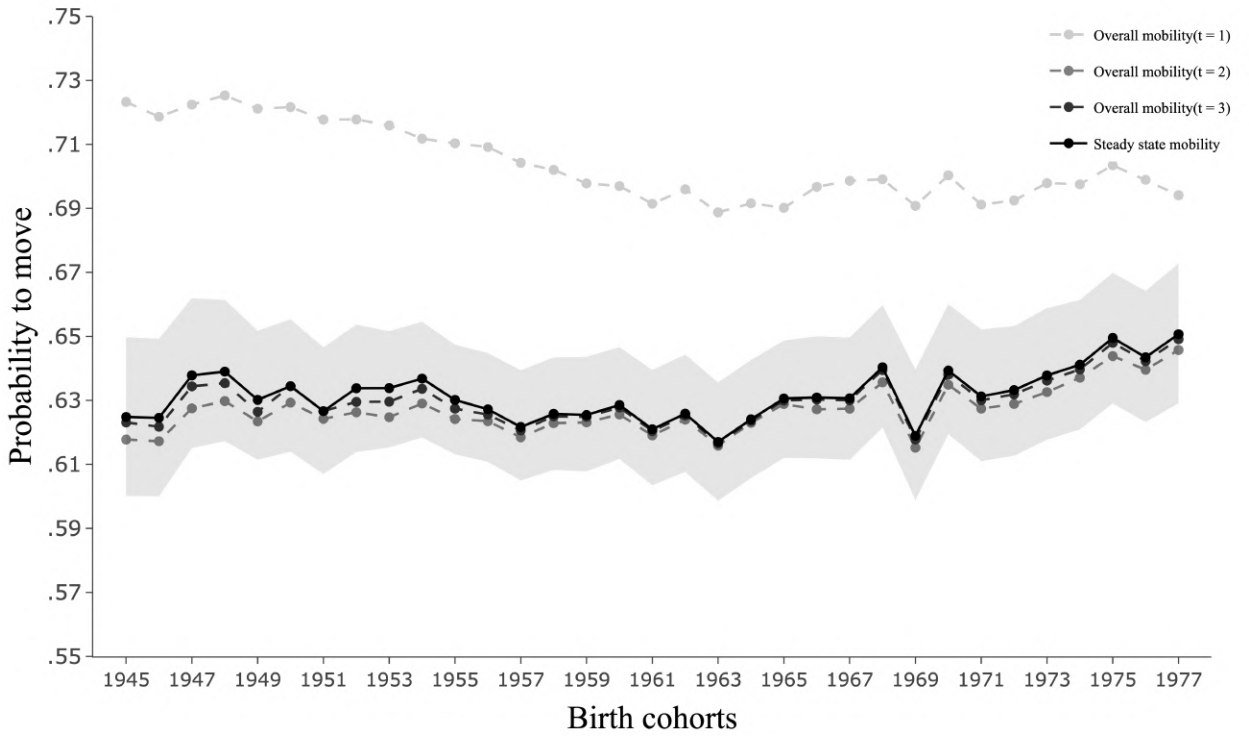


(D) Upward and downward mobility



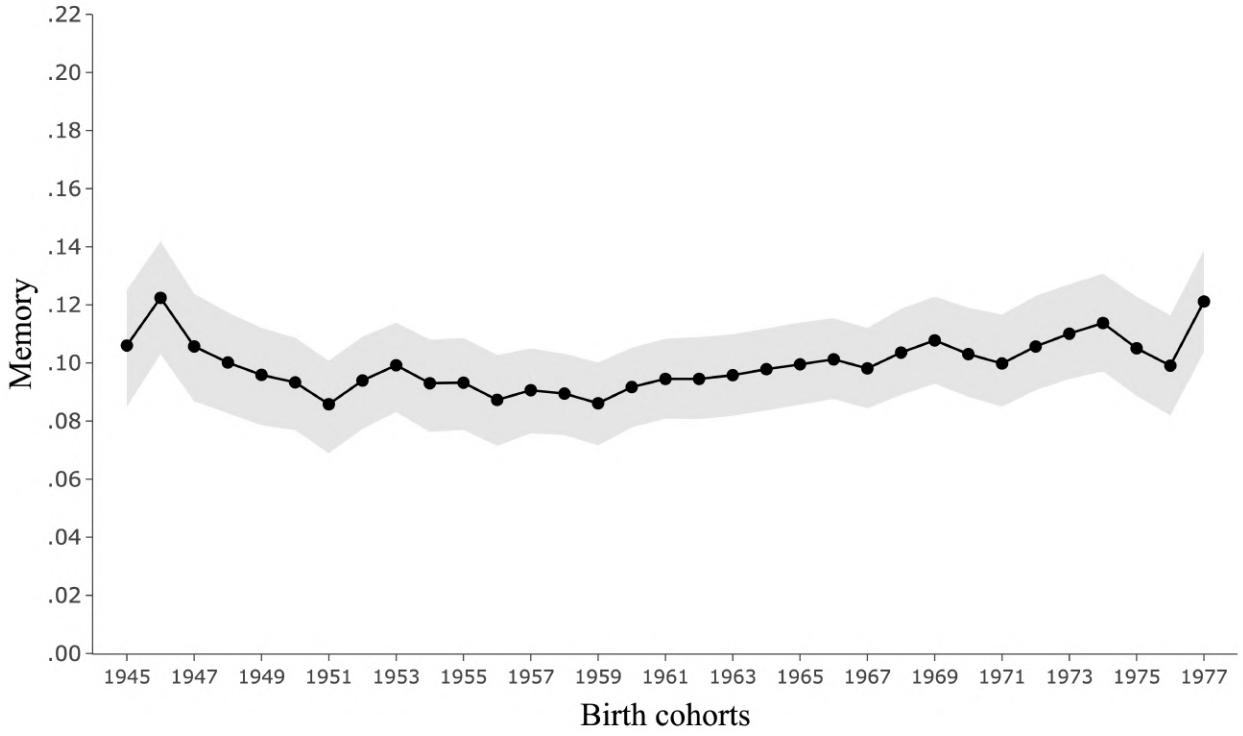
Notes: Shaded areas represent 95% confidence intervals.

Figure F.2: Overall mobility (OM_t) across synthetic generations based on father-daughter pairs



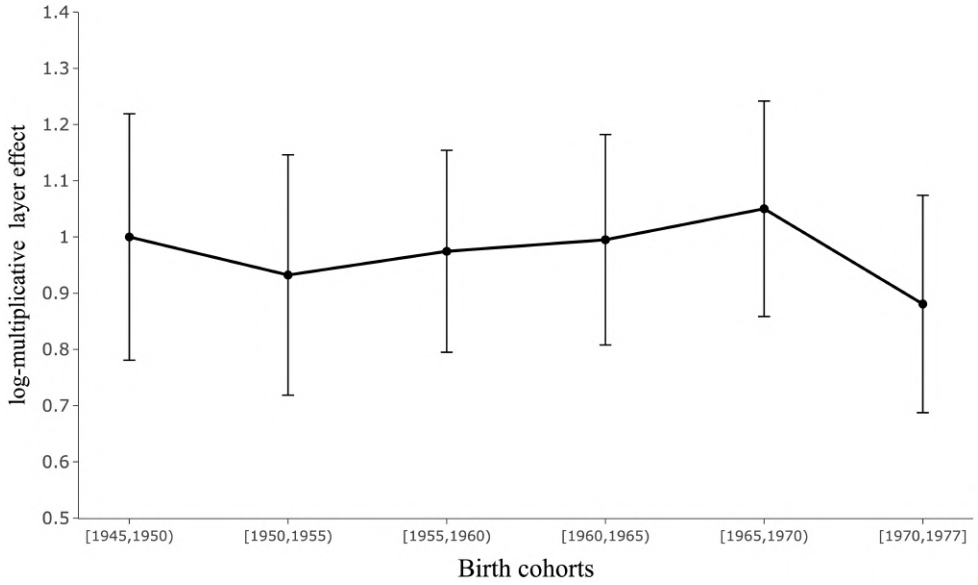
Notes: This figure illustrates the evolution of overall mobility across generations in a stationary Markov chain. By $t = 4$, the Markov chains for most of the cohorts have converged to their respective steady-state distributions, where there is no structural mobility. Shaded areas represent 95% confidence intervals, which are shown only for the trend in steady-state mobility.

Figure F.3: Aggregate intergenerational memory at generation $t = 1$ (AIM_1) based on father-daughter pairs



Notes: Shaded areas represent 95% confidence intervals.

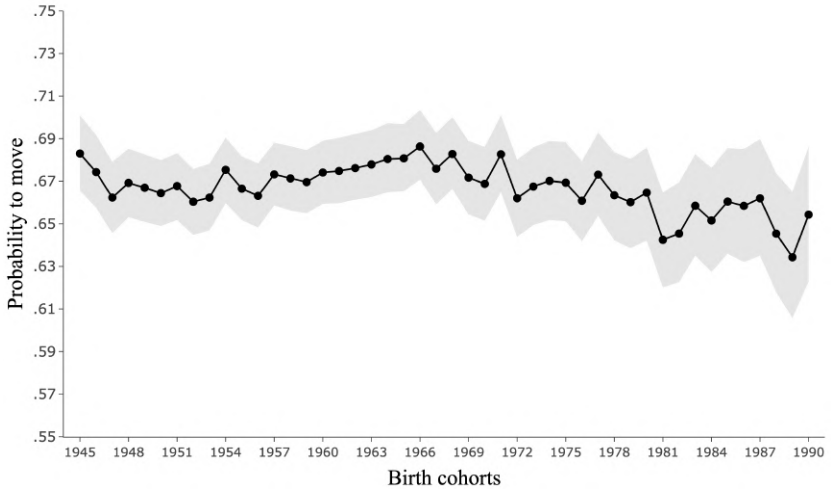
Figure F.4: Log-multiplicative layer effects based on father-daughter pairs



Notes: This figure plots the log-multiplicative layer effect across birth cohorts using ∼5-year bins. The vertical bars represent 95% confidence intervals.

Figure F.5: Measures of movement at generation $t = 1$ based on father-son pairs

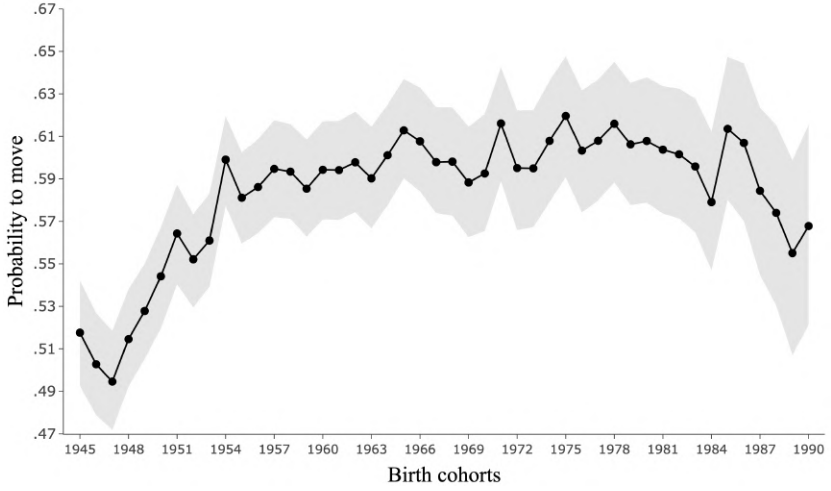
(A) Overall mobility (OM_1)



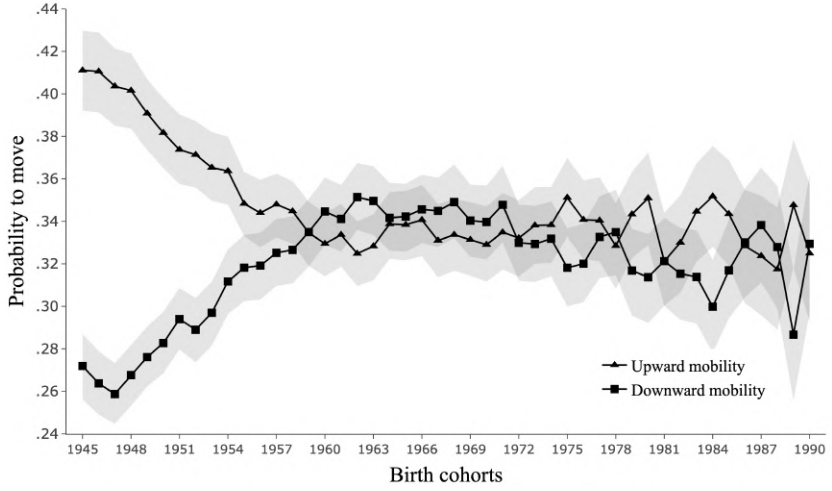
(B) Structural mobility (SM_1)



(C) Exchange mobility (EM_1)

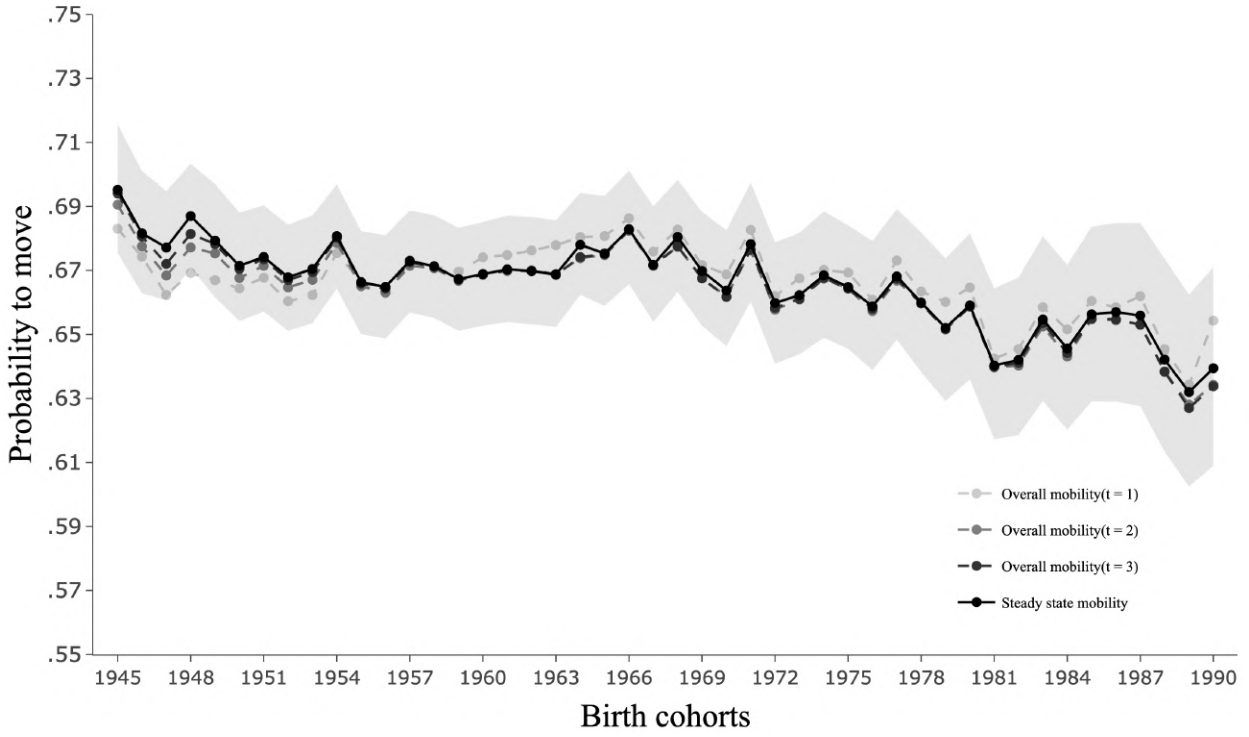


(D) Upward and downward mobility



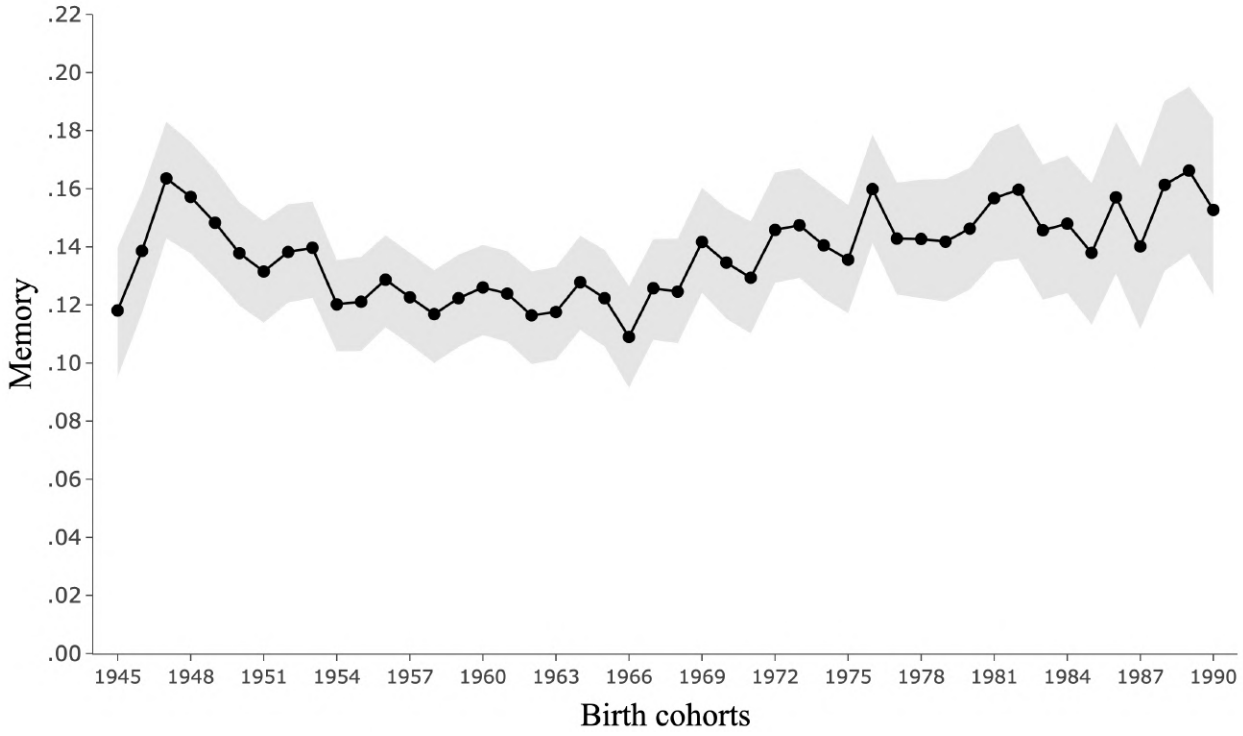
Notes: Shaded areas represent 95% confidence intervals.

Figure F.6: Overall mobility (OM_t) across synthetic generations based on father-son pairs



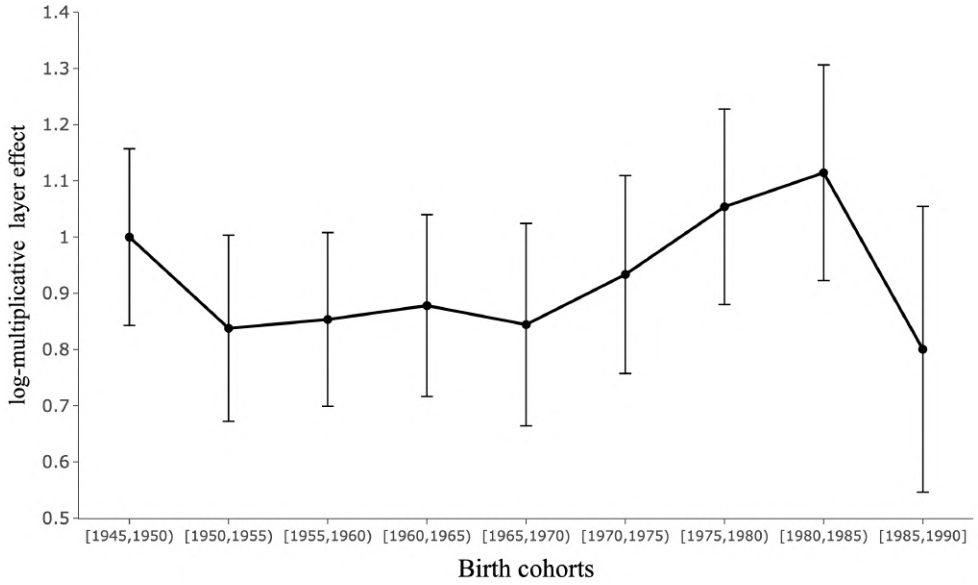
Notes: This figure illustrates the evolution of overall mobility across generations in a stationary Markov chain. By $t = 4$, the Markov chains for most of the cohorts have converged to their respective steady-state distributions, where there is no structural mobility. Shaded areas represent 95% confidence intervals, which are shown only for the trend in steady-state mobility.

Figure F.7: Aggregate intergenerational memory at generation $t = 1$ (AIM_1) based on father-son pairs



Notes: Shaded areas represent 95% confidence intervals.

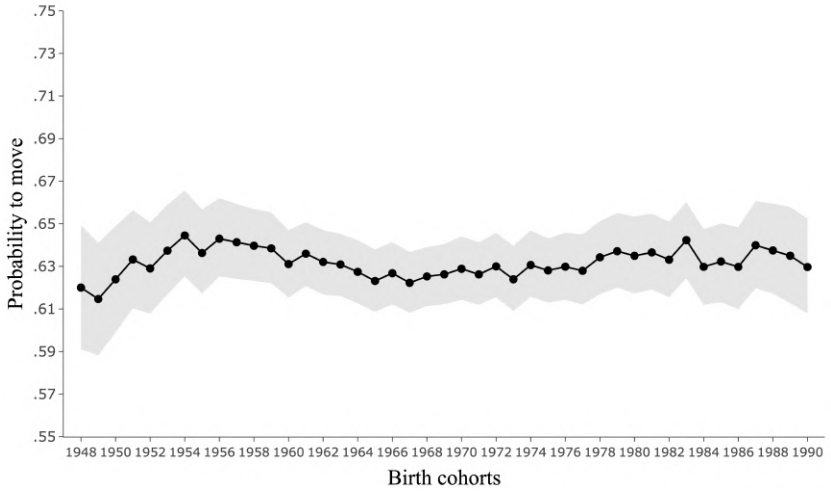
Figure F.8: Log-multiplicative layer effects based on father-son pairs



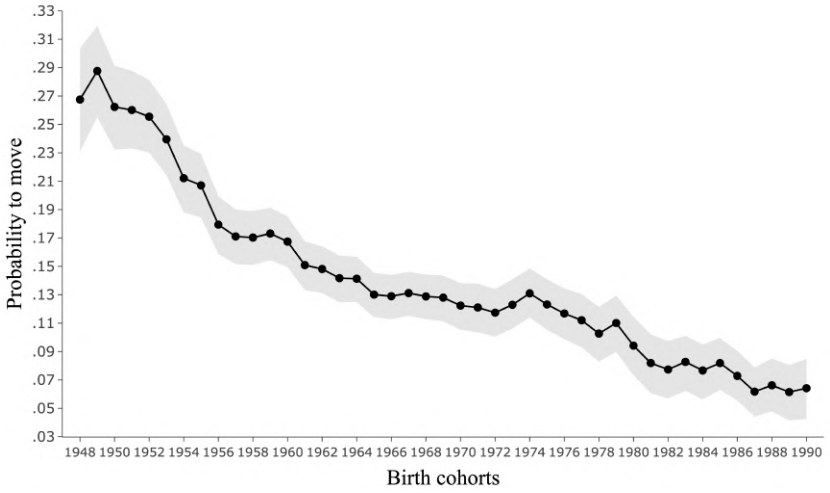
Notes: This figure plots the log-multiplicative layer effect across birth cohorts using 5-year bins. The vertical bars represent 95% confidence intervals.

Figure F.9: Measures of movement at generation $t = 1$ based on mother-child pairs

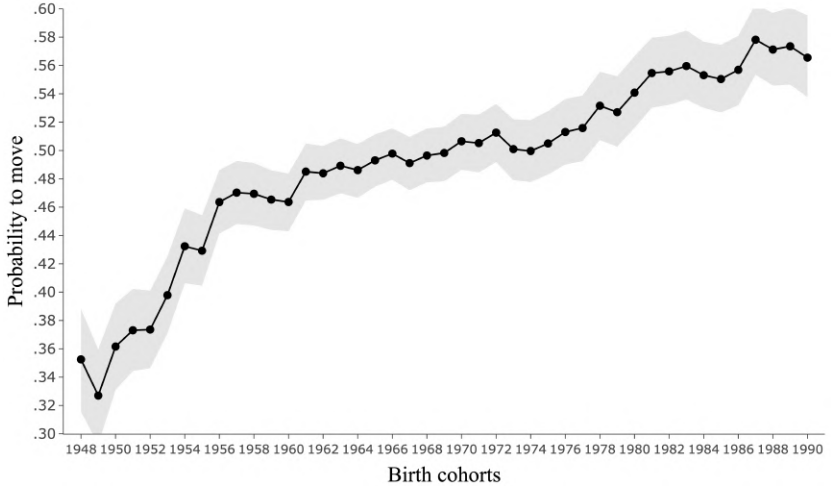
(A) Overall mobility (OM_1)



(B) Structural mobility (SM_1)



(C) Exchange mobility (EM_1)

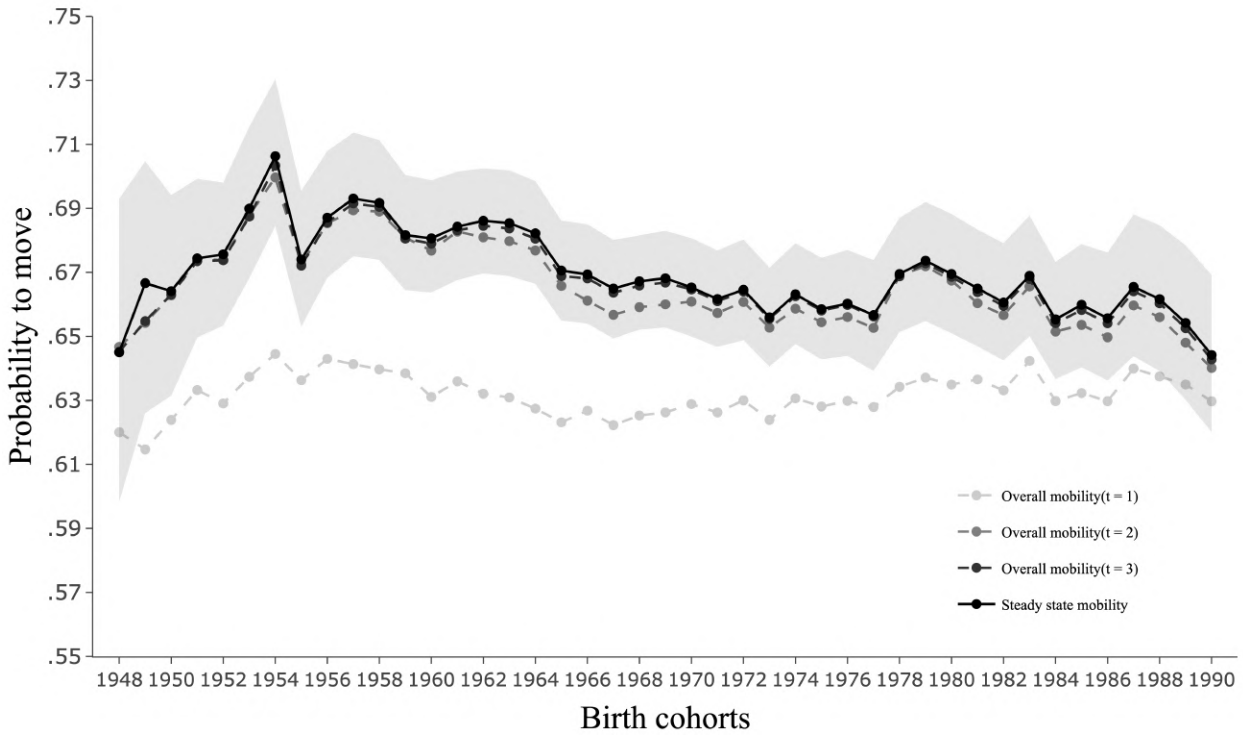


(D) Upward and downward mobility



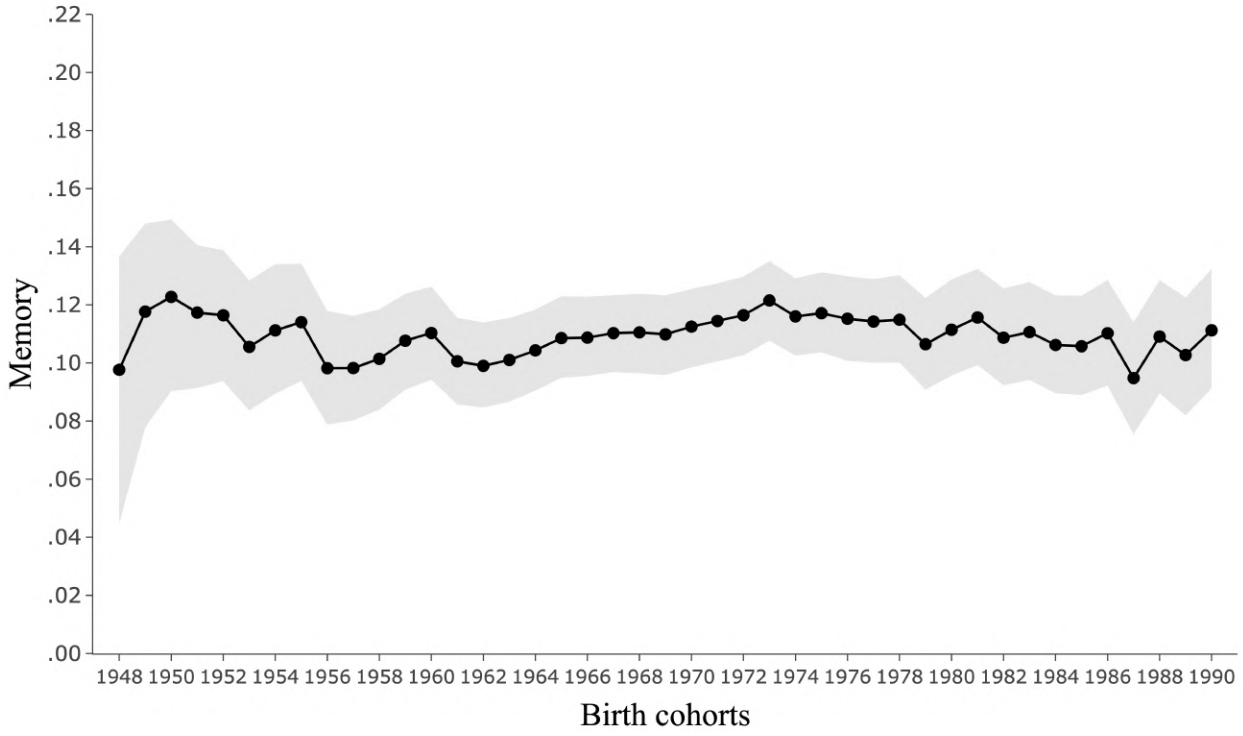
Notes: Shaded areas represent 95% confidence intervals.

Figure F.10: Overall mobility (OM_t) across synthetic generations based on mother-child pairs



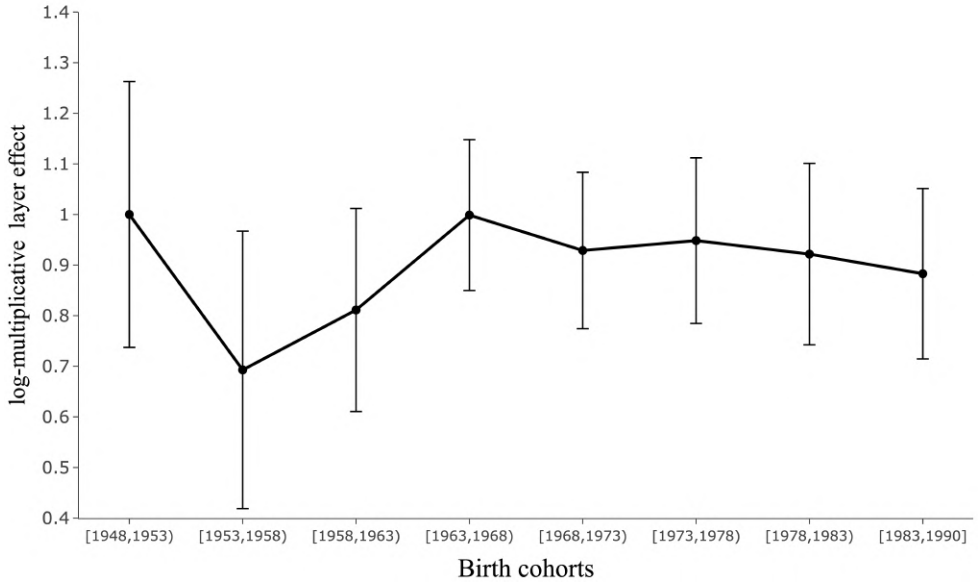
Notes: This figure illustrates the evolution of overall mobility across generations in a stationary Markov chain. By $t = 4$, the Markov chains for most of the cohorts have converged to their respective steady-state distributions, where there is no structural mobility. Shaded areas represent 95% confidence intervals, which are shown only for the trend in steady-state mobility.

Figure F.11: Aggregate intergenerational memory at generation $t = 1$ (AIM_1) based on mother-child pairs



Notes: Shaded areas represent 95% confidence intervals.

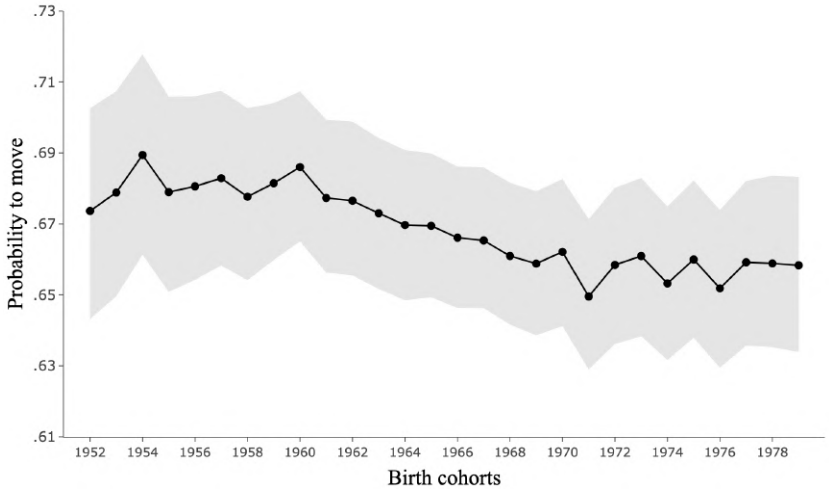
Figure F.12: Log-multiplicative layer effects based on mother-child pairs



Notes: This figure plots the log-multiplicative layer effect across birth cohorts using 5-year bins. The vertical bars represent 95% confidence intervals.

Figure F.13: Measures of movement at generation $t = 1$ based on mother-son pairs

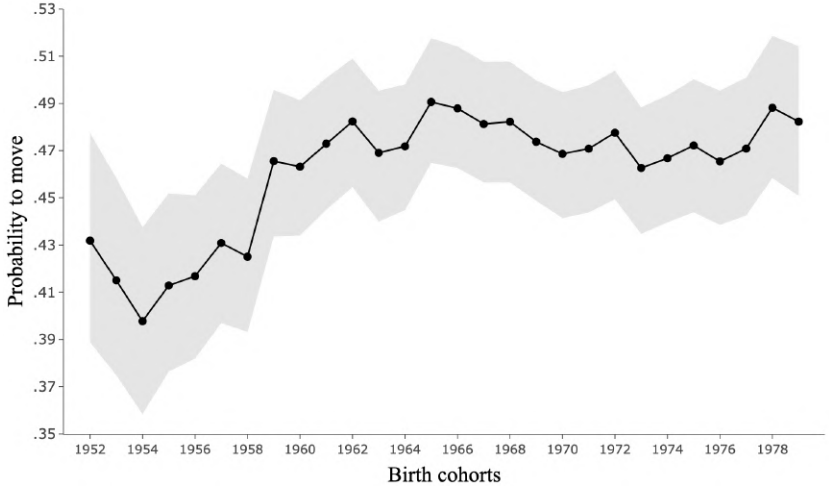
(A) Overall mobility (OM_1)



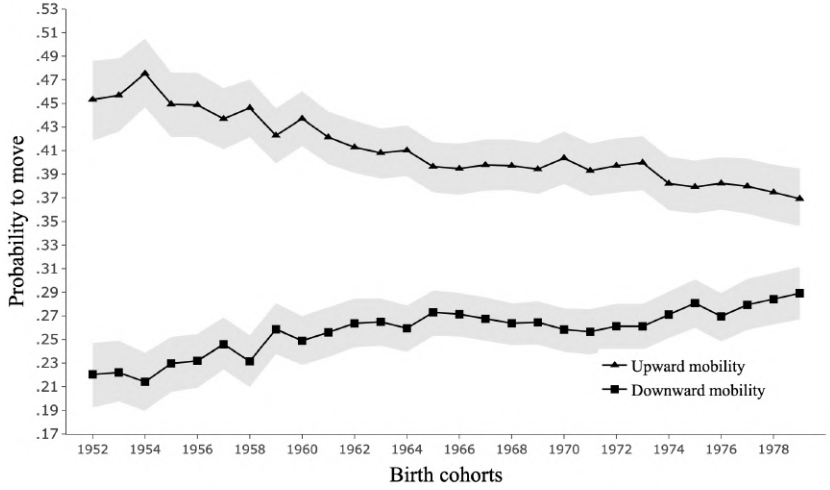
(B) Structural mobility (SM_1)



(C) Exchange mobility (EM_1)

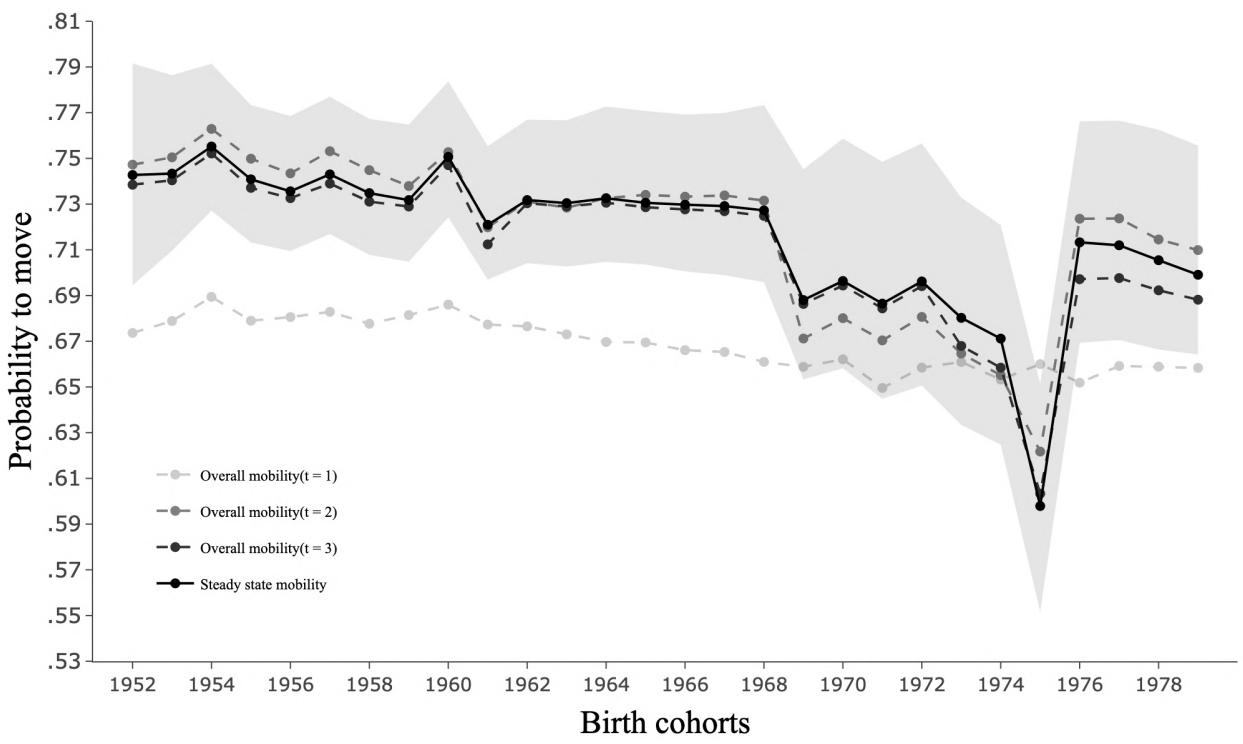


(D) Upward and downward mobility



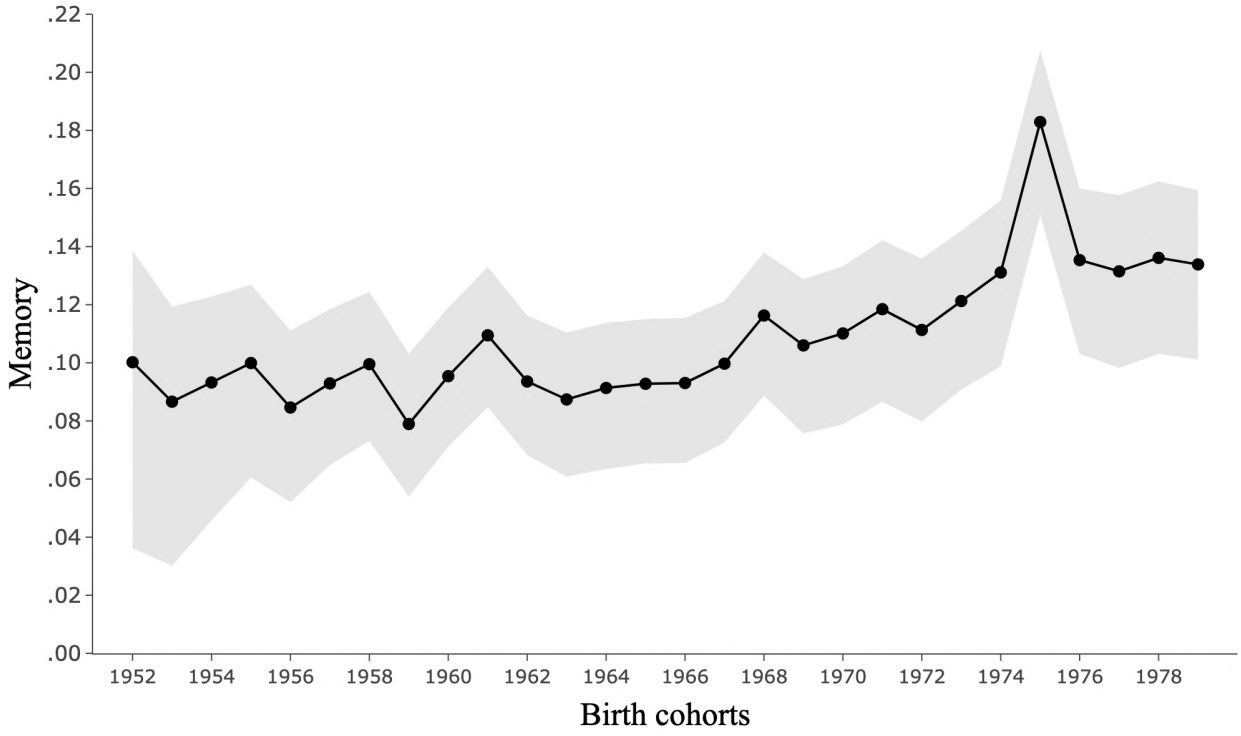
Notes: Shaded areas represent 95% confidence intervals.

Figure F.14: Overall mobility (OM_t) across synthetic generations based on mother-son pairs



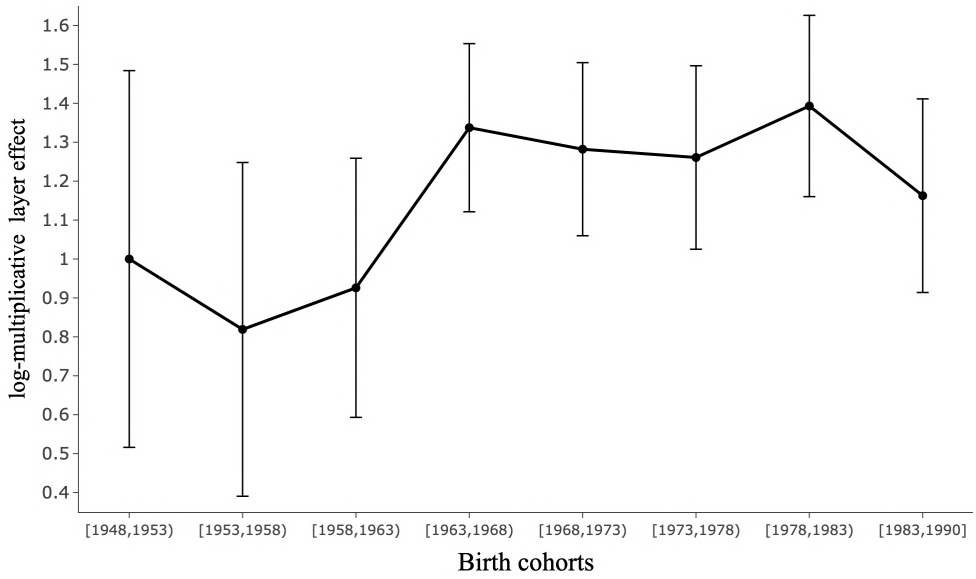
Notes: This figure illustrates the evolution of overall mobility across generations in a stationary Markov chain. By $t = 4$, the Markov chains for most of the cohorts have converged to their respective steady-state distributions, where there is no structural mobility. Shaded areas represent 95% confidence intervals, which are shown only for the trend in steady-state mobility.

Figure F.15: Aggregate intergenerational memory at generation $t = 1$ (AIM_1) based on mother-son pairs



Notes: Shaded areas represent 95% confidence intervals.

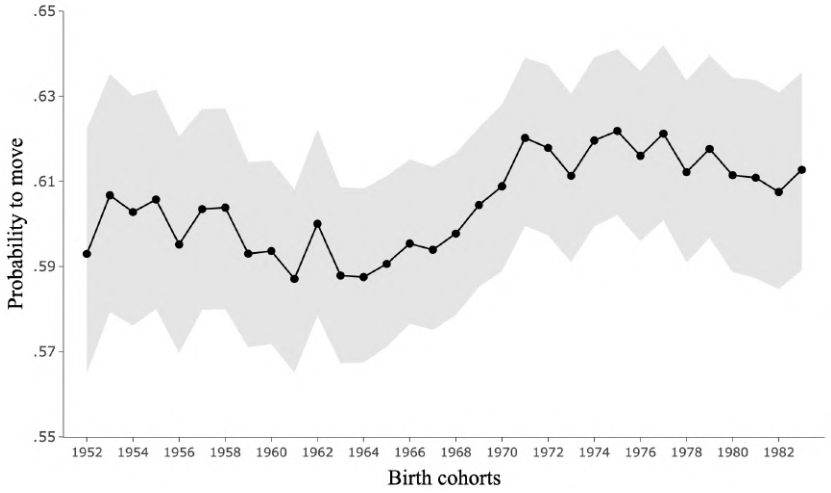
Figure F.16: Log-multiplicative layer effects based on mother-son pairs



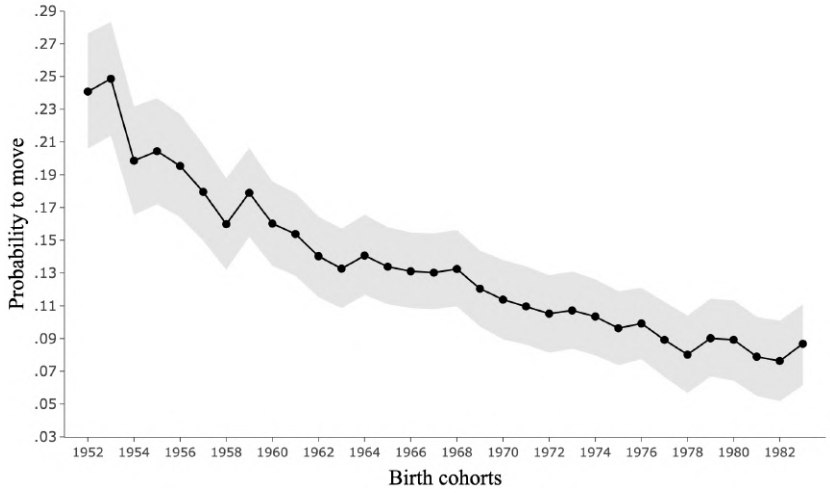
Notes: This figure plots the log-multiplicative layer effect across birth cohorts using 5-year bins. The vertical bars represent 95% confidence intervals.

Figure F.17: Measures of movement at generation $t = 1$ based on mother-daughter pairs

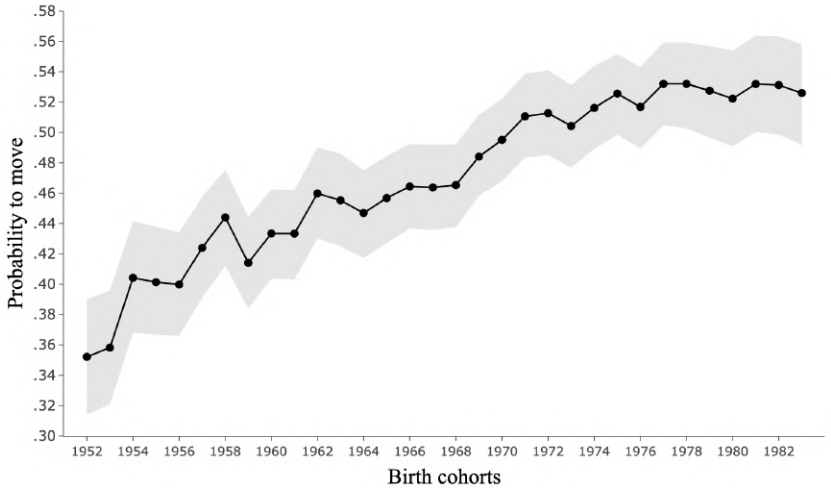
(A) Overall mobility (OM_1)



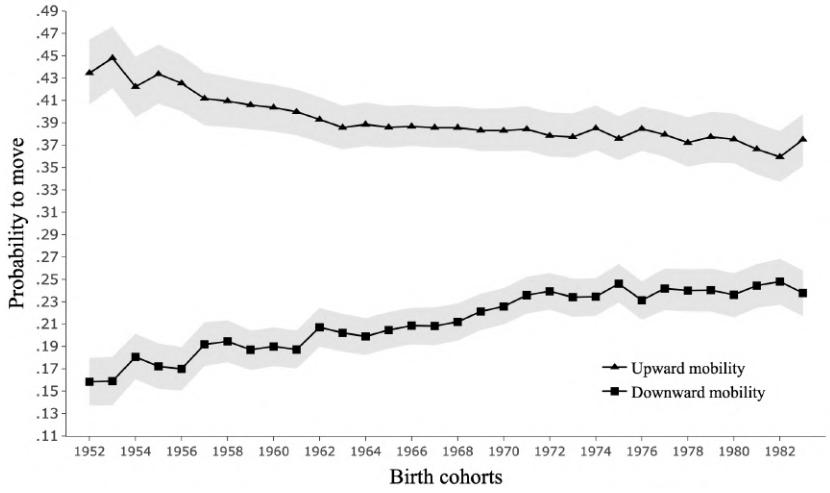
(B) Structural mobility (SM_1)



(C) Exchange mobility (EM_1)

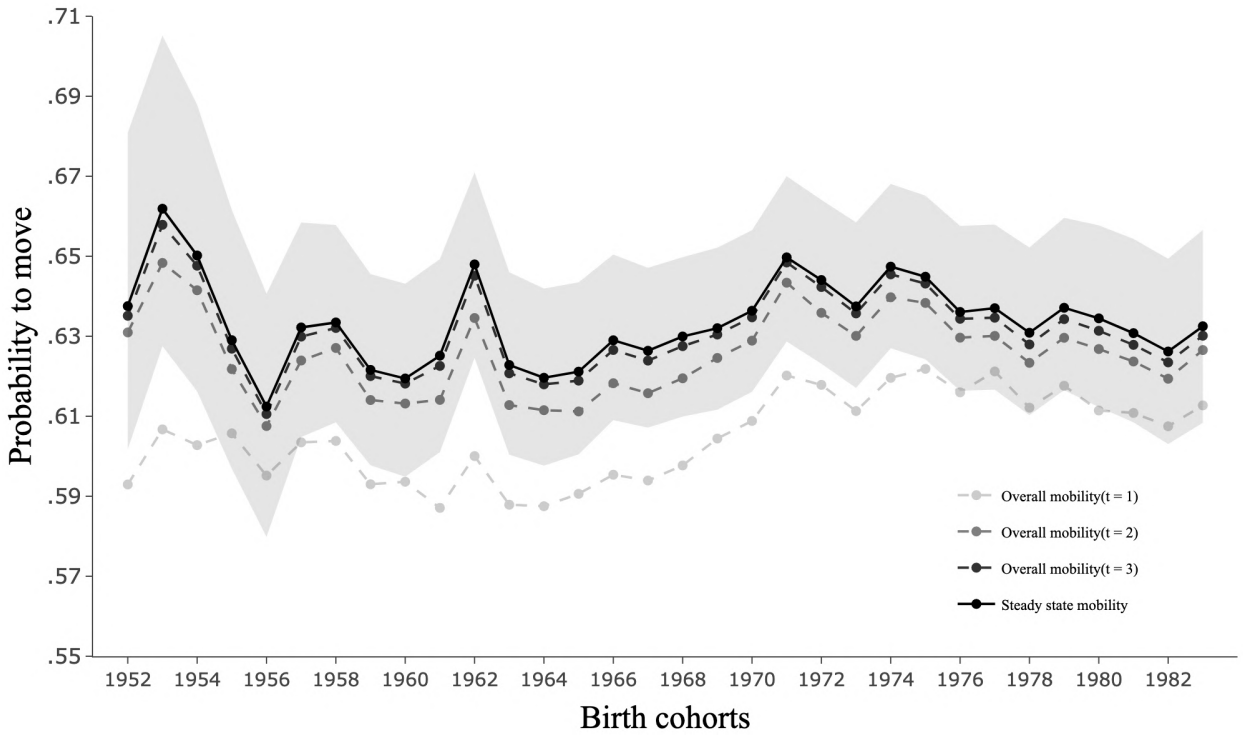


(D) Upward and downward mobility



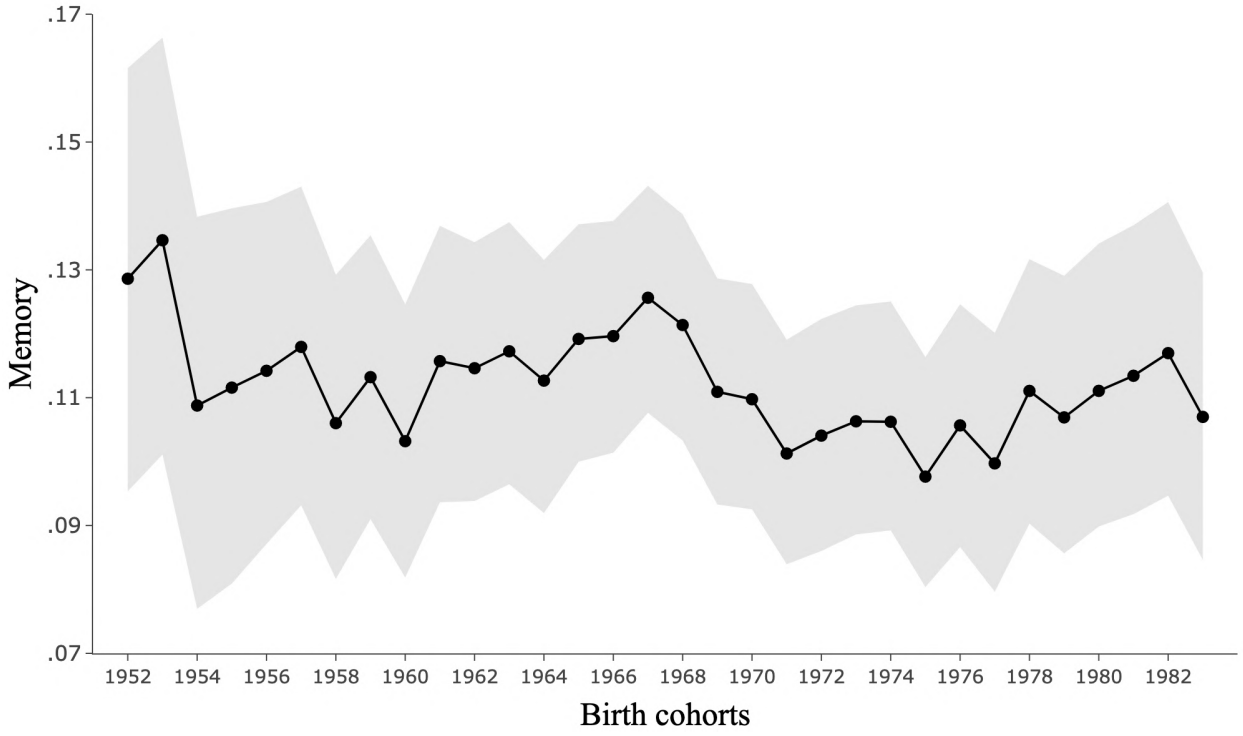
Notes: Shaded areas represent 95% confidence intervals.

Figure F.18: Overall mobility (OM_t) across synthetic generations based on mother-daughter pairs



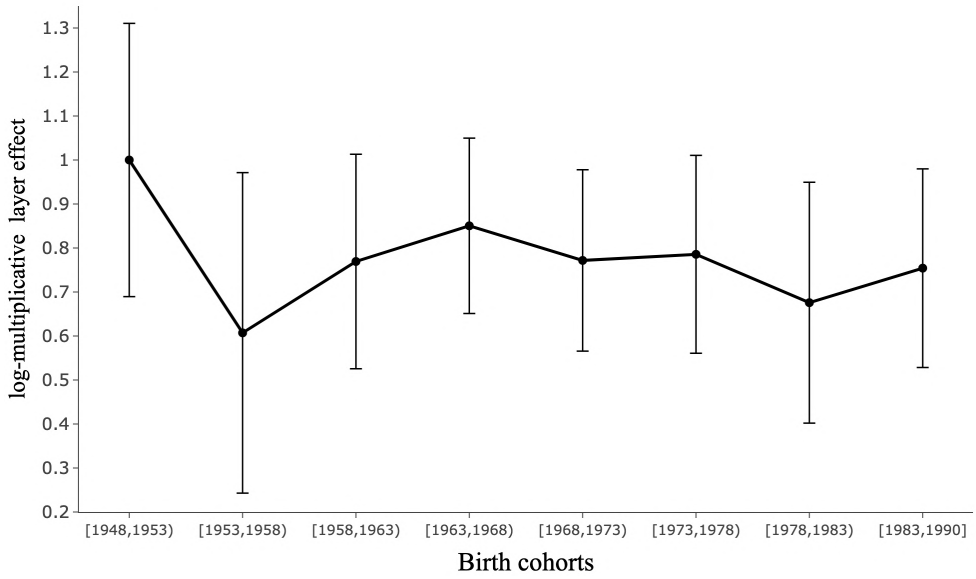
Notes: This figure illustrates the evolution of overall mobility across generations in a stationary Markov chain. By $t = 4$, the Markov chains for most of the cohorts have converged to their respective steady-state distributions, where there is no structural mobility. Shaded areas represent 95% confidence intervals, which are shown only for the trend in steady-state mobility.

Figure F.19: Aggregate intergenerational memory at generation $t = 1$ (AIM_1) based on mother-daughter pairs



Notes: Shaded areas represent 95% confidence intervals.

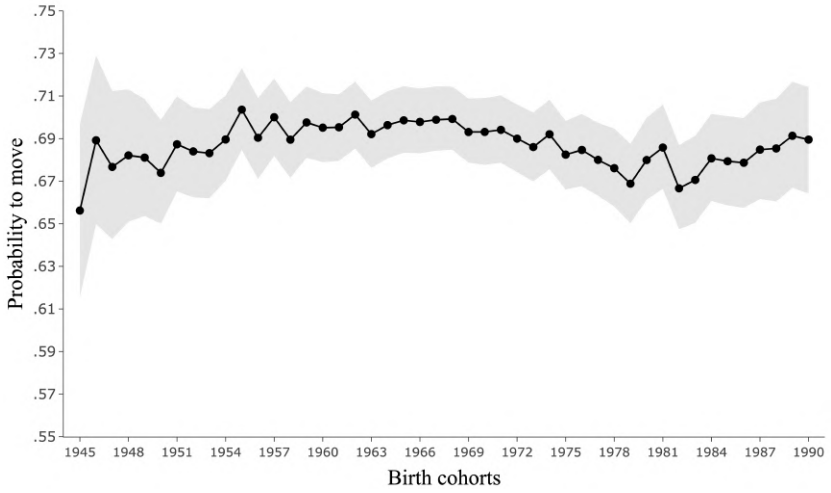
Figure F.20: Log-multiplicative layer effects based on mother-daughter pairs



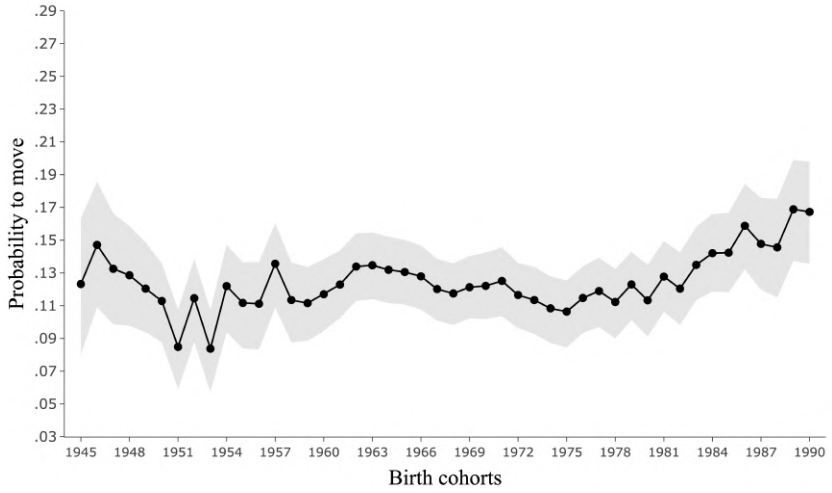
Notes: This figure plots the log-multiplicative layer effect across birth cohorts using 5-year bins. The vertical bars represent 95% confidence intervals.

Figure F.21: Measures of movement at generation $t = 1$ based on parent with higher status-child pairs

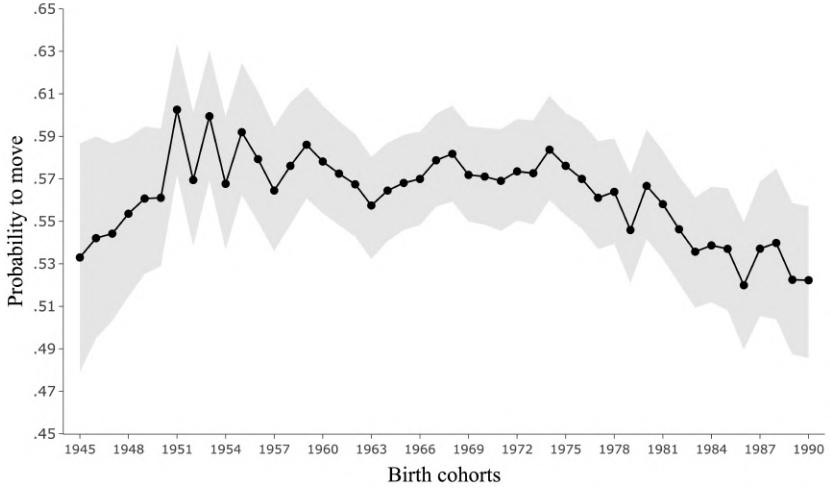
(A) Overall mobility (OM_1)



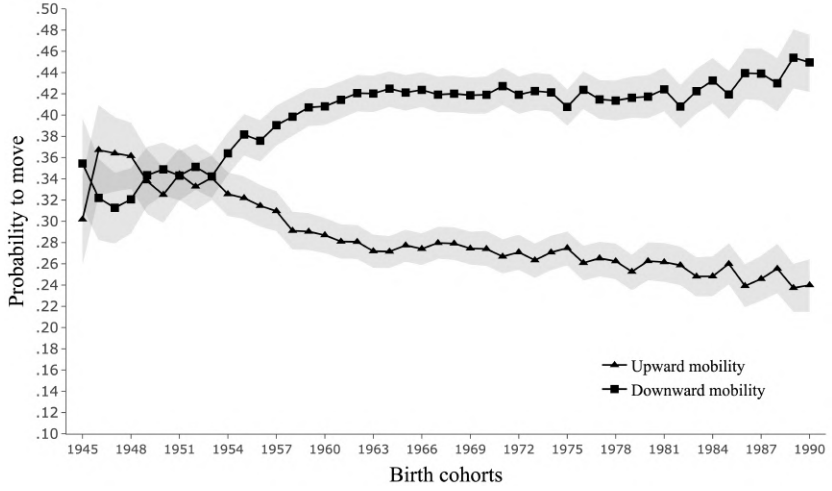
(B) Structural mobility (SM_1)



(C) Exchange mobility (EM_1)

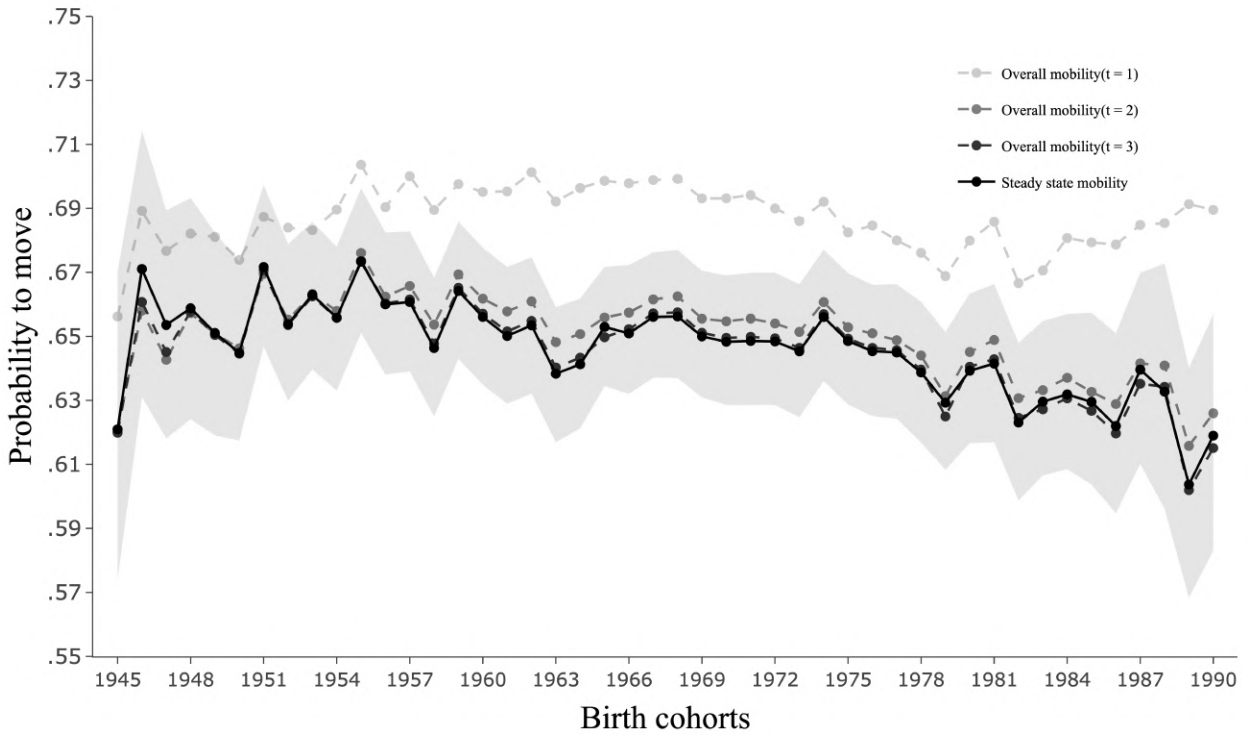


(D) Upward and downward mobility



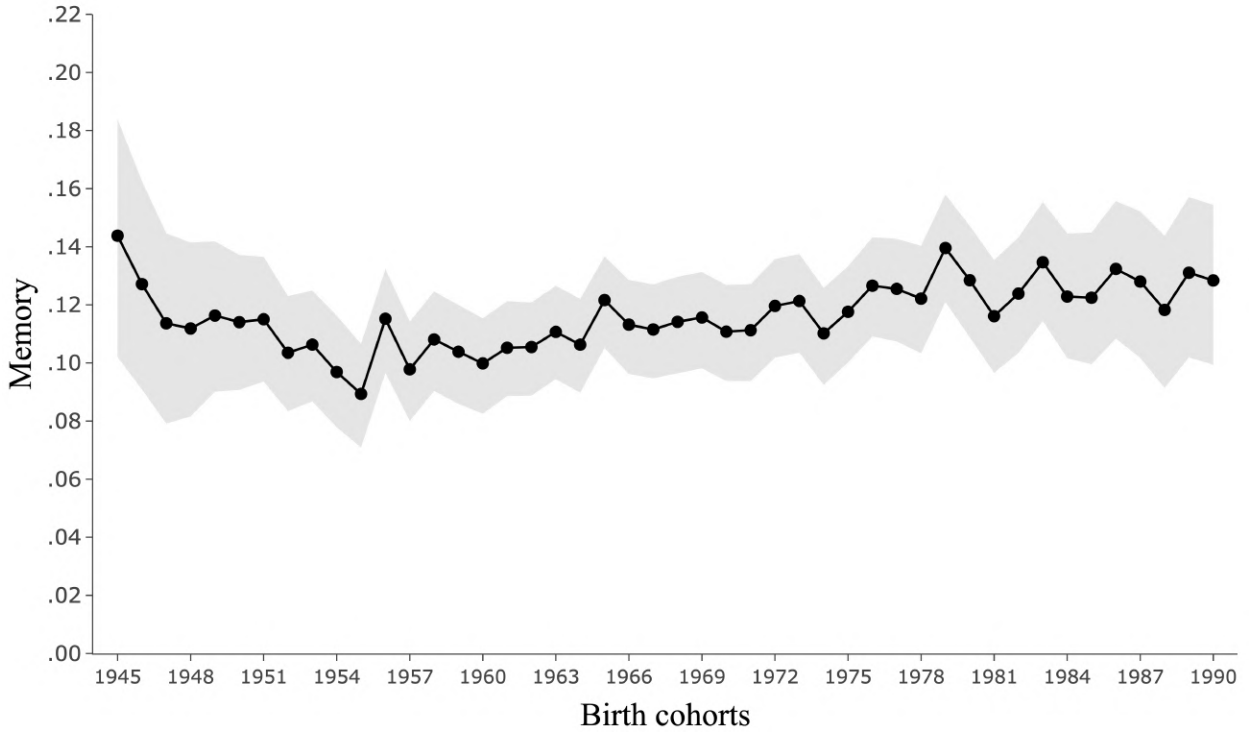
Notes: Shaded areas represent 95% confidence intervals.

Figure F.22: Overall mobility (OM_t) across synthetic generations based on parent with higher status-child pairs



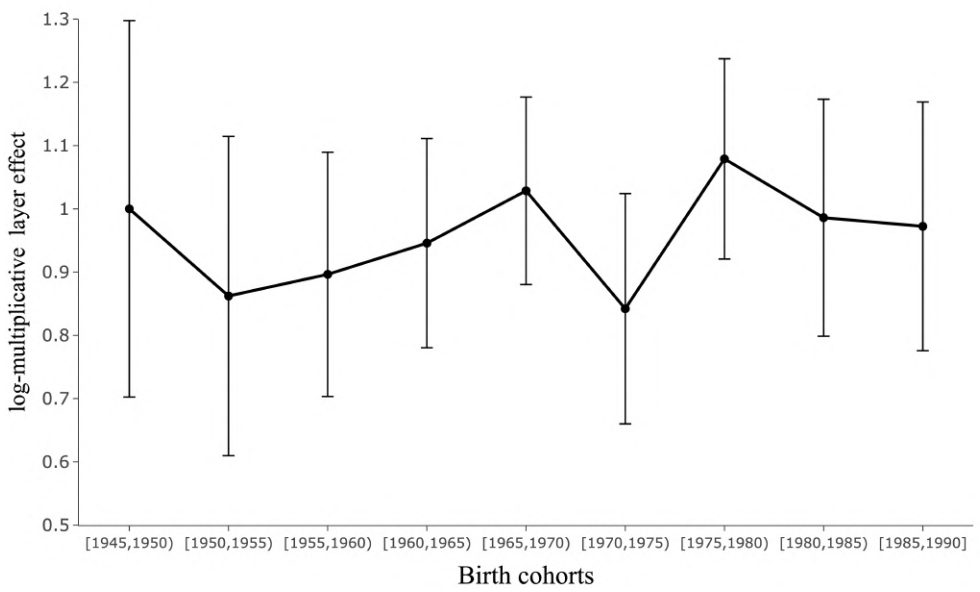
Notes: This figure illustrates the evolution of overall mobility across generations in a stationary Markov chain. By $t = 4$, the Markov chains for most of the cohorts have converged to their respective steady-state distributions, where there is no structural mobility. Shaded areas represent 95% confidence intervals, which are shown only for the trend in steady-state mobility.

Figure F.23: Aggregate intergenerational memory at generation $t = 1$ (AIM_1) based on parent with higher status-child pairs



Notes: Shaded areas represent 95% confidence intervals.

Figure F.24: Log-multiplicative layer effects based on parent with higher status-child pairs



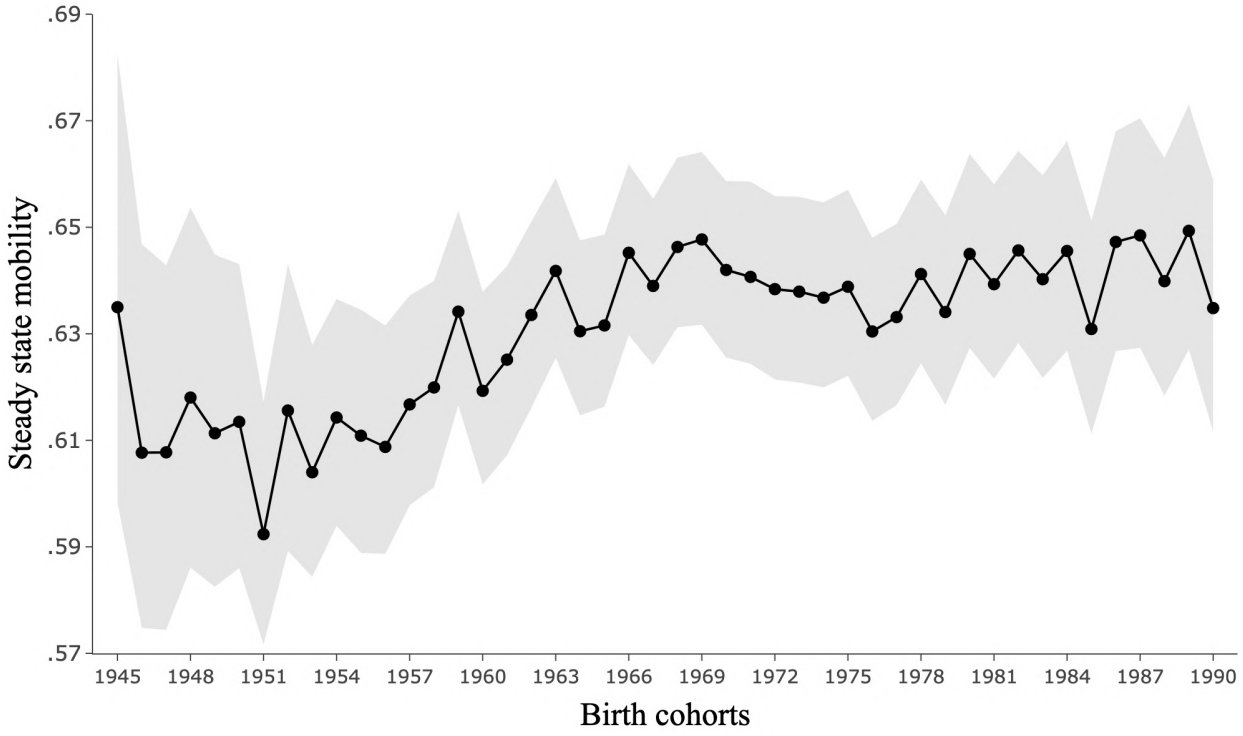
Notes: This figure plots the log-multiplicative layer effect across birth cohorts using ∼5-year bins. The vertical bars represent 95% confidence intervals.

Figure F.25: Aggregate intergenerational memory at generation $t = 1$ (AIM_1) for educational attainment, based on mother-child pairs



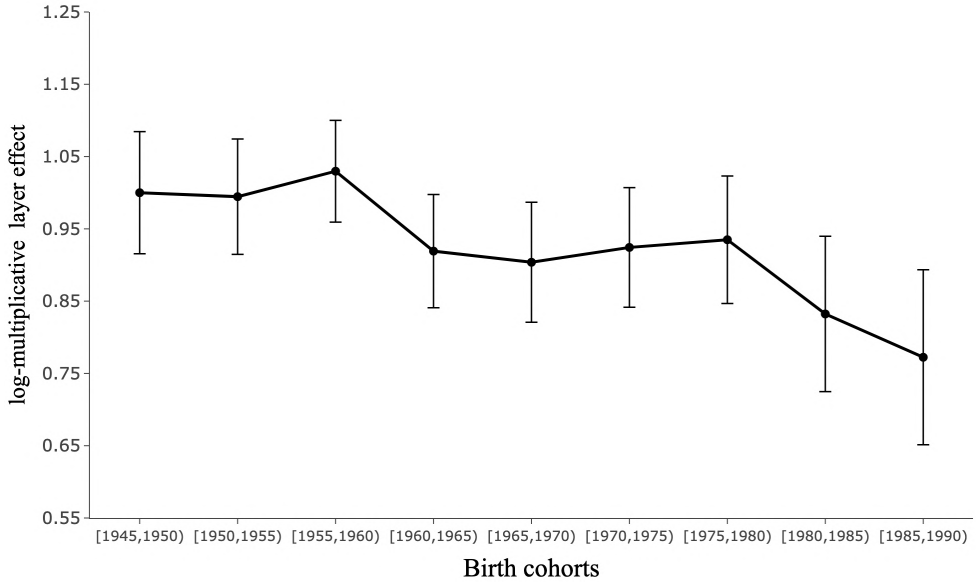
Notes: Shaded areas represent 95% confidence intervals.

Figure F.26: Steady-state mobility (SSM) for educational attainment, based on mother-child pairs



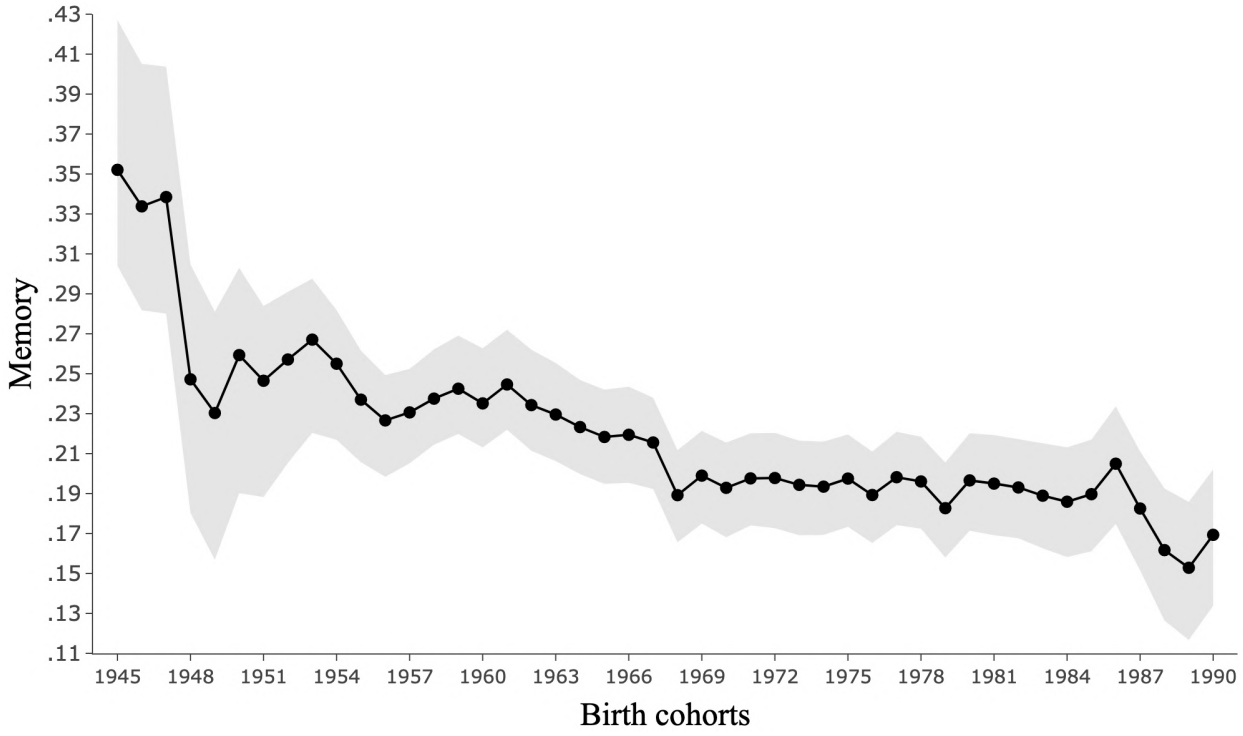
Notes: Shaded areas represent 95% confidence intervals.

Figure F.27: Log-multiplicative layer effects for educational attainment, based on mother-child pairs



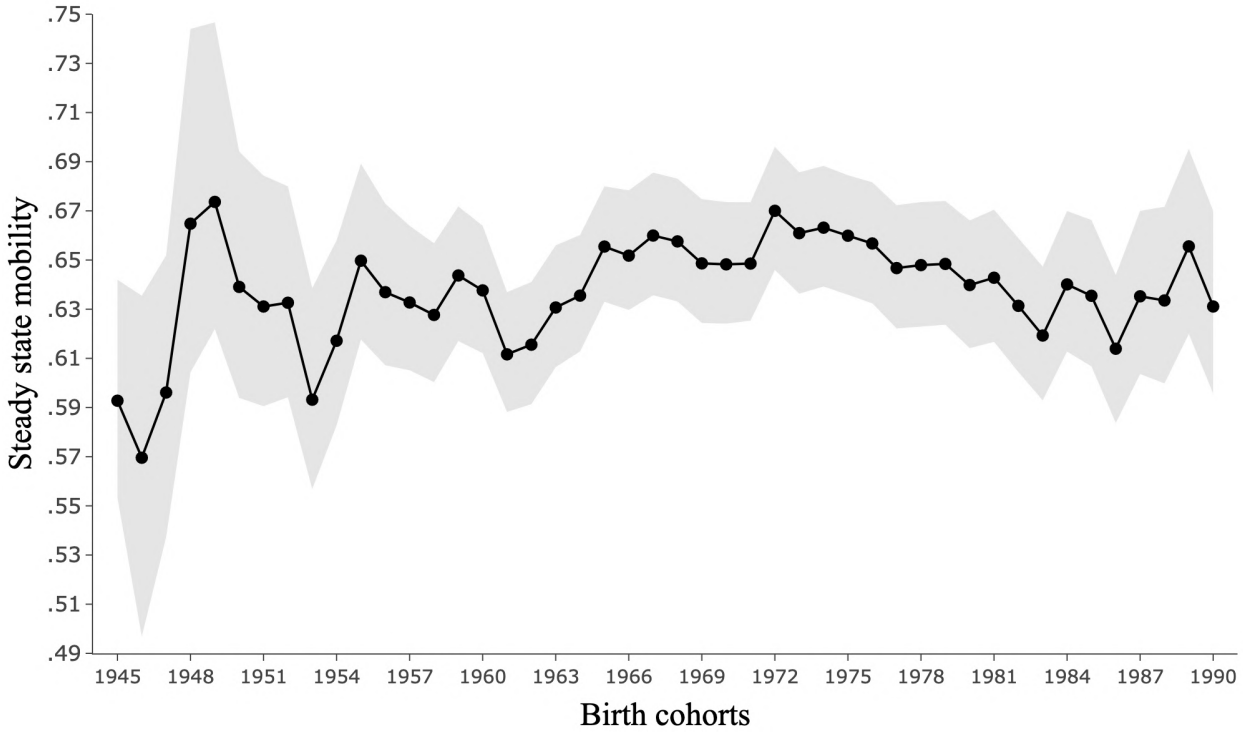
Notes: This figure plots the log-multiplicative layer effect across birth cohorts using 5-year bins. The vertical bars represent 95% confidence intervals.

Figure F.28: Aggregate intergenerational memory at generation $t = 1$ (AIM_1) for educational attainment, based on mother-son pairs



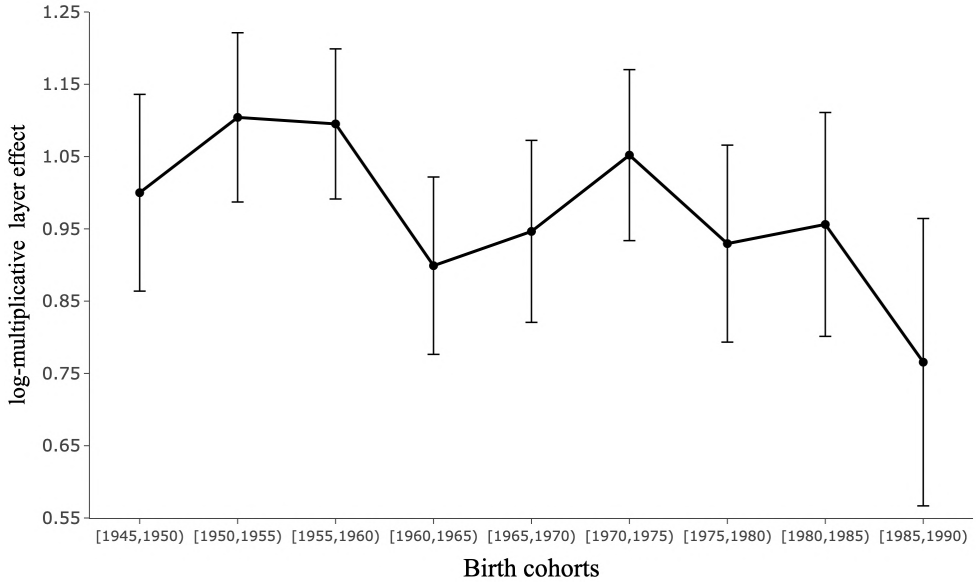
Notes: Shaded areas represent 95% confidence intervals.

Figure F.29: Steady-state mobility (SSM) for educational attainment, based on mother-son pairs



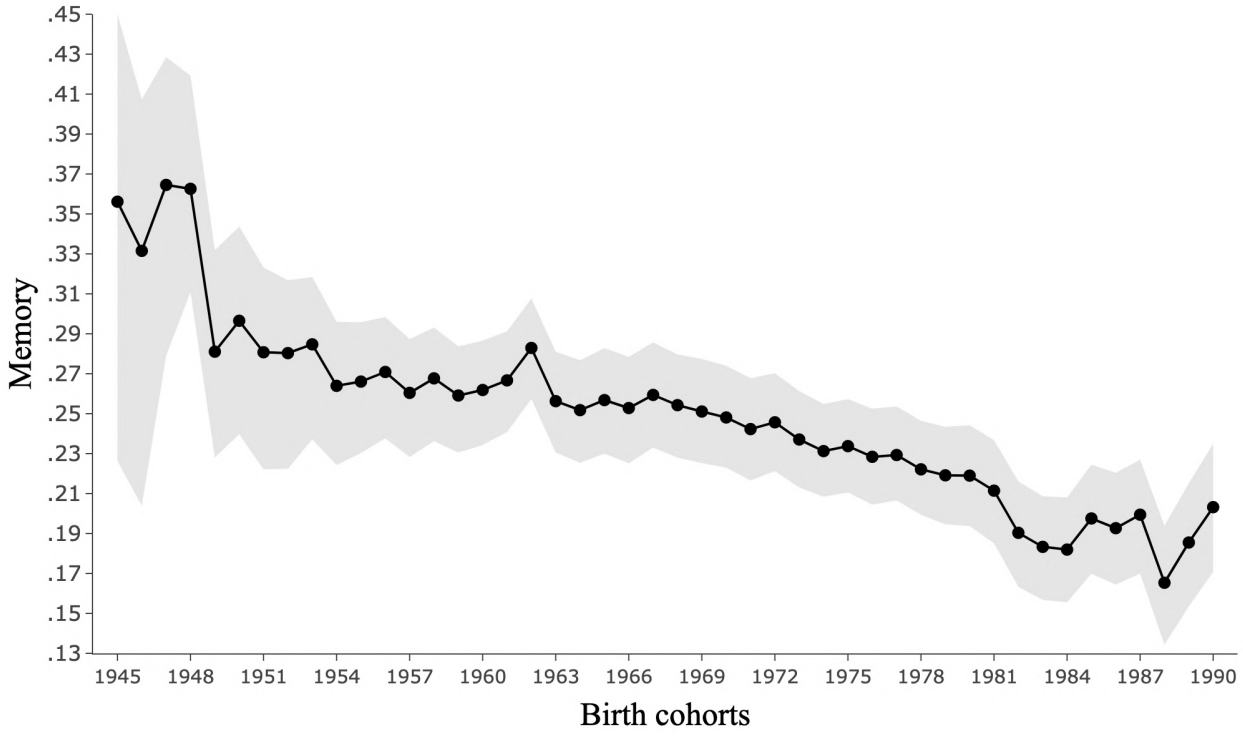
Notes: Shaded areas represent 95% confidence intervals.

Figure F.30: Log-multiplicative layer effects for educational attainment, based on mother-son pairs



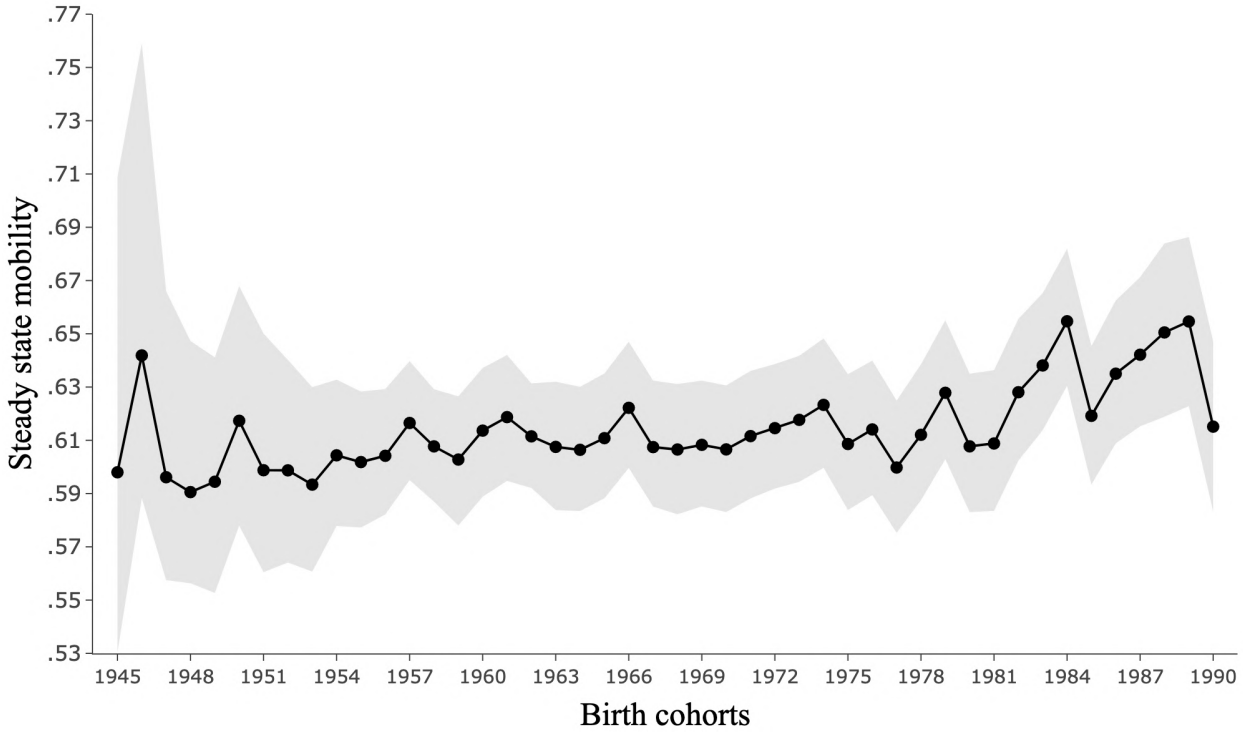
Notes: This figure plots the log-multiplicative layer effect across birth cohorts using 5-year bins. The vertical bars represent 95% confidence intervals.

Figure F.31: Aggregate intergenerational memory at generation $t = 1$ (AIM_1) for educational attainment, based on mother-daughter pairs



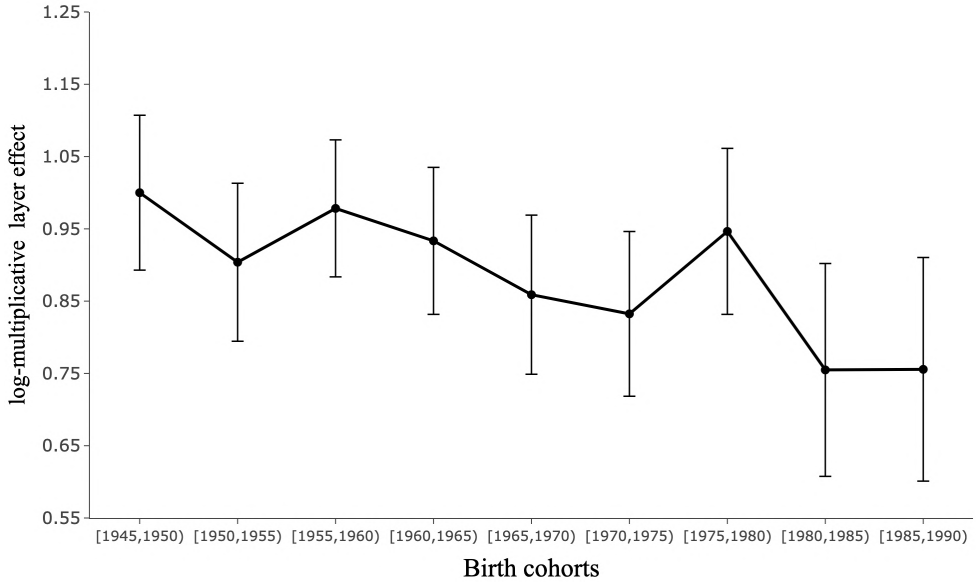
Notes: Shaded areas represent 95% confidence intervals.

Figure F.32: Steady-state mobility (SSM) for educational attainment, based on mother-daughter pairs



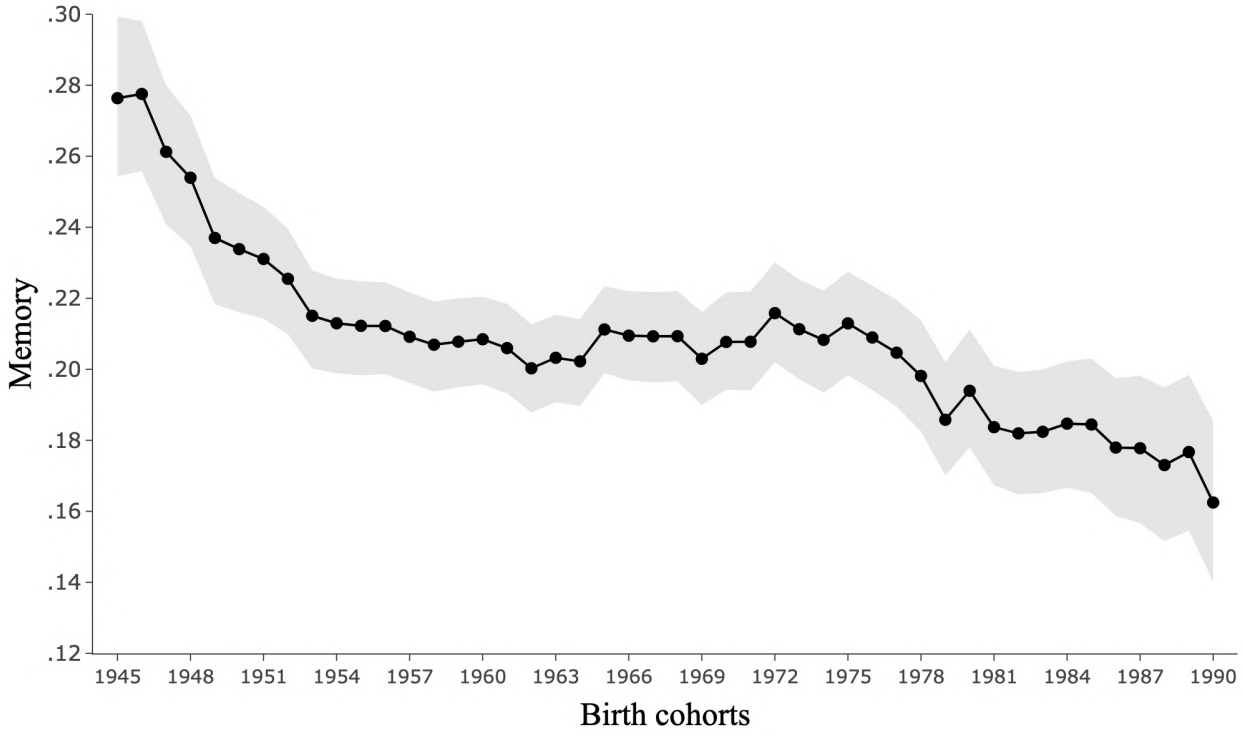
Notes: Shaded areas represent 95% confidence intervals.

Figure F.33: Log-multiplicative layer effects for educational attainment, based on mother-daughter pairs



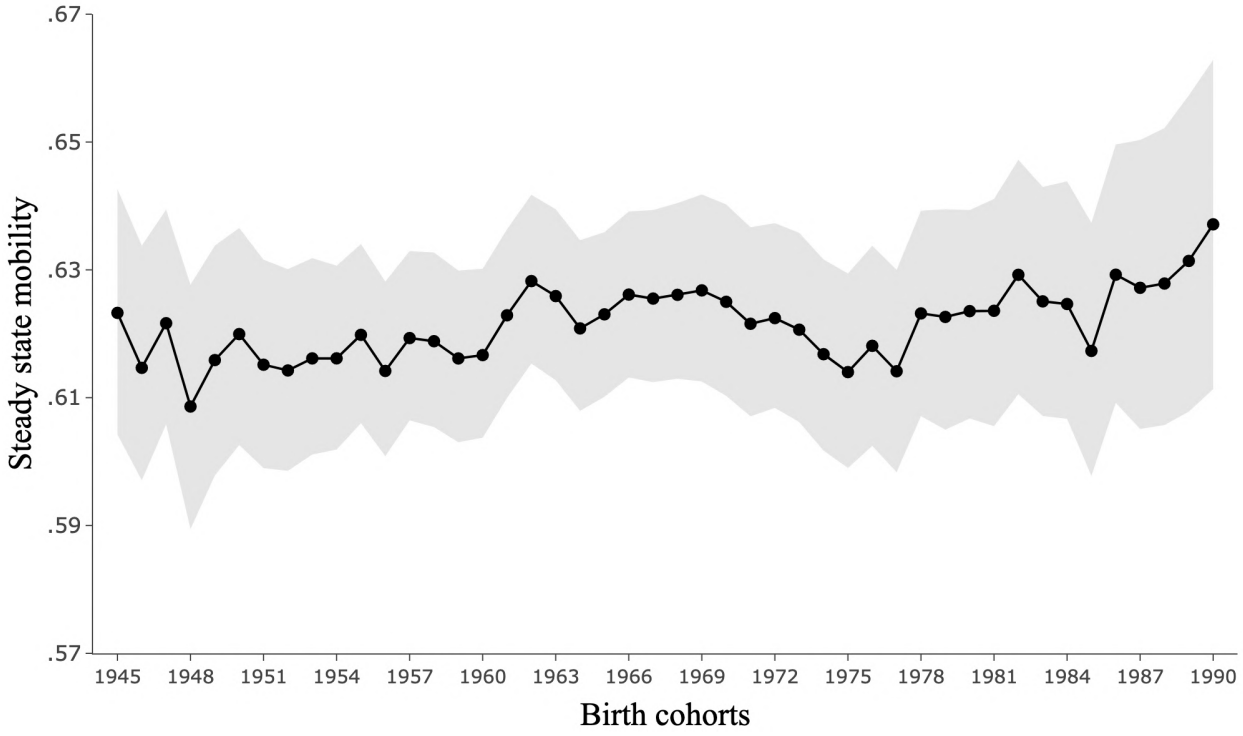
Notes: This figure plots the log-multiplicative layer effect across birth cohorts using 5-year bins. The vertical bars represent 95% confidence intervals.

Figure F.34: Aggregate intergenerational memory at generation $t = 1$ (AIM_1) for educational attainment, based on highest-educated parent-child pairs



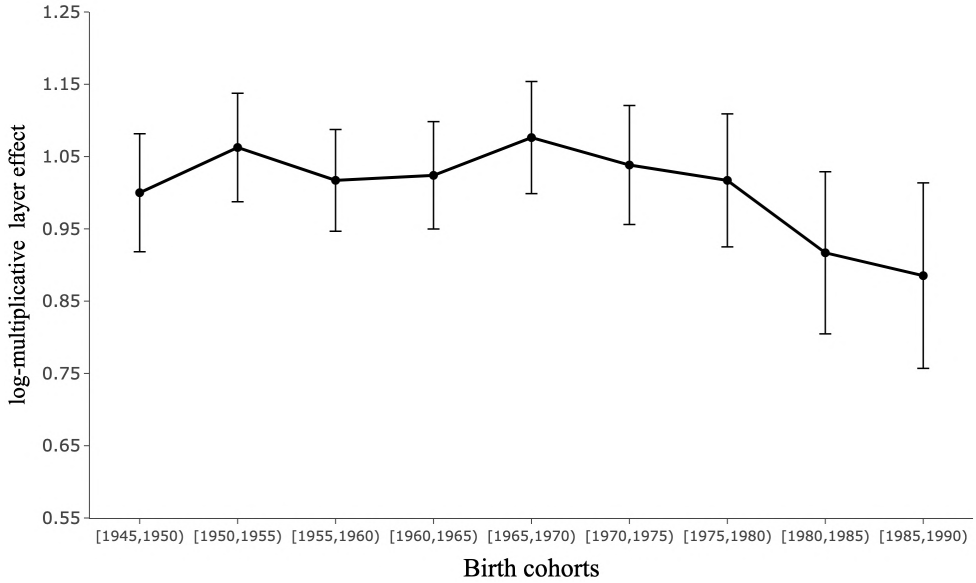
Notes: Shaded areas represent 95% confidence intervals.

Figure F.35: Steady-state mobility (SSM) for educational attainment, based on highest-educated parent-child pairs



Notes: Shaded areas represent 95% confidence intervals.

Figure F.36: Log-multiplicative layer effects for educational attainment, based on highest-educated parent-child pairs



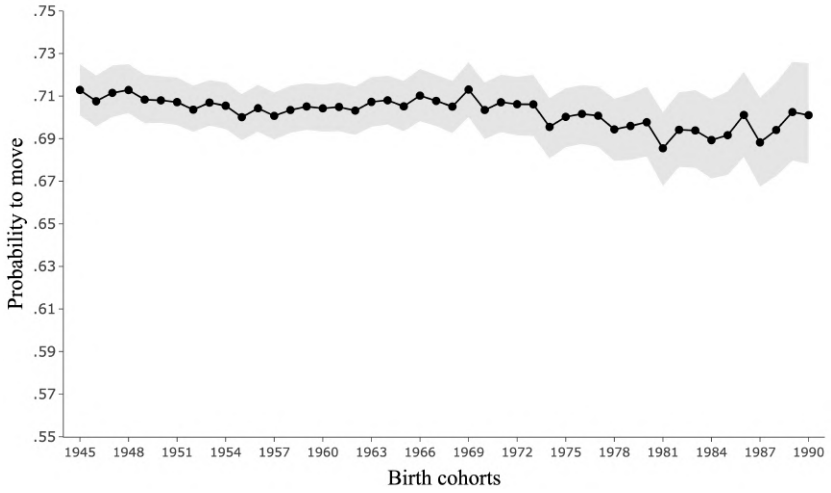
Notes: This figure plots the log-multiplicative layer effect across birth cohorts using 5-year bins. The vertical bars represent 95% confidence intervals.

G Trends by Race

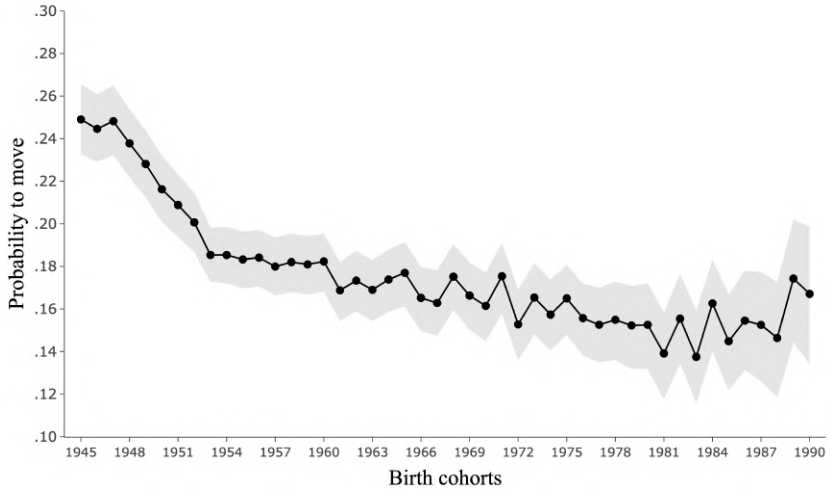
Due to sample limitations, our data include only 4,831 non-White father–child pairs among cohorts born between 1945 and 1990 who were age 25-55 at the time of their GSS interview. To examine potential heterogeneity by race, we therefore replicate our main analysis after excluding non-White pairs and focusing solely on White father–child pairs, which yields 19,395 observations. Because these cases constitute the majority of our sample in the main text, all key trends are largely unchanged when restricted to White father-child pairs.

Figure G.1: Measures of movement at generation $t = 1$ based on White father-child pairs

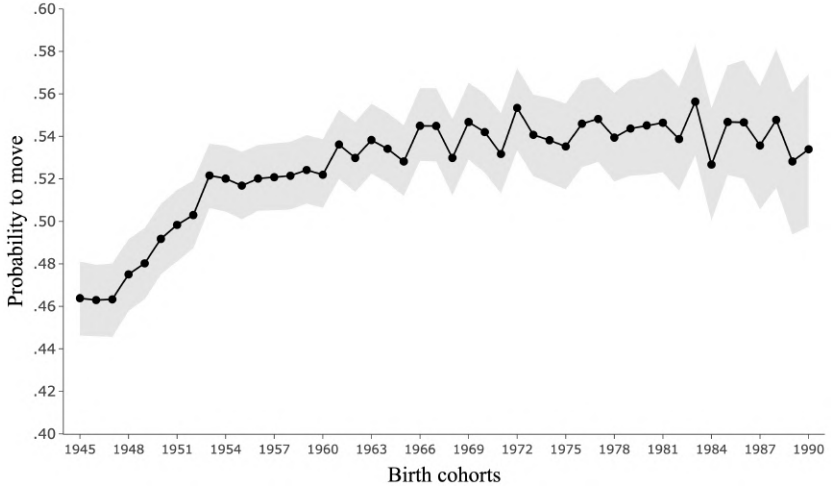
(A) Overall mobility (OM_1)



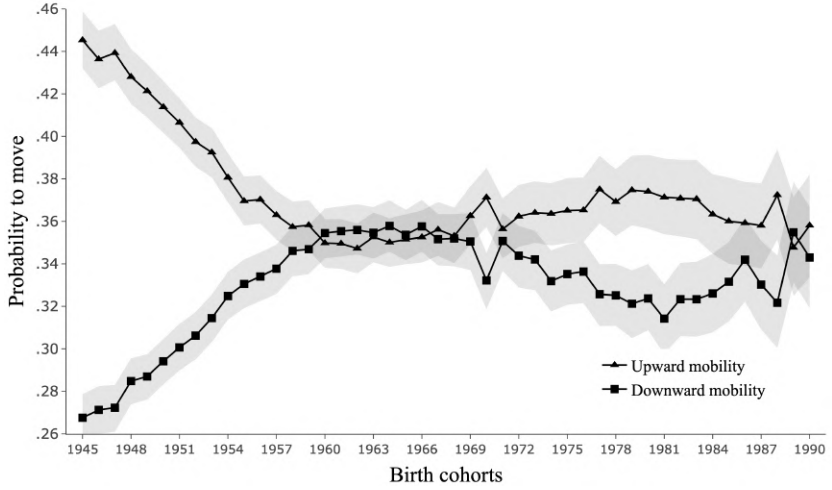
(B) Structural mobility (SM_1)



(C) Exchange mobility (EM_1)

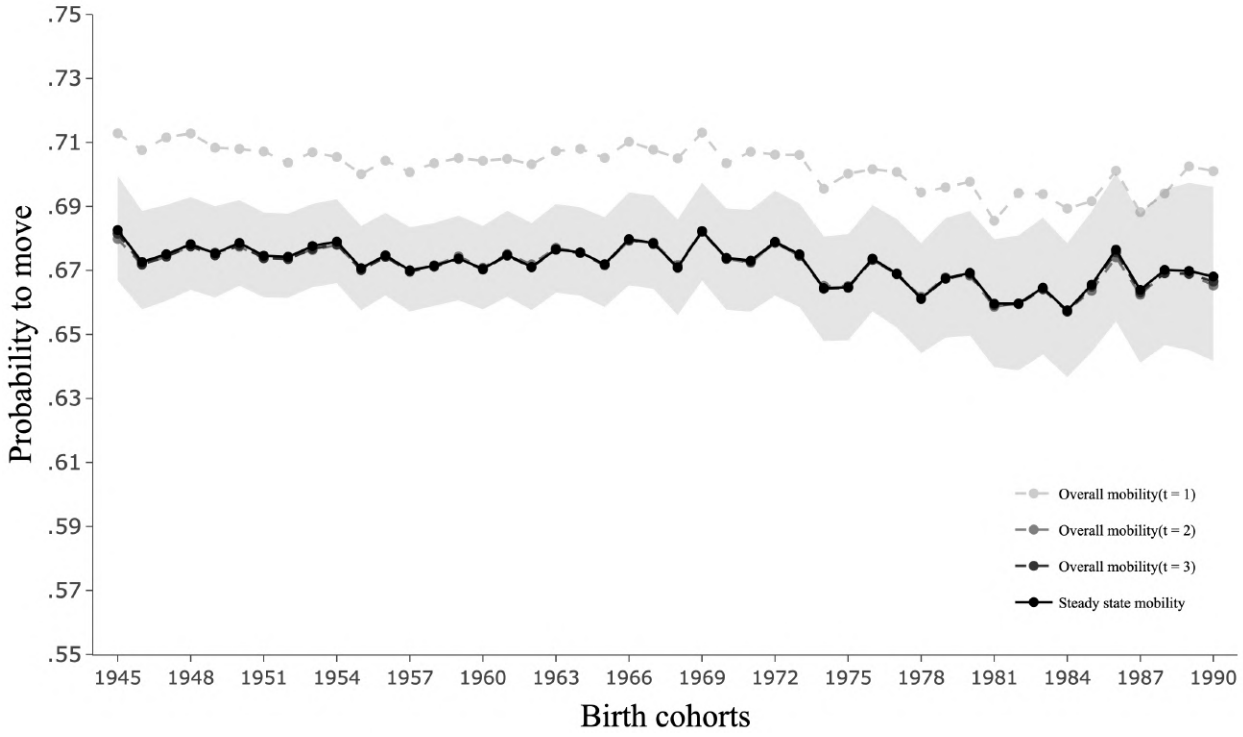


(D) Upward and downward mobility



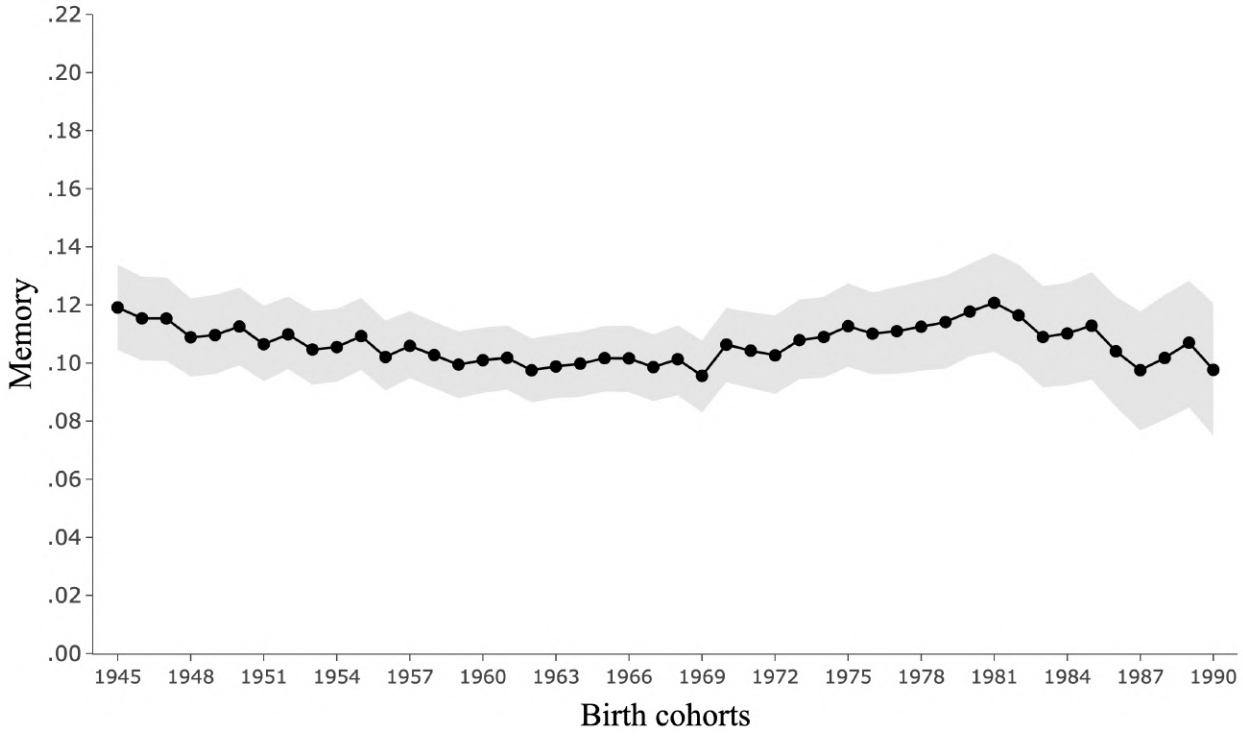
Notes: Shaded areas represent 95% confidence intervals.

Figure G.2: Overall mobility (OM_t) across synthetic generations based on White father-child pairs



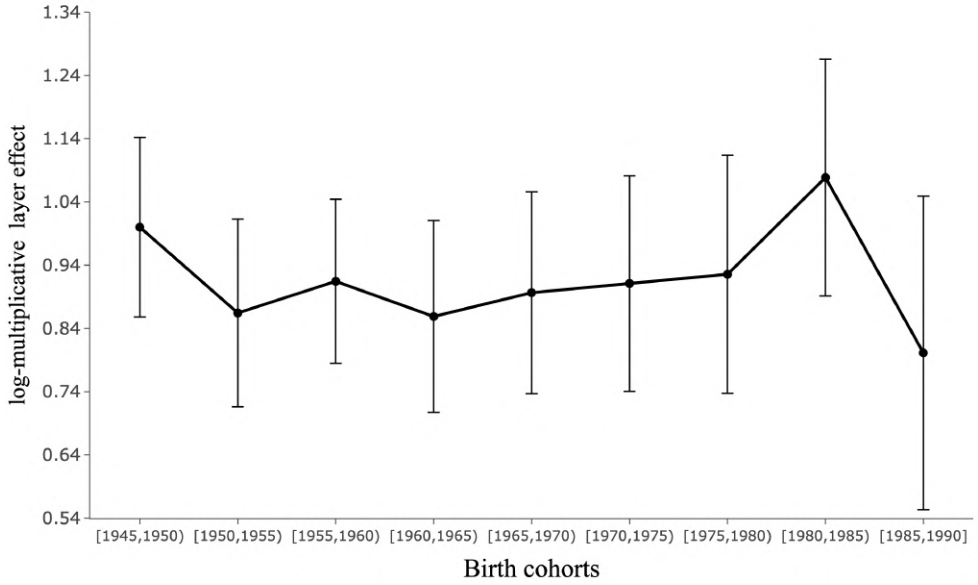
Notes: This figure illustrates the evolution of overall mobility across generations in a stationary Markov chain. By $t = 4$, the Markov chains for most of the cohorts have converged to their respective steady-state distributions, where there is no structural mobility. Shaded areas represent 95% confidence intervals, which are shown only for the trend in steady-state mobility.

Figure G.3: Aggregate intergenerational memory at generation $t = 1$ (AIM_1) based on White father-child pairs



Notes: Shaded areas represent 95% confidence intervals.

Figure G.4: Log-multiplicative layer effects based on White father-child pairs



Notes: This figure plots the log-multiplicative layer effect across birth cohorts using 5-year bins. The vertical bars represent 95% confidence intervals.

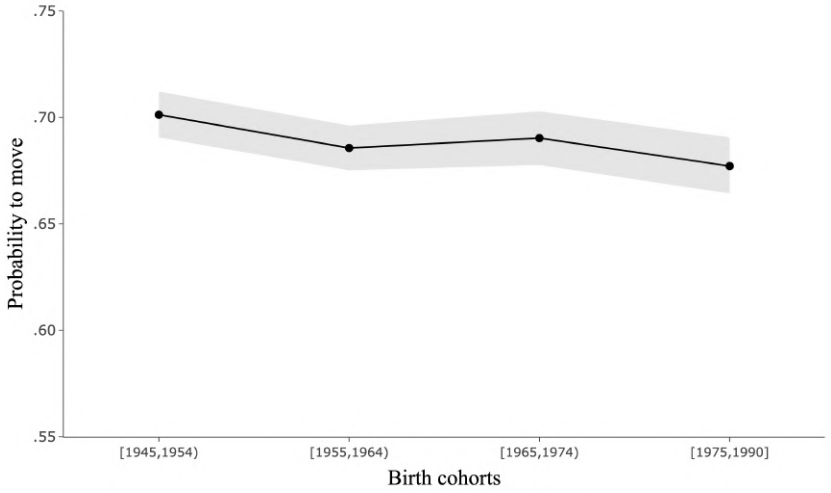
H Alternative Approaches to Smoothing

In this section, we replicate our main analyses using alternative methods for addressing sparsity in the origin-by-destination-by-cohort mobility tables. Instead of smoothing these tables with penalized splines, as in Equation 8, we construct transition matrices based on binned cohorts with 5- and ∼10-year bin widths. We then compute our measures of movement and memory from these binned matrices. The resulting estimates—presented in Figures H.1 to H.6—are broadly consistent with the findings reported in the main text.

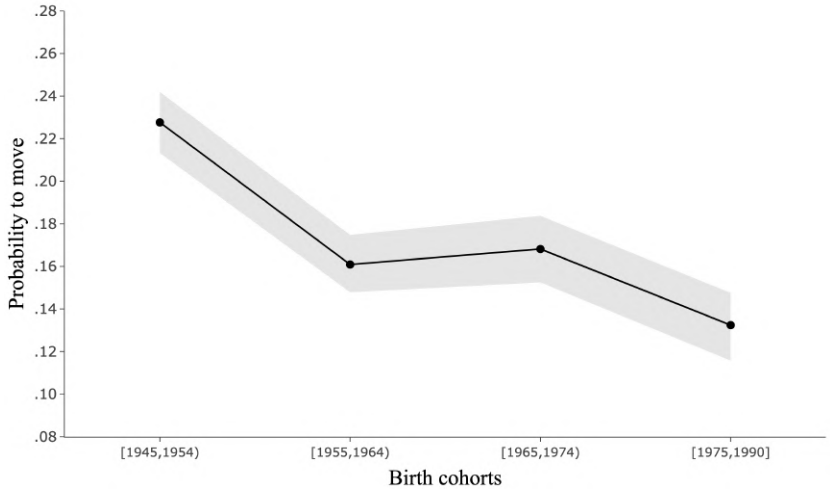
For comparison, we also present results obtained without any binning or smoothing. These estimates are shown in Figures H.7 to H.9. As expected, the unsmoothed transition matrices yield estimates that are much less precise and exhibit far more year-to-year volatility. Nevertheless, aside from this added noise, the trends appear broadly similar in that our key measures of movement and memory shown no indication of a consistent increase or decrease across cohorts.

Figure H.1: Measures of movement at generation $t = 1$ based on 10-year cohort bins

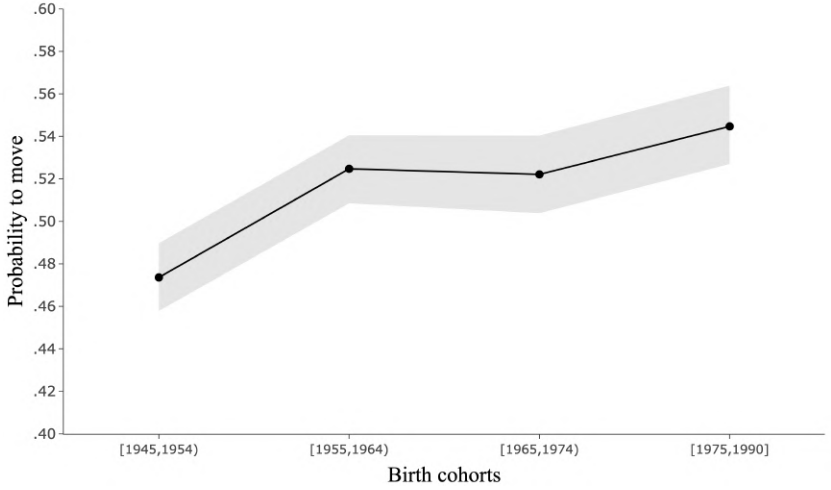
(A) Overall mobility (OM_1)



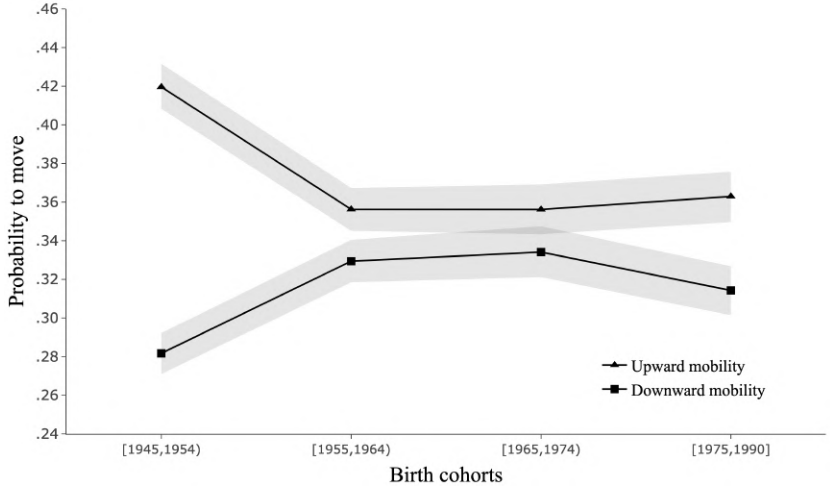
(B) Structural mobility (SM_1)



(C) Exchange mobility (EM_1)

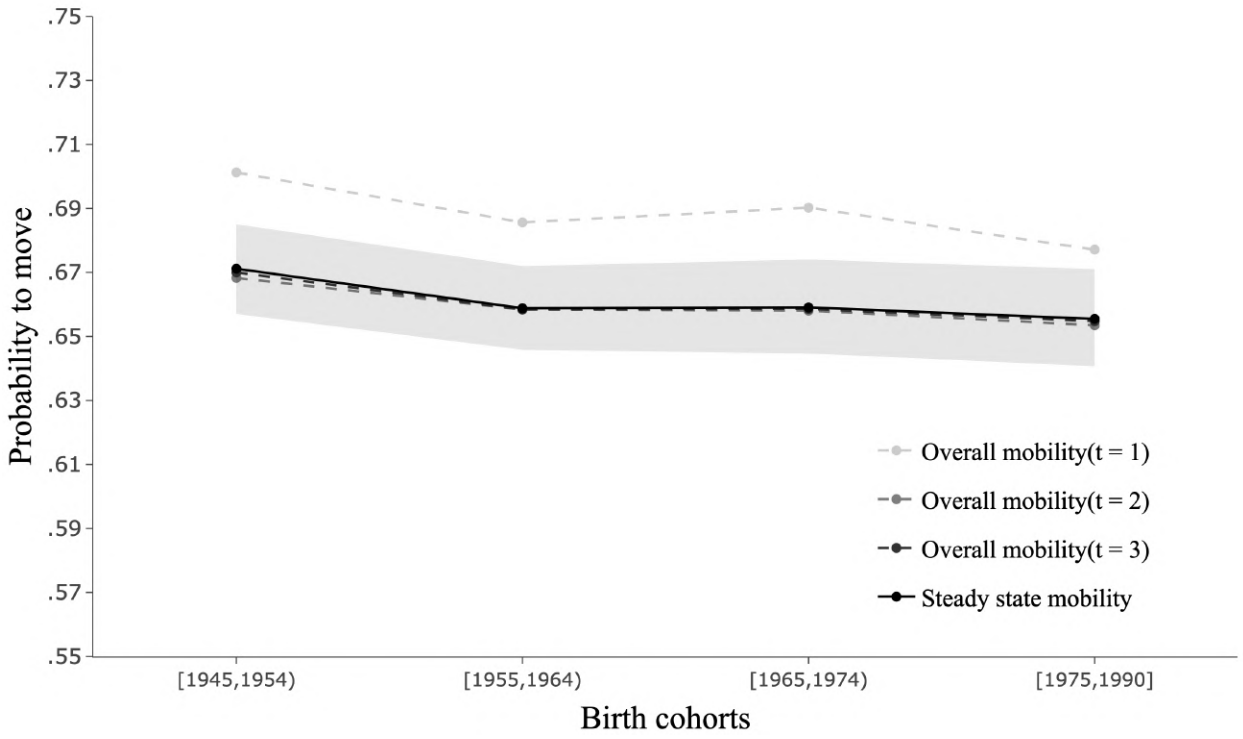


(D) Upward and downward mobility



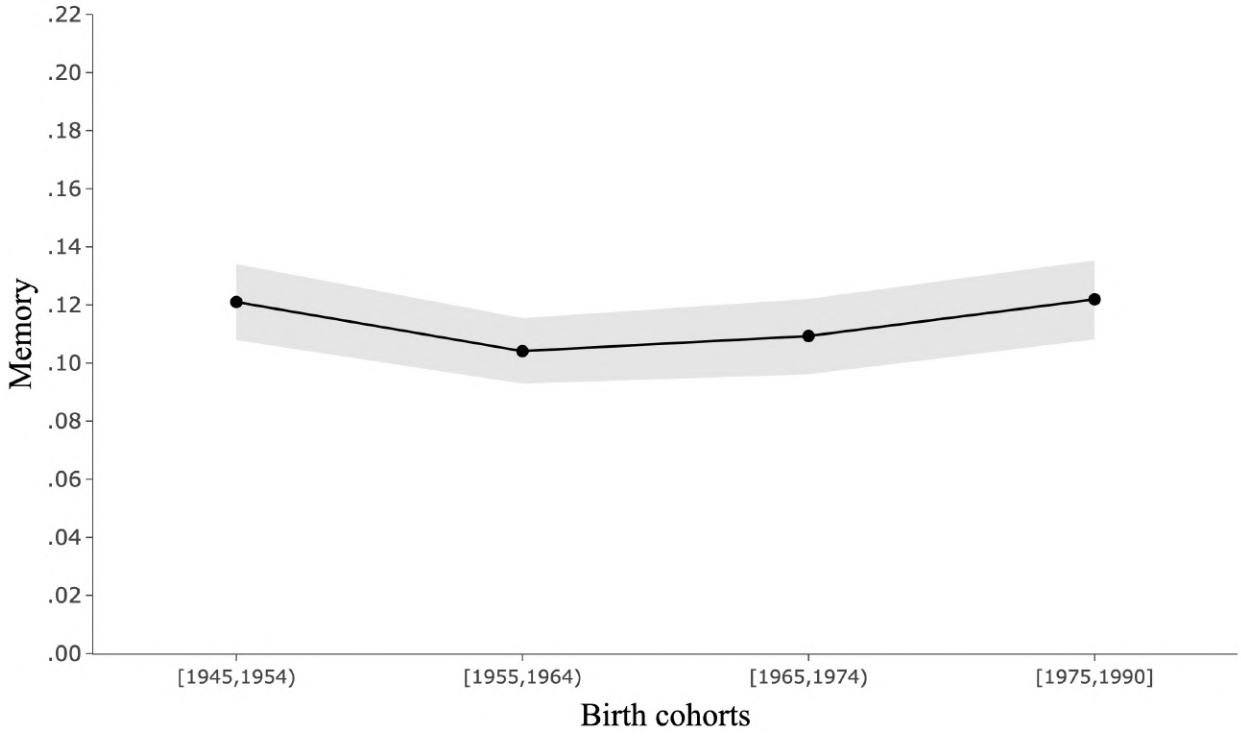
Notes: Shaded areas represent 95% confidence intervals.

Figure H.2: Overall mobility (OM_t) across synthetic generations based on 10-year cohort bins



Notes: This figure illustrates the evolution of overall mobility across generations in a stationary Markov chain. By $t = 4$, the Markov chains for most cohorts have converged to their respective steady-state distributions, where there is no structural mobility. Shaded areas represent 95% confidence intervals, which are shown only for the trend in steady-state mobility.

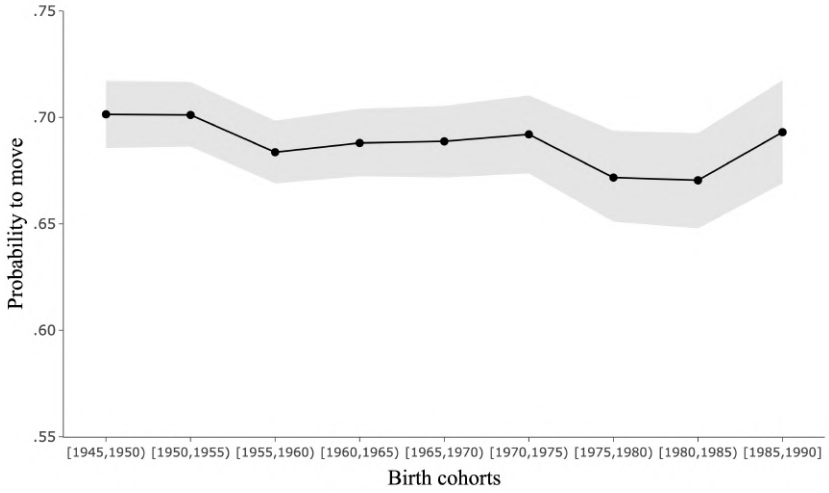
Figure H.3: Aggregate intergenerational memory at generation $t = 1$ (AIM_1) based on 10-year cohort bins



Notes: Shaded areas represent 95% confidence intervals.

Figure H.4: Measures of movement at generation $t = 1$ based on 5-year cohort bins

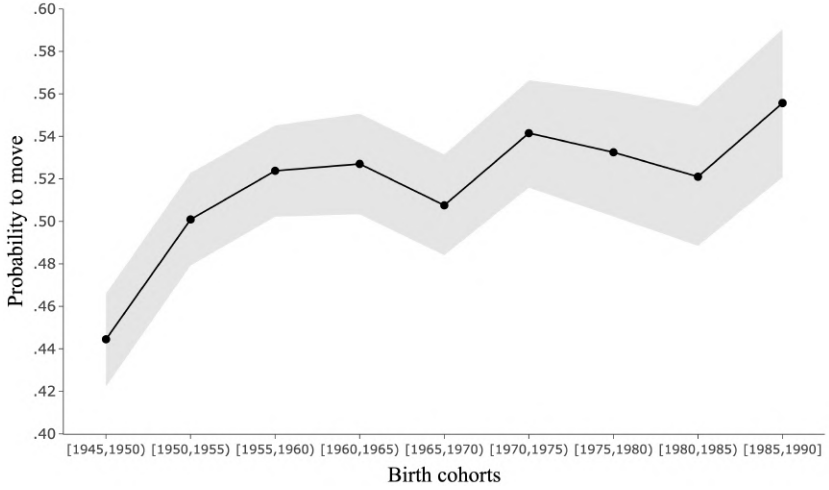
(A) Overall mobility (OM_1)



(B) Structural mobility (SM_1)



(C) Exchange mobility (EM_1)



(D) Upward and downward mobility



Notes: Shaded areas represent 95% confidence intervals.

Figure H.5: Overall mobility (OM_t) across synthetic generations based on 5-year cohort bins



Notes: This figure illustrates the evolution of overall mobility across generations in a stationary Markov chain. By $t = 4$, the Markov chains for most cohorts have converged to their respective steady-state distributions, where there is no structural mobility. Shaded areas represent 95% confidence intervals, which are shown only for the trend in steady-state mobility.

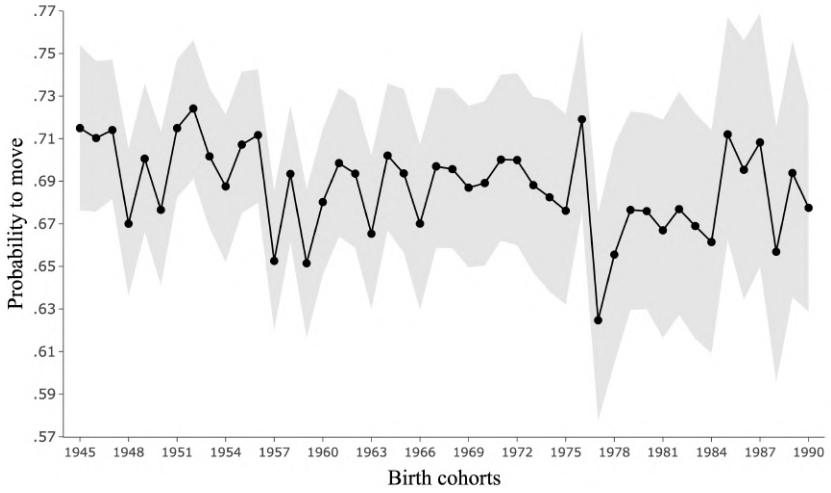
Figure H.6: Aggregate intergenerational memory at generation $t = 1$ (AIM_1) based on 5-year cohort bins



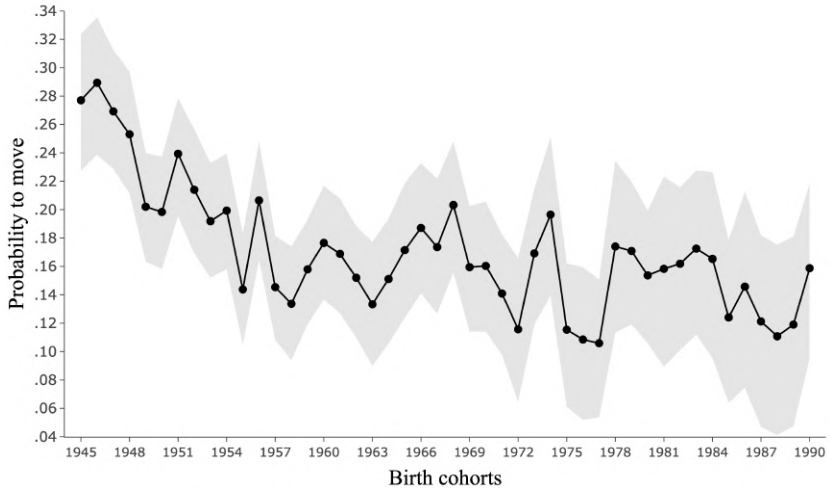
Notes: Shaded areas represent 95% confidence intervals.

Figure H.7: Measures of movement at generation $t = 1$ based on unsmoothed data

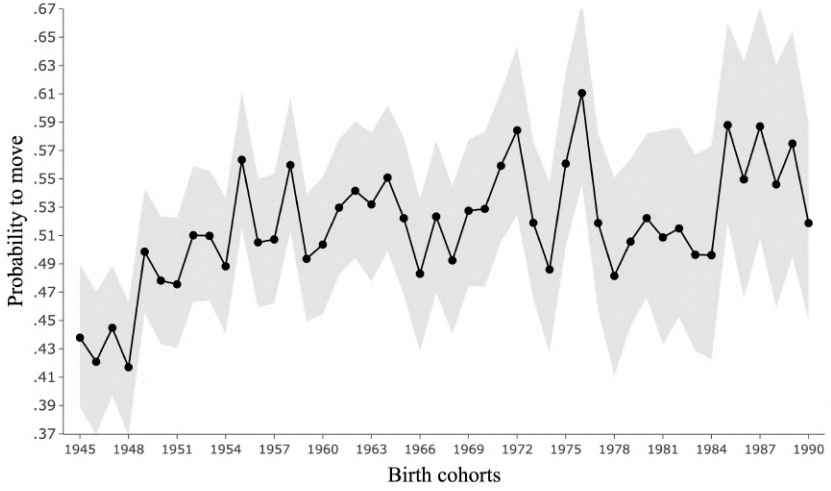
(A) Overall mobility (OM_1)



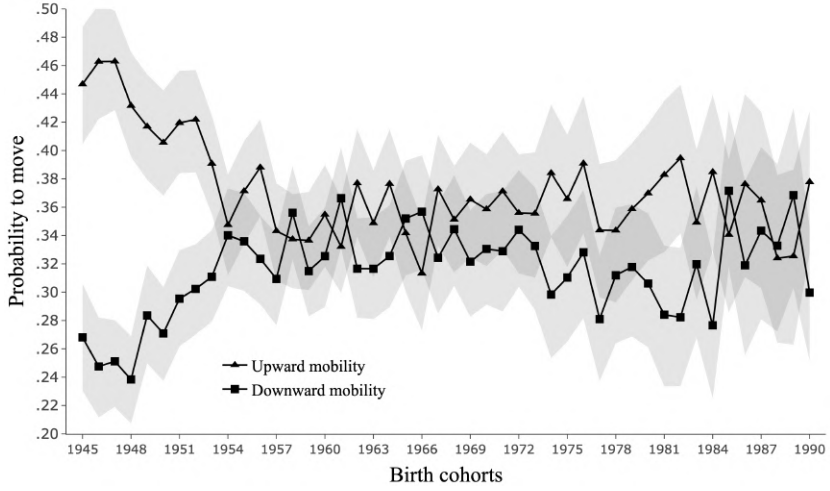
(B) Structural mobility (SM_1)



(C) Exchange mobility (EM_1)

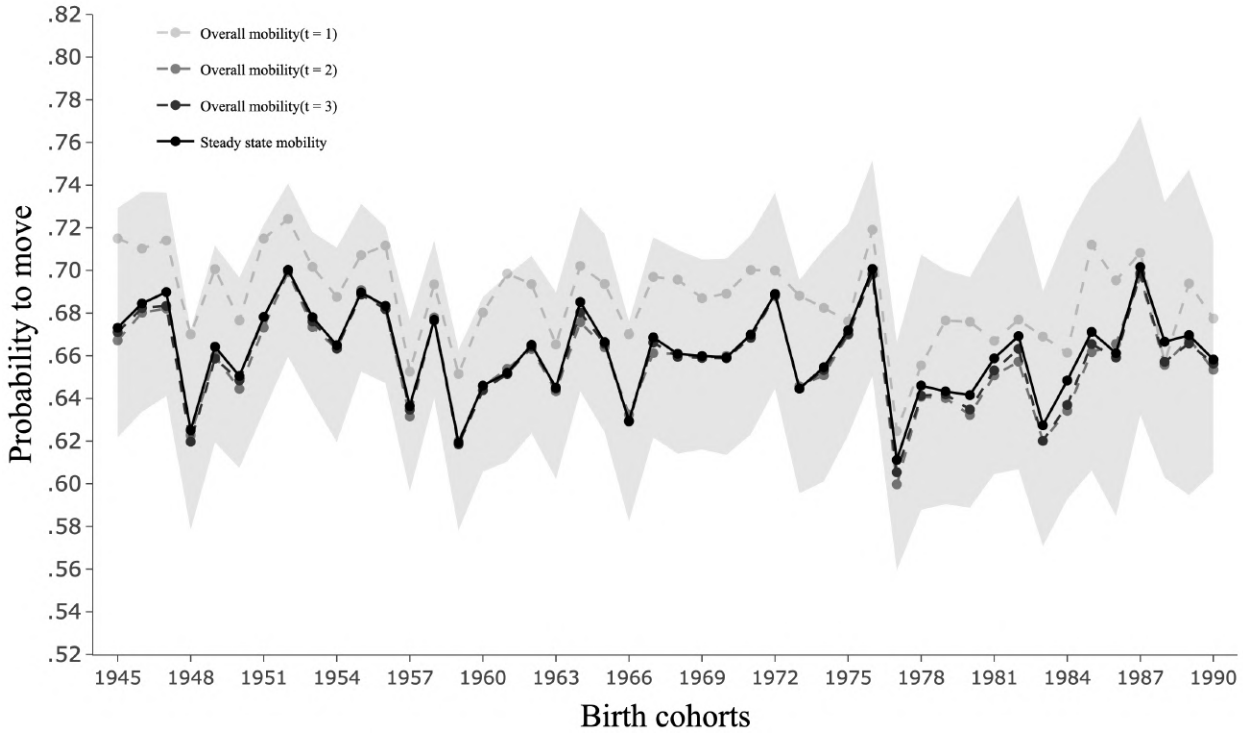


(D) Upward and downward mobility



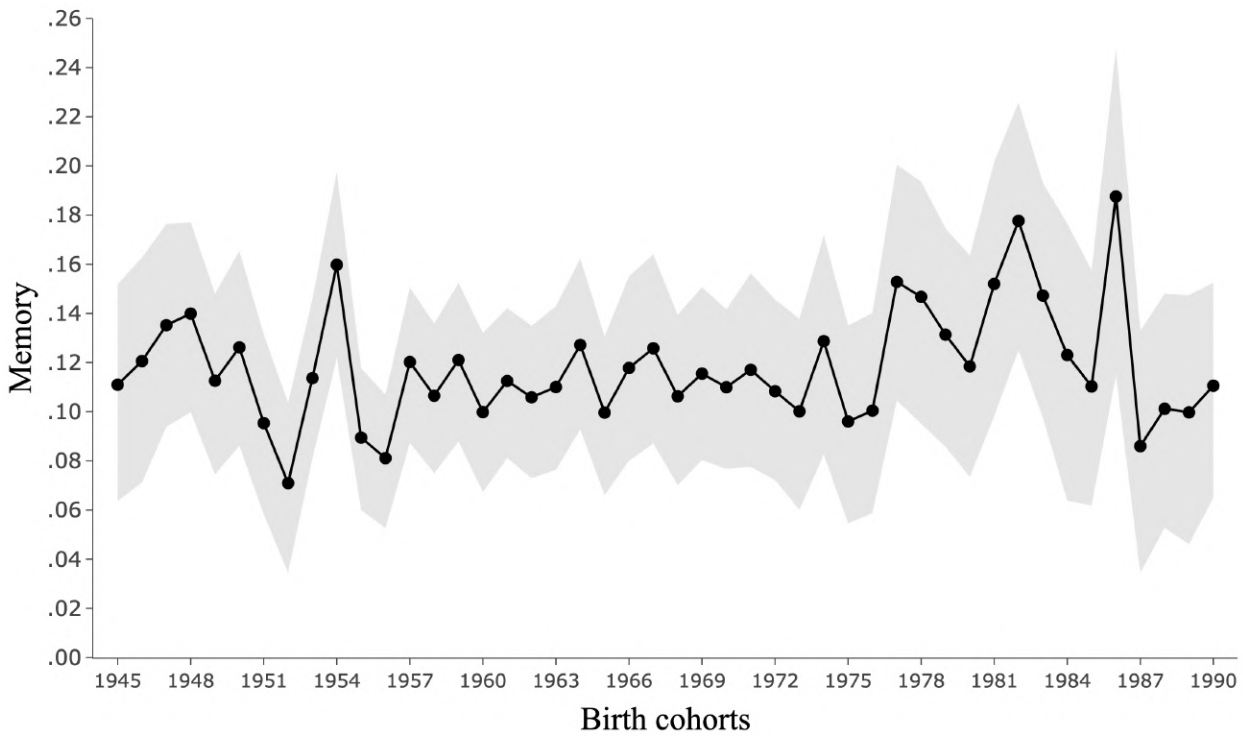
Notes: Shaded areas represent 95% confidence intervals.

Figure H.8: Overall mobility (OM_t) across synthetic generations based on unsmoothed data



Notes: This figure illustrates the evolution of overall mobility across generations in a stationary Markov chain. By $t = 4$, the Markov chains for most cohorts have converged to their respective steady-state distributions, where there is no structural mobility. Shaded areas represent 95% confidence intervals, which are shown only for the trend in steady-state mobility.

Figure H.9: Aggregate intergenerational memory at generation $t = 1$ (AIM_1) based on unsmoothed data



Notes: Shaded areas represent 95% confidence intervals.

I Income Mobility in the NLSY

In this section, we replicate our analysis using the NLSY and measures of income mobility. We construct our analytic sample and our key measures for this analysis following Bloome et al. (2018). Complete parent-child income dyads are drawn from the NLSY cross-sectional samples together with the oversamples of Black and Hispanic respondents; the military and economically disadvantaged white subsamples are excluded. To ensure that parental income broadly captures the family resources available to children before they enter the labor market, we restrict the analysis to cohorts born between 1961–1964 in the NLSY79 and 1980–1984 in the NLSY97.

For the NLSY79, parental income is measured as the average of parent-reported family income over the first five surveys beginning in 1979, subject to two requirements: the child must have been coresident with the parents in the reporting year, and at least two valid family-income observations must be available. For the NLSY97, we use family income reported in 1997—the only parent-reported family-income measure in the survey—as our primary measure of parental resources, imputing it from the average of the subsequent four years of youth-reported family income only when the 1997 value is missing. Under this construction, parental income captures family resources available to children roughly between ages 14 and 21 in the NLSY79 cohorts and ages 12 and 20 in the NLSY97 cohorts. Children's own income is measured as the average over a common age window of 27–38 in both surveys and is deflated to 2023 dollars. We then adjust income for family size; using unequivalized income yields substantively similar results.

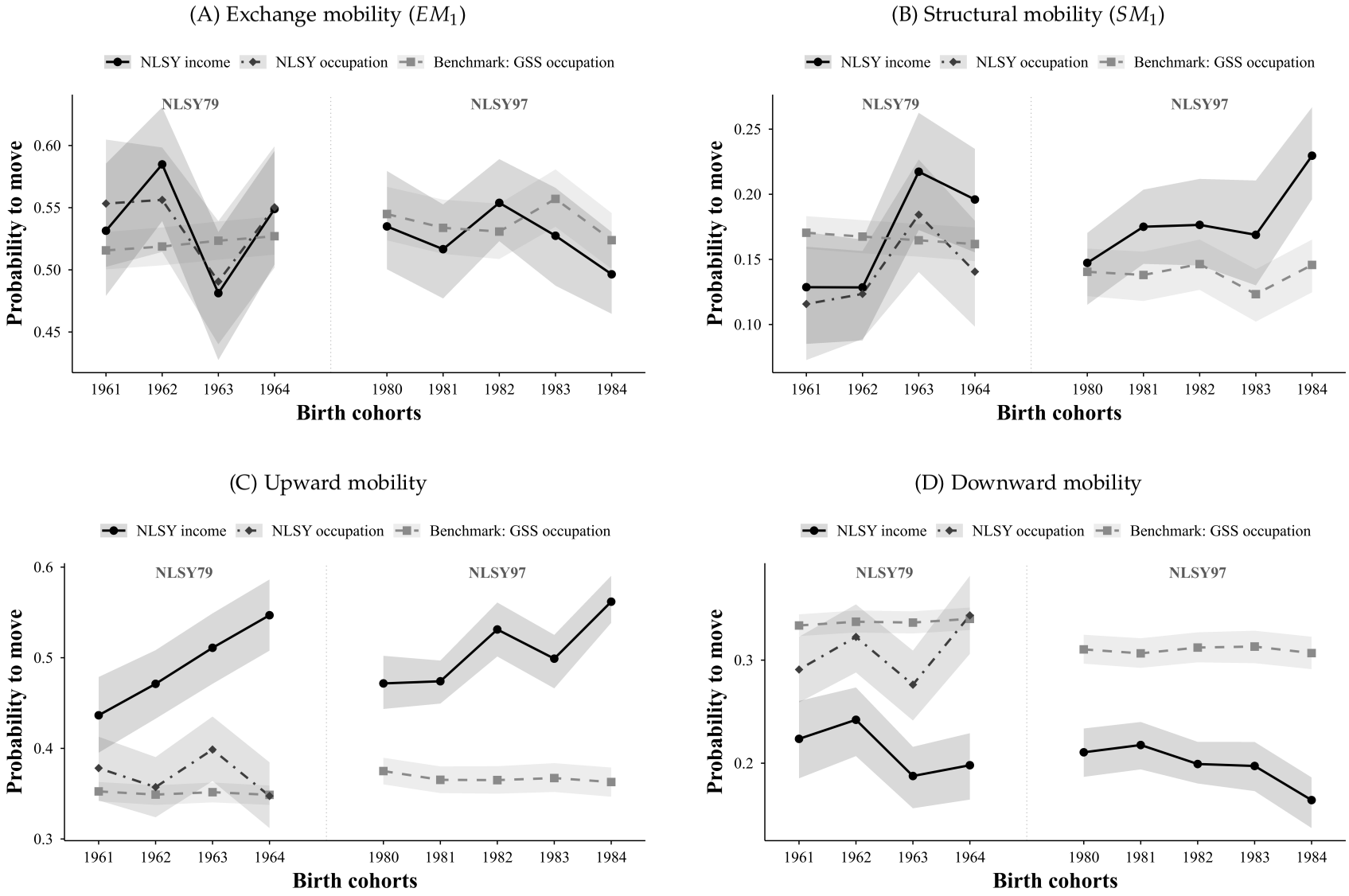
Within each survey, we define income classes using weighted quintiles of the pooled distribution of parents' and children's real family income. Because primary sampling units for the NLSY79 are not publicly available, we use the household identifier as the design unit to account for sibling correlation. For the NLSY97, we use the publicly available survey design units in a survey-based bootstrap.

To benchmark the income results, we also compute measures of occupational-class mobility in the NLSY. Because the NLSY97 does not report fathers' occupations, father-child occupational dyads can be constructed only for the NLSY79. For children, we use the occupational observation closest to age 40. This choice improves comparability with the GSS, in which occupation is observed cross-sectionally between ages 25 and 55, and age 40 is the midpoint of that window. It also provides a consistent mid-career reference point rather than allowing occupational status to depend on an arbitrary survey wave. Fathers' and children's occupations are then mapped to the EGP class typology.

The results of this analysis are presented in Figures I.1 and I.2. Taken together, they

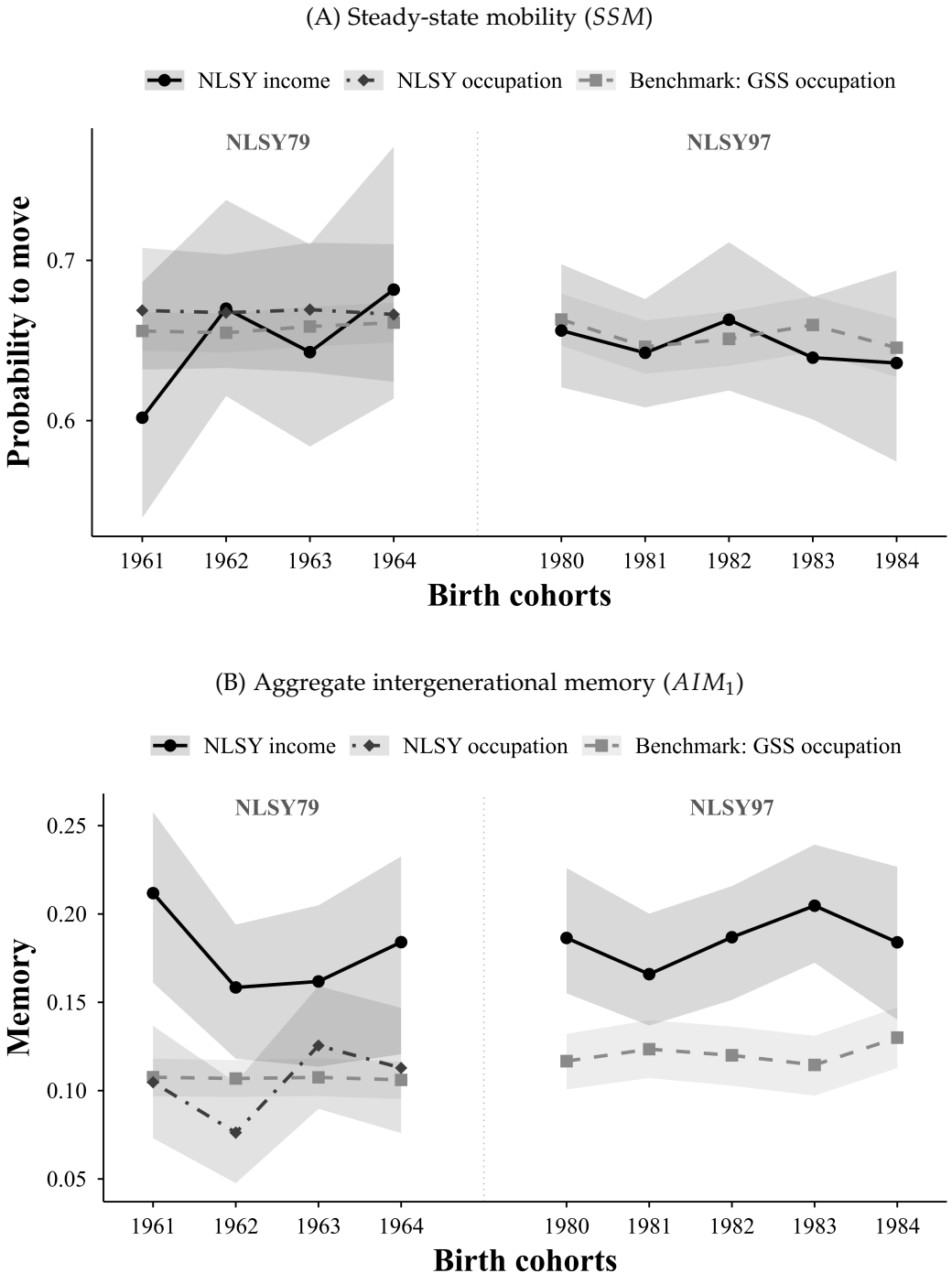
provide an external validation of the occupational-mobility trends estimated from the GSS. The NLSY79 occupational-mobility estimates align closely with the GSS in both levels and trends. The income-based estimates, although different in level, also show no sustained trend in aggregate intergenerational memory or steady-state mobility. At the same time, overall income mobility rises within both the NLSY79 and NLSY97 cohort groups, driven primarily by increases in structural and upward mobility. The stability of aggregate intergenerational memory and steady-state mobility, which are less sensitive to changes in the marginal income distributions, provides the clearest evidence that the link between parent and child income has also remained broadly stable across cohorts during the era of rising inequality. Alternative and more conventional measures of income mobility, including rank-rank correlations and intergenerational elasticities, yield cohort patterns in the NLSY very similar to our synthetic dynasty measures.

Figure I.1: Measures of movement at generation $t = 1$ based on the NLSY79 and NLSY97



Notes: This figure compares trends in intergenerational income mobility (NLSY income) and occupational mobility (NLSY occupation) among birth cohorts 1961–1964 in the NLSY79 and 1980–1984 in the NLSY97 with the corresponding trends in occupational mobility estimated from the GSS (Benchmark: GSS occupation). Shaded areas represent 95% confidence intervals.

Figure I.2: Steady-state mobility (SSM) and aggregate intergenerational memory at generation $t = 1$ (AIM_1) based on the NLSY79 and NLSY97



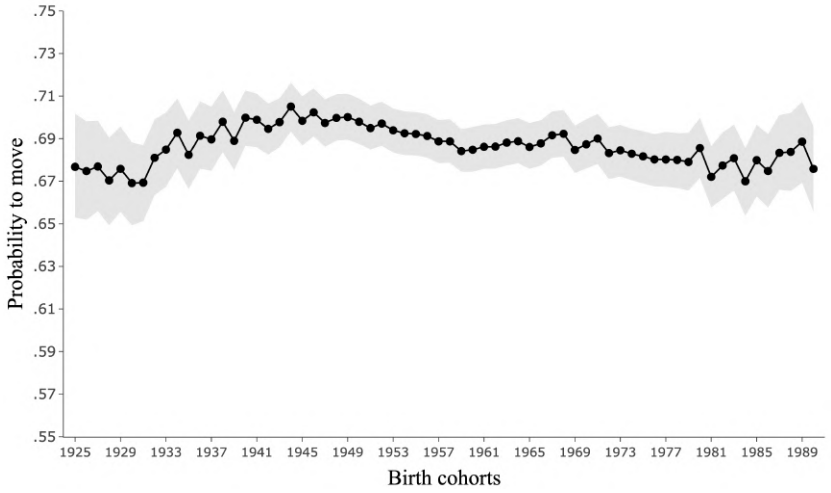
Notes: This figure compares trends in intergenerational income mobility (NLSY income) and occupational mobility (NLSY occupation) among birth cohorts 1961–1964 in the NLSY79 and 1980–1984 in the NLSY97 with the corresponding trends in occupational mobility estimated from the GSS (Benchmark: GSS occupation). Shaded areas represent 95% confidence intervals.

J An Extended Series of Cohorts

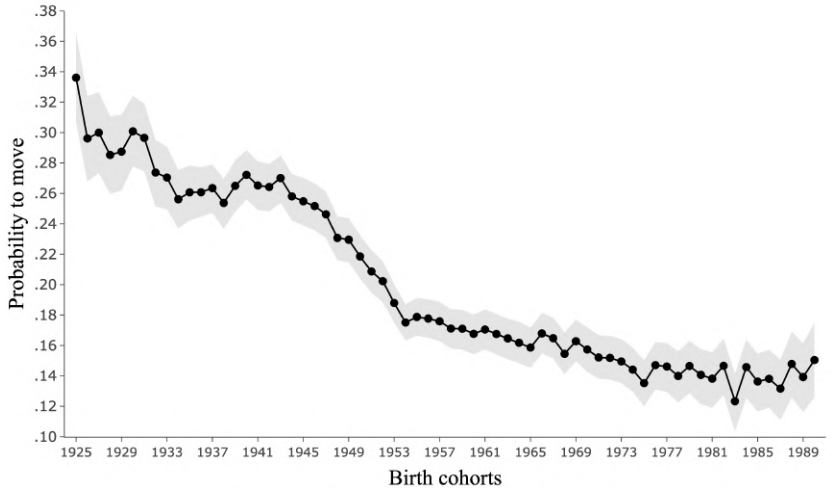
In this section, we examine mobility patterns among earlier cohorts in the GSS. Specifically, we replicate our main analysis using father-child pairs constructed for cohorts born between 1925 and 1990, applying the same age restriction of 25 to 55 at the time of the GSS interview. Including cohorts as early as 1925 reveals some distinct dynamics compared to later cohorts. Before 1945, we observe a clear upward trend in steady-state mobility, and a clear downward trend in memory and association. After 1945, however, these trends dissipate, and both movement and memory appear largely flat thereafter.

Figure J.1: Measures of movement at generation $t = 1$ based on cohorts born between 1925 and 1985

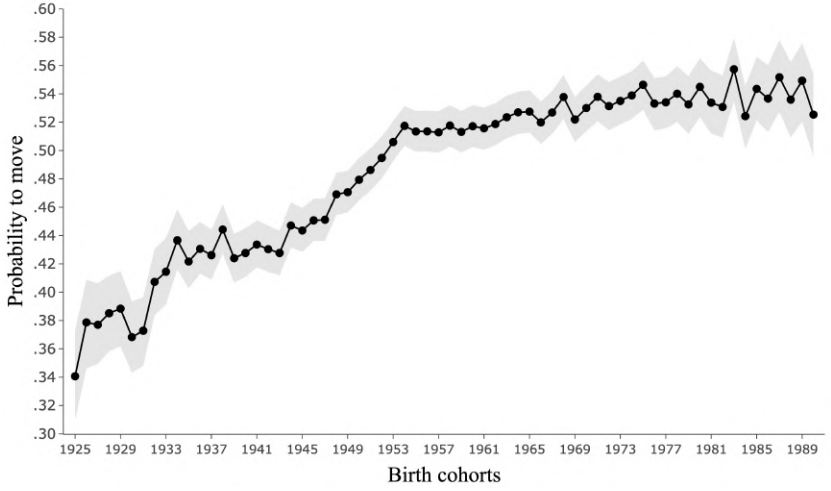
(A) Overall mobility (OM_1)



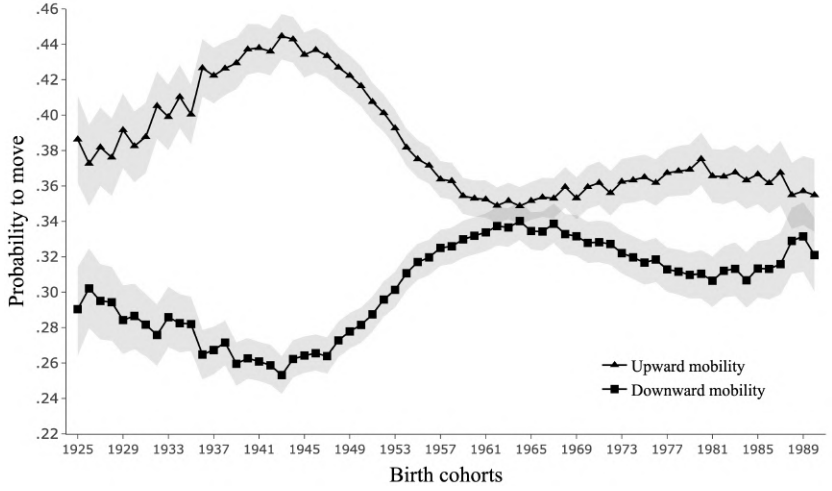
(B) Structural mobility (SM_1)



(C) Exchange mobility (EM_1)

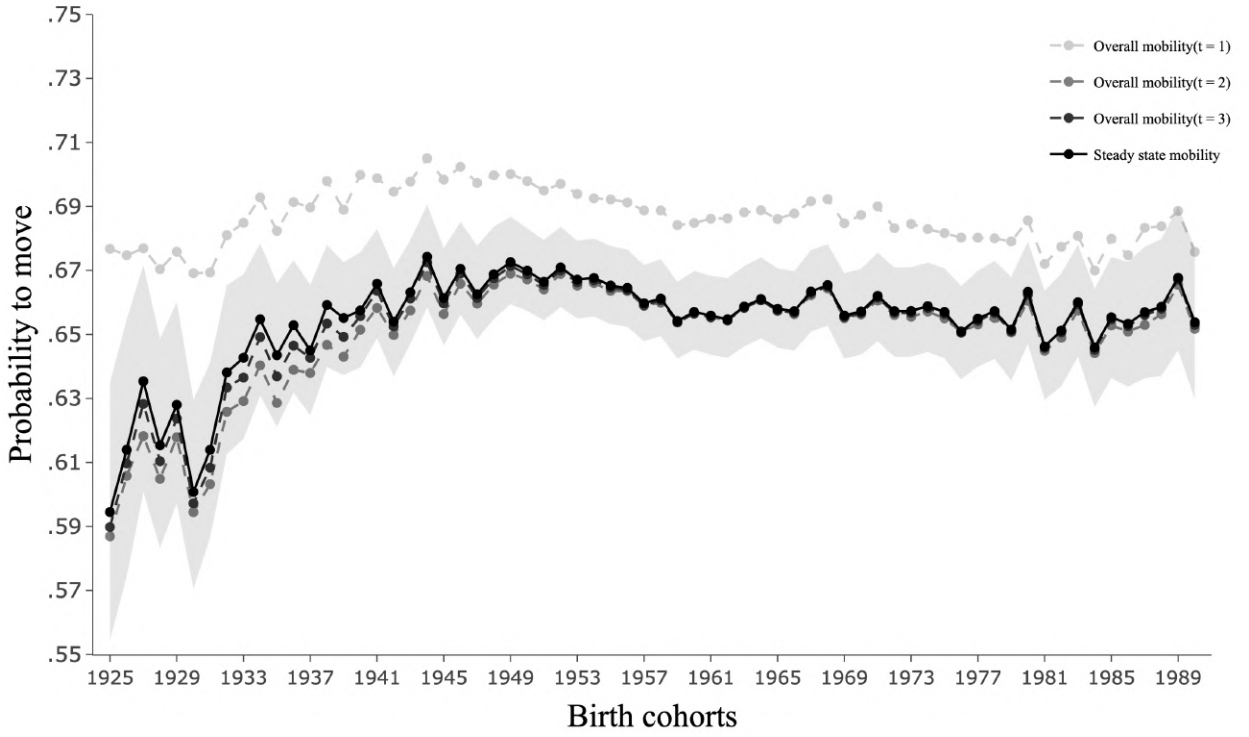


(D) Upward and downward mobility



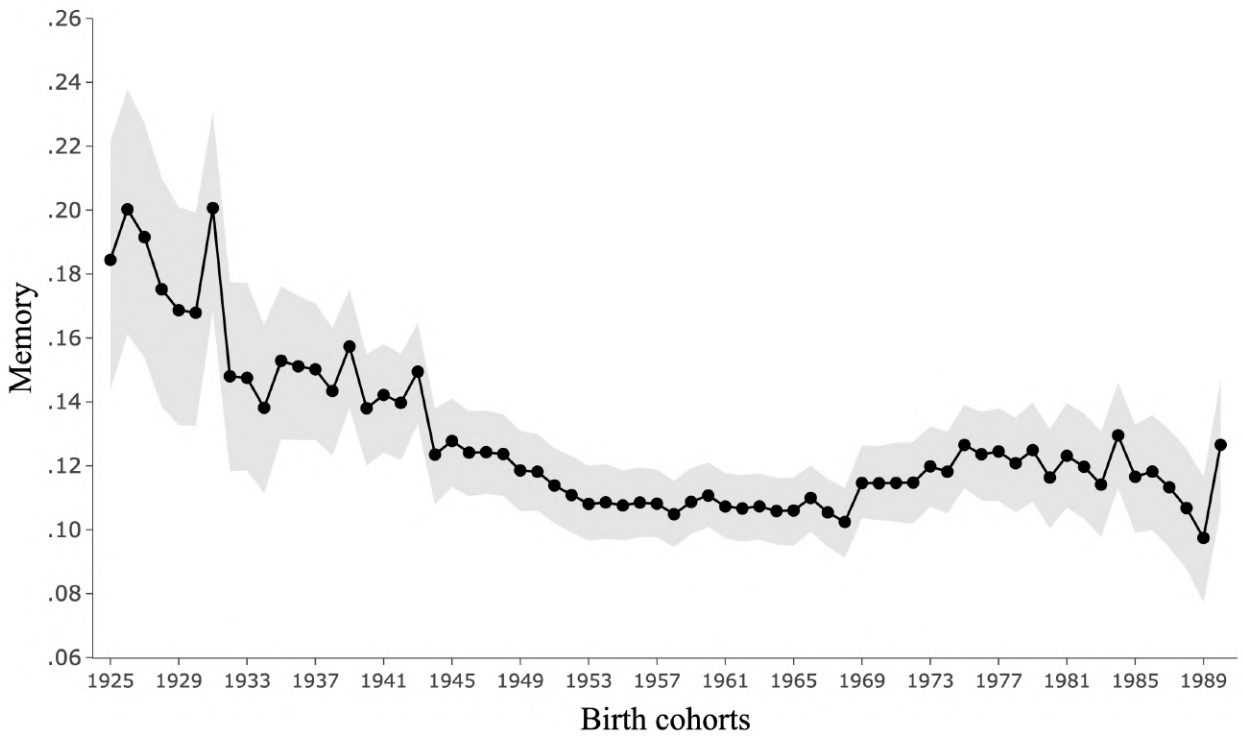
Notes: Shaded areas represent 95% confidence intervals.

Figure J.2: Overall mobility (OM_t) across synthetic generations based on cohorts born between 1925 and 1985



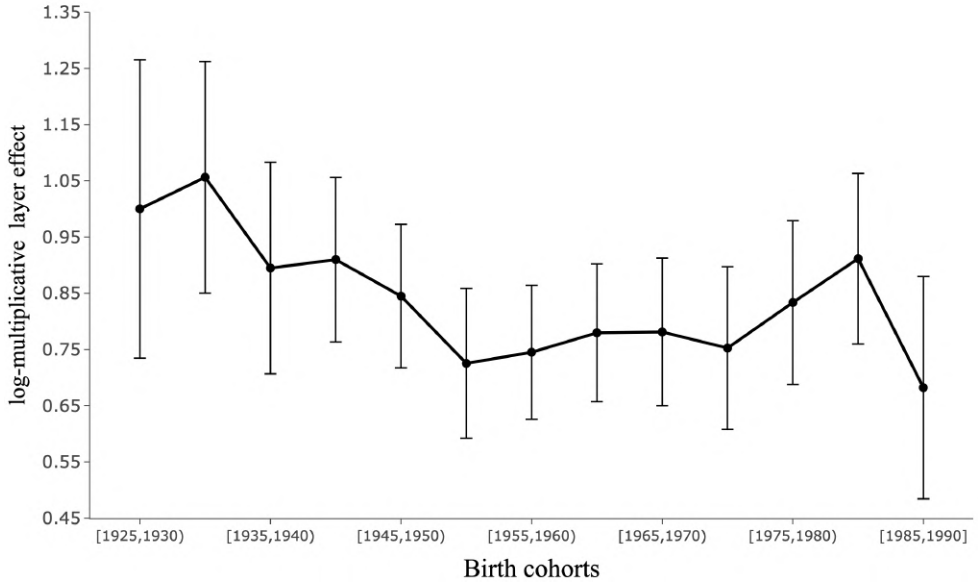
Notes: This figure illustrates the evolution of overall mobility across generations in a stationary Markov chain. By $t = 4$, the Markov chains for most of the cohorts have converged to their respective steady-state distributions, where there is no structural mobility. Shaded areas represent 95% confidence intervals, which are shown only for the trend in steady-state mobility.

Figure J.3: Aggregate intergenerational memory at generation $t = 1$ (AIM_1) based on cohorts born between 1925 and 1985



Notes: Shaded areas represent 95% confidence intervals.

Figure J.4: Log-multiplicative layer effects based on cohorts born between 1925 and 1985



Notes: This figure plots the log-multiplicative layer effect across birth cohorts using 5-year bins. The vertical bars represent 95% confidence intervals.

K Sparsity and Estimation Uncertainty

A natural concern about our results is the uncertainty in the cohort-specific transition matrices on which they are based. Although smoothing reduces random variation in the observed tables, it cannot fully eliminate the uncertainty associated with small cell counts in the underlying sample. This concern is especially pronounced for cohorts born after 1975. Because respondents from these cohorts can appear only in later GSS waves while satisfying our age restriction of 25 to 55, their transition matrices are estimated from fewer father-child dyads. Figure 1 in the main text shows this decline in sample size across both fathers' class origins and children's class destinations. At the same time, some origin-destination transitions are substantively uncommon throughout the study period. This is particularly relevant for transitions involving class 4—higher-grade manual workers, lower-grade technicians, and farmers—which is relatively small among recent cohorts.

We define a cell as sparse when the raw cell count in the parental origin-child destination contingency table is no greater than 5:

$$A_{ij,c} = \mathbf{1}\left\{N_{ij,c}^{\text{raw}} \leq 5\right\},$$

where i denotes the father's origin class, j denotes the child's destination class, and c denotes the child's birth cohort. As we discussed before, a cell can be sparse when a certain transition is less common or when the cohort sample supporting the transition matrix is relatively small. In some situations, these two sources of sparsity can occur together, making the sparsity issue more severe for later cohorts. As shown in Table K.1, under the current definition of sparsity, the median number of sparse cells in later cohorts is three times that in earlier cohorts, and these cells are more widely distributed across the transition matrix, appearing in more origin rows. For a cell involving a class that is more "dynamically distant" from other classes, a perturbation of a given size may produce a larger change in the steady-state distribution. For example, perturbations that increase inflows into class 4 from all other origins, as well as its retention, may have a sizeable effect on its long-run steady-state share.

The sparsity problem in the raw contingency table naturally raises two concerns about our results. First, does the limited sample, that is, the limited cohort size, provide reliable estimates of the joint distribution of fathers' and children's occupational classes, including both the parental-origin distribution and the transition matrix? Second, supposing that the current sample adequately represents the joint distribution, is the transition system sensitive to perturbations of transition probabilities that are close

to zero? Specifically, are our main findings of broadly stable trends robust to potential instability associated with the sparse cells in our transition matrices?

We designed two perturbation exercises to directly assess the robustness of our results to these two concerns. Throughout this section, let $\widehat{P}_c$ denote the smoothed father-to-child transition matrix for cohort c, and let $\widehat{\mu}_{0,c}$ denote the smoothed marginal distribution of fathers across the five occupational origin classes for respondents in child birth cohort c. In the main analysis, this parental-origin distribution serves as the initial marginal distribution for the Markov-chain calculations. The corresponding marginal distribution of children's destination classes implied by the estimated Markov transition matrix is $\widehat{\mu}_{1,c} = \widehat{\mu}_{0,c}\widehat{P}_c$.

Let

$$T_{ic} = \{j : A_{ij,c} = 1\}$$

denote the set of sparse destination cells in father-origin row i for cohort c, let $m_{ic} = |T_{ic}|$ denote the number of sparse cells in that row, and let

$$K_c = \sum_i m_{ic}$$

denote the total number of sparse cells in the cohort table. We use a dyad-equivalent parameter, κ, to index our perturbation exercises, where $\kappa = 1$ corresponds to one dyad-equivalent per sparse cell. The change in a sparse-cell transition probability corresponding to one dyad-equivalent can differ between the two exercises. Our primary perturbation exercise focuses on $\kappa = 1$, so a cohort with K_c sparse cells receives a total perturbation of K_c dyad-equivalents. Combined with the greater prevalence of sparsity in later cohorts, this design implies a generally larger total perturbation budget for these cohorts.

Our first exercise, which we refer to as *redistribution*, is designed to address concerns about the sensitivity of our estimated transition system, taking the estimated transition matrix as the baseline and holding the estimated father-origin marginal distribution fixed. The redistribution exercise answers the following question: *If we increase each sparsely supported transition probability by a one-dyad-equivalent amount, how do the cohort trends in all of our intergenerational mobility measures change?*

The exact one-dyad-equivalent size is defined as follows. Let n_{ic} denote the raw number of dyads in father-origin row i. We increase each sparse-cell probability by κ/n_{ic}, which, at $\kappa = 1$, corresponds to a one-dyad-equivalent increase conditional on

origin. Defining

$$S_{T,ic} = \sum_{j \in T_{ic}} \widehat{P}_{ij,c}$$

as the baseline probability mass contained in the sparse cells of that row, the perturbed probabilities are

$$\widehat{P}^{R}_{ij,c} = \widehat{P}_{ij,c} + \frac{\kappa}{n_{ic}}, \qquad j \in T_{ic},$$

and

$$\widehat{P}^{R}_{ij,c} = \widehat{P}_{ij,c} \left(\frac{1 - S_{T,ic} - \kappa m_{ic}/n_{ic}}{1 - S_{T,ic}} \right), \qquad j \notin T_{ic}.$$

Provided that positive probability mass remains in the donor cells, rearranging the second equation gives the following equality:

$$\frac{\widehat{P}^{R}_{ij,c}}{1 - S_{T,ic} - \kappa m_{ic}/n_{ic}} = \frac{\widehat{P}_{ij,c}}{1 - S_{T,ic}}, \qquad j \notin T_{ic}.$$

This construction preserves the relative shares of the donor cells and ensures that each row continues to sum to one.[1] In our perturbation exercise, the donor cells are always the non-sparse cells. When several father-origin rows contain sparse cells, each affected row is perturbed in this way. Note that we deliberately increase the sparse-cell probabilities rather than decrease them to address more directly the concern that the joint distribution estimated from the sample may understate certain transition probabilities because those transitions are rarely observed.

The second exercise, which we refer to as *augmentation*, evaluates the sensitivity of our results to uncertainty in the underlying joint distribution of fathers' and children's occupational classes. Specifically, because certain transitions are less prevalent, they may be more likely to be unobserved or underrepresented in a finite sample. We thus "augment" their representation in the exercise by considering a hypothetical sample in which additional dyads belonging to these cells had been observed. To reduce the influence of sampling noise in the GSS when evaluating these hypothetical changes in transition prevalence, we conduct our perturbation exercise on the smoothed joint distribution. Combining the smoothed joint distribution with the raw dyad count of each cohort gives us a pseudo-contingency table with reduced sampling variation. We can then ask how adding hypothetical omitted dyads to the sparse cells would change the

[1] In application, for the affected rows, the redistribution exercise requires $n_{ic} > 0$, $S_{T,ic} < 1$, and $\kappa m_{ic}/n_{ic} \leq 1 - S_{T,ic}$, so that the perturbed probabilities remain nonnegative. The total increase assigned to the sparse cells is therefore removed proportionally from the non-targeted cells in the same father-origin row.

joint distribution. Let N_c denote the raw number of father–child dyads in cohort c, and define the smoothed mass of father-origin row i as

$$w_{ic} = N_c \widehat{\mu}_{0,i,c},$$

where $\widehat{\mu}_{0,i,c}$ is the smoothed share of fathers in occupational origin class i. The baseline pseudo-count in cell (i, j) is then

$$C^0_{ij,c} = w_{ic} \widehat{P}_{ij,c}.$$

We then augment each sparse cell by κ pseudo-dyads:

$$C^A_{ij,c} = C^0_{ij,c} + \kappa A_{ij,c}.$$

After renormalizing the augmented table, the perturbed transition probabilities are

$$\widehat{P}^A_{ij,c} = \frac{w_{ic} \widehat{P}_{ij,c} + \kappa A_{ij,c}}{w_{ic} + \kappa m_{ic}},$$

and the perturbed marginal distribution of fathers across origin classes is

$$\widehat{\mu}^A_{0,i,c} = \frac{w_{ic} + \kappa m_{ic}}{N_c + \kappa K_c}.$$

Here, the one-dyad-equivalent perturbation is defined on the pseudo-count scale rather than directly on the origin-specific transition probabilities. Unlike redistribution, augmentation does not transfer a fixed amount of probability from non-sparse cells to sparse cells. Instead, at $\kappa = 1$, it adds one pseudo-dyad to each sparse cell in the smoothed pseudo-contingency table and then renormalizes the resulting table. The mass of each affected father-origin row therefore increases, as does the total mass of the cohort table. Consequently, the transition matrix, the smoothed distribution of fathers across occupational origin classes, and the implied marginal distribution of children's occupational classes can all change. When $\kappa = 0$, the normalized pseudo-contingency table reproduces our baseline smoothed joint distribution.

As our main conclusions concern trends in intergenerational mobility, we focus on the systematic impact of the perturbation exercises on our cohort-specific result series, rather than interpreting the results separately for each cohort. To characterize the trends in these series, we fit an OLS regression for each measure separately. For a measure

denoted by θ_c, the trend within cohort window W is summarized as follows:

$$\theta_c = \alpha_W + \beta_W \left(\frac{c - \bar{c}_W}{10} \right) + \varepsilon_c,$$

where $\bar{c}_W$ is the midpoint of the relevant cohort window. The primary window runs from 1945 to 1990, the same as in our baseline analysis. As sparse cells are more prevalent among later cohorts, we also consider a restricted window from 1975 to 1990 to diagnose the sensitivity of the late-cohort results. Under this parameterization, β_W gives the change in the measure per decade.

Let β_W^0 denote the slope based on the baseline transition matrices and $\beta_W^M(\kappa)$ the slope after applying mechanism $M \in \{R, A\}$. The perturbation-induced change in the trend is

$$\Delta\beta_W^M(\kappa) = \beta_W^M(\kappa) - \beta_W^0.$$

Because the baseline and perturbed regressions include exactly the same cohorts and use the same specification, $\Delta\beta$ is also equal to the slope obtained by regressing the cohort-specific perturbation effects,

$$\theta_c^M(\kappa) - \theta_c^0,$$

on the same centered and decade-scaled birth-cohort variable, $(c - \bar{c}_W)/10$, with an intercept. Table K.2 reports the baseline slope, the slope under each perturbation, and the resulting $\Delta\beta$ for both cohort windows. Figure K.1 provides the graphical counterpart, displaying the perturbation-induced slope changes for all measures under both mechanisms and in both periods.

Quantifying uncertainty in the perturbation effect requires placing the current exercise in the context of sampling variation. To do so, we use the 2,000 precomputed bootstrap replicates from our main analysis, in which we used a survey-year-stratified bootstrap and re-estimated our GAM model for each bootstrap sample. The baseline bootstrap captures both sampling variation and uncertainty arising from re-estimating the smoothing model. Applying the perturbations to the bootstrap estimates and comparing the perturbed results with their unperturbed counterparts helps us quantify uncertainty in the perturbation effect under sampling variation. Within each bootstrap replicate b, we calculate the relevant baseline and perturbed slopes and form the paired difference

$$\Delta\beta_{W,b}^M = \beta_{W,b,\text{pert}}^M - \beta_{W,b,\text{base}}.$$

The 95% interval for $\Delta\beta$ is therefore the 2.5th to 97.5th percentile range of these paired differences across bootstrap replicates. The intervals for all measures are reported

in Table K.2, while Figure K.1 displays them alongside the baseline-to-perturbed slope change, $\Delta\beta$. As $\Delta\beta$ captures the change induced by the perturbation, its magnitude and sign indicate the size and direction of the slope change, while the width of the interval reflects its uncertainty. An interval that crosses zero represents uncertainty about the direction of the change; it does not by itself imply a reversal of the underlying trend. To assess how frequently the perturbed trends align with the direction of our baseline results, $P(\text{direction retained})$ in Table K.2 reports the proportion of bootstrap replicates in which the perturbed slope has the same sign as the deterministic baseline slope.

To better understand the size of the perturbation effect, we further benchmark it against the variation in results generated by the unperturbed bootstrap. As several of our measures depend on the invariant distribution, and the steady-state distribution is itself determined by the transition matrix, we first compare the total-variation distance between the baseline and perturbed stationary distributions with the corresponding distances generated by the unperturbed bootstrap. Table K.1 shows that, under both perturbation exercises, the stationary-distribution effects at $\kappa = 1$ fall below the total-system bootstrap 95th-percentile benchmark in the reported median comparisons. However, the late-cohort effects are much closer to this upper quantile of the bootstrap variation.

The direct comparison of the perturbation-induced slope changes with variation generated by the total bootstrap system is presented in Table K.3. The total-system benchmark is based on

$$u_{W,b}^{\text{total}} = \beta_{W,b,\text{base}} - \beta_W^0,$$

which quantifies the difference between the slope for a measure in bootstrap replicate b and the deterministic baseline slope. Because it is constructed from the complete bootstrap replicate, it captures ordinary uncertainty throughout the estimated system. For measures that depend on both the father-origin marginal and the transition matrix, it includes variation in both components.

Another useful benchmark can be defined in relation to the sparse cells: if we focus on the flagged sparse cells, how much variation in our results can be generated by bootstrap changes at these locations? To answer this question, we use the existing bootstrap replicates to vary the flagged sparse cells, together with the normalization adjustments required elsewhere in the table. We refer to this as a targeted bootstrap-system reference. For comparison with the redistribution exercise, we replace the flagged sparse cells of the baseline smoothed transition matrix with the corresponding bootstrapped transition probabilities and rescale the remaining cells of each affected father-origin row so that the rows still sum to one, while holding the father-origin marginal distribution fixed at its baseline level. In parallel with the augmentation exercise, we instead update the

flagged cells of the baseline smoothed pseudo-contingency table with the corresponding bootstrapped values on the same pseudo-count scale and then renormalize the table, so that both the origin marginal distribution and the transition law can change. These constructions are designed to closely mirror our augmentation and redistribution exercises using variation generated by the bootstrap. Let $u_{W,b}^{\text{target}}$ denote the difference between the slope obtained from the corresponding targeted bootstrap reference and the deterministic baseline slope. We summarize the comparisons using

$$R_{\text{total}} = \frac{|\Delta\beta|}{q_{.95}\left(|u_{W,b}^{\text{total}}|\right)}$$

and

$$R_{\text{target}} = \frac{|\Delta\beta|}{q_{.95}\left(|u_{W,b}^{\text{target}}|\right)},$$

where the quantiles are taken across bootstrap replicates. These ratios are displayed in Table K.3. Figure K.2 benchmarks the perturbation effects against bootstrap variation. The light-gray and dark-gray bands show the total-system and targeted sparse-cell bootstrap reference ranges of slope deviations from the baseline estimate, respectively, whereas the point-and-interval marks show the perturbation-induced slope change, $\Delta\beta$, and its paired-bootstrap 95% interval, as also shown in Figure K.1.

The perturbation results show that our main conclusions are not overturned by the one-dyad-equivalent perturbations. As shown in Table K.2 and Figure K.1, the majority of our measures retain their baseline trend direction over the full period, and the slope changes are relatively mild. Small sign changes occur in the individual memory measures for classes 1 and 5, while more pronounced changes in magnitude occur in the long-run measures specifically related to class 4. The slope change for class 5 memory is approximately 0.001 index units per decade in absolute value, against a nearly flat baseline trend.

The more pronounced changes in the class-4-specific long-run measures reveal an important feature of our Markov measures: for a primitive transition matrix, every class is reachable from every other class. Therefore, perturbation effects should not be evaluated in isolation. A perturbation to a particular cell can affect the steady-state distribution through the connections among states in the transition system.[1] As shown in Figure E.2,

[1]For finite irreducible transition matrices P and $\widetilde{P} = P + E$, Hunter's exact perturbation identity is: (Hunter, 2005):

$$\widetilde{\boldsymbol{\pi}} - \boldsymbol{\pi} = -\widetilde{\boldsymbol{\pi}} E N,$$

where $\boldsymbol{\pi}$ and $\widetilde{\boldsymbol{\pi}}$ are the corresponding stationary row vectors, $N_{\ell j} = \pi_j m_{\ell j}$ for $\ell \neq j$, $N_{jj} = 0$, and $m_{\ell j}$

class 4 generally takes the longest to reach from other origins, and these passage times tend to increase across cohorts. As the perturbation exercise is conducted on all sparse cells, it can alter both inflows into class 4 and its retention. Where these changes redirect probability toward class 4 from destinations with long passage times into it, they can produce a sizeable proportional increase in its steady-state share. Consistent with this mechanism, the decreasing trend in the steady-state share of class 4 is attenuated, as is the increasing trend in the average MFPT into class 4 from other origins. These changes are especially pronounced among later cohorts, where the perturbation budget is larger. How much weight to place on this sensitivity depends on the plausibility of the perturbations under the underlying data-generating process. The baseline estimates indicate increasing difficulty in reaching class 4, and the perturbations attenuate rather than reverse the full-period trends in its stationary share and mean first passage time. Although these class-4-specific quantities experience sizeable changes, the perturbations do not overturn our main conclusions about aggregate mobility.

The findings for movement measures are particularly stable. The perturbation exercises preserve the full-period trend directions, although their magnitudes change. As shown in Table K.2 and Figure K.1, both perturbations slightly strengthen the decline in structural mobility, whose full-period slope changes from -2.111 percentage points per decade at baseline to -2.432 under redistribution and -2.426 under augmentation. They also reinforce the increasing trend in exchange mobility, whose slope rises from 1.581 to 1.955 and 2.015, respectively. The nearly flat, though slightly declining, trend in overall mobility at $t = 1$ is further attenuated toward zero, changing from -0.530 to -0.477 under redistribution and -0.411 under augmentation, as is the decline in steady-state mobility. The directions of the upward- and downward-mobility trends are also preserved. Table K.3 further indicates that these slope changes remain below the total-system 95th-percentile benchmark. Thus, the perturbations reinforce rather than weaken the main interpretation of Figure 2: broad stability in overall mobility conceals offsetting declines in structural mobility and increases in exchange mobility.

The aggregate findings for memory are also preserved. The full-period slope in

is the baseline mean first passage time from class ℓ to class j. For a transfer of probability mass ε within origin row r, from destination d to destination k, this becomes

$$\widetilde{\pi}_j - \pi_j = \widetilde{\pi}_r \, \varepsilon \left(N_{dj} - N_{kj} \right).$$

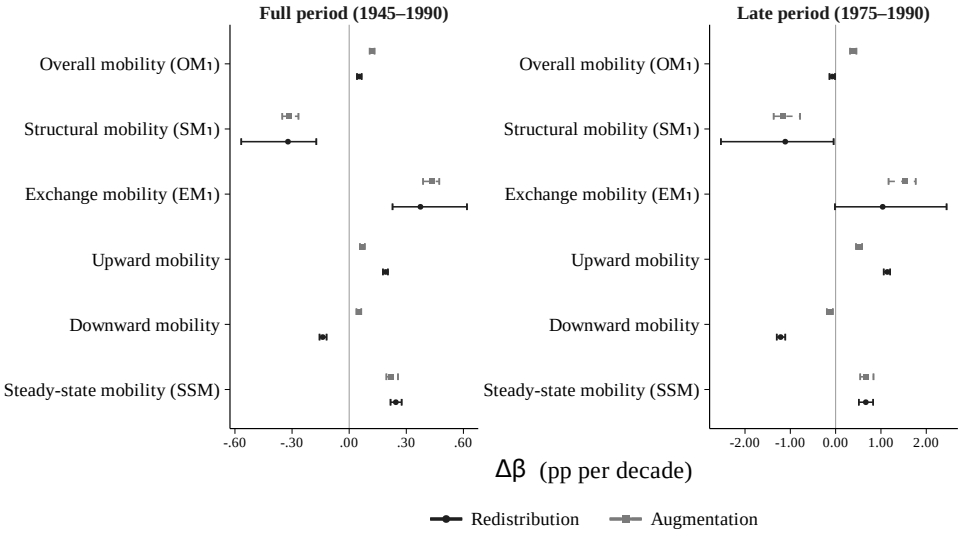
Thus, the effect depends on how much probability we move, the affected origin's stationary share after perturbation, and the difference in baseline mean first passage-time weights between the donor and recipient destinations. Redirecting probability directly into class 4 from destinations with long passage times into class 4 can therefore produce a substantial proportional change in its stationary share. A small stationary share alone does not ensure insensitivity to perturbations.

aggregate intergenerational memory remains close to zero, changing from 0.002 index units per decade at baseline to 0.002 under redistribution and 0.001 under augmentation. Greater sensitivity is confined primarily to more granular results, though these shifts are nevertheless small relative to total-system bootstrap uncertainty, with R_{total} reaching at most 0.45 among the full-period memory measures, corresponding to class 2 under redistribution. The perturbations therefore do not threaten the conclusion that aggregate intergenerational memory has remained largely stable, and the associated full-period slope changes remain below the total-system bootstrap 95th-percentile benchmark.

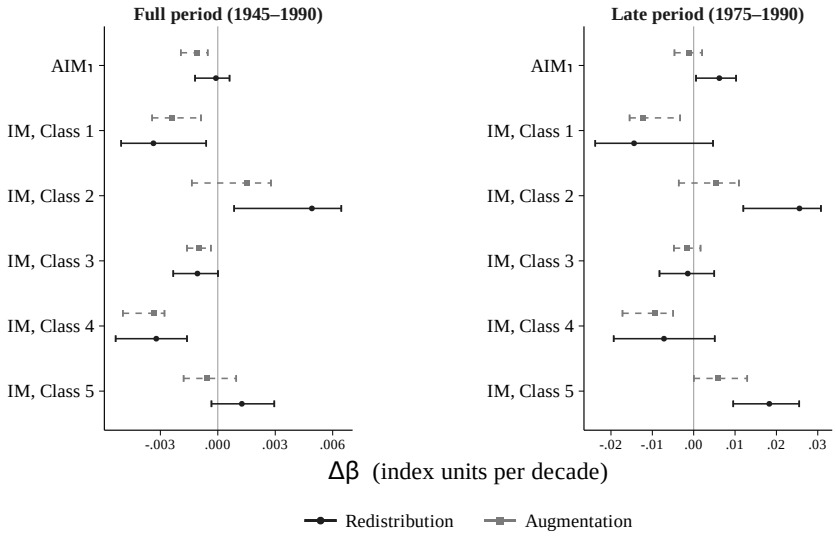
Taken together, the perturbation analysis supports our major conclusions: trends in overall mobility and aggregate intergenerational memory remain largely stable over the full period, with overall mobility masking offsetting changes in structural and exchange mobility. Although some class-specific memory slopes change sign, these changes are small relative to the uncertainty captured by the bootstrap. The principal exceptions are the steady-state share of class 4 and the mean first passage time into it. Their greater sensitivity is consistent with the influence of sparse transitions involving class 4 on its long-run dynamics.

Figure K.1: Perturbation-induced changes in estimated cohort trends ($\Delta\beta$) at $\kappa = 1$

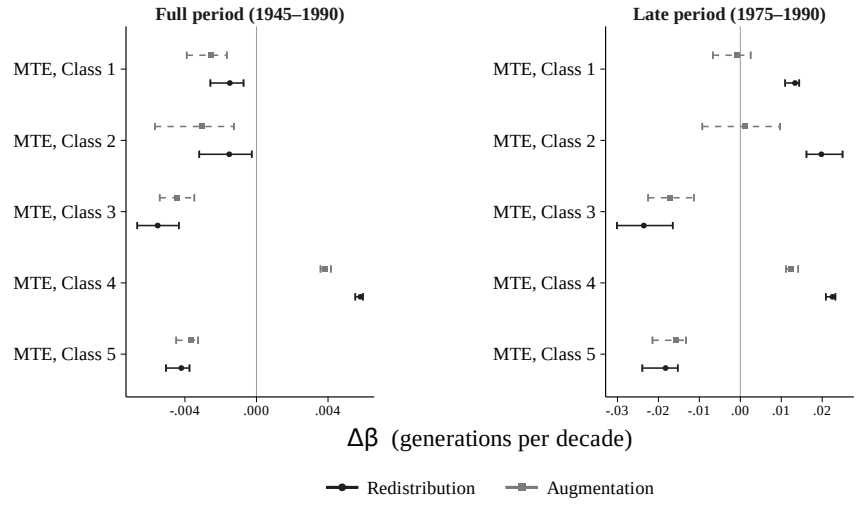
(A) Movement measures



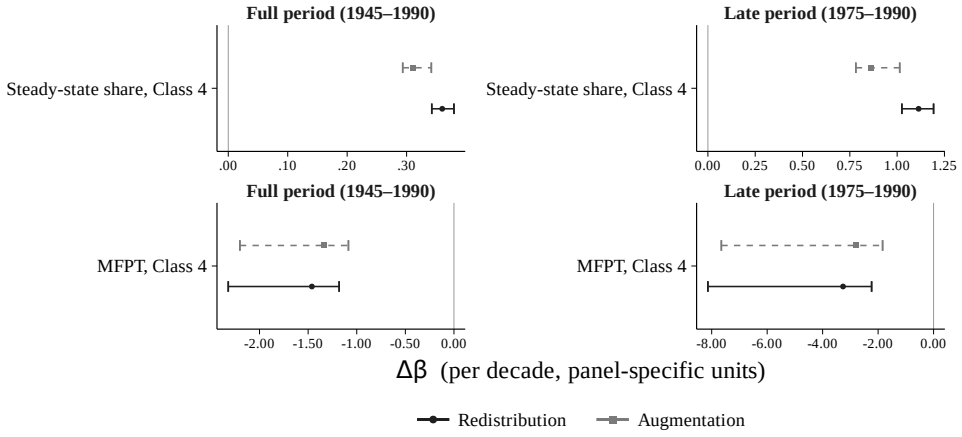
(B) Memory measures



(C) Movement class-specific measures

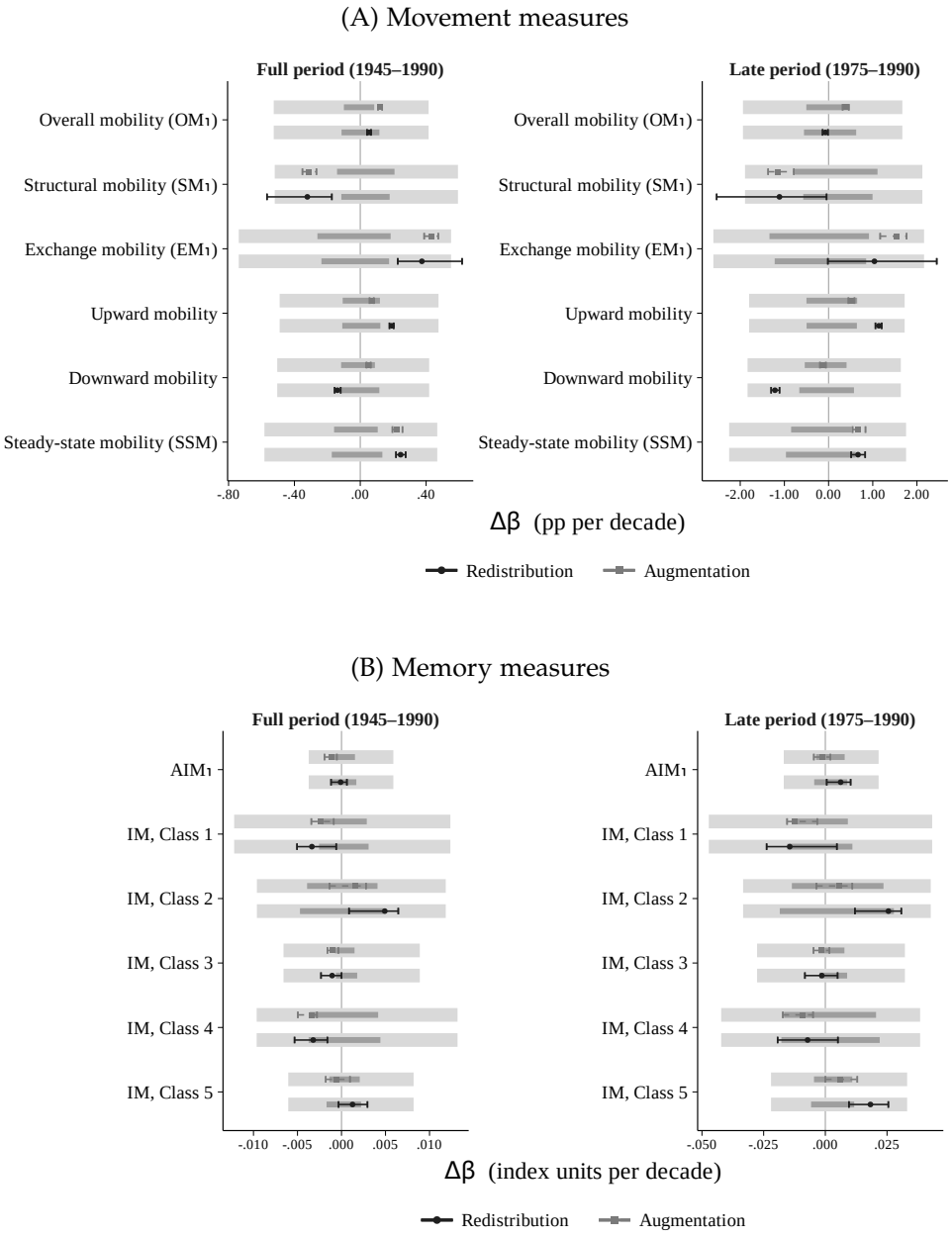


(D) Class-4-specific measures

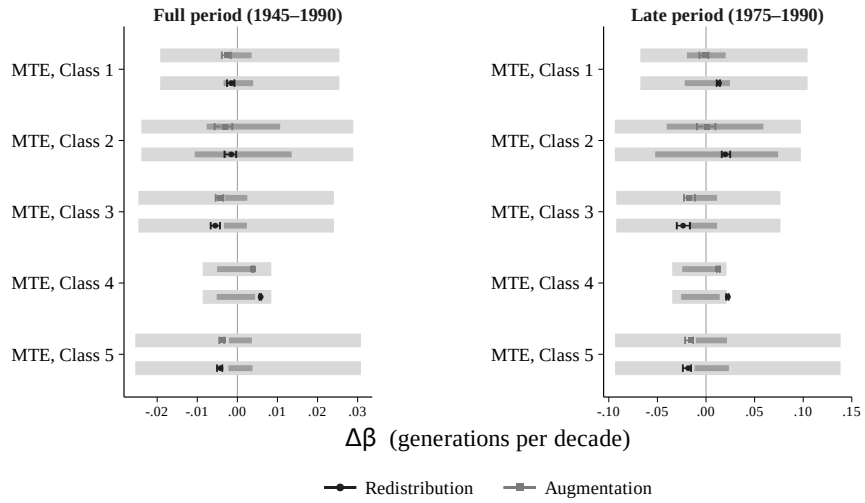


Notes: This figure displays the perturbation-induced slope changes ($\Delta\beta$) for all measures under both the redistribution and augmentation mechanisms, in both the full period (1945–1990) and the late period (1975–1990). Panel (A) reports movement measures; panel (B) reports memory measures; panel (C) reports movement class-specific measures (mean time to exit); and panel (D) reports Class-4-specific measures. Black circles with solid intervals denote redistribution exercise; gray squares with dashed intervals denote augmentation exercise. Points denote the baseline value of $\Delta\beta$; intervals are its associated 95% percentile paired-bootstrap intervals.

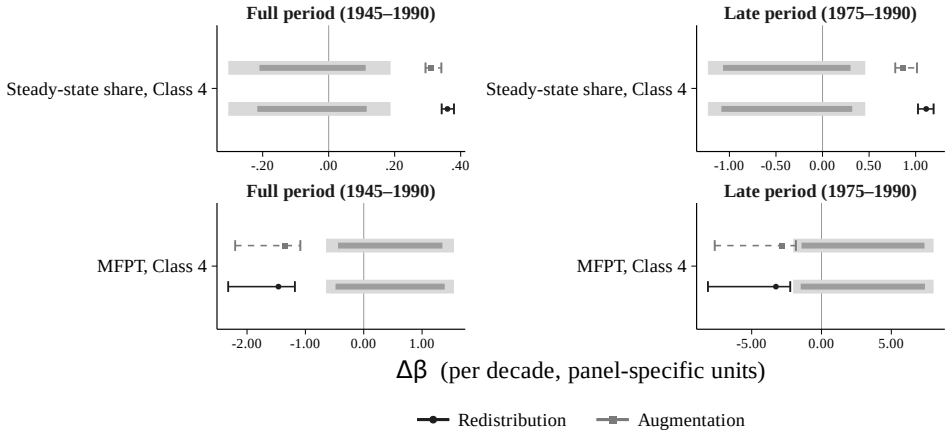
Figure K.2: Perturbation-induced slope changes relative to bootstrap benchmark distributions



(C) Movement class-specific measures



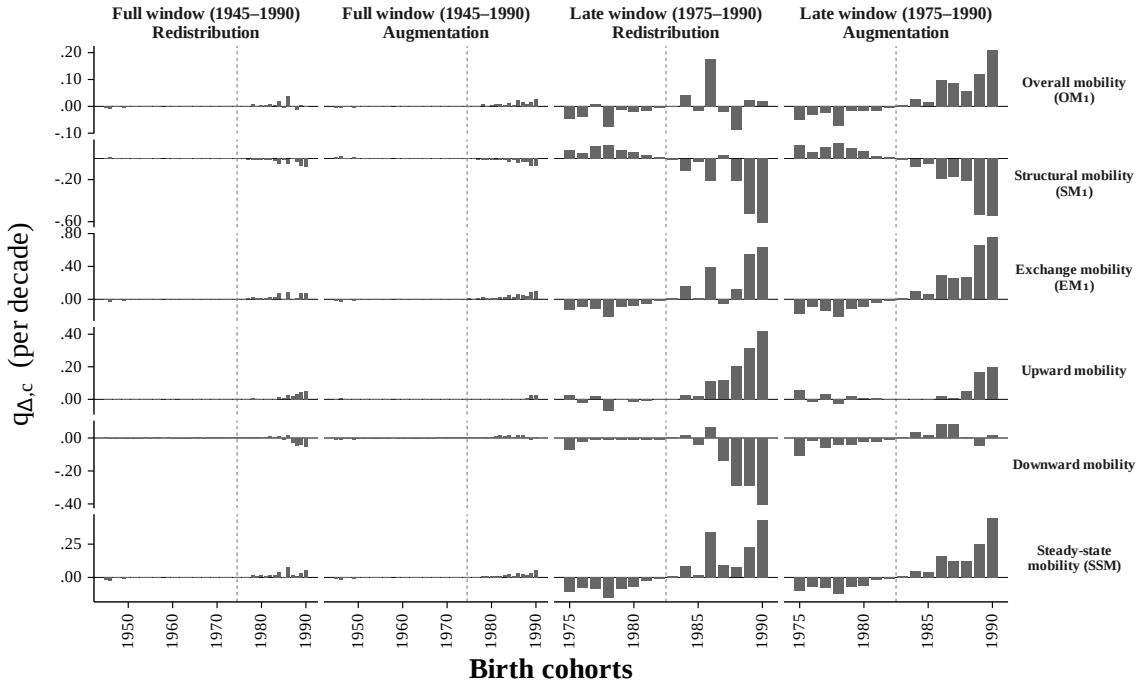
(D) Class-4-specific measures



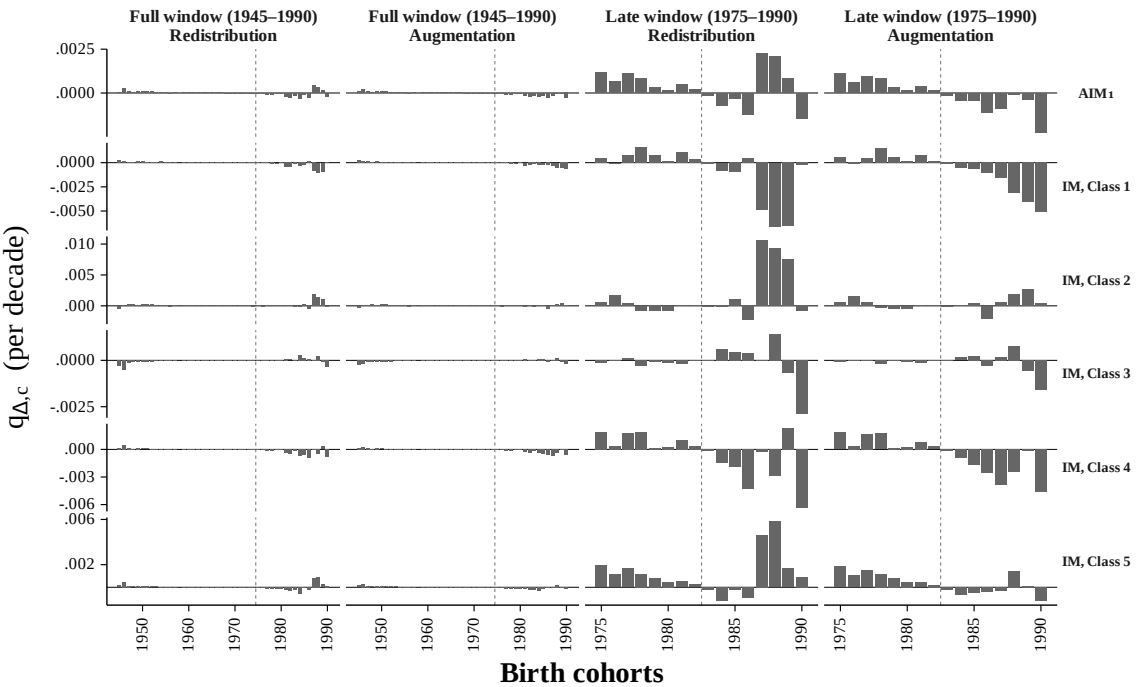
Notes: This figure compares the perturbation-induced slope changes with bootstrap variation in the estimated cohort trends. Panel (A) reports movement measures; panel (B) reports memory measures; panel (C) reports movement class-specific measures (mean time to exit); and panel (D) reports Class-4-specific measures. Light-gray bands show the total-system bootstrap slope-movement ranges, while dark-gray bands show the targeted sparse-cell ranges. Black circles with solid intervals denote redistribution, and gray squares with dashed intervals denote augmentation. The points represent deterministic $\Delta\beta$, and the intervals are paired-bootstrap 95% percentile intervals for $\Delta\beta$. The benchmark bands and point–interval marks represent different distributions: the bands calibrate the magnitude of the shift and are not confidence intervals for the plotted $\Delta\beta$ values.

Figure K.3: Cohort-specific contributions to perturbation-induced trend changes

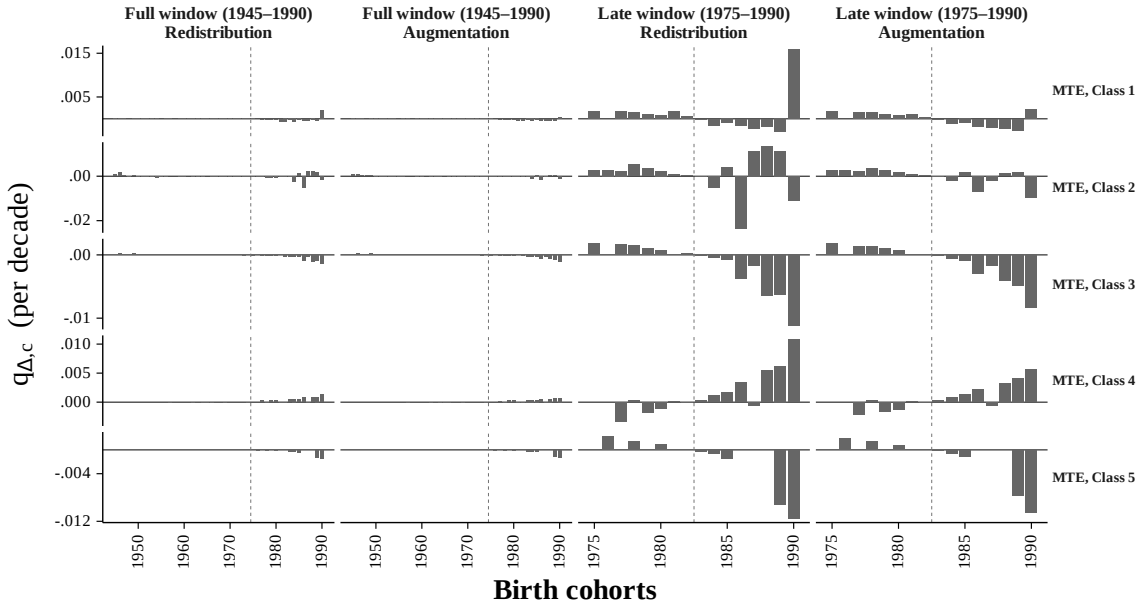
(A) Movement measures



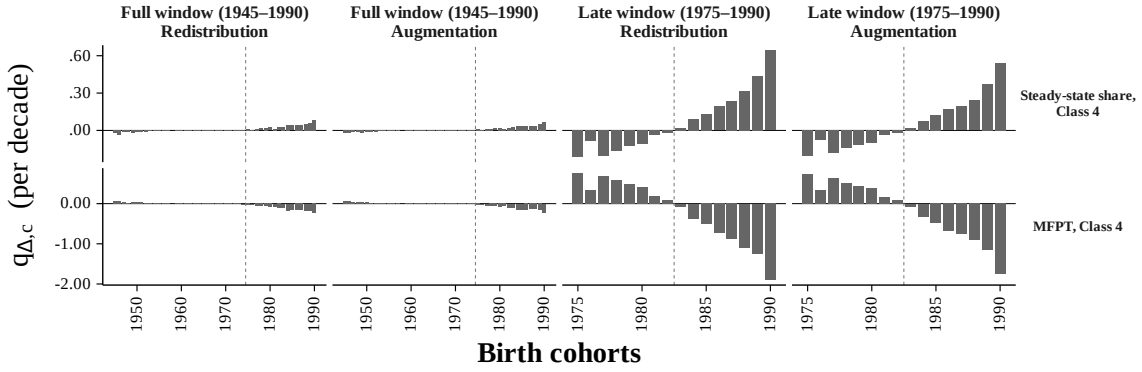
(B) Memory measures



(C) Movement class-specific measures



(D) Class-4-specific measures



Notes: This figure displays each cohort's contribution to the perturbation-induced slope change, $q_{\Delta,c} = h_{W,c}\left[\theta_c^M(\kappa) - \theta_c^0\right]$, where $h_{W,c}$ is the OLS slope weight for cohort c in window W. Panel (A) reports movement measures; panel (B) reports memory measures; panel (C) reports movement class-specific measures (mean time to exit); and panel (D) reports Class-4-specific measures. Within each mechanism and cohort window, these contributions sum exactly to $\Delta\beta$. The full- and late-window contributions use their own centering and denominators. The vertical dividers mark 1975 in the full window and 1983 in the late window. The figure shows that, for several sensitive trends, recent cohorts account for a large share of the perturbation-induced slope change.

Table K.1: Sparse-cell perturbation design and bootstrap calibration at $\kappa = 1$.

Mechanism	Era	μ_0 changes	med. sparse cells	med. affected rows	med. budget	med. stationary TV	total q50	total q95	med. $R_{\text{total}}(1)$	$\kappa_{\text{boot95,total}}$	med. TV(μ_0)	med. TV(μ_1)	capped cohorts
Redistribution	early	no	2	2	2	0.0053	0.0105	0.0191	0.269	3.80	0.0000	0.0038	0
Redistribution	late	no	6	4	6	0.0195	0.0159	0.0292	0.702	1.42	0.0000	0.0165	0
Augmentation	early	yes	2	2	2	0.0044	0.0105	0.0191	0.238	4.56	0.0026	0.0032	0
Augmentation	late	yes	6	4	6	0.0154	0.0159	0.0292	0.538	1.92	0.0063	0.0149	0

Notes: A cell is sparse when its raw dyad count is at most five; the sparse-cell mask is constructed from the original raw counts and held fixed across mechanisms, κ values, and bootstrap replicates. Let K_c denote the number of sparse cells in cohort c. At $\kappa = 1$, the cohort-specific input budget is K_c dyad-equivalents—one per sparse cell. The budget column reports the median K_c within each era. Redistribution moves probability toward sparse cells within each father-origin row while holding $\widehat{\mu}_{0,c}$, the smoothed marginal distribution of fathers across occupational origin classes, fixed. Augmentation adds κ pseudo-dyads to each sparse cell, allowing the transition matrix, the father-origin marginal $\widehat{\mu}_{0,c}$, and the implied child-destination marginal $\widehat{\mu}_{1,c}$ to change. Stationary TV is the total-variation distance between the perturbed and baseline stationary distributions. For each cohort, total q50 and q95 are the 50th and 95th percentiles of the perturbation-free total-system bootstrap stationary-TV distribution. $R_{\text{total}}(1)$ is calculated cohort by cohort as stationary TV at $\kappa = 1$ divided by total q95 and then summarized by its median within each era. $\kappa_{\text{boot95,total}}$ is the mechanism-specific perturbation magnitude at which stationary TV reaches the cohort's total-system q95; entries report medians across cohorts. "Capped cohorts" counts cohorts for which the requested redistribution exceeds its feasibility ceiling; none are capped at $\kappa = 1$. Early = 1945–1974; late = 1975–1990.

Table K.2: Cohort-trend results under both sparse-cell perturbation mechanisms ($\kappa = 1$).

Measure	Baseline β	Redist. β	Redist. $\Delta\beta$	Redist. $\Delta\beta$ 95% CI	Redist. $P(\text{dir.})$	Augm. β	Augm. $\Delta\beta$	Augm. $\Delta\beta$ 95% CI	Augm. $P(\text{dir.})$
Panel A: full period, 1945–1990									
Measures of movement									
Overall mobility (OM_1)	-0.530	-0.477	+0.053	[0.041, 0.065]	0.99	-0.411	+0.119	[0.108, 0.133]	0.98
Structural mobility (SM_1)	-2.111	-2.432	-0.321	[-0.567, -0.172]	1.00	-2.426	-0.316	[-0.351, -0.266]	1.00
Exchange mobility (EM_1)	+1.581	+1.955	+0.374	[0.228, 0.619]	1.00	+2.015	+0.435	[0.388, 0.473]	1.00
Upward mobility	-1.206	-1.014	+0.192	[0.177, 0.203]	1.00	-1.137	+0.069	[0.057, 0.082]	1.00
Downward mobility	+0.676	+0.537	-0.139	[-0.156, -0.119]	0.98	+0.725	+0.050	[0.038, 0.064]	1.00
Mean time to exit									
Average MTE	+0.009	+0.008	-0.001	[-0.002, -0.001]	0.95	+0.007	-0.002	[-0.003, -0.002]	0.95
MTE, Class 1	+0.037	+0.036	-0.001	[-0.003, -0.001]	1.00	+0.035	-0.003	[-0.004, -0.002]	1.00
MTE, Class 2	+0.041	+0.039	-0.002	[-0.003, 0.000]	1.00	+0.038	-0.003	[-0.006, -0.001]	1.00
MTE, Class 3	-0.042	-0.048	-0.006	[-0.007, -0.004]	1.00	-0.047	-0.004	[-0.005, -0.003]	1.00
MTE, Class 4	-0.016	-0.010	+0.006	[0.006, 0.006]	0.99	-0.012	+0.004	[0.004, 0.004]	1.00
MTE, Class 5	+0.025	+0.021	-0.004	[-0.005, -0.004]	0.96	+0.022	-0.004	[-0.004, -0.003]	0.96
Intergenerational memory									
AIM_1	+0.002	+0.002	+0.000	[-0.001, 0.001]	0.85	+0.001	-0.001	[-0.002, -0.001]	0.73
IM, Class 1	+0.002	-0.002	-0.003	[-0.005, -0.001]	0.41	-0.001	-0.002	[-0.003, -0.001]	0.46
IM, Class 2	+0.004	+0.009	+0.005	[0.001, 0.006]	0.95	+0.005	+0.002	[-0.001, 0.003]	0.85
IM, Class 3	-0.002	-0.003	-0.001	[-0.002, 0.000]	0.72	-0.003	-0.001	[-0.002, 0.000]	0.68
IM, Class 4	+0.007	+0.004	-0.003	[-0.005, -0.002]	0.81	+0.003	-0.003	[-0.005, -0.003]	0.78
IM, Class 5	+0.000	+0.001	+0.001	[0.000, 0.003]	0.73	-0.001	-0.001	[-0.002, 0.001]	0.55
Steady-state quantities									
Steady-state mobility (SSM)	-0.367	-0.122	+0.245	[0.217, 0.276]	0.74	-0.146	+0.221	[0.195, 0.256]	0.77
Steady-state share, Class 4	-0.699	-0.339	+0.360	[0.342, 0.380]	1.00	-0.388	+0.311	[0.293, 0.342]	1.00
Mean first passage time									
MFPT into Class 4	+2.127	+0.666	-1.461	[-2.321, -1.181]	1.00	+0.786	-1.342	[-2.202, -1.086]	1.00
Panel B: late period, 1975–1990									
Measures of movement									
Overall mobility (OM_1)	-0.099	-0.173	-0.073	[-0.135, -0.014]	0.62	+0.285	+0.385	[0.318, 0.458]	0.42

continued

Measure	Baseline β	Redist. β	Redist. $\Delta\beta$	Redist. $\Delta\beta$ 95% CI	Redist. $P(\text{dir.})$	Augm. β	Augm. $\Delta\beta$	Augm. $\Delta\beta$ 95% CI	Augm. $P(\text{dir.})$
Structural mobility (SM_1)	+0.103	-1.009	-1.112	[-2.532, -0.045]	0.17	-1.051	-1.154	[-1.368, -0.786]	0.15
Exchange mobility (EM_1)	-0.202	+0.836	+1.038	[-0.016, 2.448]	0.30	+1.337	+1.539	[1.168, 1.767]	0.17
Upward mobility	-0.729	+0.412	+1.141	[1.061, 1.203]	0.33	-0.211	+0.518	[0.449, 0.586]	0.60
Downward mobility	+0.630	-0.584	-1.214	[-1.300, -1.111]	0.21	+0.496	-0.133	[-0.195, -0.062]	0.68
Mean time to exit									
Average MTE	-0.002	+0.001	+0.003	[0.001, 0.004]	0.41	-0.006	-0.004	[-0.007, -0.002]	0.55
MTE, Class 1	+0.033	+0.047	+0.013	[0.011, 0.014]	0.92	+0.033	-0.001	[-0.007, 0.003]	0.85
MTE, Class 2	-0.038	-0.018	+0.020	[0.016, 0.025]	0.66	-0.037	+0.001	[-0.009, 0.010]	0.82
MTE, Class 3	-0.047	-0.071	-0.024	[-0.030, -0.017]	0.97	-0.064	-0.017	[-0.023, -0.011]	0.96
MTE, Class 4	-0.022	+0.001	+0.023	[0.021, 0.023]	0.62	-0.009	+0.012	[0.011, 0.014]	0.86
MTE, Class 5	+0.064	+0.046	-0.018	[-0.024, -0.015]	0.87	+0.048	-0.016	[-0.021, -0.013]	0.88
Intergenerational memory									
AIM_1	-0.007	+0.000	+0.006	[0.001, 0.010]	0.42	-0.008	-0.001	[-0.005, 0.002]	0.73
IM, Class 1	-0.012	-0.026	-0.014	[-0.024, 0.005]	0.90	-0.024	-0.012	[-0.015, -0.003]	0.87
IM, Class 2	-0.010	+0.015	+0.026	[0.012, 0.031]	0.18	-0.005	+0.005	[-0.004, 0.011]	0.53
IM, Class 3	-0.001	-0.002	-0.001	[-0.008, 0.005]	0.53	-0.003	-0.002	[-0.005, 0.002]	0.50
IM, Class 4	-0.025	-0.032	-0.007	[-0.019, 0.005]	0.97	-0.034	-0.009	[-0.017, -0.005]	0.98
IM, Class 5	-0.003	+0.016	+0.018	[0.010, 0.026]	0.06	+0.003	+0.006	[0.000, 0.013]	0.25
Steady-state quantities									
Steady-state mobility (SSM)	-0.030	+0.636	+0.666	[0.511, 0.829]	0.35	+0.634	+0.664	[0.543, 0.835]	0.35
Steady-state share, Class 4	-0.410	+0.704	+1.113	[1.025, 1.193]	0.21	+0.452	+0.861	[0.782, 1.014]	0.38
Mean first passage time									
MFPT into Class 4	+1.284	-1.980	-3.264	[-8.137, -2.234]	0.16	-1.530	-2.815	[-7.651, -1.838]	0.26

Notes: Slopes are reported per decade: percentage points for proportion measures, generations for mean-time-to-exit and first-passage measures, and index units for intergenerational-memory measures. Redist. denotes within-row redistribution, and Augm. denotes pseudo-dyad augmentation. Both mechanisms use the same fixed sparse-cell mask and the same cohort-specific input budget, κK_c, at $\kappa = 1$. For each mechanism, $\Delta\beta = \beta_{\text{pert}} - \beta_{\text{base}}$. The reported 95% interval is the unadjusted 2.5th–97.5th percentile range of the paired replicate-level values of $\Delta\beta$; no additional bias correction is applied. $P(\text{dir.})$ is $P(\text{direction retained})$, the share of bootstrap replicates in which the perturbed slope has the same sign as the deterministic baseline slope.

Table K.3: Perturbation-induced trend changes relative to bootstrap slope variation ($\kappa = 1$).

Panel A: full period, 1945–1990

Measure	Mech.	Baseline β	Total-bootstrap β 95% range	Perturbed β	$\Delta\beta$	Paired $\Delta\beta$ 95% CI	Total $\lvert u\rvert$ q95	R_{total}	Targeted $\lvert u\rvert$ q95	R_{target}	Outside total 95%
Overall mobility (OM_1)	Augm.	-0.530	[-1.056, -0.115]	-0.411	+0.119	[0.108, 0.133]	0.478	0.25	0.092	1.29	–
Overall mobility (OM_1)	Redist.	-0.530	[-1.056, -0.115]	-0.477	+0.053	[0.041, 0.065]	0.478	0.11	0.115	0.46	–
Structural mobility (SM_1)	Augm.	-2.111	[-2.630, -1.517]	-2.426	-0.316	[-0.351, -0.266]	0.559	0.56	0.184	1.71	–
Structural mobility (SM_1)	Redist.	-2.111	[-2.630, -1.517]	-2.432	-0.321	[-0.567, -0.172]	0.559	0.58	0.162	1.98	–
Exchange mobility (EM_1)	Augm.	+1.581	[0.842, 2.132]	+2.015	+0.435	[0.388, 0.473]	0.664	0.66	0.236	1.84	–
Exchange mobility (EM_1)	Redist.	+1.581	[0.842, 2.132]	+1.955	+0.374	[0.228, 0.619]	0.664	0.56	0.216	1.74	–
Upward mobility	Augm.	-1.206	[-1.696, -0.731]	-1.137	+0.069	[0.057, 0.082]	0.486	0.14	0.115	0.61	–
Upward mobility	Redist.	-1.206	[-1.696, -0.731]	-1.014	+0.192	[0.177, 0.203]	0.486	0.40	0.117	1.64	–
Downward mobility	Augm.	+0.676	[0.171, 1.094]	+0.725	+0.050	[0.038, 0.064]	0.464	0.11	0.101	0.49	–
Downward mobility	Redist.	+0.676	[0.171, 1.094]	+0.537	-0.139	[-0.156, -0.119]	0.464	0.30	0.120	1.16	–
Average MTE	Augm.	+0.009	[0.000, 0.020]	+0.007	-0.002	[-0.003, -0.002]	0.010	0.19	0.002	0.83	–
Average MTE	Redist.	+0.009	[0.000, 0.020]	+0.008	-0.001	[-0.002, -0.001]	0.010	0.13	0.003	0.48	–
MTE, Class 1	Augm.	+0.037	[0.018, 0.063]	+0.035	-0.003	[-0.004, -0.002]	0.023	0.11	0.003	0.76	–
MTE, Class 1	Redist.	+0.037	[0.018, 0.063]	+0.036	-0.001	[-0.003, -0.001]	0.023	0.07	0.004	0.40	–
MTE, Class 2	Augm.	+0.041	[0.017, 0.070]	+0.038	-0.003	[-0.006, -0.001]	0.026	0.12	0.010	0.32	–
MTE, Class 2	Redist.	+0.041	[0.017, 0.070]	+0.039	-0.002	[-0.003, 0.000]	0.026	0.06	0.012	0.12	–
MTE, Class 3	Augm.	-0.042	[-0.067, -0.018]	-0.047	-0.004	[-0.005, -0.003]	0.024	0.18	0.003	1.57	–
MTE, Class 3	Redist.	-0.042	[-0.067, -0.018]	-0.048	-0.006	[-0.007, -0.004]	0.024	0.23	0.003	1.86	–
MTE, Class 4	Augm.	-0.016	[-0.025, -0.008]	-0.012	+0.004	[0.004, 0.004]	0.009	0.45	0.005	0.81	–
MTE, Class 4	Redist.	-0.016	[-0.025, -0.008]	-0.010	+0.006	[0.006, 0.006]	0.009	0.68	0.005	1.16	–
MTE, Class 5	Augm.	+0.025	[0.000, 0.056]	+0.022	-0.004	[-0.004, -0.003]	0.029	0.13	0.003	1.18	–
MTE, Class 5	Redist.	+0.025	[0.000, 0.056]	+0.021	-0.004	[-0.005, -0.004]	0.029	0.15	0.003	1.24	–
AIM_1	Augm.	+0.002	[-0.002, 0.008]	+0.001	-0.001	[-0.002, -0.001]	0.005	0.21	0.001	0.82	–
AIM_1	Redist.	+0.002	[-0.002, 0.008]	+0.002	+0.000	[-0.001, 0.001]	0.005	0.02	0.002	0.07	–
IM, Class 1	Augm.	+0.002	[-0.011, 0.014]	-0.001	-0.002	[-0.003, -0.001]	0.012	0.20	0.003	0.90	–
IM, Class 1	Redist.	+0.002	[-0.011, 0.014]	-0.002	-0.003	[-0.005, -0.001]	0.012	0.28	0.003	1.17	–
IM, Class 2	Augm.	+0.004	[-0.006, 0.015]	+0.005	+0.002	[-0.001, 0.003]	0.011	0.14	0.004	0.38	–
IM, Class 2	Redist.	+0.004	[-0.006, 0.015]	+0.009	+0.005	[0.001, 0.006]	0.011	0.45	0.005	1.04	–
IM, Class 3	Augm.	-0.002	[-0.009, 0.007]	-0.003	-0.001	[-0.002, 0.000]	0.008	0.12	0.001	0.81	–
IM, Class 3	Redist.	-0.002	[-0.009, 0.007]	-0.003	-0.001	[-0.002, 0.000]	0.008	0.13	0.002	0.68	–
IM, Class 4	Augm.	+0.007	[-0.003, 0.020]	+0.003	-0.003	[-0.005, -0.003]	0.012	0.28	0.004	0.86	–
IM, Class 4	Redist.	+0.007	[-0.003, 0.020]	+0.004	-0.003	[-0.005, -0.002]	0.012	0.27	0.004	0.77	–

continued

Measure	Mech.	Baseline β	Total-bootstrap β 95% range	Perturbed β	$\Delta\beta$	Paired $\Delta\beta$ 95% CI	Total $\lvert u\rvert$ q95	R_{total}	Targeted $\lvert u\rvert$ q95	R_{target}	Outside total 95%
IM, Class 5	Augm.	+0.000	[-0.006, 0.008]	-0.001	-0.001	[-0.002, 0.001]	0.007	0.08	0.002	0.31	–
IM, Class 5	Redist.	+0.000	[-0.006, 0.008]	+0.001	+0.001	[0.000, 0.003]	0.007	0.17	0.002	0.64	–
Steady-state mobility (SSM)	Augm.	-0.367	[-0.950, 0.100]	-0.146	+0.221	[0.195, 0.256]	0.534	0.41	0.141	1.57	–
Steady-state mobility (SSM)	Redist.	-0.367	[-0.950, 0.100]	-0.122	+0.245	[0.217, 0.276]	0.534	0.46	0.157	1.56	–
Steady-state share, Class 4	Augm.	-0.699	[-1.003, -0.511]	-0.388	+0.311	[0.293, 0.342]	0.267	1.16	0.182	1.71	Yes
Steady-state share, Class 4	Redist.	-0.699	[-1.003, -0.511]	-0.339	+0.360	[0.342, 0.380]	0.267	1.35	0.186	1.94	Yes
MFPT into Class 4	Augm.	+2.127	[1.482, 3.674]	+0.786	-1.342	[-2.202, -1.086]	1.343	1.00	1.134	1.18	Yes
MFPT into Class 4	Redist.	+2.127	[1.482, 3.674]	+0.666	-1.461	[-2.321, -1.181]	1.343	1.09	1.147	1.27	Yes
Panel B: late period, 1975–1990											
Overall mobility (OM_1)	Augm.	-0.099	[-2.037, 1.570]	+0.285	+0.385	[0.318, 0.458]	1.789	0.22	0.476	0.81	–
Overall mobility (OM_1)	Redist.	-0.099	[-2.037, 1.570]	-0.173	-0.073	[-0.135, -0.014]	1.789	0.04	0.591	0.12	–
Structural mobility (SM_1)	Augm.	+0.103	[-1.789, 2.226]	-1.051	-1.154	[-1.368, -0.786]	1.978	0.58	0.983	1.17	–
Structural mobility (SM_1)	Redist.	+0.103	[-1.789, 2.226]	-1.009	-1.112	[-2.532, -0.045]	1.978	0.56	0.890	1.25	–
Exchange mobility (EM_1)	Augm.	-0.202	[-2.809, 1.960]	+1.337	+1.539	[1.168, 1.767]	2.386	0.64	1.193	1.29	–
Exchange mobility (EM_1)	Redist.	-0.202	[-2.809, 1.960]	+0.836	+1.038	[-0.016, 2.448]	2.386	0.44	1.100	0.94	–
Upward mobility	Augm.	-0.729	[-2.528, 0.993]	-0.211	+0.518	[0.449, 0.586]	1.784	0.29	0.592	0.87	–
Upward mobility	Redist.	-0.729	[-2.528, 0.993]	+0.412	+1.141	[1.061, 1.203]	1.784	0.64	0.570	2.00	–
Downward mobility	Augm.	+0.630	[-1.204, 2.265]	+0.496	-0.133	[-0.195, -0.062]	1.741	0.08	0.491	0.27	–
Downward mobility	Redist.	+0.630	[-1.204, 2.265]	-0.584	-1.214	[-1.300, -1.111]	1.741	0.70	0.625	1.94	–
Average MTE	Augm.	-0.002	[-0.036, 0.040]	-0.006	-0.004	[-0.007, -0.002]	0.039	0.10	0.012	0.33	–
Average MTE	Redist.	-0.002	[-0.036, 0.040]	+0.001	+0.003	[0.001, 0.004]	0.039	0.07	0.015	0.18	–
MTE, Class 1	Augm.	+0.033	[-0.034, 0.138]	+0.033	-0.001	[-0.007, 0.003]	0.090	0.01	0.020	0.04	–
MTE, Class 1	Redist.	+0.033	[-0.034, 0.138]	+0.047	+0.013	[0.011, 0.014]	0.090	0.15	0.023	0.59	–
MTE, Class 2	Augm.	-0.038	[-0.132, 0.060]	-0.037	+0.001	[-0.009, 0.010]	0.097	0.01	0.052	0.02	–
MTE, Class 2	Redist.	-0.038	[-0.132, 0.060]	-0.018	+0.020	[0.016, 0.025]	0.097	0.20	0.066	0.30	–
MTE, Class 3	Augm.	-0.047	[-0.139, 0.030]	-0.064	-0.017	[-0.023, -0.011]	0.086	0.20	0.014	1.21	–
MTE, Class 3	Redist.	-0.047	[-0.139, 0.030]	-0.071	-0.024	[-0.030, -0.017]	0.086	0.27	0.016	1.50	–
MTE, Class 4	Augm.	-0.022	[-0.056, -0.001]	-0.009	+0.012	[0.011, 0.014]	0.029	0.42	0.022	0.56	–
MTE, Class 4	Redist.	-0.022	[-0.056, -0.001]	+0.001	+0.023	[0.021, 0.023]	0.029	0.77	0.024	0.95	Yes
MTE, Class 5	Augm.	+0.064	[-0.030, 0.202]	+0.048	-0.016	[-0.021, -0.013]	0.122	0.13	0.020	0.80	–
MTE, Class 5	Redist.	+0.064	[-0.030, 0.202]	+0.046	-0.018	[-0.024, -0.015]	0.122	0.15	0.022	0.85	–
AIM_1	Augm.	-0.007	[-0.023, 0.015]	-0.008	-0.001	[-0.005, 0.002]	0.019	0.06	0.007	0.16	–
AIM_1	Redist.	-0.007	[-0.023, 0.015]	+0.000	+0.006	[0.001, 0.010]	0.019	0.32	0.008	0.80	–
IM, Class 1	Augm.	-0.012	[-0.059, 0.032]	-0.024	-0.012	[-0.015, -0.003]	0.045	0.27	0.012	1.00	–
IM, Class 1	Redist.	-0.012	[-0.059, 0.032]	-0.026	-0.014	[-0.024, 0.005]	0.045	0.32	0.014	1.05	–

continued

Measure	Mech.	Baseline β	Total-bootstrap β 95% range	Perturbed β	$\Delta\beta$	Paired $\Delta\beta$ 95% CI	Total $\lvert u\rvert$ q95	R_{total}	Targeted $\lvert u\rvert$ q95	R_{target}	Outside total 95%
IM, Class 2	Augm.	-0.010	[-0.044, 0.033]	-0.005	+0.005	[-0.004, 0.011]	0.039	0.14	0.021	0.26	–
IM, Class 2	Redist.	-0.010	[-0.044, 0.033]	+0.015	+0.026	[0.012, 0.031]	0.039	0.65	0.025	1.02	–
IM, Class 3	Augm.	-0.001	[-0.029, 0.031]	-0.003	-0.002	[-0.005, 0.002]	0.031	0.05	0.006	0.25	–
IM, Class 3	Redist.	-0.001	[-0.029, 0.031]	-0.002	-0.001	[-0.008, 0.005]	0.031	0.05	0.007	0.19	–
IM, Class 4	Augm.	-0.025	[-0.067, 0.014]	-0.034	-0.009	[-0.017, -0.005]	0.041	0.23	0.019	0.49	–
IM, Class 4	Redist.	-0.025	[-0.067, 0.014]	-0.032	-0.007	[-0.019, 0.005]	0.041	0.18	0.021	0.35	–
IM, Class 5	Augm.	-0.003	[-0.025, 0.030]	+0.003	+0.006	[0.000, 0.013]	0.030	0.20	0.010	0.60	–
IM, Class 5	Redist.	-0.003	[-0.025, 0.030]	+0.016	+0.018	[0.010, 0.026]	0.030	0.62	0.010	1.77	–
Steady-state mobility (SSM)	Augm.	-0.030	[-2.281, 1.724]	+0.634	+0.664	[0.543, 0.835]	2.138	0.31	0.732	0.91	–
Steady-state mobility (SSM)	Redist.	-0.030	[-2.281, 1.724]	+0.636	+0.666	[0.511, 0.829]	2.138	0.31	0.827	0.81	–
Steady-state share, Class 4	Augm.	-0.410	[-1.641, 0.049]	+0.452	+0.861	[0.782, 1.014]	1.066	0.81	0.947	0.91	Yes
Steady-state share, Class 4	Redist.	-0.410	[-1.641, 0.049]	+0.704	+1.113	[1.025, 1.193]	1.066	1.04	0.973	1.14	Yes
MFPT into Class 4	Augm.	+1.284	[-0.744, 9.310]	-1.530	-2.815	[-7.651, -1.838]	6.763	0.42	6.370	0.44	Yes
MFPT into Class 4	Redist.	+1.284	[-0.744, 9.310]	-1.980	-3.264	[-8.137, -2.234]	6.763	0.48	6.608	0.49	Yes

Notes: Per-decade units as in the trend table. The total-bootstrap β 95% range is the unadjusted percentile range of baseline bootstrap slopes; it is not the bias-adjusted confidence interval reported in the main analysis. u_{total} is the displacement of each stored replicate's full-system baseline slope from the deterministic baseline slope (replicate transition matrices and father-origin marginals vary jointly); u_{target} is the mechanism-specific targeted displacement (redistribution: targeted transition-law variation with the father-origin marginal held fixed; augmentation: targeted joint-table variation with replicate-specific father-origin marginals). $R_{\text{total}} = |\Delta\beta|/q_{.95}(|u_{\text{total}}|)$ and $R_{\text{target}} = |\Delta\beta|/q_{.95}(|u_{\text{target}}|)$ are effect-size calibrations. "Outside total 95%" identifies deterministic perturbed slopes that lie outside the central 95% range of unperturbed total-system bootstrap slopes. The paired $\Delta\beta$ interval remains the uncertainty statement for the perturbation-induced change.